ANTICANCER PROPERTY AND MODE OF ACTION OF METAL(II) COMPLEXES OF INTERCALATING LIGAND AND AMINO ACID

VON SZE TIN

MASTER OF SCIENCE

FACULTY OF ENGINEERING AND SCIENCE
UNIVERSITI TUNKU ABDUL RAHMAN
SEPTEMBER 2012

ANTICANCER PROPERTY AND MODE OF ACTION OF METAL(II) COMPLEXES OF INTERCALATING LIGAND AND AMINO ACID

By

VON SZE TIN

A thesis submitted to the Department of Bioscience and Chemistry,
Faculty of Engineering and Science,
Universiti Tunku Abdul Rahman,
In partial fulfillment of the requirements for the degree of
Master of Science
September 2012

ABSTRACT

ANTICANCER PROPERTY AND MODE OF ACTION OF METAL(II) COMPLEXES OF INTERCALATING LIGAND AND AMINO ACID

Von Sze Tin

Over the last few years, a lot of research has been done to develop novel metal-based anticancer drugs, with the aim of increase clinical effectiveness, reduce toxic side effect, and broadening the spectrum of activity. Nowadays, breast cancer is the most common cancer in women in most parts of the world. A woman in Malaysia has a 1 in 20 chance of getting breast cancer in her lifetime. This research attempts to screen different metal complexes of 1,10-phenanthroline (a known intercalating molecule) and amino acid, with the general formula [M(phen)(edda)] [M(II) = Cu, Co, Zn; phen = 1,10-phenanthroline; edda = *N,N'*-ethylenediaminediacetate]. Low IC_{50} value of 2.8 µM [Cu(phen)(edda)], 5 µM [Zn(phen)(edda)] and 13.5 µM [Co(phen)(edda)] on breast cancer cells, MCF7 for 72 h were observed. The corresponding IC_{50} values for [Cu(phen)(edda)], [Zn(phen)(edda)] and [Co(phen)(edda)] on breast normal cells, MCF10A in 72 h are 10.4 µM, 32 µM and 28 µM respectively. These cytotoxicity studies showed that [M(phen)(edda)] exhibit selectivity towards breast cancer cells over normal cells. The log *P* values for [Zn(phen)(edda)] is 0.70, [Cu(phen)(edda)] is 0.33 and [Co(phen)(edda)] is 0.30. It is interesting to note that three compounds have good drug-like property as their values obey Log *P* < 5 for drug-like property based on Lipinski's Rule of Five. Besides, morphological studies show apoptosis

occurred as characterized by nuclear condensation (performed by using DAPI staining), membrane blebbing, extension of microspikes and apoptotic body formation. Besides, fluorescent micrographs of Annexin V-FITC/Propidium Iodide double staining of 2.8 µM [Cu(phen)(edda)], 5 µM [Zn(phen)(edda)] and 13.5 µM [Co(phen)(edda)] treated-MCF7 cells induced apoptosis in time dependent manner. An accumulation of cells in S phase were observed in MCF7 cells treated with 5 µM [Zn(phen)(edda)] treatment. In contrast, no cell cycle arrest was detected when treated with 2.8 µM [Cu(phen)(edda)] and 13.5 µM [Co(phen)(edda)]. Moreover, 2.8 µM [Cu(phen)(edda)], 5 µM [Zn(phen)(edda)] and 13.5 µM [Co(phen)(edda)]-treated MCF7 cells showed an increasing mitochondrial membrane depolarization in time dependent manner by using JC-1 staining. Topoisomerases have been identified as the cellular target of a number of important anticancer agents. The order of inhibitory effect on topoisomerase I activity in this study is [Zn(phen)(edda)] > [Co(phen)(edda)] > [Cu(phen)(edda)].

ACKNOWLEDGEMENTS

would also want to thank my co-supervisor, Dr. Lee Hong Boon from Cancer Research Initiative Foundation, for all her support, advice and discussion from the initial to the final level enabled me to develop an understanding of the subject.

Besides, I am sincerely grateful to my co-researchers, Tan Kong Wai and Seng Hoi Ling for their support, friendship and technical assistance in the laboratory. The team has been a source of friendships as well as good advice and collaboration.

Especially, I would like to give my special thanks to my family whose patient love and encouragement enabled me to complete this work. For my parents, who have raised me with a love of science and supported me in all my pursuits. Also, for the presence of my brother, Victor Von who is staying together with me in Kuala Lumpur for more than three of my years here. Thank you.

Lastly, I offer my regards and blessings to all of those who supported me in any respect during the completion of the project.

This dissertation/thesis entitled "**ANTICANCER PROPERTY AND MODE OF ACTION OF METAL(II) COMPLEXES OF INTERCALATING LIGAND AND AMINO ACID**" was prepared by VON SZE TIN and submitted as partial fulfillment of the requirements for the degree of Master of Science in Faculty of Engineering and Science at Universiti Tunku Abdul Rahman.

Approved by:

_____

(Assoc. Prof. Dr. Ng Chew Hee)   Date:…………………..
Supervisor
Department of Chemical Science
Faculty of Science
Universiti Tunku Abdul Rahman

_____

(Dr. Lee Hong Boon)   Date:…………………..
Co-supervisor
Cancer Research Initiative Foundation (CARIF)
Subang Jaya Medical Centre

Date: _____

SUBMISSION OF DISSERTATION/THESIS

It is hereby certified that **VON SZE TIN** (ID No: **07UEM08780**) has completed this thesis/dissertation entitled "ANTICANCER PROPERTY AND MODE OF ACTION OF METAL(II) COMPLEXES OF INTERCALATING LIGAND AND AMINO ACID" under the supervision of Assoc. Prof. Dr. Ng Chew Hee (Supervisor) from the Department of Chemical Science, Faculty of Science, and Dr. Lee Hong Boon (Co-Supervisor) from Cancer Research Initiative Foundation, Subang Jaya Medical Centre.

I understand that the University will upload softcopy of my thesis/dissertation in pdf format into UTAR Institutional Repository, which may be made accessible to UTAR community and public.

Yours truly,

_____
(VON SZE TIN)

DECLARATION

I hereby declare that the dissertation is based on my original work except for quotations and citations which have been duly acknowledged. I also declare that it has not been previously or concurrently submitted for any other degree at UTAR or other institutions.

VON SZE TIN

Date:

TABLE OF CONTENTS

Page

CHAPTER

LIST OF TABLES

LIST OF FIGURES

LIST OF ABBREVIATIONS

^{o}C	Degree Celsius
μg	Microgram
μm	Micrometer
ψm	Mitochondrial membrane potential
μM	Micromolar
M	Molar
%	Percentage
v/v	Volume per volume
w/v	Weight per volume
14-3-3σ	Putative tumor suppressor involved in cell-cycle progression and epithelial polarity
AIF	Apoptosis inducing factor
Apaf-1	Apoptotic peptidase activating factor 1
AJCC	American Joint Committee on Cancer
ASR	Age-standardized incidence
ATCC	American Type Culture Collection
ATP	Adenosine triphosphate
BAX	Bcl-2–associated X protein
Bel-7402	Human liver carcinoma cell line
BGC-823	Human stomach carcinoma cell line
BCL-XL	B-cell lymphoma-extra large
Bp	Base pair
BRCA	Breast cancer
CDKs	Cyclin-dependent kinases
CIP1/WAF1	Cyclin-dependent kinase inhibitor
Cl_2	Chloride
cm	centimetre
Co(II)	Cobalt(II)
Cu(II)	Copper(II)
Cr(VI)	Chromium
DAPI	4',6-diamidino-2-phenylindole
dATP	Deoxyadenosine triphosphate
DHE	Dihydroethidium
DIABLO	Direct inhibitor of apoptosis-binding protein with low isoelectric point
DiOC6	3,3'-dihexyloxacarbocyanine iodide
DMEM	Dulbecco's modified eagle medium
DMSO	Dimethyl sulfoxide
DNA	Deoxyribonucleic acid
DNase	Deoxyribonuclease
DR5	Death receptor 5
EDDA	*N,N'*-ethylenediaminediacetic acid
EDTA	Ethylenediaminetetraacetic acid
EGFR	Epidermal growth factor receptor

ETC	Electron transport chain
FACS	Fluorescence activated cell sorting
Fas	Death receptor on cell surface that leads to apoptosis
FAS1	Tumor necrosis factor receptor superfamily member 6 isoform 1
FasL	Fas ligand
FBS	Fetal bovine serum
FITC	Fluorescein isothiocyanate
g	Gram
GADD45	Growth arrest and DNA damage protein
h	Hour
H_2DCFDA	2',7'-dichlorodihydrofluorescein diacetate
H_2O	Water molecule
H_2O_2	Hydrogen peroxide
HCl	Hydrochloride/Hydrochloric acid
Hela	Human cervix carcinoma cell line
HL-60	Human promyelocytic leukemia cell line
IC_{50}	Concentration of the metal complexes at which the percentage of viability was reduced by 50%)
IGF-BP3	Insulin-like growth factor-binding protein-3
JC-1	5,5',6,6'-tetrachloro-1,1',3,3'-tetraethylbenzimidazol-carbocyanine iodide
Kb	Kilo base pair
L	Litre
Log P	Partition coefficient
MCF7	Human breast cancer cell line
MCF10A	Human breast normal cell line
MDA-MB-435	Human galactophore carcinoma cell line
MDM2	Murine double minute 2
MEM	Minimum essential medium
mg	Milligram
Mg	Magnesium
min	Minute
ml	Millilitre
mm	Millimetre
mM	Millimolar
MTT	3-(4,5-dimethylthiazol-2-yl)-2,5-diphenyltetrazolium bromide
NaCl	Sodium chloride
NaOH	Sodium hydroxide
nDNA	Nuclear deoxyribonucleic acid
NEAA	Non-Essential amino acids
Nm	Nanometer
O_2^-	Superoxide
•OH	Hydroxyl radical
p53	Tumor protein 53
PBS	Phosphate-buffered saline
PC-3MIE8	Human prostate carcinoma cell line
PCNA	Proliferating cell nuclear antigen
Phen	Phenanthroline

PI	Propidium iodide
PS	Phosphatidylserine
RNase	Ribonuclease
ROS	Reactive oxygen species
Rpm	Rotation per minute
RPMI	Roswell park memorial institute medium
s	Second
SDS	Sodium dodecyl sulfate
SE	Standard deviation
smac	Second mitochondria-derived activator of caspase
TAE	Tris–acetate EDTA
TGFα	Transforming growth factor α
TNF	Tumor necrosis factor
Topo	Topoisomerase
Tris	Tris(hydroxymethyl)aminomethane
TUNEL	Terminal deoxynucleotidyl transferase dUTP nick end labeling
UV	Ultraviolet
viz.	Namely or that is to say
WIP1	Wild-type p53-induced phosphatase 1
Zn(II)	Zinc(II)

CHAPTER 1.0

INTRODUCTION

The success of the clinical use of *cis*-[PtCl$_2$(NH$_3$)$_2$], known as *cis*-diamminedichloroplatinum(II) or cisplatin, has stimulated considerable interest in developing other metal complexes as new anticancer agents. In view of the emergence of drug-resistant cancer and some undesirable side effects of cisplatin, there have been extensive studies from many laboratories worldwide to develop new metal-based drug leads that could overcome the drug resistance and with fewer side effects (Stewart, 2007). The severe limitations prompted many researchers to develop alternative strategies based on different metals and probably aimed at different mechanism of actions.

The study of transition metal complexes with tetradentate edda-type ligands (edda = an ion of *N,N'*-ethylenediaminediacetic acid) was the subject of a large number of investigations for many years (Brubaker *et al.*, 1971; Radanović, 1984; Sabo *et al.*, 2002). Metal chelation chemistry may be important even in drugs that are not intentionally designed as metal chelators. A large fraction of drugs on the market are known or expected to bind metals with appreciable affinity. How this affects their actions is worthy of exploration. Chelates are inorganic agents that have good clinical effects in treatment of various types of cancer as cytotoxic agent (Tripathi *et al.*, 2007). Various chelates based on cobalt, copper and zinc are reported as cytotoxic

agent (Chohan *et al.*, 2006; Miesel and Weser, 2006; Ferry *et al.*, 1998). 1,10-phenanthroline (1,10-phen) is a versatile ligand capable of forming highly stable complexes with transition metal ions (Maki and Sakuraba, 1969). Also, 1,10-phen itself has anticancer property (Devereux *et al.*, 2006). One of the most biologically active of the metal–phen complexes is $[Cu(phen)_2]^{2+}$. Moreover, a recent study of the synthesis of some $[Cu(phen)_2]^{2+}$ phenanthroline compounds along with their *in vitro* anticancer properties have been reported (Zhang *et al.*, 2004; Thati *et al.*, 2007; Barceló-Oliver *et al.*, 2007). Insufficiently, it is hard to search literature review of $[Co(phen)_2]^{2+}$ and $[Zn(phen)_2]^{2+}$ on anticancer work. It is also important to point out the publication of initial research work of this thesis shown that anticancer neutral octahedral ternary metal(II) complexes of 1,10-phen and edda, [M(phen)(edda)] (M = Cu, Co, Ni, Zn) could interact with DNA through binding to it by intercalation and clearly evident that DNA being a target for this family of compounds has been verified (Ng *et al.*, 2008). In the initial stage of this study, [Cu(phen)(edda)], [Co(phen)(edda)] and [Zn(phen)(edda)] were found to have low IC_{50} values in comparison to other similar anticancer agents, *viz.* [Co(4-MPipzcdt)(phen)_2]Cl, [Zn(4-MPipzcdt)(phen)_2]Cl, [Co(4-MPipzcdt)_2(phen)], [Zn(4-MPipzcdt)_2(phen)], [Cu(phen)(L-Thr)(H_2O)](ClO_4), [Cu(H_2O)(phen)(tp)_2](ClO_4)_2·H_2O and [Cu(H_2O)(phen)(dmtp)_2](ClO_4)_2 (Kalia *et al.*, 2009; Zhang *et al.*, 2004; Boutaleb-Charki *et al.*, 2009). Metal complexation with improved chelator designs are needed to enhance selectivity, affinity, stability, lipophilicity, and oral activity, while maintaining low toxicity and low cost. Additionally, increasing knowledge of the biological activities of simple metal complexes guided many researchers to the

development of promising chemotherapeutic compounds which target specific physiological or pathological processes.

Breast cancer is still a leading cause of cancer death among women in developed and non-developed countries (Porter, 2009). Numerous similarities have long been found between cell lines and tumors. It has been proven that breast cancer cell lines are considered as representative models of transformed cells *in vivo* (Lacroix and Leclercq, 2004). Moreover, it has been well established that the MCF7 cell line is a novel tool for the study of breast cancer resistance to chemotherapeutic drug such as doxorubicin and adriamycin because it appears to mimic the heterogeneity of tumor cells *in vivo* (Simstein *et al.*, 2003). The human breast cancer cell line, MCF7 provides an unlimited source of homogenous self-replicating material, free of contaminating stromal cells, and can be easily cultured in simple standard media. Such a cell line is ideal to study the interaction between a potential anticancer drug and cancer cells (Ray *et al.*, 2006).

A key goal in the development of novel cancer therapeutics is to achieve tissue specificity and minimize side effects in other tissues while maintaining activity against local and metastatic disease (Roberts *et al.*, 2007). This emphasizes the need for the development of novel therapeutics with increased selectivity and efficacy. There is an urgent need to develop selective treatments for cancer. Current treatments are not selective enough and cause debilitating and toxic side effects therefore compromising the effectiveness of the treatment. In the search for novel and effective treatment modalities for

human breast cancer, much attention has focused on exploiting the cytostatic and cytotoxic effects of inorganic transition metal complexes (Tim, 2006).

Besides, the implications for the design of novel anticancer drugs have proceeded to the next wave of drug delivery systems, particularly with respect to systems for oral administration. In terms of oral delivery, the types of aqueous solubility problems attendant to large compound size and high lipophilicity are well handled by respective physicochemical characterization and here refers to Lipinski's Rule of Five (Lipinski *et al.*, 2001; Chuprina *et al.*, 2010). Lipinski's Rule of Five is a rule to evaluate drug-likeness, or determine if a chemical compound with a certain pharmacological or biological activity has properties that would make it a likely orally active drug in humans. It is based on the observation that most medication drugs are relatively small and lipophlic molecules (Lipinski *et al.*, 2001). Indeed, the drug development process from the target identification to the final product being marketed is a time and money consuming process, with the total research and development costs reported as being up to US$802 million dollars and an average of 12 years taken (DiMasi *et al.*, 2003). This has been updated by 64% to US$1.32 billion in 2006 and projected an increase of another 64% by 2012 to an average research and development costs of US$2.16 billion or closely resembling 2.7 times the US$802 million (Light and Warbuton, 2011). Of the hundreds and thousands of novel compounds that many researchers invent, typically only a fraction of these have drug-like properties to become a drug product. Therefore, one of the approaches used in this drug discovery is lipophilicity (log *P*) measurement which conducted in parallel with *in vitro* antitumor

inhibiting studies; such an early compound identification stage permits further selection of drug nominees with desirable absorption, distribution and metabolism properties. When properly designed, it may bring about significant shortening of timelines and reducing costs between discovery and clinical development.

Cell death has been considered a degenerative phenomenon affecting the metabolic activity of the cell (Farber, 1982). One mode of cell death, apoptosis, is the universal mechanism which refers to morphological alterations exhibited by dying cells that include rounding, membrane blebbing, chromatin condensation, and fragmentation. Cells undergoing apoptosis often fragment into membrane-bound apoptotic bodies that are readily phagocytosed and digested by macrophages or neighboring cells without generating an inflammatory response (Essbauer and Ahne, 2002). These changes distinguish apoptosis from cell death by necrosis. Necrosis refers to the morphology most often seen when cells die from severe and sudden injury, such as ischemia. In necrosis, there are early changes in mitochondrial shape and function, the cell loses its ability to regulate osmotic pressure and consequently swells and ruptures. Cell contents are spilled into the surrounding tissue, resulting in the generation of a local inflammatory response (Hines and Allen-Hoffmann, 1996). Changes in nuclear morphology and in organelle structure as well as specific phenomena at the cell surface level, namely surface blebbing, spike and blister formation are often considered as markers associated with apoptosis (Collins, 1997). In order to conduct such research, apoptosis is targeted for the

loss of phospholipid asymmetry of the plasma membrane which characterized by the early exposure of phosphatidylserine (Van Engeland *et al.*, 1998).

Another mode of cell death involves components of the cell cycle machinery which are frequently altered in human cancer. Most anticancer drugs such as antimetabolites, alkylating agents and platinum based drugs target the S-phase of the cell cycle which involves DNA replication or synthesis phase (Humer *et al.*, 2008; Singh *et al.*, 2009; Temmink *et al.*, 2007). Among them, the agents that disturb the cell cycle have been one of particular interest, since cell cycle regulation is the basic mechanism underlying cell fate, i.e., proliferation, differentiation or induced cell death (Hartwell and Kastan, 1994). Thus, uncontrolled cell proliferation is one of the main hallmarks of cancer. This is related to tumor cells damage in genes that are directly involved in the regulation of cell cycle (Waldman *et al.*, 1996).

Anticancer drugs were recently shown to be able to target the DNA, mitochondria, topoisomerase as well as proteosome. Doxorubicin is one of the most common prescribed antitumor drugs for the treatment of breast cancer but the cardiotoxicity of this anthracycline derivative limits its clinical use. It induces cell death by targeting mitochondria (Pereira and Oliveira, 2010). In particular, mitochondrial permeability transition is considered a critical early event in the apoptotic process (Zamzami *et al.*, 1996; Kroemer, 1999). Most chemotherapeutic drugs induce cancer cell apoptosis whereby a cell activates its own destruction by initiating a series of cascading events including the loss of the mitochondrial membrane potential ($\Delta\psi_m$) (Elmore, 2007). Besides, a

rapid collapse of $\Delta\psi_m$ is always found in chemotherapeutic agents-induced apoptosis in cancer cells (Zamzami *et al.*, 1995). Importantly, the DNA topoisomerases are enzymes that can alter the topology of DNA by transiently breaking one or two strands of DNA, passing a single- or double-stranded DNA through the break and finally religating the break. These nuclear enzymes are involved in a number of crucial cellular processes, including DNA replication, transcription, and recombination, and now viewed as important therapeutic targets for cancer chemotherapy (Fukuda *et al.*, 1996). Many researchers have reported that targeting human DNA topoisomerase I (topo I) represents a new generation of antitumor agents (Bailly, 2003; Santos *et al.*, 2004; Pommier and Cushman, 2009). In addition, Coleman *et al.* (2002) have reported that laboratory studies indicated cells responsive to topo I–targeted drugs have elevated levels of topo I, require active DNA replication, and may require a functional apoptotic pathway.

The complexes investigated for their anticancer property and mode of action are [Cu(phen)(edda)], [Co(phen)(edda)] and [Zn(phen)(edda)]. In these complexes, there are two ligands coordinated. An intercalating ligand, 1,10-phen, coordinates through two nitrogen atoms while the other ligand is an amino acid, edda, coordinates through the amino nitrogen and the carboxylate oxygen atoms. The resultant entity is a neutral molecule with an octahedral structure (Figure 1.1). As the coordination sphere of these neutral [M(phen)(edda)] complexes is saturated and their ligands are strongly bound, they cannot bind covalently to DNA. However, the edda ligand has both hydrogen-bonding donors and acceptors interacting with DNA while the phen

moiety can intercalate into the adjacent DNA base pairs. Thus, non-covalent interactions with DNA are envisaged. Interestingly, the chelated tetradentate edda ligand can adopt two possible configurations; symmetrical-*cis* (sy-*cis*) and unsymmetrical-*cis* (unsy-*cis*), where the two glycinato moieties of the edda ligand are distinctly different in their orientation (Ng *et al.*, 2008; Seng *et al.*, 2008; Radanović *et al.*, 1995).

This study was designed to understand the anticancer activity and investigate the mode of action of newly synthesized metal-based drugs of [Cu(phen)(edda)], [Co(phen)(edda)] and [Zn(phen)(edda)] on human breast cancer MCF7 cell line by performing several tests including cytotoxicity test, cell cycle analysis and apoptosis analysis. Besides, the partition coefficient of [M(phen)(edda)], as a measure of membrane permeability was also determined. This can be done by calculating the log *P* value in lipophilicity test, a traditional method to evaluate the drug-likeness. In addition, there is a preliminary investigation into whether these [M(phen)(edda)] complexes have multiple biological targets. Another objective involves finding out whether there might be a difference in the ability of the complexes to induce different cell death mechanism by changing the type of metal in this series of [M(phen)(edda)] complexes. Also, this work presented here represents the preliminary assessment of the potential application of [Cu(phen)(edda)], [Co(phen)(edda)] and [Zn(phen)(edda)] as novel therapeutic agents for the treatment of cancer. This project has been published in two journal papers (Ng *et al.*, 2008; Von *et al.*, 2011).
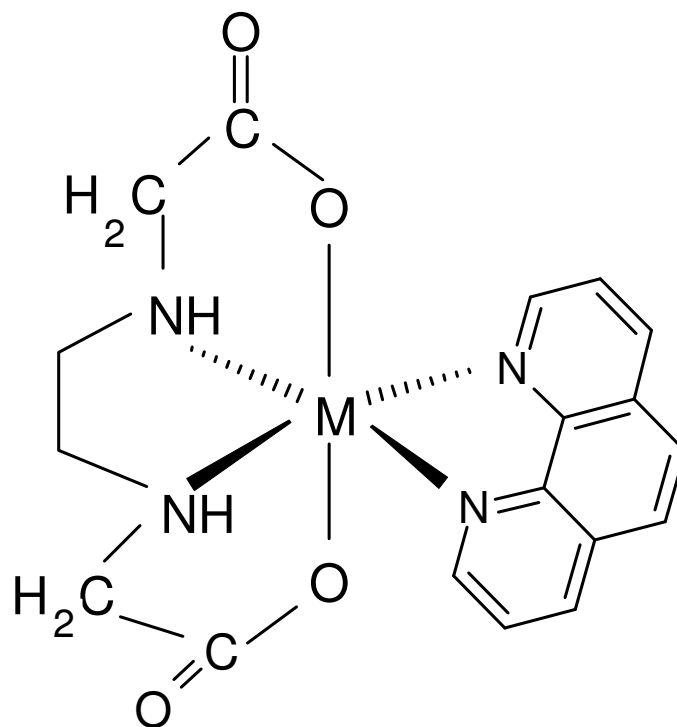
Figure 1.1: Structure of Ternary Transition Metal Complexes of 1,10-phenanthroline and *N,N'*-ethylenediaminediacetic acid. [M = Copper(II), Cobalt(II) and Zinc(II)].

CHAPTER 2.0

LITERATURE REVIEW

2.1   Cancer

All cancer originates from normal cells which are the body's basic units of life. Cancer is a group of diseases that cause cells in the body to change and grow out of control. Although there are many kinds of cancer, all of them start because of out-of-control growth of abnormal cells. The body is made up of hundreds of millions of living cells. Normal body cells grow, divide, and die in an orderly function. In the beginning stage of a person's life, normal cells divide more rapidly to allow the person to grow. After the person becomes an adult, most cells divide only to replace worn-out, damaged, or dying cells and to repair injuries. However, sometimes this orderly process goes wrong. Cancer cell growth is different from normal cell growth because cancer cells continue to grow and divide. Instead of dying, cancer cells keep on growing and form new cancer cells. Being able to grow out of control and invade other tissues is what makes cells cancerous. Cancer harms the body when damaged cells divide uncontrollably to form lumps and this extra cells form masses of tissue called tumors.

There are three biological properties that unify or characterize all cancers, *viz.* (namely), (i) they have uncontrolled growth; (ii) the capacity of

cancer cells to invade and destroy normal tissue, and (iii) the capacity of the primary tumor to break off seeds that spread to distant organs throughout the body (Toumi, 2010). Not all tumors are cancerous. There are two types of tumors which can be benign or malignant. Benign tumors are not cancerous. They usually grow slowly and can be removed; in most cases they do not come back. Cells in benign tumors are localized and do not spread to other parts of the body or invade and destroy nearby tissue. In contrast, malignant tumors are cancerous. This form of tumors can invade and damage tissues and organs near the tumor. Therefore, cells in these tumors can spread from one part of the body to another and this process itself is called metastasis. In most cases the cancer cells form a tumor. But some cancers, such as leukemia, do not form tumors. Instead, these cancer cells are in the blood and bone marrow (American Cancer Society, 2010). When cancer cells get into the bloodstream or lymph vessels, they can travel to other parts of the body. When a tumor starts to spread to other parts of the body and begins to grow, invading and destroying other healthy tissues and forming new tumors, it is said to have metastasized (McCutcheon, 2006). Consequently, this results in a severe condition that is very difficult to treat.

There are over 200 different types of cancer, and each is classified by the type of cell that is initially affected (Dangoor, 2011). Metastatic cells have the same cell type as the original or primary tumor from which it spread. No matter where a cancer may spread, it is always named after the place where it started. According to the American Cancer Society (2010), breast cancer, for example, that has spread to the liver is still called breast cancer, not liver

cancer. Different types of cancer can behave very differently. For example, lung cancer and breast cancer are very different diseases. They grow at different rates and respond to different treatments. That is why people with cancer need treatment that is aimed at their own kind of cancer (American Cancer Society, 2010).

Toumi (2010) has reported that cancer causes more deaths than AIDS, tuberculosis, and malaria combined. One in eight deaths worldwide is due to cancer. Based on the GLOBOCAN 2008 estimates, cancer has grabbed the lives of about 7.6 million people in the world which constitutes 2.8 million in economically developed countries and 4.8 million in economically developing countries (Center *et al.*, 2011; Jemal *et al.*, 2011). Hence, there are about 20,000 cancer deaths a day. Center *et al.* (2011) also reported that by 2030, the global burden is expected to grow to 21.4 million new cancer cases and 13.2 million cancer deaths due to the growth and aging of the population, and reductions in childhood mortality and deaths from infectious diseases in developing countries.

2.2   Breast Cancer

Despite the billions of dollars spent on breast cancer research, incidence rates have been climbing steadily in industrialized countries since the era of 1940s (Evans, 2006). Primary cause of death in women from cancer worldwide each year is cancer of the female breast, and it is the most common cancer in women in both developing and developed countries.

Breast cancer begins in breast tissue, which is made up of glands for milk production, called lobules, and the ducts that connect lobules to the nipple. The remainder of the breast is made up of fatty, connective, and lymphatic tissue. Most masses are benign; that is, they are not cancerous, do not grow out of control or invade and are not life-threatening. Some breast cancers are called *in situ* because they are confined within the ducts (ductal carcinoma *in situ*) or lobules (lobular carcinoma *in situ*) of the breast. Nearly all cancers at this stage can be cured. Many oncologists believe that lobular carcinoma *in situ* (lobular neoplasia) is not a true cancer but an indicator of increased risk for developing invasive cancer in the breast (Bandi *et al.*, 2009).

There are a few different types of lumps that can form in the breasts. But, only one of these types can be caused by breast cancer. It is called the malignant lump or tumor. It is developed from the cells of the breast and made up of abnormal breast cells which grow out of control and multiply (Figure 2.1). Each of these cells has an irregular shape and a pebbly surface which is comparable to the surface of a golf ball. The lump is very solid and hard like a raw of carrot slice. Most cancerous breast tumors are invasive. These cancers start in the lobules or ducts of the breast but have broken through the duct or glandular walls and begin to spread to the surrounding tissue of the breast. In order for malignant breast tumors to grow, they need to be fed. They form new blood vessels to get their nutrients and this process is known as angiogenesis. As the malignant breast tumor grows, it starts to spread into nearby tissue. This process is called invasion. Cells can also break away from the primary site and these tumors can spread to other parts of the body. The cells spread by traveling

through the blood stream and lymphatic system. This process is called metastasis. When malignant breast cells appear in a new location, they begin to multiply and grow out of control again as is growing in another part of the body; it is still called breast cancer. The most common locations of metastatic breast cancer are the lungs, liver, bones and brain (Komen, 2009). Specifically, a malignant tumor is a group of cancer cells that may invade surrounding tissue or metastasize to distant areas of the body. This property makes cancer so dangerous. A breast self examination may not be capable of finding out if the lump is moving as the normal healthy tissue around the lump also moves. A mammogram is best advised in order to get a proper diagnosis. A biopsy will provide even more information on the lump.

The seriousness of invasive breast cancer is strongly influenced by the stage of the disease; that is, the extent or spread of the cancer when it is first diagnosed. There are two main staging systems for cancer. The American Joint Committee on Cancer (AJCC) classification of tumors uses information on tumor size and how far it has spread within the breast and nearby organs (T), lymph node involvement (N), and the presence or absence of distant metastases (spread to distant organs) (M) (Bandi *et al.*, 2009). Once the T, N, and M are determined, a stage of I, II, III, or IV is assigned (Edge *et al.*, 2010). Stage I is an early stage of cancer and stage IV is the most advanced. Thus, the groups are classified with increasing severity of disease. The AJCC staging system is commonly used in clinical settings. A simpler system used for staging of cancer is known as the SEER Summary Stage system and is more commonly used in reporting to cancer registries and for public health research and planning.

Understanding of this system is as follows: (i) local-stage tumors are cancers confined to the breast; (ii) regional-stage tumors have spread to surrounding tissue or nearby lymph nodes; and (iii) distant-stage cancers have metastasized to distant organs (Bandi *et al.*, 2009).
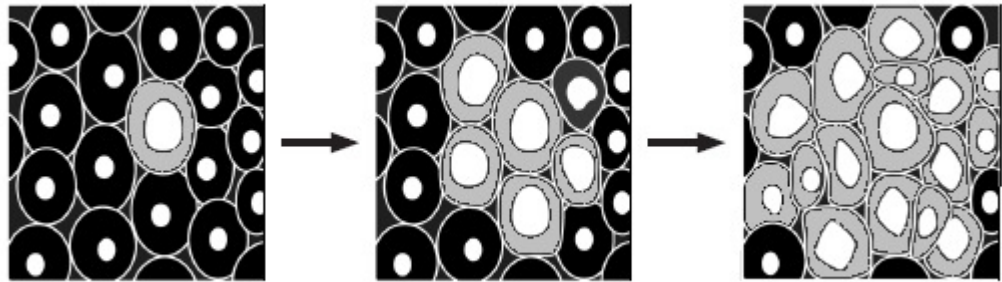
Figure 2.1: Diagram of Breast Cancer Malignant Growth. Black color circles represent normal healthy breast cells. Grey color circles represent malignant lump or tumor cells which spread to the surrounding tissue of the breast.

2.2.1   Overview of Breast Cancer in the World

Worldwide, breast cancer is the most frequently diagnosed cancer in women. An estimated 1.4 million new cases of invasive breast cancer were reported to occur among women in 2008. North America, Australia, and Northern and Western Europe have the highest incidence of breast cancer; intermediate levels are reported in Eastern Europe; and large parts of Africa and Asia have the lowest rates (Centre *et al.*, 2011).

An estimated 458,400 breast cancer deaths in women were reported in 2008 (Centre *et al.*, 2011). Breast cancer is the leading cause of cancer death among women worldwide. Low and middle income countries have historically

reported lower rates of breast cancer than high income countries. However, over the past twenty to thirty years, data gathered shows a trend of increasing incidence of breast cancer and death in lower income countries (Kamangar *et al.*, 2006; Igene, 2008). Porter (2009) reported that over million of new cases of breast cancer would be diagnosed worldwide in 2009; low and middle income countries would be burdened with 45% of breast cancer cases and 55% of breast cancer related deaths.

Increased in the incidence of breast cancer and increased in the burden of breast cancer deaths worldwide was also experienced by lower income countries. The causes of increasing incidence had been attributed to changes in the prevalence of reproductive risk factors, lifestyle changes, nutrition, physical inactivity and genetic and biological differences between ethnic and racial groups (Colditz *et al.*, 2006). Reported rates may reflect only the women who have the highest standard of living. Thus, current global figures cannot truly reflect the underlying economic and cultural diversity driving increased incidence and related mortality.

Breast cancer incidence is highest in the more-developed regions of the world, in urban populations, and in Caucasian women. In 2007, almost 45,700 women were diagnosed with breast cancer in United Kingdom (UK) with an estimated 125 women suffered from this disease a day. Besides, 277 men were also diagnosed with breast cancer in UK in 2007. The Globocan database for 2008 revealed that many African and Asian countries, including Uganda, South Korea, and India, incidence and mortality rates of breast cancer have been

rising. In general, incidence rates are high in Western and Northern Europe, Australia/New Zealand, and North America; intermediate in South America, the Caribbean, and Northern Africa; and low in sub-Saharan Africa and Asia (Figure 2.2) (Jemal *et al.*, 2011; Centre *et al.*, 2011).
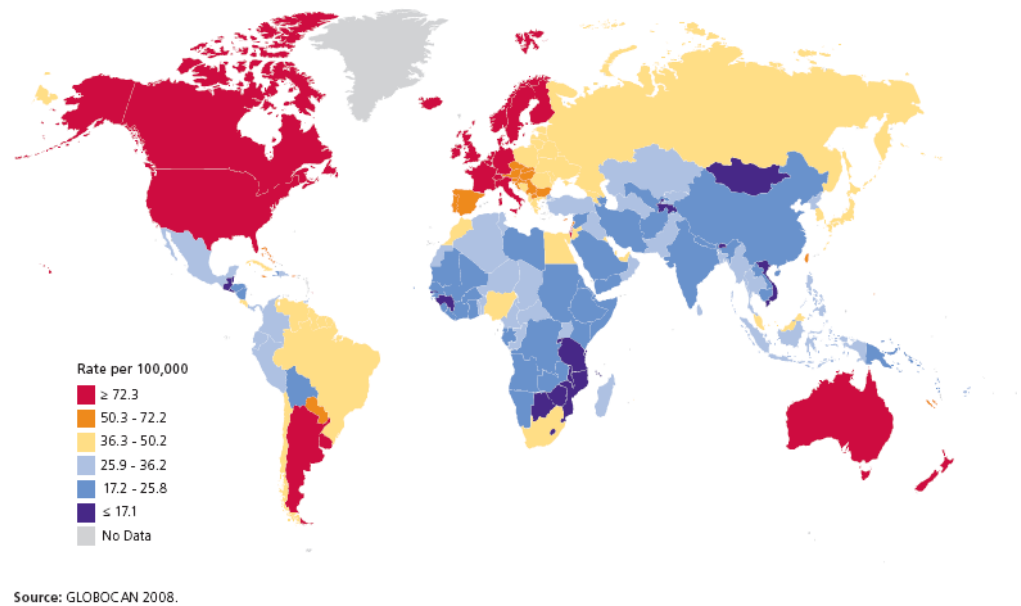
Source: Centre *et al.*, 2011.

Figure 2.2: International Variation in Age-standardized Breast Cancer Incidence Rates.

2.2.2 Incidence of Breast Cancer in Malaysia

In Malaysia, breast cancer is the main cause of cancer death in women which accounts for about 11% of all medically certified deaths (Narimah *et al.*, 1999). This disease has become increasingly important as a public health concern with the development and progress that has been achieved in this country.

Over the past several decades, the risk of breast cancer in developed countries has increased by one to two percent annually. While data for developing countries are limited, cancer registries stated that the increase in incidence is more noticeable in regions of the world which are particularly to be areas of low incidence such as the Asian continent and Africa (Sasco, 2001). Although it appears that the incidence of breast cancer in Malaysia is lower than in the developed countries, the difference may be related to the difficulties in getting accurate data and cancer patients under reporting of the cases (Hisham and Yip, 2003). Lim *et al.* (2008) have reported the cancer incidence cases from 2003 to 2005 and revealed that cancer is one of the major health problems in Malaysia. The most frequent cancer in Malaysians was breast cancer (18.0%) followed by large bowel cancer (11.9%) and lung cancer (7.4%) (Figure 2.3). Besides, breast cancer ranks first in incidence out of all cancers among females with 31.3%, followed by cancers of the cervix uterus (10.6%), large bowel (9.9%), ovary (4.3%), leukemia (3.7%) and lung (3.6%) (Figure 2.4).

Breast cancer was the commonest overall cancer as well as the commonest cancer in women amongst all races from the age of 20 years in Malaysia from year 2003 to 2005 (Table 2.1). Within a three-year period from 2003 to 2005, 11952 new cases were reported to the National Cancer Registry (Table 2.2). Breast cancer formed 31.3% of the total number of newly diagnosed cancer cases in women, with a similar percentage in each of the major ethnic groups: Malays (33.6%), Chinese (30.6%) and Indians (31.2%). The age-standardized rate for females was 47.4 per 100,000 women. In

comparison, there were 257 men with breast cancer, with an ASR of 1.2 per 100,000 men (Lim *et al.* 2008).

According to Lim *et al.* (2008), the incidence of breast cancer in Chinese women (ASR of 59.9 per 100,000) was higher than Malays (ASR of 34.9) and Indians (ASR of 54.2) (Table 2.2). Chinese women in Malaysia had a risk of 1 in 16 of getting breast cancer in their lifetime as compared to Indians (1 in 17) and Malays (1 in 28). The peak incidence of breast cancer occurred in the 50-60 years age group except in Indians where the incidence surged the peak after the age of 60 years old (Table 2.1). Local cancer centers have participated in multicentre trials such as those on novel anticancer drugs.

TheStar.com (2010) reported that the Universiti Sains Malaysia Hospital (HUSM) has recorded about 10 new advanced breast cancer patients entering their facilities each month, with five to six of them eventually passing away from the disease. The reasons for these unfortunate statistics are due to their traditional practices. The exact cause of breast cancer is unknown. Women with a family history of the disease have an increased risk of getting breast cancer. Carriers of the BRCA I and BRCA II genes, especially, have at least a 40 to 85 per cent risk of getting cancer (Grabrick *et al.*, 2000). Other risk factors include exposure to radiation, a history of benign breast lumps, obesity; diet especially one high in fat, early menarche (first menstrual bleeding) and late menopause (Wahid, 1999). The possibility that hormone replacement therapy causes breast cancer is still a topic of discussion. Most women in Malaysia present with a lump in the breast in over 90% of cases (Yip *et al.*,

2006). The lump is usually painless, grows slowly and may alter the contour or size of the breast. It may also cause skin changes, an inverted nipple or bloodstained nipple discharge. The lymph gland in the armpit will be swollen if affected by the cancer cells. In late stages, the growth may ulcerate through the skin and become infected. Bone pain, tenderness over the liver, severe headaches, shortness of breath and a chronic persistent cough may be an indication of the cancer spreading to the other organs in the body (Wahid, 1999).

Table 2.1: Female Breast Cancer Incidence in Age-specific per 100,000 Population, by Ethnicity in Peninsular Malaysia from 2003 to 2005.

Ethnic groups	Age groups							
	0-9	10-19	20-29	30-39	40-49	50-59	60-69	>70
All races	0.1	0.2	3.7	37.3	117.4	154.0	141.5	105.1
Malay	0.1	0.2	2.8	33.0	94.9	113.0	89.6	59.8
Chinese	0.1	0.1	3.7	40.4	149.7	194.0	188.8	140.5
Indian	0.0	0.4	4.7	29.6	100.1	174.0	200.0	202.9

Table 2.2: Female Breast Cancer Incidence per 100,000 Population and Age-standardized Incidence (ASR), by Ethnicity in Peninsular Malaysia from 2003 to 2005.

Ethnic groups	No.	%	CR	ASR
All races	11952	100.0	41.3	47.4
Malay	4969	41.6	27.7	34.9
Chinese	5051	42.3	66.1	59.9
Indian	1265	10.6	47.0	54.2

Figure of Ten Most Frequent Cancers in Peninsular Malaysia in 2003-2005

Type of cancers	Percentage of all cancers (%)
BREAST	18.0
LARGE BOWEL	11.9
LUNG	7.4
CERVIX UTERI	6
LEUKAEMIA	4.9
NASOPHARYNX	4.7
LYMPHOMA	4.6
STOMACH	3.5
PROSTATE GLAND	3.2
OTHER SKIN	2.6
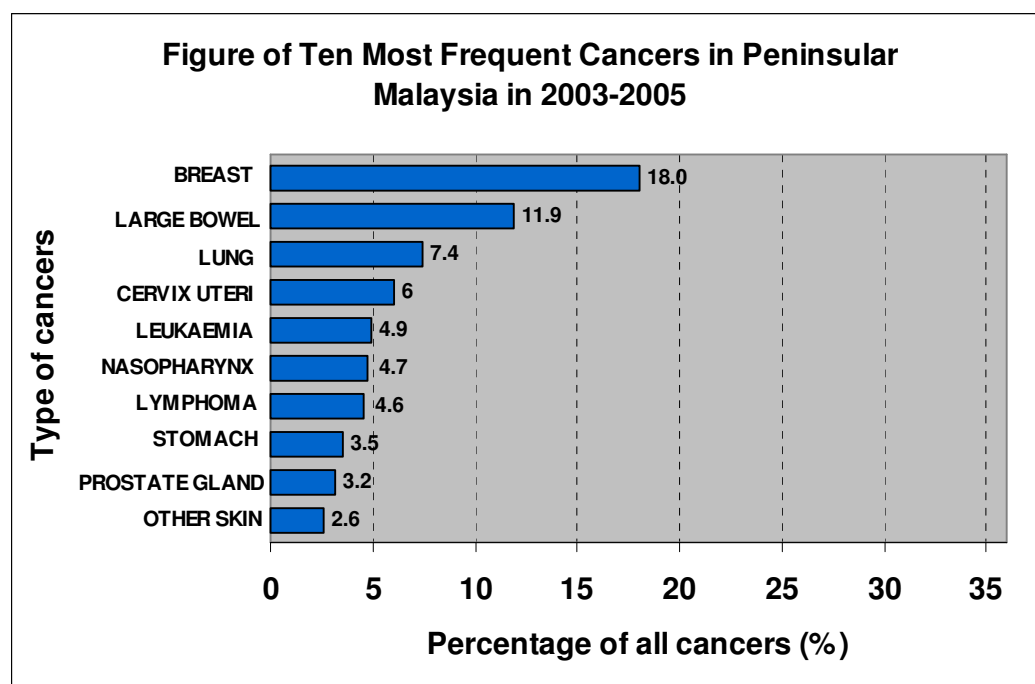
Figure 2.3: Ten Most Frequent Cancers in Peninsular Malaysia in 2003-2005.
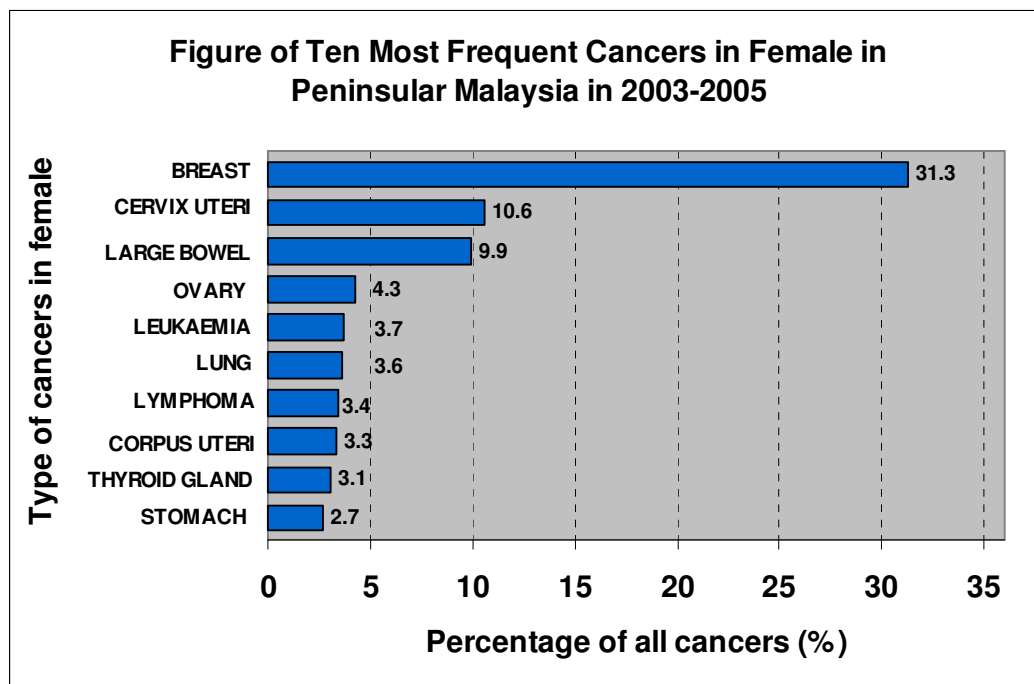
Figure 2.4: Ten Most Frequent Cancers in Females in Peninsular Malaysia in 2003-2005.

2.3   Transition Metal Complexes in Medicinal Chemistry

Transition metal complexes have been recognized as having beneficial and useful applications in medicinal biochemistry. Transition metal complexes show rich coordination chemistry, varying from tetrahedral to square planar and to octahedral. Transition metal complexes are cationic, neutral or anionic species in which a transition metal is coordinated by ligands. They can interact with a number of negatively charged molecules due to the different oxidation states they possess. This activity of transition metals has started the development of metal-based drugs with promising pharmacological application and may offer unique therapeutic opportunities.

Metal complex or coordination compound is a structure consisting of a central metal atom, bonded to a surrounding array of molecules or anions. Metal ions and metal coordination compounds are known to affect cellular processes in a dramatic way. This metal effect influences not only natural processes, such as cell division and gene expression, but also non-natural processes, such as toxicity, carcinogenicity, and antitumor chemistry (Reedijk, 2003).

Ligands that adequately bind metal ions and also have specific targeting features are gaining in popularity due to their ability to enhance the efficacy of less complicated metal-based agents. Ligands can be introduced into a system to limit the adverse effects of metal ion overload, inhibit selected metalloenzymes or facilitate metal ion redistribution. Some researchers mentioned that effects include modifying reactivity and lipophilicity, stabilizing specific oxidation states and contributing to substitution inertness. Multifunctional ligands for metal-based binding medicinal agents offer many possibilities and can play an integral role in muting the potential toxicity of a metallodrug to have a positive impact in the areas of diagnosis and therapy. Multifunctional ligands have found application at the forefront of all areas of medicinal inorganic chemistry (Storr *et al.*, 2006).

Medicinal inorganic chemistry can exploit the unique properties of metal ions for the design of new drugs. The discovery and development of the antitumor compound *cis*-diamminedichloroplatinum(II), cisplatin played a profound role in establishing the field of medicinal inorganic chemistry

(Jamieson and Lippard, 1999). Cisplatin has entered the clinical application and has developed into one of the most frequently used and most effective cytostatic drug for treatment of solid carcinomas (Köpf-Maier, 1994). Other metals like gallium, germanium, tin, bismuth, titanium, ruthenium, rhodium, iridium, molybdenum, copper, gold were shown to be effective against tumors in man and animals (Köpf-Maier, 1994).

With the advancement in the field of inorganic chemistry, the role of transition metal complexes as therapeutic compounds has become more and more noticeable. Research has shown significant progress in the use of transition metal complexes as drugs to treat several human diseases like carcinomas, lymphomas, infection control, anti-inflammatory, diabetes, and neurological disorders (Yasumatsu *et al.*, 2007; Harrison *et al.*, 1985; Pereira *et al.*, 2007; Chohan *et al.*, 2004). Development of transition metal complexes as drugs is not an easy task because considerable effort is required to get a compound of interest. The searching of ternary metal complexes, which are potentially important for the therapeutic application, is still slowly progressing. Development of new methodologies such as combinatorial chemistry will be helpful in the synthesis of inorganic compounds as therapeutic agents. New approaches are needed to investigate their biological activity so as to understand the reactions of metal complexes under physiological conditions, to improve the specificity of their interactions, and take into account of the potential toxicity of synthetic metal complexes which could add significantly to the current clinical research and practice.

The wide range of coordination numbers and geometries, accessible redox states, thermodynamic and kinetic characteristics, and the intrinsic properties of the cationic metal ion and ligand itself offer the medicinal chemist a wide spectrum of reactivities that can be used. Although metals have long been used for medicinal purposes in a more or less empirical fashion (Thompson and Orvig, 2006), the potential of metal-based anticancer agents has only been noticed and explored since the landmark discovery of the biological activity of cisplatin (Jung and Lippard, 2007). This classic anticancer drug remains one of the most effective chemotherapeutic agents in clinical use. However, the clinical use of cisplatin against solid tumor and haematological malignancies, including cancers of the gastrointestinal, renal, neurological even when administered at standard doses is severely limited by dose-limiting side effects such as visual-, neuro-, hepato-, oto- and nephrotoxicity (Chu *et al.*, 1993; Tsang *et al.*, 2009). In addition to the high systemic toxicity, inherent or acquired resistance is also a problem often associated with platinum-based drugs, which further limits their clinical use. Much effort has been devoted to the development of new platinum drugs and the elucidation of cellular responses to them to alleviate these limitations (Van Zutphen and Reedijk, 2005). These problems have also prompted chemists to develop alternative strategies based on different metals and aimed at different targets.

2.4   New Types of Drugs

Despite the fact that cisplatin is effective for several types of solid tumors, its use has been limited by toxic side effects and tumor resistance that often leads to the occurrence of secondary malignancies (Strumberg *et al.*, 2002). However, discovery and use of cisplatin have encouraged investigators or researchers to search for and develop novel non platinum-containing metal compounds with superior anticancer activity and low side effects.

A novel DNA-binding metal compound with antitumor activity and clinical efficacy must fulfill the requirements, *viz.* (*i*) good intrinsic properties, including saline solubility and enough stability to arrive intact at the cellular target; (*ii*) efficient transport properties in blood and through membranes; (*iii*) efficient DNA-binding properties but slow reactivity with proteins; (*iv*) the ability to differentiate between cancerous and normal cells; and (*v*) activity against tumors that are, or have become, resistant to cisplatin and derivatives. This latter requirement usually implies a structure that is distinct from cisplatin-type species (Reedijk, 2003).

Cancer research is still ongoing all over the world. Each time a new treatment makes it through all the stages of research and clinical trials, it will have a large number of published research papers about it. Most of the new treatments have been proven to stop or slow the growth of the cancer as well as to extend the lives of patient with some cancers. But amongst those papers, by comparing the treatment challenges, some of them showed that it did not work

26

better than the existing treatment. According to Smith (2011), United Kingdom National Institute for Health and Clinical Excellence did not believe that the evidence submitted by the drug's manufacturer, AstraZeneca proved that fulvestrant, which can be used to delay the growth of a particular type of advanced breast cancer, works significantly better than existing treatments, which are aromatase inhibitors for postmenopausal women who have oestrogen-receptor-positive, locally advanced or metastatic breast cancer, and who have already received anti-oestrogen therapy (e.g. tamoxifen), and so its widespread use would not be a good use of resources which also came at relatively high costs. Aromatase inhibitors and anti-oestrogens are types of drug used to treat breast cancer (Howell and Dowsett, 2004). Besides, a further concern that has emerged is that trastuzumab, when given in combination with other breast cancer drugs such as anthracylines and cyclophosphamide, may increase the risk of patients experiencing adverse heart effects (Keidan, 2007; Tan-Chiu *et al.*, 2005). Trastuzumab is effective in treating human epidermal growth factor receptor 2 (HER2)–positive breast cancer (Tan-Chiu *et al.*, 2005).

One of the most challenging problems is that many drugs' abilities and therapeutic effects are limited or otherwise reduced because of the partial degradation that occurs before they reach a desired target in the body. Drugs based on metallic compounds (gallium, germanium, tin and bismuth), early-transition metal complexes (titanium, vanadium, niobium, molybdenum and rhenium) and late-transition metal complexes (ruthenium, rhodium, iridium, platinum, copper and gold) have all shown some potential for chemotherapy (Köpf-Maier, 1994). Preclinical and clinical investigations showed that the

development of new metal agents with modes of action different from cisplatin is possible. Thus, complexes with iron, cobalt, or gold central atoms have shown promising results in preclinical studies and compounds with titanium, ruthenium, or gallium central atoms have already been evaluated in phase I and phase II clinical trials (Ott and Gust, 2007). However, their mechanisms of action are still unknown or not completely known.

Many researchers have discovered new metal-based drugs which were shown to have anticancer property. Titanium complexes such as titanocene dichloride had been recognized as active anticancer drug against breast and gastrointestinal carcinomas (Christodoulou *et al.*, 1998; O'Connor *et al.*, 2006). Gold complexes also showed anticancer activity and these complexes acted through a mechanism different from that of cisplatin (Au *et al.*, 2008). The target site of gold complexes was found to be mitochondria and not DNA. Rather, the cytotoxicity was mediated by their ability to slow down mitochondrial function and inhibit protein synthesis (McKeage *et al.*, 2002). Certain gold complexes with aromatic bipyridyl ligands have shown cytotoxicity against cancer cells (Marcon *et al.*, 2002). The 2-[(dimethylamino)methyl]phenyl gold(III) complex has also proven to be antitumor agent against various human cancers (Messori *et al.*, 2000). A lanthanum compound has also been used to treat various forms of cancer (Kapoor, 2009). Li *et al.* (2006) have reported that lanthanum(III) complexes containing 2-methylene–1,10-phen units bridged by aliphatic diamines exhibited good cytotoxic activities against HL-60 (human promyelocytic leukemia) cells, PC-3MIE8 (human prostate carcinoma) cells, BGC-823

(human stomach carcinoma) cells, MDA-MB-435 (human galactophore carcinoma) cells, Bel-7402 (human liver carcinoma) cells, and Hela (human cervix carcinoma) cells. Besides, Ansari *et al.* (2009) found that some complexes of manganese(III) induced tumor selective apoptosis of human cells. Many ruthenium complexes that were studied were found to be having antiproliferative effects on human ovarian cancers. Ruthenium complexes with oxidation state +2 or +3 show antitumor activity against metastatic cancers. Complexes of transition metal like iron have shown remarkable anti-proliferative properties (Lange *et al.*, 2008; Ray *et al.*, 2007; Sun *et al.*, 2007). Four oxovanadium(IV) complexes with 1,10-phen or 4,7-dimethyl-1,10-phen exhibited potent cytotoxic activity against human acute lymphoblastic leukemia cells, and their cytotoxic activity was modulated by the coordination environment (Dong *et al.*, 2007).

Cobalt, copper and zinc are transition metals which are generally regarded as nutritionally essential microelements for humans. They are involved in various regulatory processes, such as catalysis of biochemical reactions, especially redox reactions or reactions-involving oxygen. Examples are enzymes cytochrome oxidase containing copper ion, and DNA polymerase containing zinc ion (Aggett, 1985; Fraga, 2005; Raikwar *et al.*, 2008). Furthermore, late 3d transition metal ions, Co(II), Cu(II) and Zn(II), are classified as "borderline" between 'hard' (a-class) and 'soft' (b-class) metals regarding their metal-DNA interactions as they show more affinity for both the heterocyclic bases and the phosphate group in contrast to 'soft' (b-class) metals like Pt(II), and they have enhanced binding strength (Arjmand *et al.*, 2010).

Apart from being essential elements, they may be less toxic than non-essential metals such as platinum. The mechanisms by which organisms control metal ions and their role in cellular regulation has become an area of great scientific interest. These metals have been shown to be involved in cell-cell signaling, signal transduction, as well as, influencing transcription and translation *via* metal responsive regulators (Eide and Guerinot, 1997; Formigari *et al.*, 2008; Marzano *et al.*, 2009; Jungwirth *et al.*, 2011; McCann *et al.*, 2012). Among the metal complexes so far investigated, those of phen have attracted much attention for their various functions. Complexes of 1,10-phen have been shown to exhibit interesting clinical activities including antitumor, antibacterial, antifungal and antimicrobial activities (Barceló-Oliver *et al.*, 2007).

2.4.1   Copper Complexes as Anticancer Agents

The variety of metal ion functions in biology has stimulated the development of new metallodrugs other than platinum drugs with the aim to obtain compounds acting *via* alternative mechanism of action. Among non-platinum compounds, copper complexes are potentially attractive as anticancer agents (Marzano *et al.*, 2009).

For many years, researchers have actively investigated copper compounds based on the assumption that endogenous metals may be less toxic (Linder, 2001). Copper-chelating compounds have also shown promising results in both preclinical and clinical studies (Chen *et al.*, 2009; Yu *et al.*, 2006). It has been established that the properties of copper-coordinated

compounds are largely determined by the nature of ligands and donor atoms bound to the metal ion (Rajendiran *et al.*, 2007; Goodgame *et al.*, 1991; Chaviara *et al.*, 2005).

Copper is an essential trace element in all living organisms (Cabrera *et al.*, 2008). Copper becomes toxic in the case of excessive intracellular accumulation playing a role in apoptotic processes as well as initiating the generation of reactive oxidative species (ROS), such as superoxide ion (O_2^-), hydrogen peroxide (H_2O_2), and hydroxyl radical (•OH) (Dock and Vahter, 1999). Copper is readily absorbed from the diet through the small intestine and is usually excreted via bile through the gastrointestinal tract (Wapnir, 1998). The balance between the intracellular and extracellular content of copper is driven by cellular transport systems that regulate the uptake, export and intracellular compartmentalization (Harris, 1991).

Recently, many researchers have shown that copper(II), Cu(II) compounds have anticancer property and some examples include Cu(II)-doxorubicin chelate, [Cu(phen)(L-Thr)(H_2O)](ClO_4)] (L-Thr = L-threonine) and [Cu(4,7-dimethyl-1,10-phen)(glycinate)NO_3] or known as casiopeina II (Monti, 1990; Zhang *et al.*, 2004; De Vizcaya-Ruiz *et al.*, 2000). Cu(II) complexes of 1,10-phen-5,6-dione, [Cu(phendione)$_3$](ClO_4)$_2$]·$4H_2O$ showed a cytotoxic response 3 and 35 times greater than that observed for the metal-based anticancer agent, cisplatin, on two neoplastic (A-498 and Hep-G2) cell lines (Deegan *et al.*, 2006). Besides, *trans-bis*(salicylaldoximato)copper(II) showed cytotoxicity comparable to that of adriamycin by inducing cell cycle

arrest and apoptosis (Elo, 2004). In addition, the exposure of normal and tumor cells to the mixtures of ascorbate and copper chelates, especially Cu(II)-1,10-phen and Cu(II)-2,9-dimethyl-1,10-phen complexes, resulted in the killing of a large proportion of cancer cell population. These copper(II) chelates in combination with ascorbate showed different degrees of DNA-scission and antiproliferative activity (Chiou and Ohtsu, 1985). Tsang *et al.* (1996) have reported that incubation of a human hepatoma cell line (Hep-G2) with $[Cu(phen)_2]^{2+}$ resulted in internucleosomal DNA fragmentation, a hallmark of apoptosis. Additionally, other Cu(II) complexes of 1,10-phen was also shown to up-regulate DNA-binding activity of p53, a pivotal molecule in the regulation of cell progression, cell survival and apoptosis (Verhaegh *et al.*, 1997).

2.4.2 Cobalt Complexes as Anticancer Agents

Cobalt is recognized as an essential metal element widely distributed in the biological system such as cells and body, and the interaction of cobalt complex with DNA has attracted much attention (Vaidyanathan and Nair, 2003; Mozaffar *et al.*, 2004; Wang *et al.*, 2004). Besides, the antiproliferative activity of the cobalt complexes in MCF7 and MDA-MB-231 human breast cancer cells was determined previously and very promising results were obtained (Gust *et al.*, 2004; Schlenk *et al.*, 2008; Fu *et al.*, 2009). Cobalt(II), Co(II) metal ions have significant biomedical applications but are toxic at higher concentration. This element forms an essential part of Vitamin B12, a group of closely related polypyrrole compounds such as cyanocobalamin,

methylcobalamin and deoxyadenosyl cobalamin (Kobayashi and Shimizu, 1999; Banerjee and Ragsdale, 2003; Zhang *et al.*, 2009). Cobalt acts as catalyst in a variety of enzyme system functions and in coenzymes in several biochemical processes. In addition, cobalt is essential for the production of red blood cells. In this respect, its roles range from weak ionic enzymatic cofactors to highly specific substances known as metalloenzymes (Underwood, 1977; Pedada *et al.*, 2009). Recently, Co(II) complexes of new ligand 2-((2-((benzo[d]oxazol-2-yl)methoxy)phenoxy)methyl)benzoxazole and nitrate exhibited strong intercalation binding affinity and cytotoxicity against four different cancer cell lines (A549, Hep G2, K562, K562/ADM) (Jiang *et al.*, 2010). Besides, a new *bis*(N-benzyl-benzotriazole)dichloridocobalt(II) complex $(Co(bbt)_2Cl_2)$ could interact with DNA by electrostatic binding and also intercalation. Cobalt causes DNA strand breaks by its capacity to produce ROS known to be highly reactive against DNA and other biomolecules (De Boeck *et al.*, 2003). In addition, Co^{2+} ions, in the presence of ultraviolet (UV) radiation or oxidants such as hydrogen peroxide, can induce increased levels of DNA damage *in vitro* (De Boeck *et al.*, 1998).

2.4.3 Zinc Complexes as Anticancer Agents

Zinc is one of the essential trace elements. Zinc plays an essential role in DNA transcription and is required in a large number of enzymes involved in cell signaling, differentiation as well as in DNA binding of many nuclear regulatory elements (Kimura and Kikuta, 2000; Beyersmann and Haase, 2001). It impacts on key immunity mediators, enzymes, peptides, cytokines,

regulators lymphoid cell activation, proliferation and apoptosis. Reducing inflammatory cytokines reduces the risk of regrowth of the tumour after surgery (Franke *et al.*, 2005; Bowman *et al.*, 2006; Clark *et al.*, 2007). Besides, zinc is intimate to synthesis of DNA and an integral constituent of DNA polymerase, reverse transcriptase, RNA polymerase, tRNA synthetase, and the protein chain elongation factor (Tipton and Cook, 1963). Zinc is involved in RNA and DNA synthesis, and therefore cell division. In addition, zinc has been identified as a part of about 120 enzymes. Among them are carbonic anhydrase, carboxypeptidase, alkaline phosphatase, oxidoreductases, transferases, ligases, hydrolases, lyases, and isomerases (Vallee and Falchuk, 1981). These experimental findings about zinc and nucleic acids are interesting in view of the clinical observation that a number of functions dependent on protein synthesis are suppressed by zinc deficiency. These include growth, cellular immunity, longevity, fertility, hair growth, wound healing, and plasma protein levels (Khursheed, 2009). There is 2 – 3 g of zinc present in the human body (second to iron in body content) and about 1 mg/L in plasma.

Some researchers have focused on zinc levels in the body in people with cancer and other diseases (Halyard *et al.*, 2007). Cancer cells must fight to establish survival. They can only manifest if the environment allows. Therefore, the nutritional approach to cancer prevention is to provide an environment hostile to malignant cells. One way to do this is to improve general immunity using nutrients such as zinc (Kristal *et al.*, 1999; Meyer *et al.*, 2005). The higher the zinc status before chemotherapy treatment leads to higher chance of remission (absence of disease activity in patients with a

chronic illness) (Sprenger *et al.*, 1983). Zinc supplementation may improve the clinical course of general conditions in cancer patients.

Interestingly, Zn^{2+} is also a strong inducer of oxidative stress. In neurons, Zn^{2+} can trigger ROS production through mitochondrial pathways by interfering with the activity of the electron transport chain (ETC) (Brown *et al.*, 2000; Sensi *et al.*, 2000). Zn^{2+} can also modulate extra-mitochondrial pathways involved in ROS generation by promoting the increased activity of NADPH oxidase, protein kinase C (PKC) activation, as well as induction of neuronal nitric oxide synthase (nNOS) which together with superoxide can produce harmful peroxynitrite ($ONOO^-$) (Zou *et al.*, 2002; Korichneva, 2005; Chen *et al.*, 2010). One of the major targets of ROS-dependent Zn^{2+} release involves the metallothioneins (Frazzini *et al.*, 2006; Valko *et al.*, 2007). In a recent study of human hsp72 and hsp70B' induction in colon cell lines by $ZnCl_2$, several cell-specific effects were found, indicating a potentially useful selectivity in human cellular responses to zinc ions (Noonan *et al.*, 2007). Besides, water soluble zinc ionophore 1-hydroxypyridine-2-thione (ZnHPT) can increase the intracellular concentrations of free zinc and to produce an antiproliferative activity in exponential phase A549 human lung cancer cultures and with no observable toxicity *in vivo* (Magda *et al.*, 2008). Moreover, [Zn(3-Me-pic)$_2$(phen)]·5H$_2$O can inhibit topo I efficiently and is cytotoxic against MCF7 cell line (Seng *et al.*, 2008). A ternary zinc(II) complex of 1,10-phen and edda binds to duplex oligonucleotide ds(AT)$_6$ more selectively than ds(CG)$_6$ and efficiently kills MCF7 breast cancer cells by inducing cell cycle arrest (Ng *et al.*, 2008).

2.5   Apoptosis (Programmed cell death)

Apoptosis is a naturally occurring process by which a cell is directed to programmed cell death. Kerr *et al.* (1972) were the first to provide evidence that cell may undergo at least two distinct types of cell death. The first type of cell death is known as necrosis, while another type is known as apoptosis (Figure 2.5).

Necrosis is referred to as accidental cell death which can occur in a matter of second, caused by physical or chemical damage and considered a "cell murder" process, i.e. severe chemical and mechanical injury. Necrosis is characterized by cytoplasm swelling, destruction of organelles and disruption of the plasma membrane, leading to the release of intracellular contents and inflammation (Collins *et al.*, 1997). Unlike necrosis, apoptosis produces apoptotic bodies that attract phagocytes to engulf and quickly remove them before the contents of the cell leak onto surrounding cells and cause damage. Apoptosis is a much slower series of events than necrosis, requiring from a few hours to several days, depending on the initiator (Willingham, 1999).
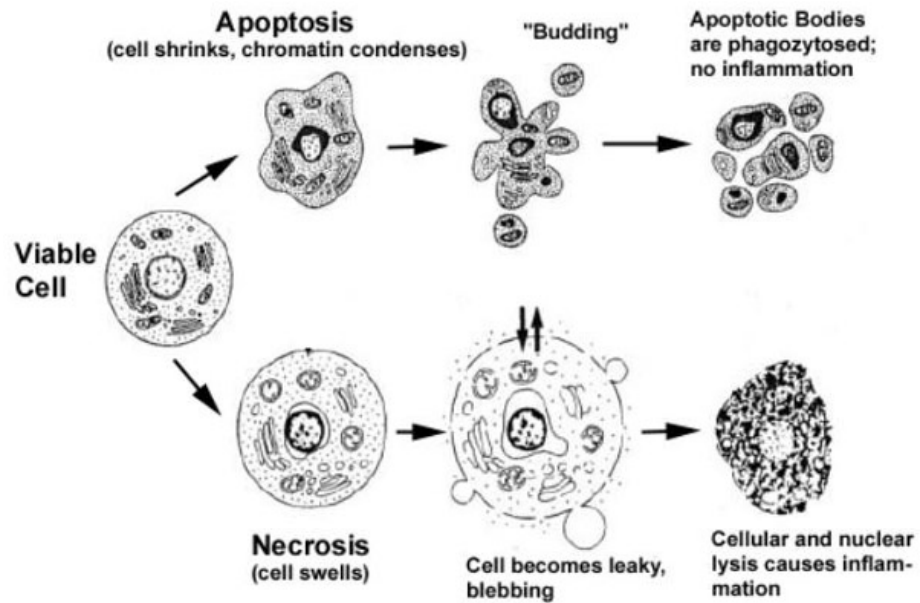
Figure 2.5: Hallmarks of the Apoptotic and Necrotic Cell Death Process.
Apoptosis includes cellular shrinking, chromatin condensation and margination
at the nuclear periphery with the eventual formation of membrane-bound
apoptotic bodies that contain organelles, cytosol and nuclear fragments and are
phagocytosed without triggering inflammatory processes. The necrotic cell
swells, becomes leaky and finally is disrupted and releases its contents into the
surrounding tissue resulting in inflammation.

2.5.1   Morphological Evidence of Apoptosis

Apoptosis involves cell shrinkage, blebbing of the plasma membrane,
chromatin condensation, echinoid spike formation, surface blister formation
and DNA degradation (Figure 2.6) (Elmore, 2007; Willingham, 1999). The
plasma membrane retains their integrity for a quite long period and is usually
surrounded by healthy neighboring cells. *In vitro*, apoptotic cells are ultimately
fragmented into multi membrane-enclosed spherical apoptotic bodies. *In vivo*,
apoptotic bodies are usually not seen as the apoptotic cells are scavenged by
phagocytes (Bizik *et al.*, 2004). Phagocytes can not only recognize and ingest

all the membrane-bound products of apoptosis and substantially intact apoptotic cells but also apoptotic bodies detaching during blebbing and zeiosis of the dying cell (Wylhe *et al.*, 1980). Morphological features of apoptosis may reflect macrophage recognition, ingestion and degradation of dying cells before chromatin condensation takes place (Mower *et al.*, 1994).

The first stage that can be observed in this apoptosis analysis was that cells treated with the compounds became rounded and this occurred because the protein structures that formed the cytoskeleton were digested by specialized peptidases that were activated inside the cell. In the second stage, the chromatin (DNA and its packaging proteins in the cell nucleus) should undergo initial degradation and condensation. Chromatin then underwent further condensation into compact patches against the nuclear envelope (Santos *et al.*, 2000). At this stage, the double membrane that surrounds the nucleus should still appear complete. However, Kihlmark *et al.* (2001) reported that specialized peptidases had already advanced in the degradation of nuclear pore proteins and had begun to degrade the lamin that underlies the nuclear envelope. It must be noted, also, that, while the previous stage of initial chromatin condensation had been observed in non-apoptotic forms of programmed cell death, this advanced stage called pyknosis is considered a hallmark of apoptosis. In addition, the nuclear envelope would become discontinuous and the DNA inside underwent fragmentation (a process referred to as karyorrhexis). The nucleus would break into several discrete chromatin bodies or nucleosomal units due to the degradation of DNA (Nagata, 2000). In the next stage, the cell membrane would show irregular buds and then

occurrence of blebbings. Apoptosis would then proceed to a subsequent stage after a long interval of surface blebbing. This third stage should be characterized by the frequent protrusion of surface microspikes or echinoid protrusions (Majno and Joris, 1995). After the final extension of these echinoid protrusions, the cells would show complete cessation of all active movement (Collins *et al.*, 1997). Permeability of the cell surface happened only when cells that had undergone the terminal blistering event. After this immobile stage, the cells would begin to show surface blisters that gradually expanded (Noureini and Wink, 2009). The cell then broke apart into several vesicles called apoptotic bodies, which would then be phagocytosed. Dying cells that underwent the final stages of apoptosis would display phagocytotic molecules, such as phosphatidylserine on their cell surface (Li *et al.*, 2003). The biochemical and morphological events that affect programmed cell death usually lead to a unique and highly controlled series of events (Figure 2.7) known as apoptosis (Kerr *et al.*, 1972).

| Normal | Blebs | Spikes | Blisters |
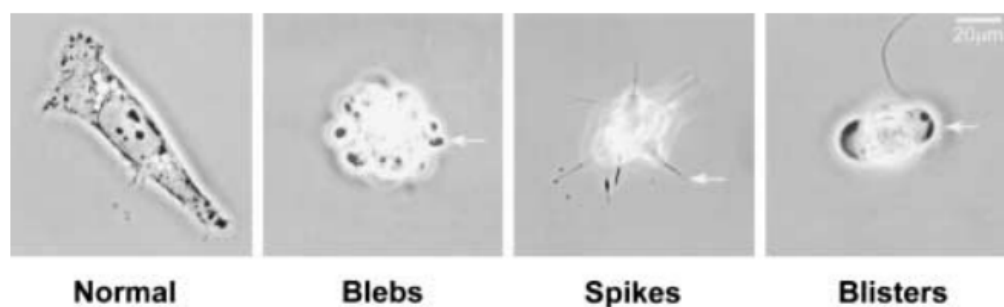
Figure 2.6: Surface Morphological Features of Apoptotic Cells in Culture. These images demonstrate the hallmark sequential features (arrows) of apoptotic cells detected by phase contrast microscopy, including blebs, echinoid spikes, and surface blisters. These images were generated using KB human carcinoma cells induced to go into apoptosis using ricin (Willingham, 1999).

Morphologic Features in Apoptosis
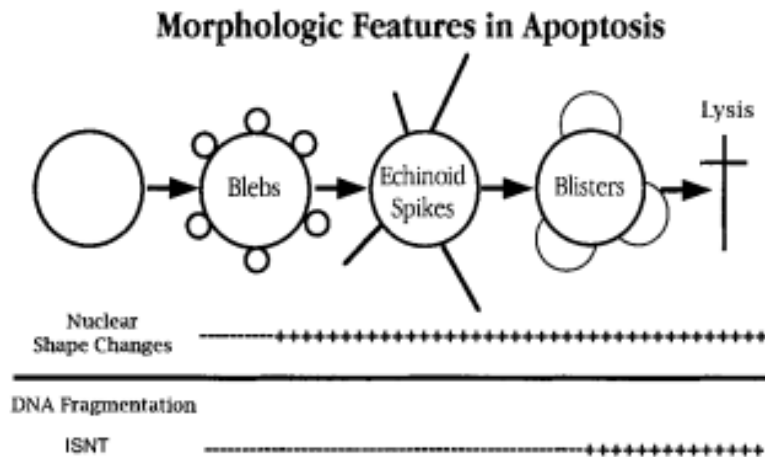
Source: Collins *et al.*, 1997.

Figure 2.7: Schematic Summary of the Surface Morphological, Nuclear Shape and Major DNA Fragmentation Events during Apoptosis.

2.5.2 Annexin V

A critical stage of apoptosis involves the acquisition of surface changes. In normal healthy cell, phosphatidylserine (PS) is located mainly in the internal layer of the cell membrane and has a variety of unique structural and regulatory functions. One of these plasma membrane alterations during apoptosis is the translocation of PS from the inner side of the plasma membrane to the outer layer, i.e. PS becomes exposed at the external surface of the cell. The PS exposure may represent a hallmark in detecting dying cells (Fink and Cookson, 2005). The Annexin V, with anticoagulant properties has proven to be a useful tool in detecting apoptotic cell due to its ability to preferentially bind negatively charged phospholipid-like PS. By conjugating fluorescein isothiocyanate (FITC) to Annexin V, it is possible to identify and quantitate apoptotic cells on a single-cell basis by flow cytometer.

Propidium iodide (PI) is widely used in conjunction with Annexin V to determine if cells are viable, apoptotic, or necrotic through differences in plasma membrane integrity and permeability (Hingorani *et al.*, 2011; Rieger *et al.*, 2011). The Annexin V/PI protocol is a commonly used approach for studying apoptotic cells. PI is used more often than other nuclear stains because it is economical, stable and a good indicator of cell viability, based on its inability to stain living viable or early apoptotic cells due to the presence of an intact plasma membrane (Rieger *et al.*, 2011). In late apoptotic and necrotic cells, the integrity of the plasma and nuclear membranes decreases, allowing PI to pass through the membranes and intercalate into nucleic acids (Darzynkiewicz *et al.*, 1992; Rieger *et al.*, 2011).

In the Annexin V-FITC/PI assay, FITC-labelled Annexin V (green fluorescence) binding was assessed in cell staining together with dye exclusion of PI (red fluorescence). The test described in dot-plot quadrants representing populations of healthy intact cells (Annexin V-FITC$^-$/PI$^-$) are in the lower left quadrant, early apoptotic cells (Annexin V-FITC$^+$/PI$^-$) are in the lower right quadrant, late apoptotic cells (Annexin V-FITC$^+$/PI$^+$) are in the upper right quadrant and necrotic cells (Annexin V-FITC$^-$/PI$^+$) are in the upper left quadrant (Figure 2.8). The Annexin V-FITC/PI assay offers the possibility of detecting early phases of apoptosis before the loss of cell membrane integrity and permits measurement of the kinetics of apoptotic death in relation to the cell cycle.
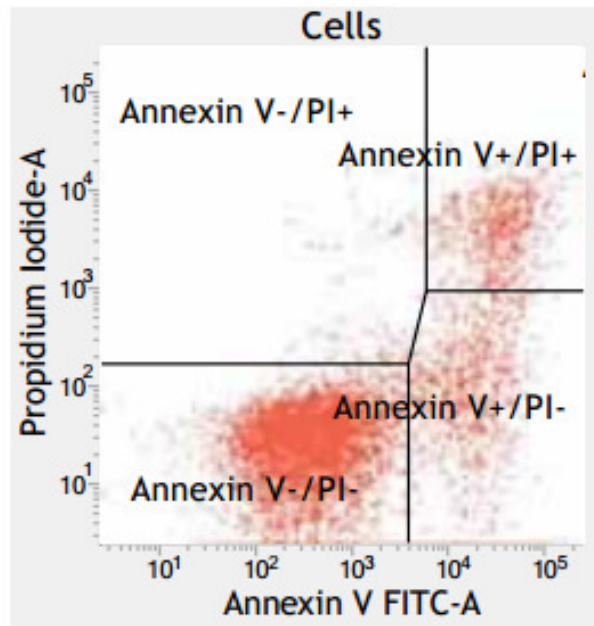
Source: Hingorani *et al.*, 2011.

Figure 2.8: Flow Cytometric Analysis of Apoptotic Cells Stained with Annexin V-FITC and Propidium Iodide. Jurkat cells were treated with 5 µm of camptothecin for 4 h followed by staining with Annexin V-FITC and propidium iodide (PI). Staining with PI differentiates necrotic or late apoptotic cells. PI stained cells are easily distinguished from the early apoptotic population (Annexin V-FITC^{+}/PI^{-}) located at the lower quadrant of the dot plot.

2.5.3 Molecular Mechanism of Apoptosis

There are three different mechanisms by which cells die by apoptosis, *viz.* (i) apoptosis triggered by internal signals; the intrinsic or mitochondrial-mediated pathway, (ii) apoptosis triggered by external signals; the extrinsic or death-receptor pathway, and (iii) apoptosis inducing factor (AIF) that may be triggered by dangerous reactive oxygen species (Susin *et al*, 1999; Kroemer *et al.*, 2007; Rastogi *et al.*, 2009).

The intrinsic signaling pathways that initiate apoptosis produce intracellular signals that act directly on targets within the cell and are mitochondrial initiated events. All of these stimuli cause changes in the inner mitochondrial membrane that result in an opening of the mitochondrial permeability transition pore. The released cytochrome c then binds to the protein apoptotic protease activating factor-1 (Apaf-1). Using the energy provided by ATP, these complexes aggregate to form apoptosomes. The apoptosomes will then bind to and activate caspase-9. Eventually, caspase-9 activates other caspases (caspase-3 and -7) creating an expanding cascade of proteolytic activity which leads to digestion of structural proteins in the cytoplasm, degradation of chromosomal DNA, and phagocytosis of the cell (Kroemer, 1999). Besides the release of cytochrome c from the intramembrane space, the intramembrane content released also contains AIF to facilitate DNA fragmentation through its migration into the nucleus and binding to DNA, which triggers the destruction of the DNA and cell death (Kroemer, 1999; Kroemer *et al.*, 2007). Therefore, AIF is involved in initiating caspase-independent pathway that can facilitate the completion of apoptosis following transfer into nuclei. Fas and the tumor necrosis factor (TNF) receptor are integral membrane proteins with their receptor domains exposed at the surface of the cell. The extrinsic pathway is activated at the cell surface when a specific ligand binds to its corresponding cell surface death receptor and activates caspase-8 (Locksley *et al.*, 2001). Caspase 8 acts similarly like caspase 9, initiates a cascade of caspase activation leading to phagocytosis of the cell. One method by which cytotoxic T cells bind to their target triggers them to produce more Fas ligands (FasL) at their surface (Elmore, 2007). They will

then bind with the Fas on the surface of the target cell leading to its death by apoptosis (Rastogi *et al.*, 2009; Elmore, 2007).

2.6 Mitochondrial Fluorescent Intensity with JC-1 staining

The membrane-permeant JC-1 dye is widely used in apoptosis studies to monitor mitochondrial health. JC-1 dye exhibits potential-dependent accumulation in mitochondria, indicated by a fluorescence emission shift in emitted light from 527 nm (*i.e.*, emission of JC-1 green fluorescent monomeric form) to 590 nm (*i.e.*, emission of red fluorescent J-aggregate) when excited at 490 nm (Hada *et al.*, 1977; Reers *et al.*, 1991). Consequently, mitochondrial depolarization is indicated by a decrease in the red/green fluorescence intensity ratio. The ratio of green to red fluorescence depends only on the membrane potential and not on other factors such as mitochondrial size, shape, and density, which may influence single-component fluorescence signals (Salido *et al.*, 2007). Both colors can be detected using the filters commonly mounted in all flow cytometers, so that green emission can be analyzed in fluorescence FL-1 channel (*x-axis*) and reddish orange emission in FL-2 channel (*y-axis*). Therefore, a careful analysis of the fluorescence ratio detected will allow researchers to make comparative measurements of membrane potential and determine the percentage of mitochondria within a population that responds to an applied stimulus (Salido *et al.*, 2007).

Energy released during the oxidation reactions in the mitochondrial respiratory chain is stored as a negative electrochemical gradient across the

mitochondrial membrane and membrane is said to be polarized (Lemasters and Ramshesh, 2007). Healthy cells which contain mitochondria that are maintaining a normal proton and pH gradient across the inner mitochondrial membrane will continue to concentrate the JC-1 dye forming J-aggregates and exhibit the classic reddish orange fluorescence (Cossarizza, 1993; Cossarizza, 2000). Obviously, JC-1 worked by migration of cationic molecules into the negative sites in the mitochondria, and it is released when the $\Delta\psi_m$ changes. In this case, JC-1 is fluorescent and the reddish orange signal decreases when the $\Delta\psi_m$ is lost (Figure 2.9). In apoptotic cells, the $\Delta\psi_m$ collapses, and the JC-1 cannot accumulate within the mitochondria. In this case, JC-1 remains in the cytoplasm in a green fluorescent monomeric form. Apoptotic cells show primarily green fluorescence and are easily differentiated from healthy cells which show red and green fluorescence. The change of the $\Delta\psi_m$ is calculated by fluorescent ratio intensity value which reflects the function of mitochondria (Cossarizza, 2000).
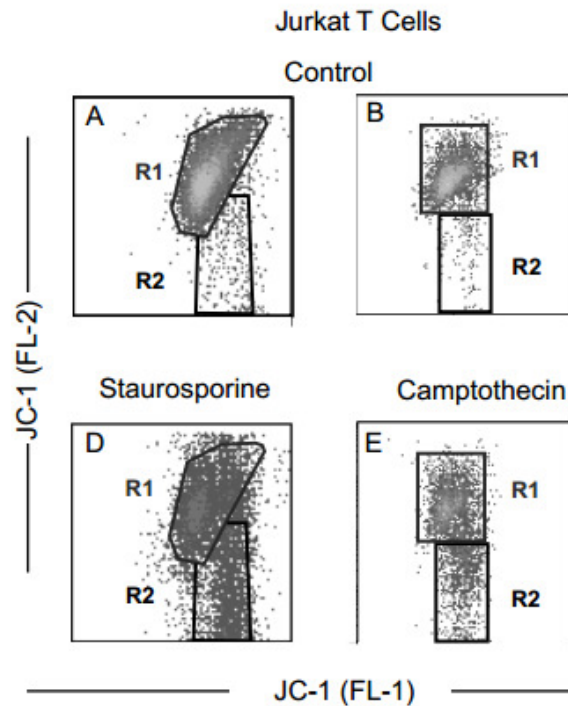
Jurkat T Cells

Figure 2.9: JC-1 Staining in Control and Apoptotic Cells. Cells (1×10^6 cells/ml) were left untreated (vehicle only, A, B) or treated with staurosporine (1µm, 4 h), camptothecin (4 µm, 4 h) to induce apoptosis (D, E). JC-1 fluorescence is seen in both the FL-2 and FL-1 channels (R1) in the control (untreated) cell populations. A dot plot of red fluorescence (FL-2 channel) versus green fluorescence (FL-1 channel) resolved healthy cells with intact mitochondrial membrane potential ($\Delta\psi_m$) from apoptotic and dead cells with lost $\Delta\psi_m$. JC-1 that fluoresces in the FL-1 channel and lacks fluorescence in the FL-2 channel is considered to correspond to mitochondria with a depolarized $\Delta\psi_m$. Thus, the data indicates that apoptosis induction was associated with depolarization of the $\Delta\psi_m$.

2.7 Cell Cycle Regulation

The cell cycle is at the center of the decisions make by a cell. Dividing cells go through a cycle consisting of, G_1 (growth or gap), S (DNA synthesis), G_2 (growth) and M phase (mitosis) (Pucci *et al.*, 2000). Specific events must happen in a particular sequence for the cell to replicate. During the G_1 phase, the cell integrates mitogenic and growth inhibitory signals and makes the

decision to proceed, or exit the cell cycle. S phase is defined as the stage in which DNA synthesis occurs. G_2 is the second gap phase during which the cell prepares for the cell to undergo division. M stands for mitosis, the phase in which the replicated chromosomes are segregated into separate nuclei and cytokinesis occurs to form two daughter cells. Taken together, G_1, S, and G_2 make up interphase. In addition, the term G_0 is used to describe cells that have exited the cell cycle and become quiescent. When cells differentiate, they usually stop dividing and therefore exit the cell cycle. Most cells that stop dividing to differentiate do so in the G_1 phase although some arrest in G_2 (Li and Brooks, 1999; Pucci *et al.*, 2000; Vermeulen *et al.*, 2003).

Overall, the cell cycle is tightly regulated, and is dependent on a cell's life history and its differentiated state. The cell cycle is controlled at several checkpoints, called checkpoint control. One is at the G_2/M transition, and another one in late G_0/G_1 phase before it enters into S phase. The control involves physical interaction between two classes of proteins, *viz.* (i) protein kinases which are specifically cyclin-dependent kinases (CDK), and (ii) cyclins (MacLachlan *et al.*, 1995; Li and Brooks, 1999).

The D-type cyclins are the first cyclins to be induced as G_0 cells are stimulated to enter the cell cycle (Sherr, 1994). Cyclin D1 is over expressed in some primary tumors and tumor cell lines (Matsushime *et al.*, 1991; Enoch and Nurse, 1990). In several animal model systems, deregulated expression of cyclin D1 has been shown to directly contribute to tumorigenesis (Wang *et al.*, 1994). Cyclin D1 gene amplification also occurs in a subset of breast,

esophageal, bladder, lung, and squamous cell carcinomas (Lovec *et al.*, 1994). Cyclin E is the next cyclin to be induced during the progression of cells through G_0/G_1. Cyclin E associates with Cdk2, and this kinase complex is required for cells to make the transition from G_0/G_1 into S phase (Ohtsubo *et al.*, 1995). Cyclin A, which accumulates at the G_1/S phase transition and persists through S phase. Cyclin A initially associates with Cdk2 and then, in late S phase, associates with Cdk1. Cyclin A-associated kinase activity is required for entry into S phase, completion of S phase, and entry into G_2/M phase. Cyclin A colocalizes with sites of DNA replication, suggesting that cyclin A may actively participate in DNA synthesis or perhaps play a role in preventing excess DNA replication (Johnson and Walker, 1999).

2.8 Drug-like Properties

Lipinski's Rule of Five states that the absorption or permeation of a drug that is not a substrate for a biological transporter is likely to be impaired when it has these properties, *viz.* (i) log P (P = Partition Coefficient) > 5; (ii) molecular weight > 500; (iii) number of hydrogen donor groups > 5; and (iv) number of hydrogen acceptor groups > 10 (Lipinski *et al.*, 2001). The critical drug-like properties can be illuminated by examining the fate of an orally administered drug. During drug development, one needs to select drug candidates with the most appropriate drug-like properties (Li, 2005). Early evaluation of chemical structure and determination of partition coefficient are therefore recommended to allow one to select drug candidates that would be more 'drug-like' as suggested by the Rule of Five.

The next stage in drug design is likely to be the development of dedicated drugs that comprise the transport (through the membranes), survival in the cell, binding to the DNA or possibly other targets, and eventually excretion from the body with minimum side effects.

2.9   Human Topoisomerase I

Human topoisomerase I (topo I) is the intracellular target of important anticancer drugs such as camptothecin and other topo I inhibitors; some of which are among the most promising anticancer drugs ever identified (Rothenberg, 1997; Pommier, 2006; Beretta *et al.*, 2008). Topo I initiates cleavage of single-strand in DNA and passes the other strand through the cleavage site before resealing the break. The reaction between double-stranded DNA and topo I produces a covalent 3'-phosphorotyrosyl adduct, usually referred to as the cleavable complex. Under physiological conditions, the DNA cleavage and ligation reactions catalyzed by the enzyme are tightly coordinated and the covalent intermediate is barely detectable. The cleavage is coupled with the religation to restore continuity to the DNA duplex (Beretta *et al.*, 2008). Camptothecin can convert topo I into a cell poison by blocking the religation step, thereby enhancing the formation of persistent DNA breaks responsible for cell death. Laboratory studies have indicated that cells responsive to topo I-targeted drugs have elevated levels of topo I, interrupting DNA replication, and may require a functional apoptotic pathway (Rothenberg, 1997; Coleman *et al.*, 2002). Therefore, a compound that potentially responds to topo I may be a good agent for anticancer therapy.

CHAPTER 3.0

MATERIALS AND METHODS

3.1   Synthesis and Characterization

The [M(phen)(edda)] complexes, which were given to me for my research, were prepared and characterized by others. The ternary complexes were prepared either by first reacting freshly prepared metal hydroxide with *N*,*N'*-ethylenediaminediacetic acid (H_2edda) and then finally by adding a methanolic or ethanolic aqueous solution of 1,10-phenanthroline (phen) or by an *in situ* method where the sequence of added reactants is H_2edda, NaOH, metal(II) salt and alcoholic aqueous phen (Ng *et al.*, 2008; Seng *et al.*, 2008; Von *et al.*, 2011). The ternary metal(II) complexes of the edda and phen precipitated out on the same day or upon slow evaporation of the solution mixtures. Slow evaporation of the respective resultant solutions yielded orange crystalline needles for [Co(phen)(edda)]·$3H_2O$, blue crystalline needles for [Cu(phen)(edda)]·$5H_2O$ and colourless crystalline needles for [Zn(phen)(edda)]·$3^1/_2H_2O$ which were suitable for X-ray crystal structure determination. The full characterization by various physical means had been reported. These complexes are neutral and octahedral in structure.

3.2   Cell Culture and Reagents

MCF7 breast carcinoma cells were purchased from ATCC (no. HTB-22). MCF10A breast epithelial cells were generously provided by Dr. Alan Khoo Soo Beng (IMR, Malaysia). MCF7 cells were cultured in Roswell Park Memorial Institute (RPMI) 1640 medium (Sigma-Aldrich, Germany) supplemented with 10% Fetal Bovine Serum (FBS) (Sigma-Aldrich, Germany) and subcultured using Trypsin-ethylenediaminetetraacetic acid (EDTA) (0.25%) solution (Sigma-Aldrich, Germany). MCF10A cells were cultured in Dulbecco's Modified Eagle Medium (DMEM) (GIBCO®, USA) supplemented with F12 nutrient mixture (GIBCO®, USA), 100 µg of water-soluble hydrocortisone (Sigma-Aldrich, Germany), Epidermal growth factor, recombinant human (Invitrogen, USA), Minimum Essential Medium with Non-Essential Amino Acids (MEM NEAA) (GIBCO®, USA), horse serum donor herd (GIBCO®, USA), insulin (Sigma-Aldrich, Germany), L-glutamine (GIBCO®, USA) and penicillin/streptomycin (GIBCO®, USA). MCF10A was similarly subcultured using Trypsin-EDTA (0.05%) solution (Mediatech, Germany).

All cell lines were maintained in the CO_2 water-jacketed incubator (NuAire Inc., USA) with an atmosphere of 5% CO_2 at 37 ^oC. On the next day after subculture, the medium was removed and supplemented with fresh medium containing serum as described earlier. After cell growth reached 70% confluence (achieved 3 - 4 days after subculture) with a change in the culture medium on alternate days, the cultures were trypsinized and passaged. One

51

portion of the cells was frozen and the remaining cells were seeded in 75 cm^2 tissue culture flasks (Nunc, Denmark) to grow for the subsequent test. [Co(phen)(edda)], [Cu(phen)(edda)] and [Zn(phen)(edda)] were synthesized and supplied by Dr. Ng Chew Hee and others (UTAR, Malaysia). This thesis is only investigates the anticancer activity and the mode of action of [Co(phen)(edda)], [Cu(phen)(edda)] and [Zn(phen)(edda)]. Each of the metal complexes was dissolved in deionized distilled water and diluted into culture media at the concentration indicated according to IC$_{50}$ value. All solutions were freshly prepared.

3.3   Cytotoxicity Assay

3.3.1   Experimental Set Up

Cells were plated at 2.5×10^5 cells/ml for MCF7 cells and at 2.5×10^5 cells/ml for MCF10A cells in 100 µl per well in 96-well micro titer plates (Orange Scientific, Belgium) and allowed to recover for 24 h. Then, the cells were incubated with or without metal complexes at 37 ^{o}C for 24, 48 and 72 h as different sets. Briefly, the cells were treated with increasing concentration of concentration of [Co(phen)(edda)], [Cu(phen)(edda)] and [Zn(phen)(edda)], and allowed to incubate for the specified duration. Cytotoxicity was expressed as IC$_{50}$ values calculated from dose–response curves {drug concentrations including a 50% reduction of cell survival in comparison to the control cultured in parallel without tested [M(phen)(edda)] complexes}. The 3-(4,5-dimethylthiazol-2-yl)-2,5-diphenyltetrazolium bromide (MTT) stock solution

(5 mg/ml in phosphate-buffered saline, PBS) was filter-sterilized and kept for no more than two weeks at 4 °C. In brief, for the MTT assay, after each period of incubation, 20 µl of MTT solution was added into each well and the cells were further incubated for 3 - 4 h under normal growth condition to allow the viable cells to convert MTT to formazan. Then, the media were discarded and formazan crystals in each well were dissolved by adding 100 µL of dimethyl sulfoxide (DMSO). For complete dissolution, the plate was shaken gently for five minutes. The assay is based on cleavage of the tetrazolium salt MTT by mitochondrial dehydrogenase to form a pinkish purple-colored insoluble formazan complex that solubilized in DMSO (Mosmann, 1983), which was then quantified by a microplate reader.

3.3.2 Measurement of Cell Viability in MTT Assay

The color intensity of the dissolved formazan which reflects the viable cell population was directly measured at 560 nm using a model 680 microplate reader (Bio-Rad, Japan). The percentage of viable cells [(mean optical density of treated sample/mean optical density of untreated sample) × 100] were plotted as a function of concentration of [M(phen)(edda)] to obtain the IC_{50} values. The viability results are shown as a graph of percentage of cell viability on the *y*-axis and concentration of the complexes on the *x*-axis. A triplicate from each time period was used in each assay and the experiment was repeated at least three times.

3.4 Partition Coefficient of [M(phen)(edda)] in n-octanol/water

The apparent octanol/water partition coefficients were similarly determined as described by Rudnev *et al.* (2006). Weighed amounts (2 – 3 mg) of [Co(phen)(edda)], [Cu(phen)(edda)] and [Zn(phen)(edda)] were partitioned between water and n-octanol for 2 h at room temperature by the shake flask method. Prepared volume of 5 ml for each phase added in centrifuge tube. Samples were centrifuged in $3000 \times g$ for 5 min and the content of complexes in the organic and aqueous phases were determined by UV-visible spectroscopy (Perkin Elmer, USA). The absorbance of the complexes in the aqueous phase before (A_o) and after partitioning (A_{aq}) were measured using appropriate λ_{max} value of each complex {λ_{max} values: [Co(phen)(edda)], 501 nm; [Cu(phen)(edda)], 684 nm; [Zn(phen)(edda)], 325 nm}. Partition coefficients can be evaluated as $\log P = \log (C_o - C_{aq})/C_{aq}$ from the complex concentrations in the aqueous phase before (C_o) and after partitioning (C_{aq}). From correlation between concentration and absorbance in Beers-Lambert law, $\log P$ is rewritten as $\log P = \log (A_o - A_{aq})/A_{aq}$. All experiments were run in triplicate.

3.5 Morphological Assessment of Apoptosis

3.5.1 Analyzing Surface Morphology of MCF7 Cells

To visualize surface morphology changes characteristic of apoptosis, 2.5×10^5 MCF7 cells were seeded in 60 mm petri dishes and grown overnight cultured with RPMI 1640 medium and supplemented with 10% FBS then

followed by incubation with 13.5 μM [Co(phen)(edda)], 2.8 μM [Cu(phen)(edda)] and 5 μM [Zn(phen)(edda)] (IC_{50} concentrations) for varying time periods (24, 48, and 72 h). In these and subsequent studies, the compound concentrations used were based on IC_{50} values. The images of the untreated control and treated cells were visualized with Eclipse TS100 phase contrast microscope (Nikon, Japan).

3.5.2 Analyzing Nuclear DNA of MCF7 Cells with DAPI Staining

To visualize nuclear DNA with 4',6-diamidino-2-phenylindole (DAPI) staining, 2.5×10^{5} MCF7 cells were seeded in a 60 mm petri dishes and grown overnight under normal growth conditions followed by incubation with 13.5 μM [Co(phen)(edda)], 2.8 μM [Cu(phen)(edda)], 5 μM [Zn(phen)(edda)] and 10 μg/ml cisplatin (positive control) for varying time periods (24, 48, and 72 h). Cells were then fixed with 3.7% formaldehyde in PBS for 15 min, washed twice with PBS, permeabilized in PBS containing 0.1% Triton X-100 for 5 min. After that, cells were washed three times with PBS followed by incubation with 1 μg/ml DAPI in the dark for 10 min. Thereafter, DNA stained cells were washed three times with PBS, mounted on microscope slide and the images were captured with BX51 fluorescence microscope (Olympus, Japan). DAPI, when bound to double-stranded DNA in the nucleus, has an excitation maximum at a wavelength of 358 nm (ultraviolet light) and its emission maximum is at 461 nm (blue light).

3.6   Apoptosis Analysis

3.6.1   Experimental Set Up

7.0×10^5 MCF7 cells were seeded in 100 mm petri dishes, allowed to recover for 24 h, and then treated with 13.5 µM [Co(phen)(edda)], 2.8 µM [Cu(phen)(edda)], 5 µM [Zn(phen)(edda)] and 10 µg/ml cisplatin and cells were collected after 24, 48 and 72 h incubation. Adhering and floating cells were included in this analysis, respectively, and poured together in the centrifuge tube. The cells were washed with PBS, trypsinized and resuspended in RPMI 1640 medium. After centrifugation for 5 min at 1500 rpm, the pellets were gently resuspended in 100 µl of 1× binding buffer (Becton Dickinson Pharmingen, Germany), 5 µl of Annexin V-FITC (Becton Dickinson Pharmingen, Germany) and 5 µl of propidium iodide (Sigma-Aldrich, Germany) were added to the above in a sterile 15 ml of round bottom polystyrene tube (Becton Dickinson, Germany) and allowed to stand for 30 min at room temperature. Then, 300 µl of 1× binding buffer was added before analyzing wiith flow cytometry.

3.6.2   Apoptosis Assessment by Annexin V-FITC/Propidium Iodide Staining

Cells were counterstained with AnnexinV-FITC and propidium iodide (PI) to distinguish between apoptotic and necrotic cells. The effects of [Co(phen)(edda)], [Cu(phen)(edda)], [Zn(phen)(edda)] and positive control

cisplatin on MCF7 were analyzed by using BD FACSCalibur flow cytometer (Becton Dickinson, Germany). The cell profiles were analyzed on Fluorescence Activated Cell Sorting (FACS) by using Cell Quest software (Becton Dickinson and Company, USA). A total of 10,000 events were acquired and the cells were properly gated for analysis. The cells populations were displayed as a dot plot divided into four quadrants with AnnexinV-FITC (*x*-axis) versus PI fluorescence (*y*-axis). The experiment was repeated at least three times with two replicates each time.

3.7   Cell Cycle Analysis

3.7.1   Experimental Set Up

7.0×10^5 MCF7 cells were seeded in 100 mm petri dishes, allowed to recover for 24 h, and then treated with 13.5 µM [Co(phen)(edda)], 2.8 µM [Cu(phen)(edda)], 5 µM [Zn(phen)(edda)] and 0.2 µg/ml nocodazole. The cells were washed with PBS. To analyze cell cycle phase distribution, adhering and floating cells were collectively harvested through trypsinization, washed and resuspended in RPMI 1640 medium after 24, 48 and 72 h incubation. After centrifugation for 5 min at 1500 rpm, the pellets were fixed in ice-cold 70% ethanol and stored at -20 $^{\circ}$C. For analysis, cells were transferred into 1 ml of PBS, incubated with RNAse A (15 µg/ml), treated with 20 µg/ml PI for 30 min at room temperature.

3.7.2   DNA Content Assessment by Propidium Iodide Staining

The effects of [Co(phen)(edda)], [Cu(phen)(edda)], [Zn(phen)(edda)] and positive control nocodazole on MCF7 cell cycle phase distribution were assessed by using BD FACSCalibur flow cytometry (Becton Dickinson, Germany). PI, when bound to nucleic acids, has an excitation maximum at 535 nm and emission maximum at 617 nm. The cell cycle profiles consist of percentage of cells in sub G_0/G_1, G_0/G_1, S and G_2/M phases were determined on FACS by using Cell Quest software (Becton Dickinson and Company, USA). A total of 10,000 events were collected and the cells were properly gated for analysis. The histogram of DNA content (*x*-axis, PI-fluorescence) versus counts (*y*-axis) was displayed. The experiment was repeated at least three times with two replicates each time.

3.8   Mitochondrial Membrane Potential Detection

3.8.1   Preparation of JC-1 solution

Firstly, lyophilized 5,5',6,6'-tetrachloro-1,1',3,3'-tetraethylbenzimidazol-carbocyanine iodide (JC-1) reagent was dissolved in 125 µl of DMSO (per vial) at room temperature to yield a JC-1 stock solution. The vial was re-capped and inverted several times to fully dissolve the reagent. The JC-1 stock solution may be aliquoted and stored at –20 °C. 1× JC-1 working solution was prepared freshly by diluting the JC-1 stock solution in a ratio 1:100 with prewarmed 1× assay buffer. That was, 125 µl of JC-1 stock

solution was mixed together with 12.375 ml of prewarmed 1× assay buffer. 0.5 ml of JC-1 working solution is required for each sample.

3.8.2 Experimental Set Up

Mitochondrial Membrane Potential Detection Kit (Becton Dickinson, USA) was used by following the manufacturer's instructions. Briefly, 7.0×10^5 MCF7 cells were seeded in 100 mm petri dishes, allowed to recover for 24 h, and then treated with 13.5 µM [Co(phen)(edda)], 2.8 µM [Cu(phen)(edda)], 5 µM [Zn(phen)(edda)] and 10 µg/ml cisplatin. The treated cells were collected after 24, 48 and 72 h incubation. Adhering and floating cells were included in this analysis, respectively, and poured together in the centrifuge tube. The cells were washed with PBS, trypsinized and resuspended in RPMI 1640 medium. After centrifugation for 5 min at 1500 rpm, each pellet was transferred into a sterile 15 ml of round bottom polystyrene tube (Becton Dickinson, Germany) and resuspended gently in 0.5 ml of freshly prepared JC-1 working solution at 37 ^{o}C in a CO_2 incubator and incubated for 15 min. Spare dye was removed by washing twice in 1× assay buffer and centrifugation for 5 min at 1500 rpm. In the first wash, 2 ml of 1× assay buffer was added to each pellet. In the second wash, 1 ml of 1× assay buffer was added to each pellet. Lastly, each pellet was resuspended gently in 0.5 ml of 1× assay buffer and cell-associated fluorescence was measured *via* BD FACSCalibur flow cytometer (Becton Dickinson, Germany).

3.8.3 Mitochondrial Membrane Potential Assessment by JC-1 staining

Breakdown of the mitochondrial membrane potential ($\Delta\psi_m$) was determined by FACS analysis using JC-1, which allows detection of changes of the $\Delta\psi_m$. The excitation peak of JC-1 is 488 nm. The approximate emission peaks of monomeric and J-aggregates forms are 527 nm and 590 nm, respectively. A total of 10,000 events were acquired and the cells were properly gated for analysis. The cell populations were displayed as a dot plot divided into two quadrants with green fluorescence monomers (*x*-axis) versus red fluorescence aggregates (*y*-axis). The experiment was repeated at least four times with two replicates each time. For the $\Delta\psi_m$ data, Wilcoxon Rank-Sum Test was used to evaluate p values.

3.9 Human DNA Topoisomerase I Inhibition Assay

The human DNA topoisomerase I (topo I) inhibitory activity was determined by measuring the relaxation of supercoiled plasmid DNA pBR322. Each reaction mixture contained 10 mM Tris(hydroxymethyl)aminomethane hydrochloride (Tris–HCl), pH 7.5, 100 mM Sodium chloride (NaCl), 1 mM Phenylmethylsulfonyl fluoride (PMSF), and 1 mM 2-mercaptoethanol, 0.25 μg plasmid DNA pBR322, 1 unit of human DNA topo I, and the [M(phen)(edda)] complexes at a specified concentration. Total volume of each reaction mixture was 20 μl and these mixtures were prepared on ice. Upon enzyme addition, reaction mixtures were incubated at 37 ^{o}C for 30 min. The reactions were terminated by the addition of 2 μl of 10% Sodium dodecyl sulfate (SDS), and

then followed by 3 µl of dye solution comprising 0.02% bromophenol blue and 50% glycerol. SDS is required to denature topo I, preventing further functional enzymatic activity. The mixtures was applied onto 1.2% agarose gel and electrophoresed for 5 h at 33 V with running buffer of Tris–acetate EDTA (TAE). The gel was stained, destained, and photographed under UV light using a Syngene Bio Imaging system and the digital image was viewed with Gene Flash software. Same protocol was applied in the human DNA topo I inhibition condition study. In a preliminary investigation into the mechanism of topo I inhibition, differential mixing of DNA, [M(phen)(edda)] and topo I were carried out; the only variation is the sequence in adding the main components. Three conditions were studied in this assay. In the first condition, human DNA topo I was incubated with the complexes at 37 ^{o}C for 30 min and then DNA was added, and the reaction mixture was incubated for another 30 min at the same temperature. In the second condition, the complexes and DNA were incubated for 30 min at 37 ^{o}C first before the addition of topo I followed by a further incubation of 30 min. In the third condition, all three reaction components were mixed simultaneously and incubated for another 30 min at the same temperature. This is a preliminary result of an investigation into the mode of action of [Co(phen)(edda)], [Cu(phen)(edda)] and [Zn(phen)(edda)] on the human DNA topo I.

3.10   Data Analysis

All experiments were performed at least three times and the results are expressed as the mean ± standard error. Statistical significance was established

at a value of $P < 0.05$. For the $\Delta\psi_m$ data, Wilcoxon Rank-Sum Test was used to

evaluate p values.

CHAPTER 4.0

RESULTS

This section describes the results of various investigations. The first involved antiproliferative action of [Co(phen)(edda)], [Cu(phen)(edda)] and [Zn(phen)(edda)] complexes on MCF10A and MCF7 cell lines. Octanol–water partition coefficient was also determined. The lipophilicity of these complexes was determined in order to help assess their drug-likeness property based on Lipinski's Rule of Five. Besides, mode of cell death such as induction of apoptosis on MCF7 cells was examined by morphological study, Annexin V-FITC/PI double staining, sub G_0/G_1 cell cycle analysis and disruption of $\Delta\psi_m$. Another mode of cell death was perturbation of cell cycle regulation and it was examined for MCF7 cells. Cell death of treated MCF7 cells could also arise from inhibition of topo I. Therefore, cell death induced by [M(phen)(edda)] could involve multiple targets.

4.1 Anticancer Property and Selectivity of [M(phen)(edda)] on Human Breast Cell Lines

4.1.1 Anticancer Property of [M(phen)(edda)] on Human Breast Cell Lines

[Co(phen)(edda)], [Cu(phen)(edda)] and [Zn(phen)(edda)] complexes were evaluated for cytotoxic activity *in vitro* against human breast normal and cancer cell lines (MCF10A and MCF7 respectively). Cell viability induced by [Co(phen)(edda)], [Cu(phen)(edda)] and [Zn(phen)(edda)] complexes on MCF10A and MCF7 cells were quantified by MTT antiproliferative assay as described in Chapter 3.0. In brief, MCF10A and MCF7 cells were transferred to 96-well micro titer plates. These MCF10A and MCF7 cells were separately treated with a range of concentrations of the compounds for 24, 48 and 72 h. The IC_{50} values (concentration of the metal complexes at which the percentage of viability was reduced by 50%) for these different compounds were estimated from the graphs and these are summarized in Table 4.1. The IC_{50} values decreased with incubation time for all complexes. Notably, the effect of the compounds examined on the cell viability of MCF10A showed lower increase in antiproliferative activity with increasing concentration of [Co(phen)(edda)], [Cu(phen)(edda)] and [Zn(phen)(edda)] complexes for all incubation times, *viz.* for 24 h (Figures 4.2-4.4), 48 h (Figures 4.5-4.7) and 72 h (Figures 4.8-4.10) h. In contrasts, cell viability of MCF7 cells treated with [Co(phen)(edda)], [Cu(phen)(edda)] and [Zn(phen)(edda)] complexes showed more strong increase in antiproliferative effect with increasing concentration of [M(phen)(edda)] (24 h: Figures 4.2-4.4; 48 h: Figures 4.5-4.7; 72 h: Figures 4.8-4.10).

Morphologically, viable MCF10A cells appeared flat and spindle-like in shape (Figure 4.1B). At 24 h, [Co(phen)(edda)] and [Zn(phen)(edda)] complexes did not seem to contribute strongly to the cytotoxicity activity on

MCF10A cells as their IC_{50} values were more than 140 µM. Treatment with [Cu(phen)(edda)] exhibited slight cytotoxicity with IC_{50} values of 30 µM (Figures 4.2-4.4). Besides, on incubating MCF10A cells with [Co(phen)(edda)], [Cu(phen)(edda)] and [Zn(phen)(edda)] complexes for 48 h, they showed some cytotoxicity activity with IC_{50} values of 128 µM, 15 µM and 50 µM, respectively (Figures 4.5-4.7). Moreover, IC_{50} values of [Co(phen)(edda)], [Cu(phen)(edda)] and [Zn(phen)(edda)] dropped to 39.5 µM, 10.4 µM and 32 µM, respectively when treated on MCF10A cells for 72 h (Figures 4.8-4.10).

Morphologically, viable MCF7 cells appeared flat and distorted diamond shape (Figures 4.1A). At 24 h, [Co(phen)(edda)] and [Zn(phen)(edda)]-treated MCF7 cells did not show cytotoxicity activity as their IC_{50} values were more than 160 µM and 140 µM, respectively. In contrast, treatment with [Cu(phen)(edda)] was found to be slightly cytotoxic on MCF7 cells with IC_{50} values of 25 µM (Figures 4.2-4.4). Incubation of MCF7 cells with [Co(phen)(edda)], [Cu(phen)(edda)] and [Zn(phen)(edda)] complexes for 48 h resulted in moderate cytotoxicity activity with IC_{50} values 58 µM, 5.5 µM and 15 µM, respectively (Figures 4.5-4.7). Moreover, the viability of the MCF7 cells decreased to 50% in response to 13.5 µM of [Co(phen)(edda)], 2.8 µM of [Cu(phen)(edda)] and 5 µM of [Zn(phen)(edda)] for 72 h incubation time and continued to decrease as the concentration of the complexes was increased (Figures 4.8-4.10). Hence, it was evident that the compounds were highly cytotoxic *in vitro*. In addition, the cell viability of [M(phen)(edda)]-treated MCF7 cells were decreased with incubation time and also in a dose-

dependent manner. The order of increasing cytotoxicity being [Co(phen)(edda)] < [Zn(phen)(edda)] < [Cu(phen)(edda)]. Clearly, the nature of the metal in [M(phen)(edda)] complex played an important role in the cytotoxicity of MCF7 human breast cancer cells.

4.1.2 Cytotoxic Selectivity towards Human Breast Cancer Cell Lines over Normal Breast Cell Lines

Comparing the results of MCF10A and MCF7 cells treated with [M(phen)(edda)], it was found that these complexes have some selective antitumor effect. The comparisons of the respective IC_{50} values showed that normal cells were less sensitive to the compounds *in vitro* (Table 4.1). When one compared the relative cytotoxicity towards both cell lines in the lower concentration range, the selectivity of these compounds were more prominent (Figures 4.8-4.10). Low IC_{50} values of 13.5 µM [Co(phen)(edda)], 2.8 µM [Cu(phen)(edda)] and 5 µM [Zn(phen)(edda)] on MCF7 cells in 72 h were observed. While, the IC_{50} values for [Co(phen)(edda)], [Cu(phen)(edda)] and [Zn(phen)(edda)] on MCF10A in 72 h are 39.5 µM, 10.4 µM, and 32 µM, respectively. Consequently, the results showed that the normal breast cell line, MCF10A was more than 80% viable after 72 h incubation based on the IC_{50} of [Co(phen)(edda)], [Cu(phen)(edda)] and [Zn(phen)(edda)] doses on MCF7 cancer cells under observation (Figures 4.8-4.10). Thus, this study showed that [Co(phen)(edda)], [Cu(phen)(edda)] and [Zn(phen)(edda)] has potential for development into anticancer drugs as they were more cytotoxic to cancer cells than normal cells.

Table 4.1: Cytotoxicity IC$_{50}$ Values for Compounds [Co(phen)(edda)], [Cu(phen)(edda)] and [Zn(phen)(edda)] against Human Cancer and Normal Cell Lines[a]

Compound	Cell Line IC$_{50}$ (µM) in Different Time Points					
	MCF7			MCF10A[b]		
	24 h	48 h	72 h	24 h	48 h	72 h
[Co(phen)(edda)]	>160.0	58.0	13.5	>140.0	128.0	39.5
[Cu(phen)(edda)]	25.0	5.5	2.8	30.0	15.0	10.4
[Zn(phen)(edda)]	>140.0	15.0	5.0	>140.0	50.0	32.0

[a] Cells were treated with increasing concentrations of the compounds for 24, 48 and 72 h. Cell viability was determined by MTT assay and IC$_{50}$ values were estimated from the graphs.
[b] Human normal cells.
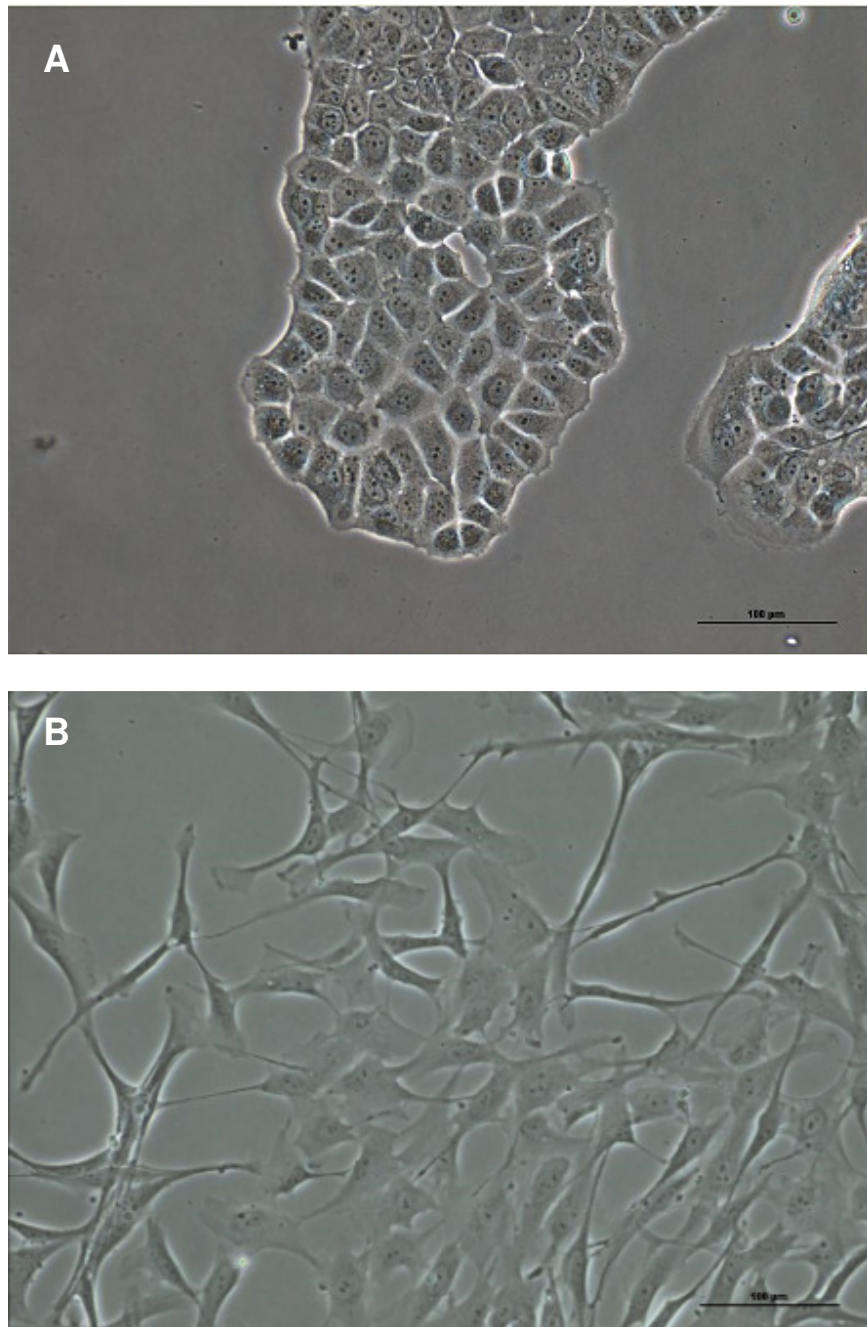
Figure 4.1: Phase-contrast Microscopy Images of Human Breast Cells.
Morphologies of human breast cancer carcinoma cells, MCF7 (A) and normal epithelial cells, MCF10A (B) without treatment were photographed. Magnification ×200, bar 100 µm (micrometer).
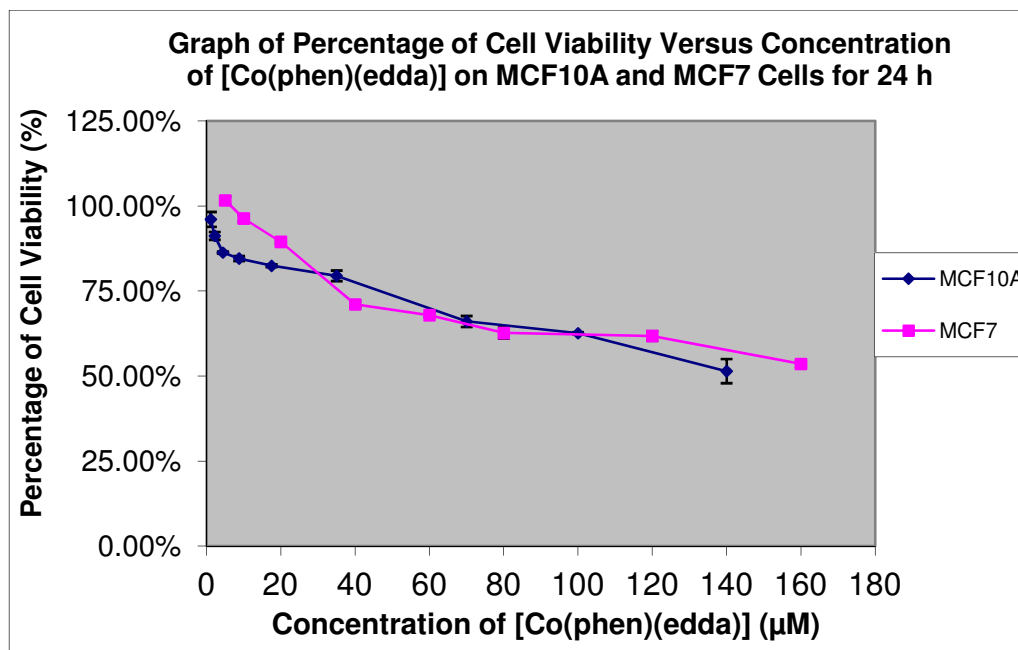
Figure 4.2: Effect of [Co(phen)(edda)] on MCF10A and MCF7 Cell Viability for 24 h Incubation Time. Results are mean ± S.E. of three independent experiments.
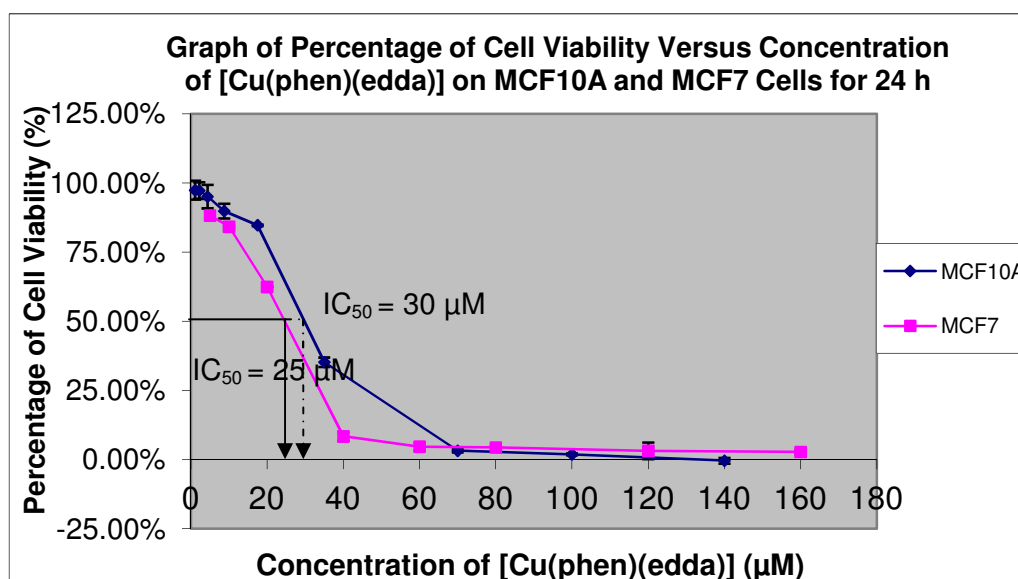
Figure 4.3: Effect of [Cu(phen)(edda)] on MCF10A and MCF7 Cell Viability for 24 h Incubation Time. The dotted line represents IC_{50} of treated MCF10A cells while solid line represents IC_{50} of treated MCF7 cells. Results are mean ± S.E. of three independent experiments.
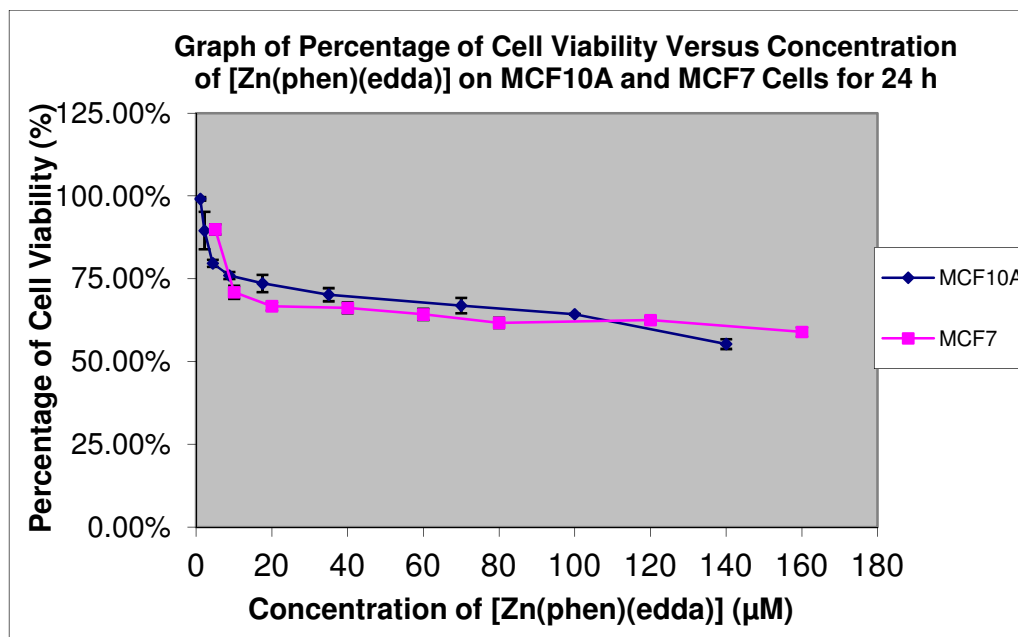
Figure 4.4: Effect of [Zn(phen)(edda)] on MCF10A and MCF7 Cell Viability for 24 h Incubation Time. Results are mean ± S.E. of three independent experiments.
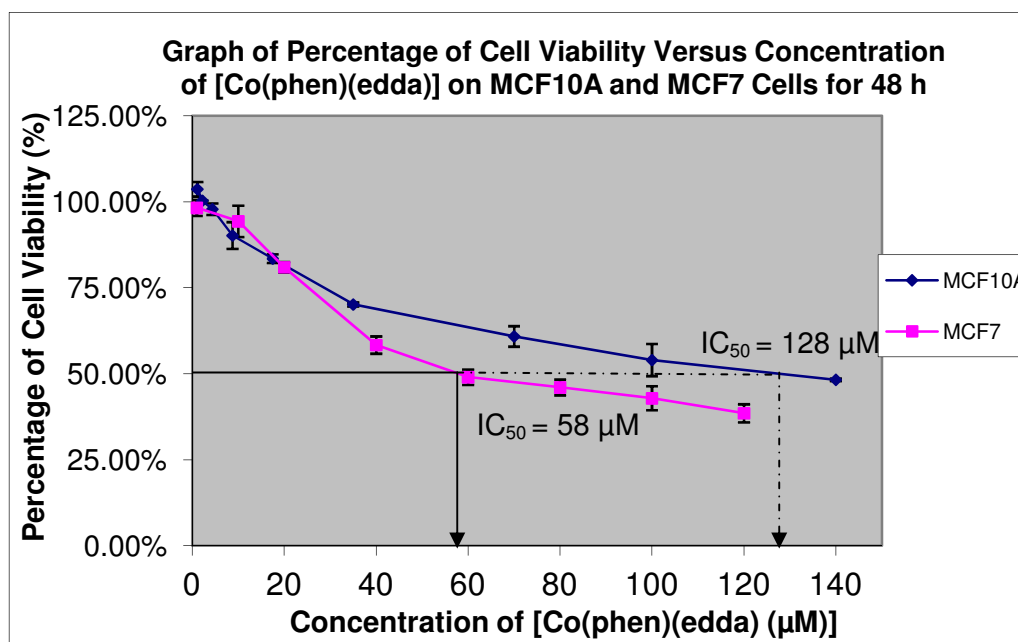
Figure 4.5: Effect of [Co(phen)(edda)] on MCF10A and MCF7 Cell Viability for 48 h Incubation Time. The dotted line represents IC_{50} of treated MCF10A cells while solid line represents IC_{50} of treated MCF7 cells. Results are mean ± S.E. of three independent experiments.
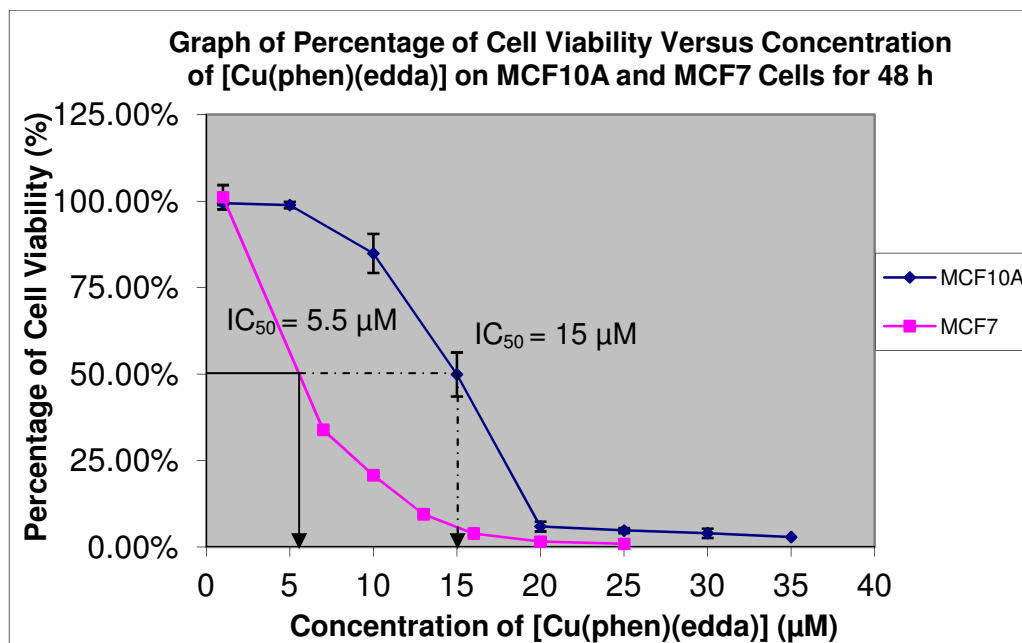
Figure 4.6: Effect of [Cu(phen)(edda)] on MCF10A and MCF7 Cell Viability for 48 h Incubation Time. The dotted line represents IC_{50} of treated MCF10A cells while solid line represents IC_{50} of treated MCF7 cells. Results are mean ± S.E. of three independent experiments.
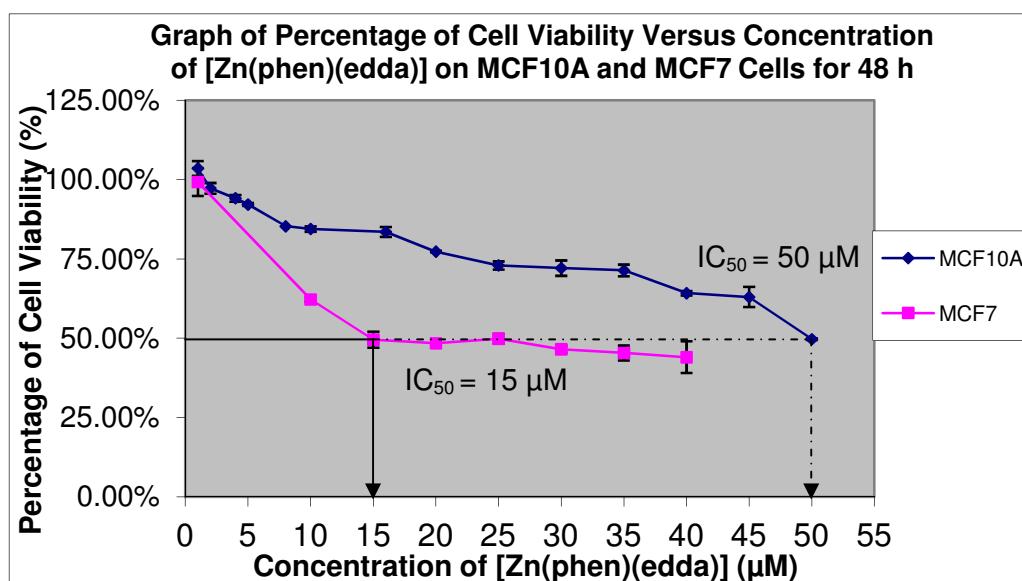
Figure 4.7: Effect of [Zn(phen)(edda)] on MCF10A and MCF7 Cell Viability for 48 h Incubation Time. The dotted line represents IC_{50} of treated MCF10A cells while solid line represents IC_{50} of treated MCF7 cells. Results are mean ± S.E. of three independent experiments.
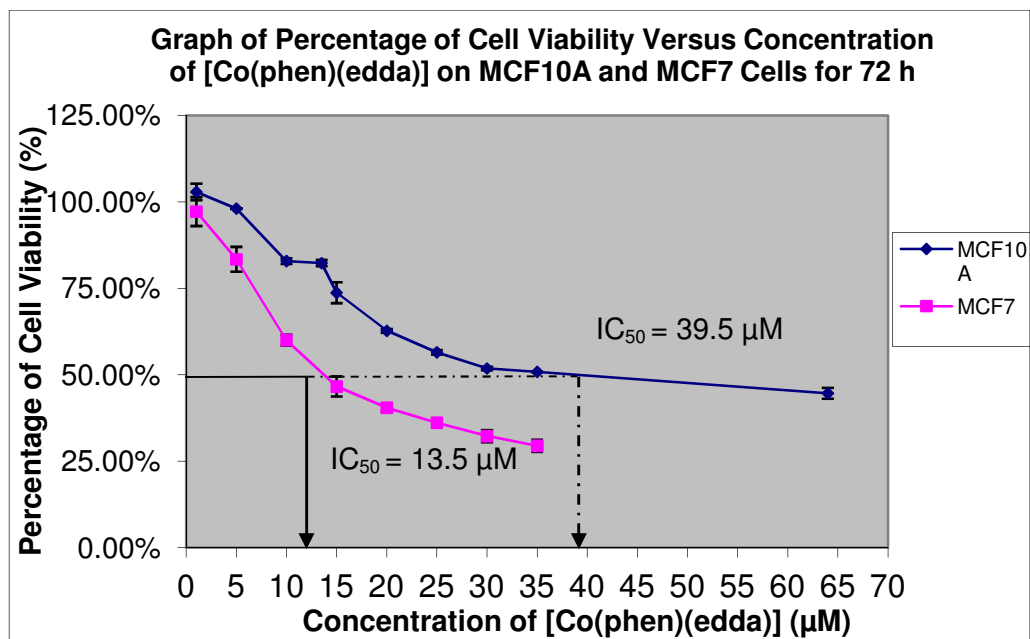
Figure 4.8: Effect of [Co(phen)(edda)] on MCF10A and MCF7 Cell Viability for 72 h Incubation Time. The dotted line represents IC_{50} of treated MCF10A cells while solid line represents IC_{50} of treated MCF7 cells. Results are mean ± S.E. of three independent experiments.
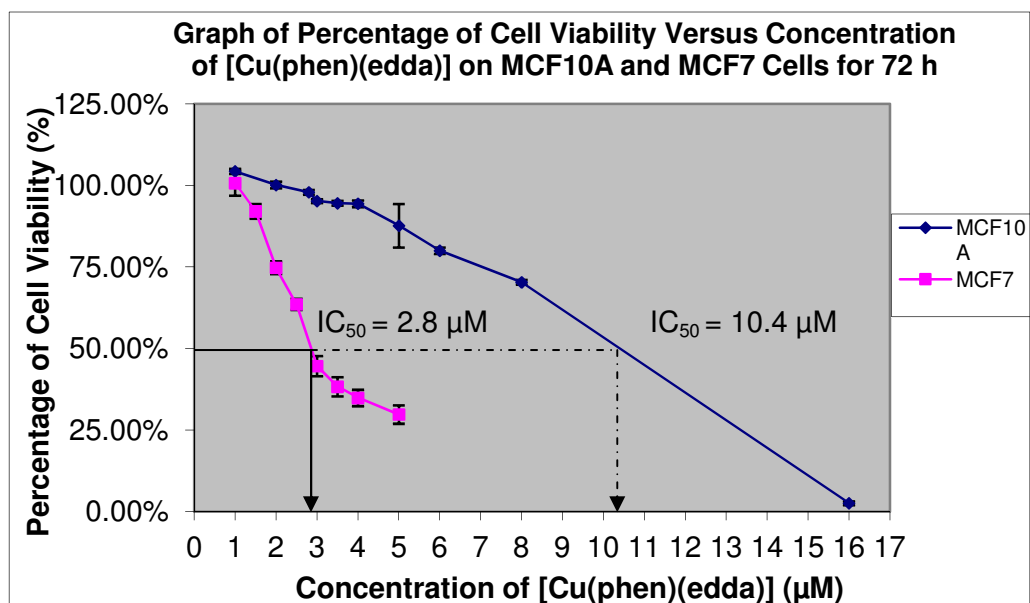
Figure 4.9: Effect of [Cu(phen)(edda)] on MCF10A and MCF7 Cell Viability for 72 h Incubation Time. The dotted line represents IC_{50} of treated MCF10A cells while solid line represents IC_{50} of treated MCF7 cells. Results are mean ± S.E. of three independent experiments.
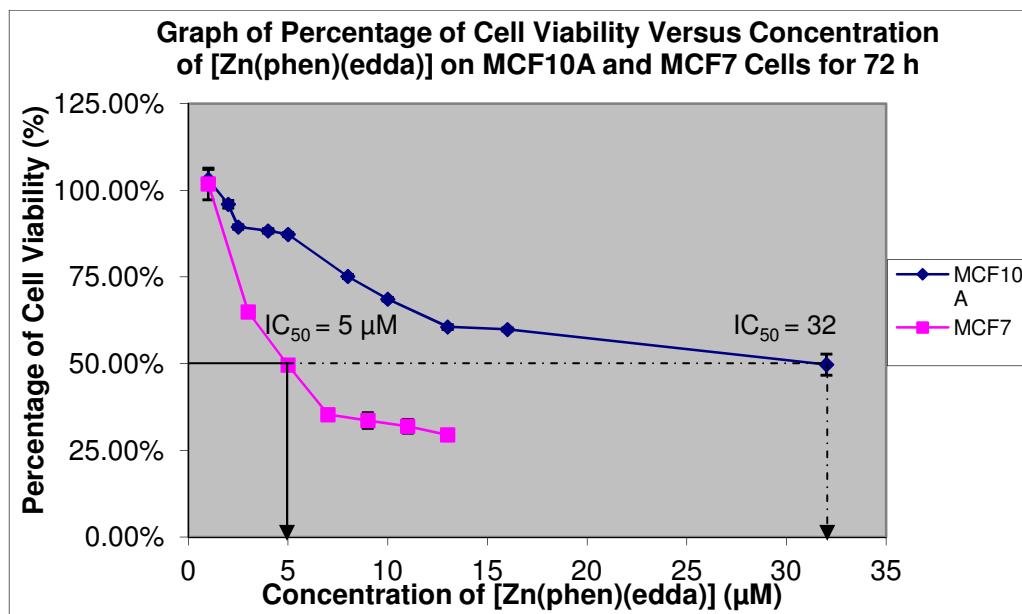
Figure 4.10: Effect of [Zn(phen)(edda)] on MCF10A and MCF7 Cell Viability for 72 h Incubation Time. The dotted line represents IC_{50} of treated MCF10A cells while solid line represents IC_{50} of treated MCF7 cells. Results are mean $\pm$ S.E. of three independent experiments.

4.2   Octanol–Water Partition Coefficients

Efficient penetration through biomembranes from intestine to bloodstream and then to the tumor cell is essential for metal complexes as an oral drug. The ability of a potential drug candidate to pass through these barriers until it binds to the target and induces the desired response is most often described by the octanol–water partition coefficient. Numerous methods for the prediction of aqueous solubility or partition coefficients have been suggested in the literature (Bodor *et al.*, 1989; Ruelle, 2000; Huang *et al.*, 2004). Briefly, the compounds were dissolved in a mixture of octanol and deionized water with 1:1 ratio and were shaken for 2 h. Subsequently, the phases were centrifuged 3000 × *g* for 5 min. Samples were analyzed using a UV-Vis spectroscopy. The log *P* (*P* = Partition Coefficient) value is known as a measure of lipophilicity. The log *P* value was calculated as log [ratio of the concentration in the octanol phase to the concentration in the aqueous phase] and as in equation log P = log $(C_o - C_{aq})/C_{aq}$. From correlation between concentration and absorbance in Beers-Lambert law, log *P* is rewritten as log *P* = log $(A_o - A_{aq})/A_{aq}$, whereby the absorbance of the complexes in the aqueous phase before (A_o) and after partitioning (A_{aq}) were measured using appropriate λ_{max} value of each complex. The log *P* values are shown in Table 4.2. These values show the comparative distribution of [Co(phen)(edda)], [Cu(phen)(edda)] and [Zn(phen)(edda)] between water and n-octanol, and the solubilizing medium mimicking the interior part of biological membranes. The results indicate that [Zn(phen)(edda)] has a mean log octanol/water partition coefficient of 0.70, whereas [Co(phen)(edda)] with low log octanol/water

partition coefficient of 0.30. The octanol/water partition coefficient of [Cu(phen)(edda)] (0.33) is intermediate to that of [Co(phen)(edda)] and [Zn(phen)(edda)] (Table 4.2). Although characteristic of only the intact complexes, such lipophilicity thresholds allow the bioavailability estimation for the compounds of interest being applied as anticancer drugs. Indeed, [Co(phen)(edda)], [Cu(phen)(edda)] and [Zn(phen)(edda)] do prefer a non-aqueous over an aqueous environment, behaving as essentially non-polar compounds. The order of increasing lipophilicity can be characterized in ascending order as [Co(phen)(edda)] > [Cu(phen)(edda)] > [Zn(phen)(edda)].

Table 4.2: Summary of Drug-related Physicochemical Properties[a] and Cytotoxicity on MCF7 Cells for the New Developed Complexes.

Complex[b]		$\log P$	IC_{50} (μM)[c]
[Co(phen)(edda)]	(467.34)	0.30 ± 0.05	13.5
[Cu(phen)(edda)]	(507.98)	0.33 ± 0.03	2.8
[Zn(phen)(edda)]	(482.81)	0.70 ± 0.02	5.0

[a] Log P values were calculated as described in chapter 3. Each value represents the mean ± S.E. of three independent experiments.
[b] Given in parentheses is the molar mass in g mol^{-1}.
[c] IC_{50} values of [M(phen)(edda)] in 72 h incubation time.

4.3 Compounds Affected Cell Morphology of MCF7 Cells

4.3.1 Effect of Compounds on Surface Morphology of MCF7 Cells

In order to determine the mode of cell killing induced by [Co(phen)(edda)], [Cu(phen)(edda)] and [Zn(phen)(edda)], phase contrast microscopic observation was performed to capture the morphological changes of cells. In these and subsequent studies, the compound concentrations used were based on IC_{50} values as mentioned in chapter 3.0. MCF7 cells are typical adherent cells and were used in this study (Figure 4.1A). Control MCF7 cells (untreated) appeared flat and retained their normal intact shape following 24, 48 and 72 h in culture. Three consecutive days after 13.5 µM [Co(phen)(edda)], 2.8 µM [Cu(phen)(edda)] and 5 µM [Zn(phen)(edda)] administration, some cells began to detach from the dish surface and were found floating in the medium. The number of floating cells increased with time, and on the third day after compounds administration, the floating material was all apoptotic cell debris as seen by microscopic observation. At 72 h, treated MCF7 cells had entirely lost their well-defined structure and became rounded and shrunken. On the other hand, untreated control MCF7 cells retained their normal size and shape while neighboring cells were closely connected to each other (Figures 4.11-4.13, C). Morphological changes of the cell membrane associated with apoptosis, including the formation of blebs, spikes and blisters, were clearly evident in MCF7 cells after treatment with 13.5 µM [Co(phen)(edda)], 2.8 µM [Cu(phen)(edda)] and 5 µM

[Zn(phen)(edda)] following 24, 48 and 72 h incubation [Figures 4.11-4.13, (2), (3), (4)]. Such changes were not observed for untreated MCF7 cells.
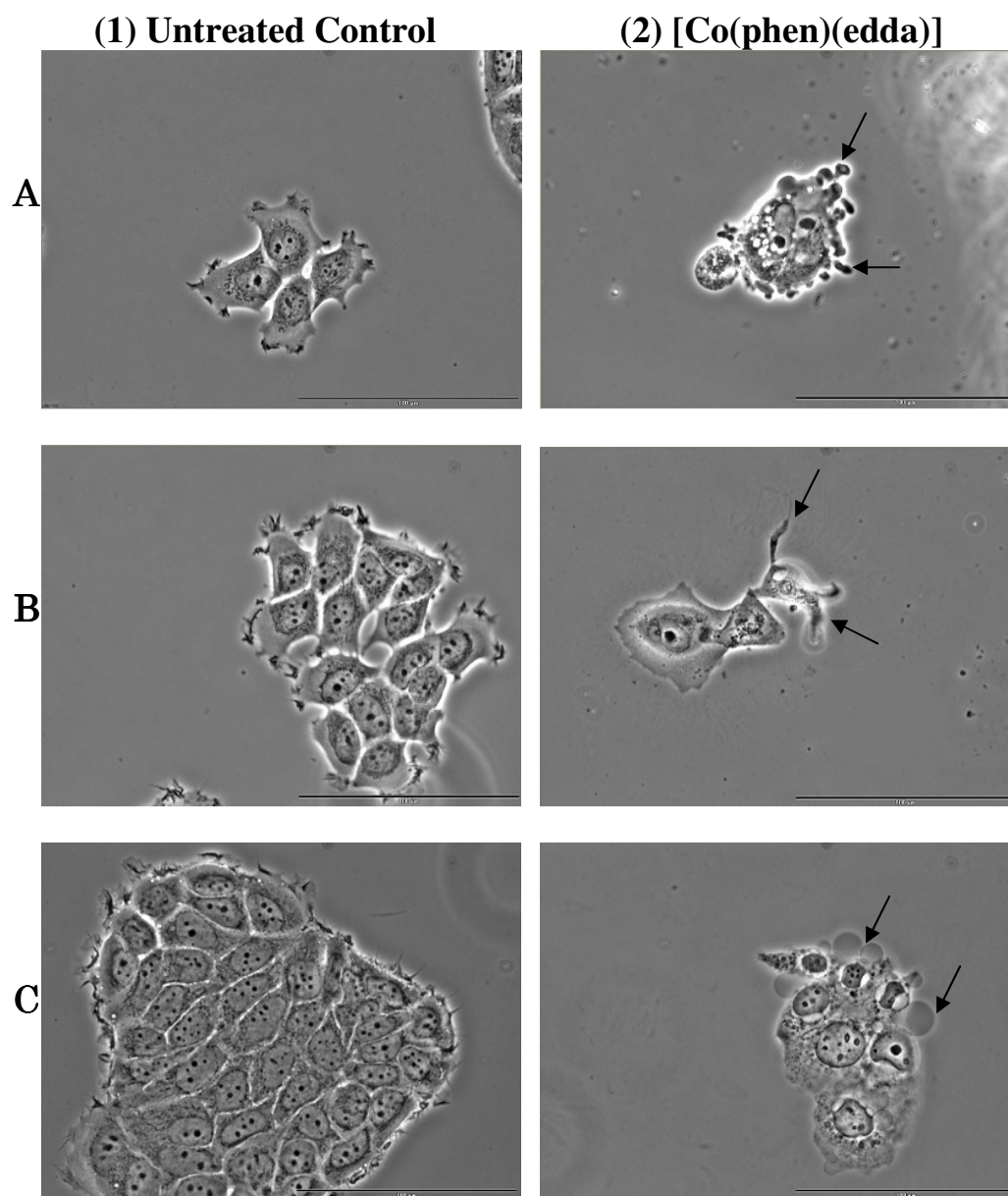
Figure 4.11: Morphological Changes of Untreated MCF7 cells and [Co(phen)(edda)]-treated MCF7 cells. After 24 (A), 48 (B) and 72 (C) h with and without treatment, the dishes were observed under phase contrast and membrane morphology was photographed. Magnification ×400, bar 100 µm.

(1) Untreated MCF7 cells were growing and appeared flat with closed diamonds, squares and triangular shape. (2) MCF7 cells treated with 13.5 µM [Co(phen)(edda)] exhibited membrane changes characteristic of apoptosis. Characteristics of apoptosis are clearly visible and are indicated by arrows: blebs (A), echinoid spikes (B), surface blisters (C).

(1) Untreated Control   **(3) [Cu(phen)(edda)]**
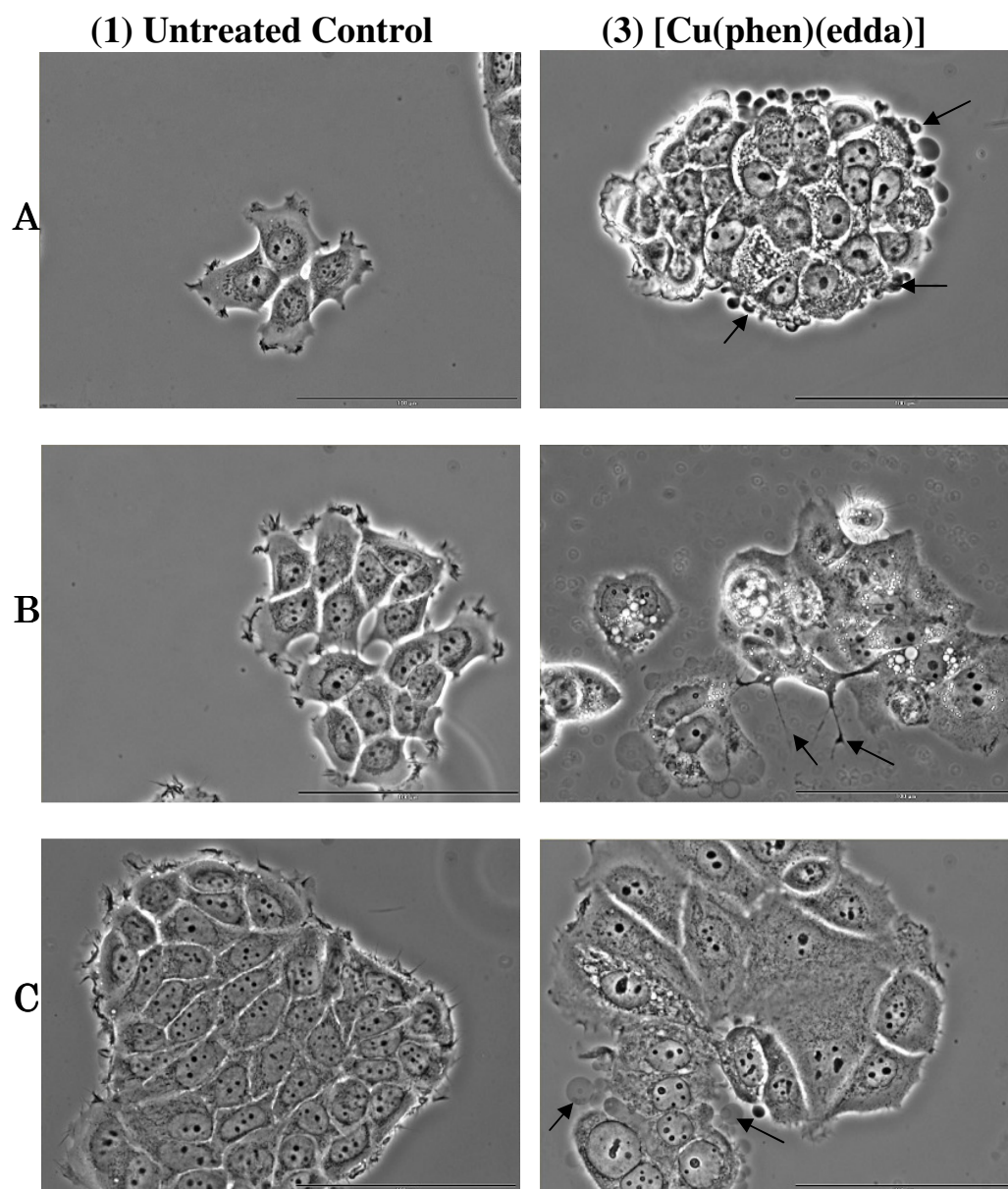
Figure 4.12: Morphological Changes of Untreated MCF7 cells and [Cu(phen)(edda)]-treated MCF7 cells. After 24 (A), 48 (B) and 72 (C) h with and without treatment, the dishes were observed under phase contrast and membrane morphology was photographed. Magnification ×400, bar 100 µm.

(1) Untreated MCF7 cells were growing and appeared flat with closed diamonds, squares and triangular shape. (3) MCF7 cells treated with 2.8 µM [Cu(phen)(edda)] exhibited membrane changes characteristic of apoptosis. Characteristics of apoptosis are clearly visible and are indicated by arrows: blebs (A), echinoid spikes (B), surface blisters (C).

(1) Untreated Control   **(4) [Zn(phen)(edda)]**
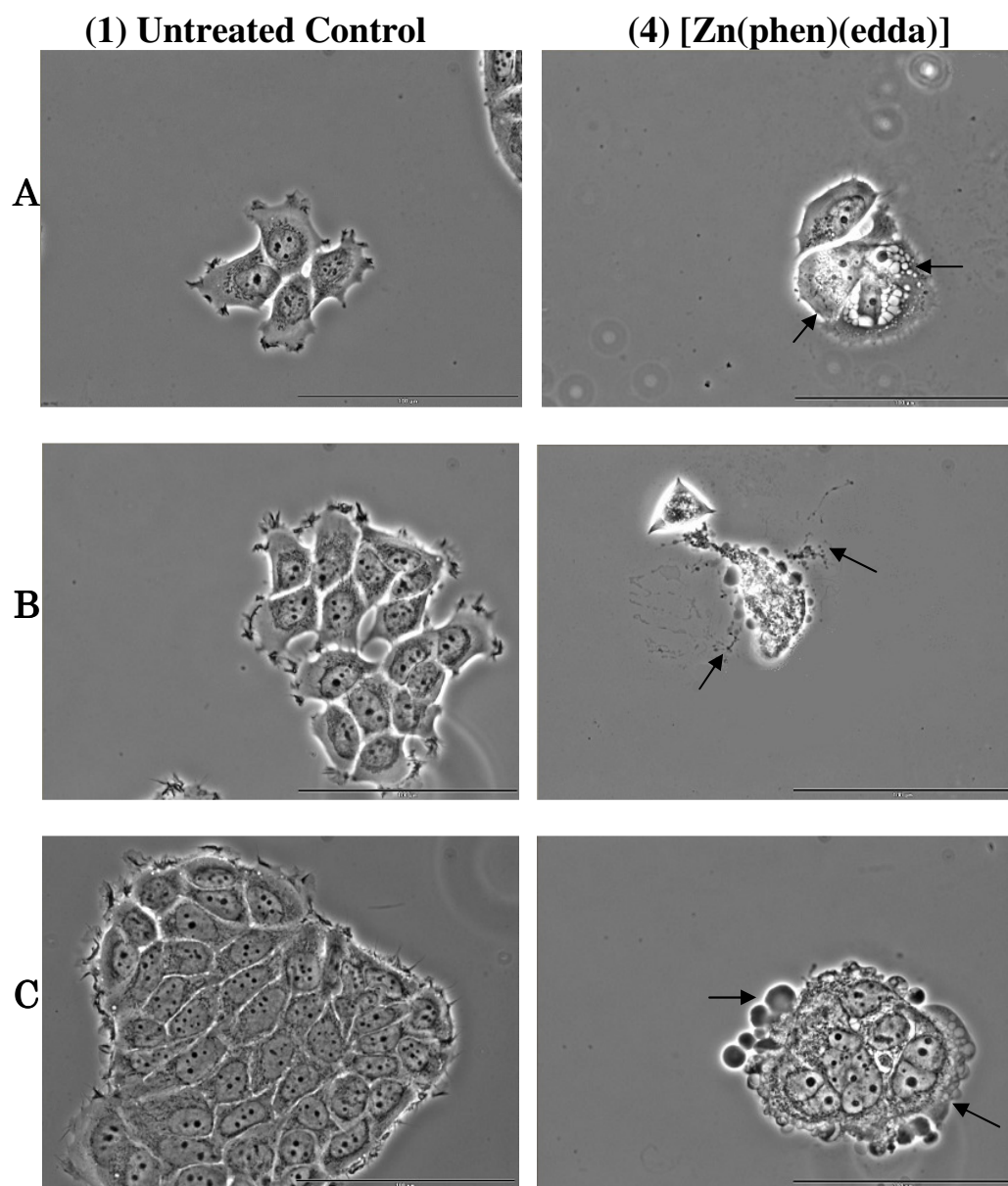
Figure 4.13: Morphological Changes of Untreated MCF7 cells and [Zn(phen)(edda)]-treated MCF7 cells. After 24 (A), 48 (B) and 72 (C) h with and without treatment, the dishes were observed under phase contrast and membrane morphology was photographed. Magnification ×400, bar 100 µm.

(1) Untreated MCF7 cells were growing and appeared flat with closed diamonds, squares and triangular shape. (4) MCF7 cells treated with 5 µM [Zn(phen)(edda)] exhibited membrane changes characteristic of apoptosis. Characteristics of apoptosis are clearly visible and are indicated by arrows: blebs (A), echinoid spikes (B), surface blisters (C).

4.3.2 Effect of Compounds on Nuclear Feature of MCF7 Cells

4',6-diamidino-2-phenylindole (DAPI) is a DNA binding dye that has been used extensively for staining cell nucleus based on relative changes in fluorescence intensity. To examine the pathway by which [Co(phen)(edda)], [Cu(phen)(edda)] and [Zn(phen)(edda)] complexes induce cell death, their effects on the nuclear integrity was analyzed by using DAPI staining and fluorescence microscopy as described in chapter 3.0. MCF7 cells were separately treated with 13.5 µM [Co(phen)(edda)], 2.8 µM [Cu(phen)(edda)] and 5 µM [Zn(phen)(edda)] (and 10 µg/ml cisplatin) for varying time periods followed by staining the cell nuclei with DAPI. Nuclear staining of the cells that were treated with the compounds for 24, 48 and 72 h are shown in Figure 4.14. DAPI staining showed nuclear condensation of MCF7 cells after the cells were treated with the compounds for 24 h (Figure 4.14, A-E) until 48 h (Figure 4.14, A'-E'). When MCF7 cells were treated with the compounds for 72 h, cells showed typical apoptotic nuclear changes (Figure 4.14, A"-E"). Interestingly, the compounds induced distinct nuclear morphological changes with more intense DAPI staining in comparison to untreated control cells, in agreement with cell viability data (Figure 4.14). The effects were more distinct in some cases in comparison to others probably due to the different efficiency of the [M(phen)(edda)] complexes. Moreover, the blue fluorescence generated from reaction between DAPI and apoptotic nuclear features on MCF7 cells treated with 13.5 µM [Co(phen)(edda)], 2.8 µM [Cu(phen)(edda)] and 5 µM [Zn(phen)(edda)] complexes were found to gradually increase in fluorescence intensity as the incubation time increased. Similarly, cisplatin acts as a positive

control also induced nuclear condensation indicating apoptotic cell death in MCF7 cells (Figure 4.14, B-B").
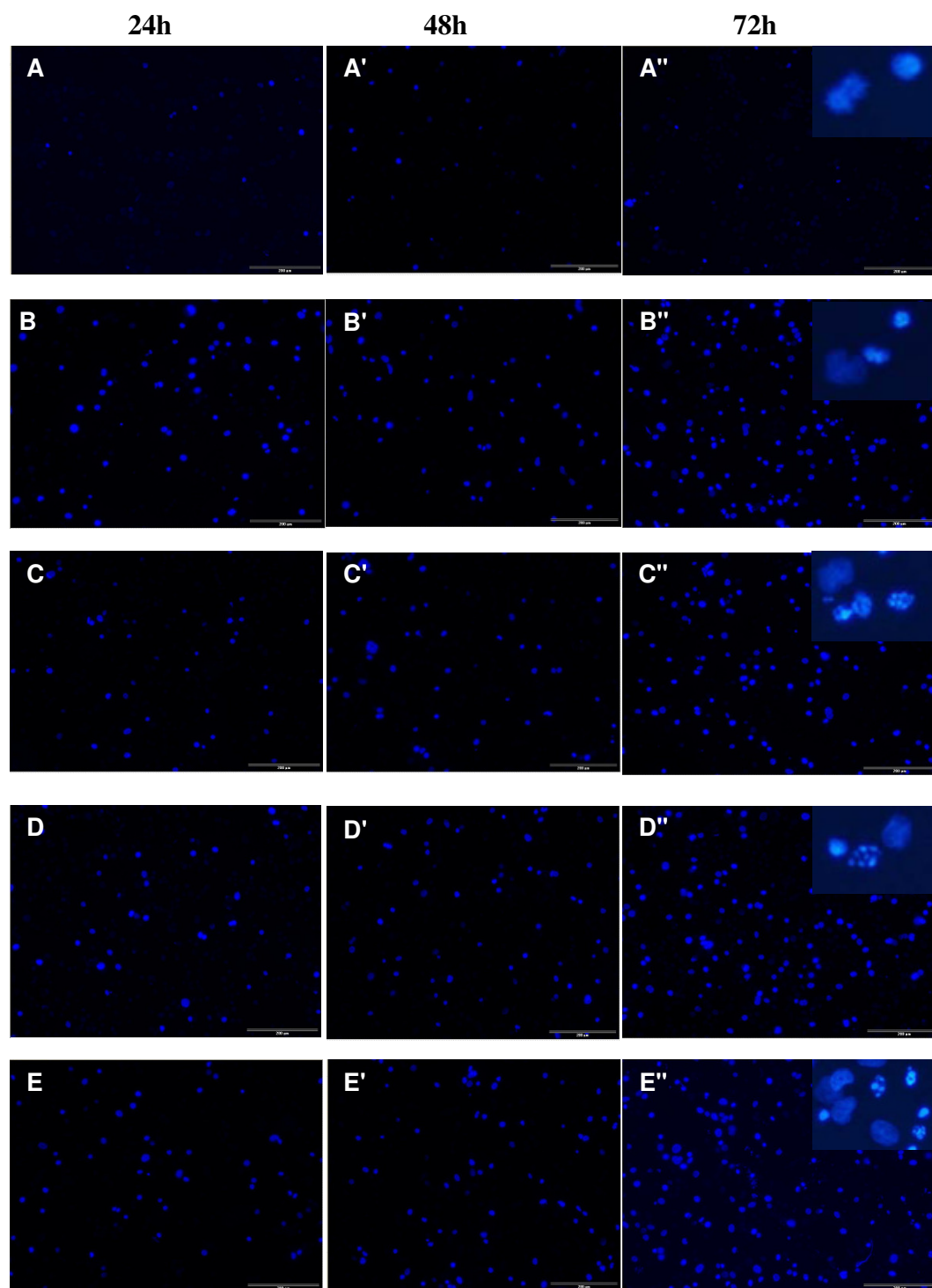
Figure 4.14: DAPI-Stained Visualization of Nuclei MCF7 Cells. Untreated MCF7 cells (A) and cells treated with 10 µg/ml cisplatin (B), 13.5 µM [Co(phen)(edda)] (C), 2.8 µM [Cu(phen)(edda)] (D) and 5 µM [Zn(phen)(edda)] (E) exhibited nuclear changes characteristic of apoptosis showed condensed apoptotic cells. After 24 (A-E), 48 (A'-E') and 72 (A"-E") h treatment, cells were isolated, fixed, permeabilized and stained with DAPI. Magnification ×100, bar 200 µm.

4.4   Analysis of Induction of Apoptosis in MCF7 Cells

To provide further evidence on the nature of cell death, Annexin V-FITC/PI staining and flow cytometry was used to investigate apoptosis. Here, we wanted to know whether [M(phen)(edda)] induce apoptosis in MCF7 cells. MCF7 cells were seeded and allowed to reach 70% confluence. Cells were collected 24 h after seeding and treatment with [Co(phen)(edda)], [Cu(phen)(edda)] and [Zn(phen)(edda)] for varying incubation periods. Unfixed MCF7 cells were labeled with PI and Annexin V-FITC and then analyzed using flow cytometer. Annexin V-FITC/PI staining can be used to monitor the progression of apoptosis from cell viability, to early-stage apoptosis, and finally to late-stage apoptosis and cell death as explained below.

An early event during apoptosis is the externalization of PS, a phospholipid normally restricted to the inner leaflet of the plasma membrane (Healy *et al.*, 1998). This apoptosis event can be monitored using Annexin V-FITC, a PS-specific binding protein. PI stains only the DNA of leaky necrotic cells and allows for a distinction between apoptotic and necrotic cells (Willingham, 1999). Cisplatin was used as a positive control in this apoptosis analysis. Cisplatin interfered with the growth of cancer cells which were eventually destroyed (Zamble *et al.*, 1998). The results were obtained from three independent experiments. The different labeling patterns in this assay identify the different cell fractions representing populations of healthy intact cells (Annexin V-FITC⁻/PI⁻) were in the lower left quadrant, early apoptotic cells (Annexin V-FITC⁺/PI⁻) were in the lower right quadrant, late apoptotic

cells (Annexin V-FITC$^+$/PI$^+$) were in the upper right quadrant and necrotic cells (Annexin V-FITC$^-$/PI$^+$) were in the upper left quadrant. This assay can help to discriminate between apoptosis and necrosis at single cell level. As shown in Figures 4.16-4.18, [Co(phen)(edda)], [Cu(phen)(edda)] and [Zn(phen)(edda)] caused higher proportions of apoptotic cells (Annexin V-FITC$^+$/PI$^-$ and Annexin V-FITC$^+$/PI$^+$) and lower proportions of necrotic cells (Annexin V-FITC$^-$/PI$^+$) in MCF7 cancer cell line examined.

Untreated MCF7 cells showed 82.10% of cells were viable healthy cells after 24 h incubation (Figure 4.19). In comparison, 10 µg/ml of cisplatin treated cells resulted in 3.45% early apoptotic cells and 36.56% late apoptotic cells [(Figure 4.15, (A)]. In MCF7 cells treated with 13.5 µM [Co(phen)(edda)] for 24 h, 7.66% cells were in early apoptosis, and 15.38% were in late apoptosis or cell death (Figure 4.19). For MCF7 cells treated with 2.8 µM [Cu(phen)(edda)] for 24 h, 11.17% cells were in early apoptosis, and 19.69% were in late apoptosis or cell death (Figure 4.19). In MCF7 cells treated with 5 µM [Zn(phen)(edda)] for 24 h, 9.48% cells were in early apoptosis, and 22.56% were in late apoptosis or cell death (Figure 4.19). Overall, the percentages of total apoptotic cells in MCF7 cells treated for 24 h with [Co(phen)(edda)], [Cu(phen)(edda)] and [Zn(phen)(edda)] complexes were 23.04%, 30.86% and 32.04%, respectively.

Proportion of untreated MCF7 cells remaining as viable healthy cells was 85.01% after 48 h (Figure 4.20). In comparison, 10 µg/ml of cisplatin treated cells resulted in 17.31% of early apoptotic cells and 38.37% of late

apoptotic cells for the same incubation period [(Figure 4.15, (B)]. In MCF7 cells treated with 13.5 µM [Co(phen)(edda)] for 48 h, 9.05% cells were in early apoptosis, and 19.28% were in late apoptosis or cell death (Figure 4.20). For MCF7 cells treated with 2.8 µM [Cu(phen)(edda)] for 48 h, 9.22% cells were in early apoptosis, and 21.35% were in late apoptosis or cell death (Figure 4.20). Finally, MCF7 cells treated with 5 µM [Zn(phen)(edda)] for 48 h, 11.13% cells were in early apoptosis, and 22.21% were in late apoptosis or cell death (Figure 4.20). In summary, for 48 h incubation, the percentages of total apoptotic cells in [Co(phen)(edda)], [Cu(phen)(edda)] and [Zn(phen)(edda)]-treated MCF7 cells were 28.33%, 30.57% and 33.34%, respectively.

After 72 h incubation, the population of untreated MCF7 cells that were viable healthy cells was 88.01% (Figure 4.21). In comparison, cells treated with 10 µg/ml of cisplatin showed 5.80% of cells at early apoptosis and 72.24% of cells at late apoptosis [(Figure 4.15, (C)]. In MCF7 cells treated with 13.5 µM [Co(phen)(edda)] for 72 h, 6.96% of cells were in early apoptosis, and 23.78% of cells were in late apoptosis or cell death (Figure 4.21). MCF7 cells treated with 2.8 µM [Cu(phen)(edda)] for 72 h, 4.14% of cells were in early apoptosis, and 28.05% were in late apoptosis or cell death (Figure 4.21). For MCF7 cells treated with 5 µM [Zn(phen)(edda)] for 72 h, 7.24% of cells were in early apoptosis, and 28.22% were in late apoptosis or cell death (Figure 4.21). The percentages of apoptotic cells in [Co(phen)(edda)], [Cu(phen)(edda)] and [Zn(phen)(edda)]-treated MCF7 cells were 30.74%, 32.19% and 35.46%, respectively. Interestingly, the compounds showed a progression from early-stage apoptosis and finally to late-stage

apoptosis [Figures 4.16-4.18]. The apoptotic cells were significantly increased in a time-dependent manner. Hence, these results showed that the [M(phen)(edda)] compounds induced apoptosis in MCF7 cells.

(a) Untreated Control **(b) Cisplatin**
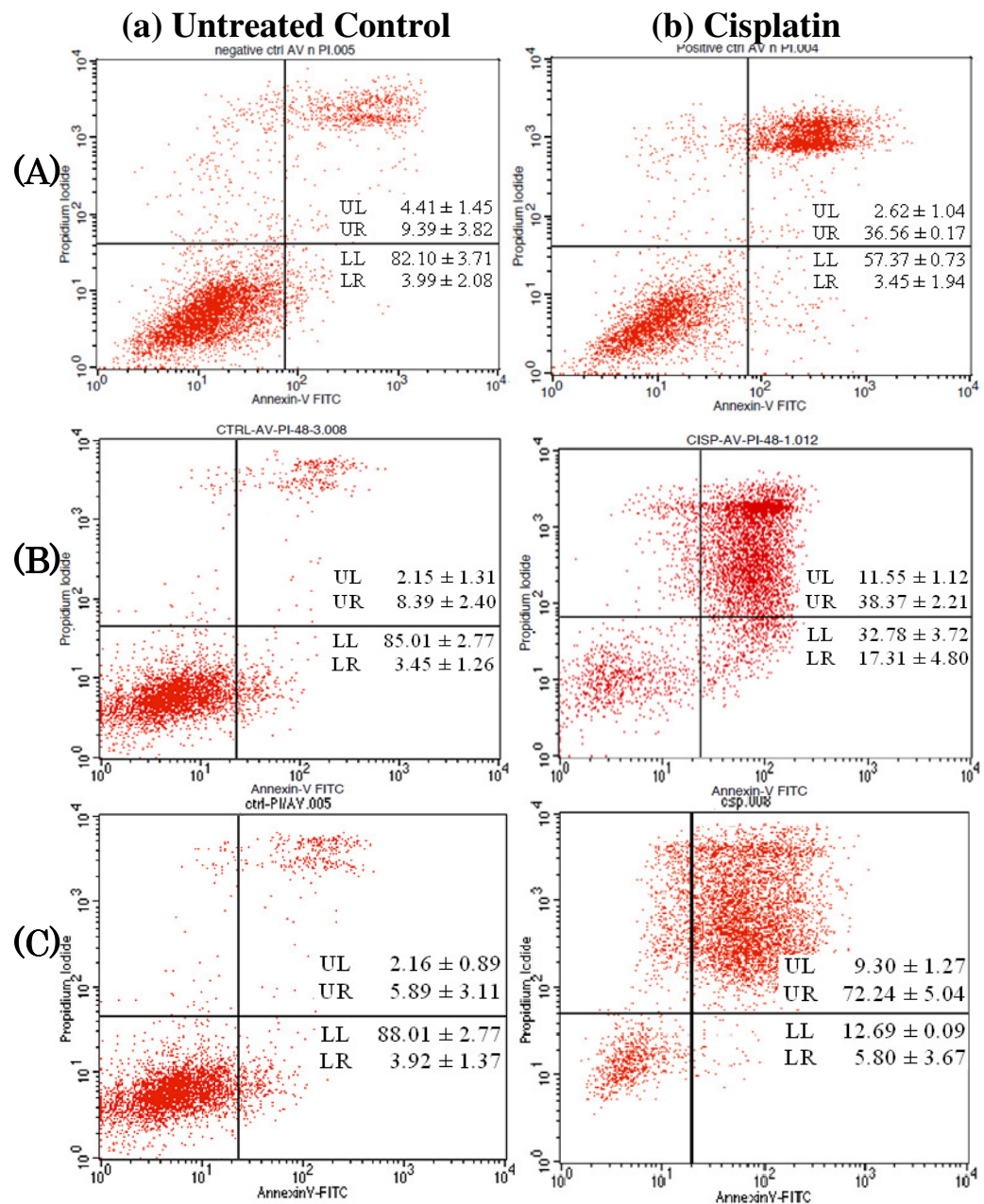
Figure 4.15: FACS Analysis of Induction of Apoptosis of Untreated MCF7 Cells Versus Cisplatin-treated MCF7 Cells For 24, 48 and 72 h. Cells were harvested and stained with annexin V-FITC (*x*-axis) and propidium iodide (*y*-axis) analyzed by flow cytometry. The percentage of cells in viable condition (LL), necrosis (UL), early (LR) and late (UR) apoptosis is indicated in each quadrant and determined by Cell Quest analysis software in dot-plots. Data represented mean values of three independent experiments and same as the following figures.

(a) Untreated cells showed a majority of viable healthy cells with 82.10%, 85.01% and 88.01% after 24 (A), 48 (B) and 72 (C) h incubation on MCF7 cells. (b) With treatment of 10 µg/ml of cisplatin, increased number of apoptotic cells observed as compared to control. Cisplatin was used as a positive control.
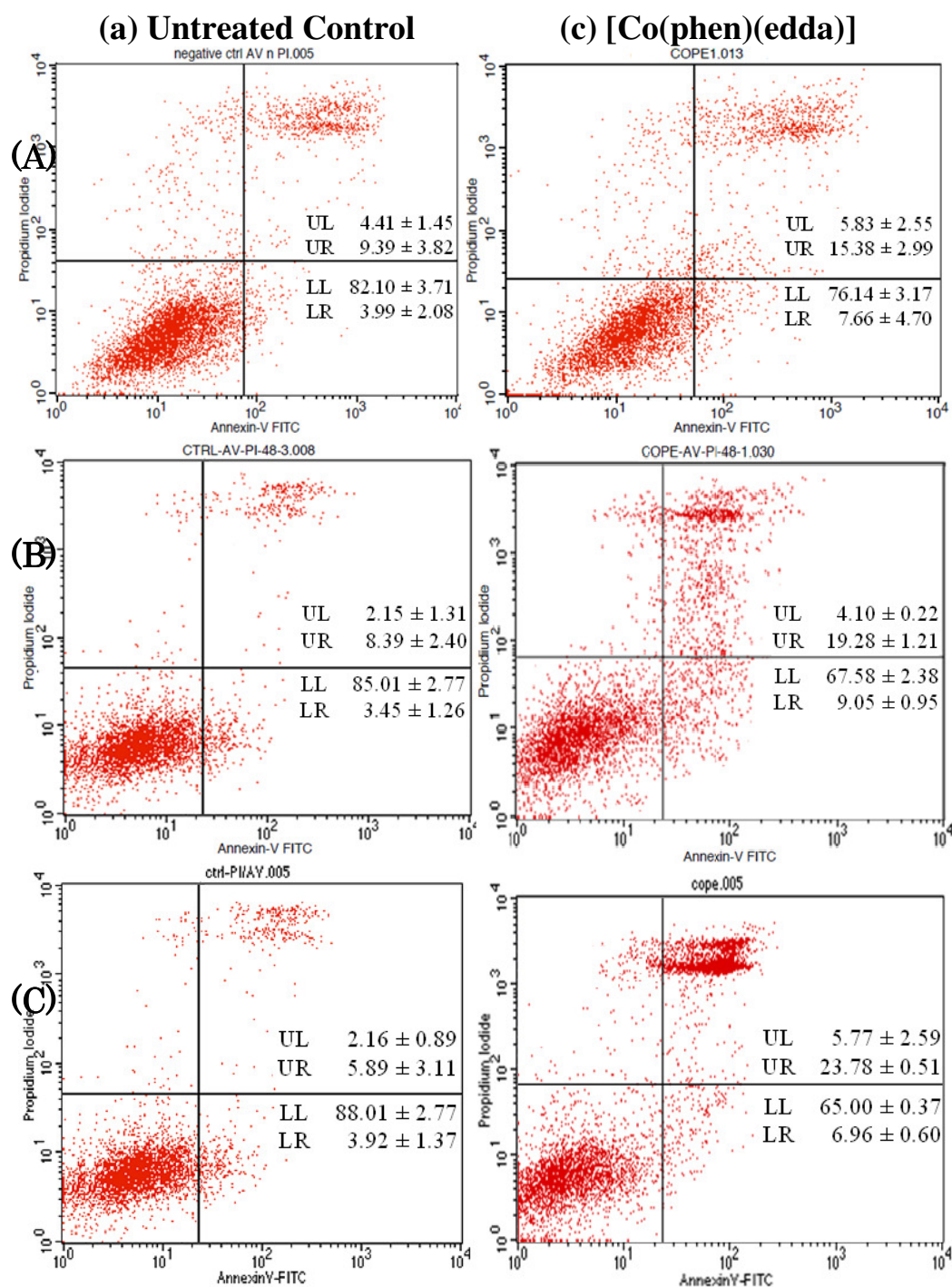
Figure 4.16: FACS Analysis of Induction of Apoptosis of Untreated MCF7 Cells Versus [Co(phen)(edda)]-treated MCF7 Cells For 24, 48 and 72 h.

(a) Untreated cells showed a majority of viable healthy cells with 82.10%, 85.01% and 88.01% after 24 (A), 48 (B) and 72 (C) h incubation on MCF7 cells. (b) MCF7 cells treated with 13.5 µM [Co(phen)(edda)] for three separate days showed increased number of apoptotic cells as compared to control.
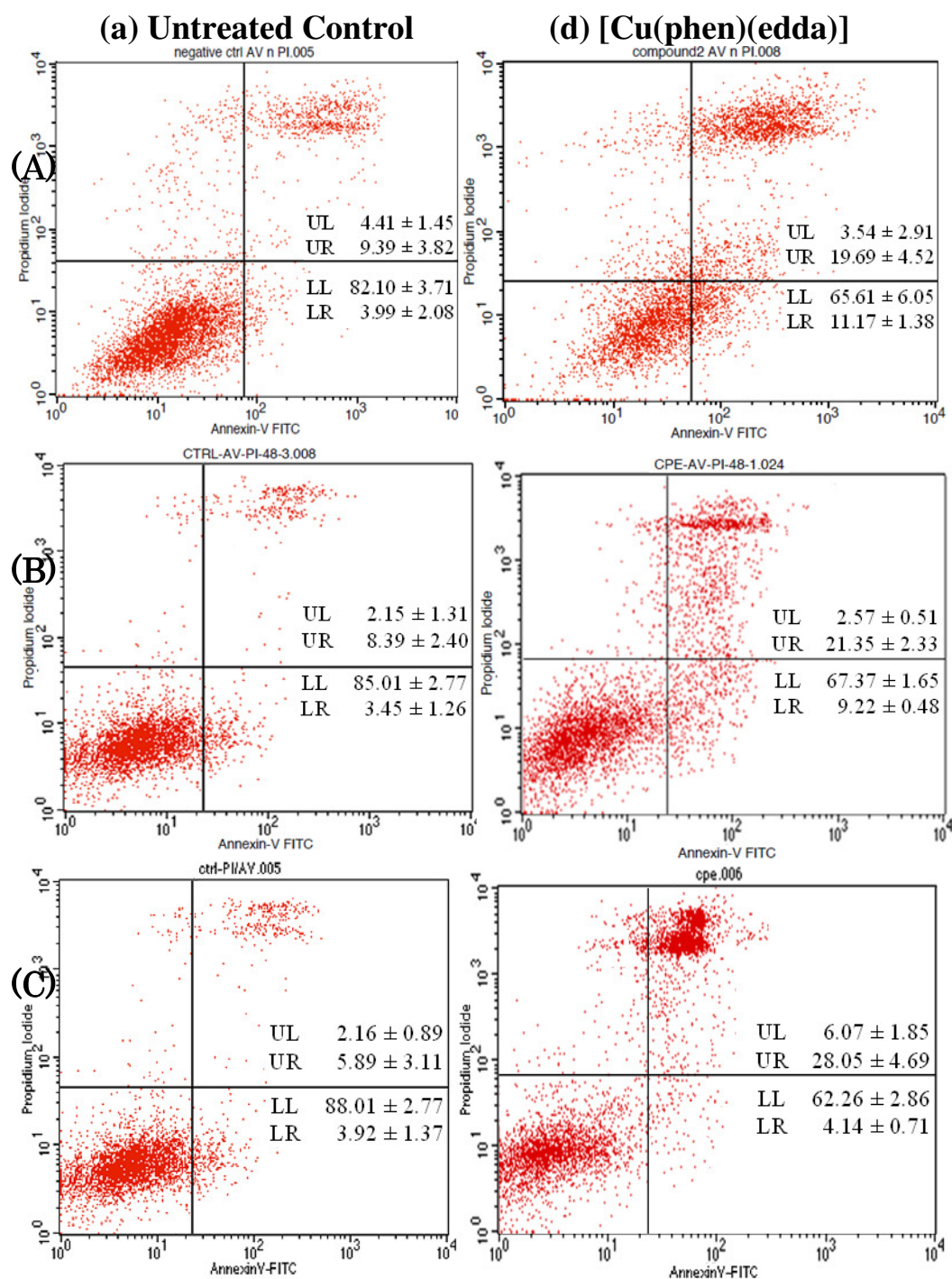
Figure 4.17: FACS Analysis of Induction of Apoptosis of Untreated MCF7 Cells Versus [Cu(phen)(edda)]-treated MCF7 Cells For 24, 48 and 72 h.

(a) Untreated cells showed a majority of viable healthy cells with 82.10%, 85.01% and 88.01% after 24 (A), 48 (B) and 72 (C) h incubation on MCF7 cells. (d) MCF7 cells treated with 2.8 µM [Cu(phen)(edda)] for three separate days showed increased number of apoptotic cells as compared to control.

(a) Untreated Control   (e) [Zn(phen)(edda)]
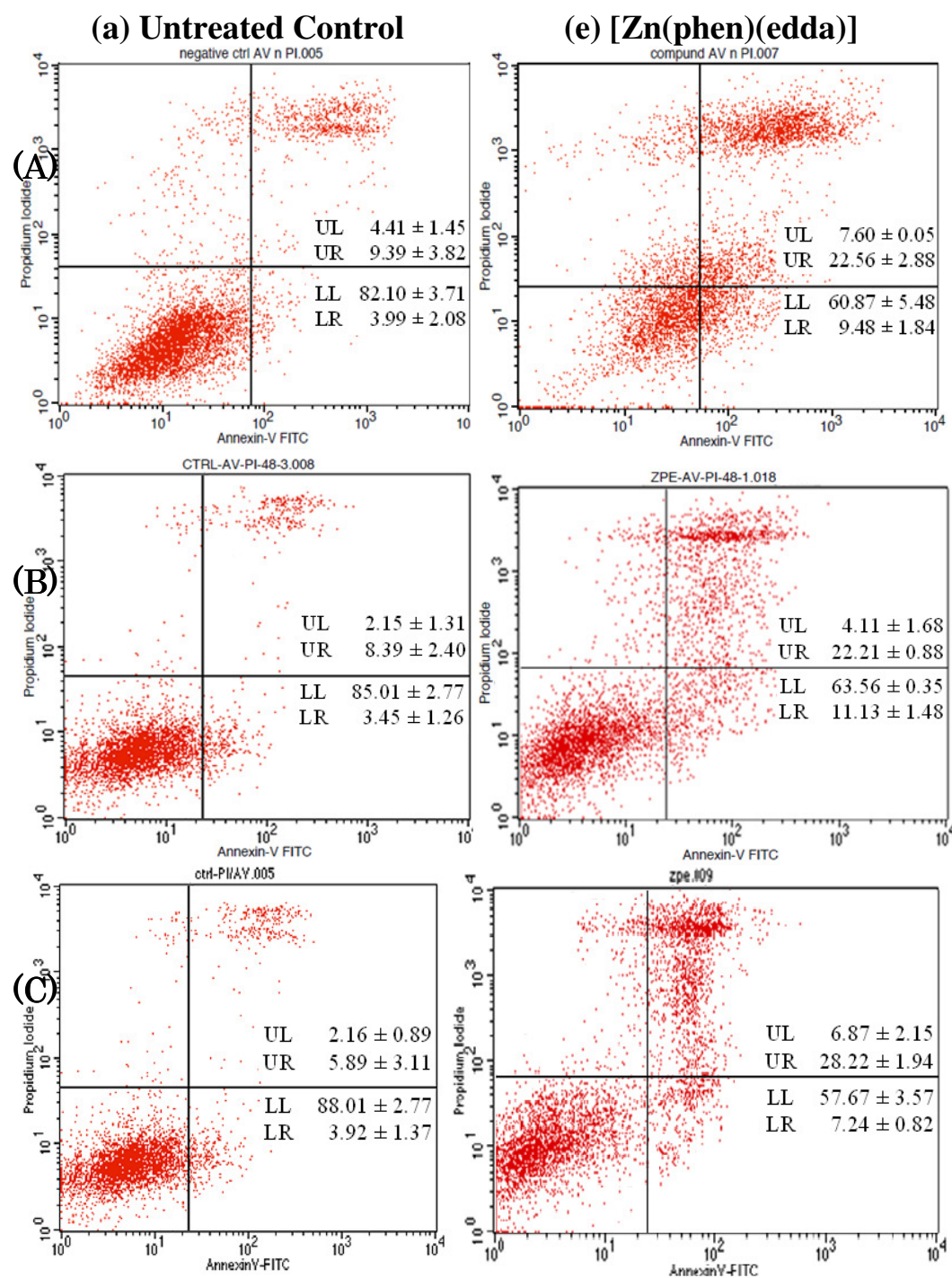
Figure 4.18: FACS Analysis of Induction of Apoptosis of Untreated MCF7 Cells Versus [Zn(phen)(edda)]-treated MCF7 Cells For 24, 48 and 72 h.

(a) Untreated cells showed a majority of viable healthy cells with 82.10%, 85.01% and 88.01% after 24 (A), 48 (B) and 72 (C) h incubation on MCF7 cells. (e) MCF7 cells treated with 5 µM [Zn(phen)(edda)] for three separate days showed increased number of apoptotic cells as compared to control.
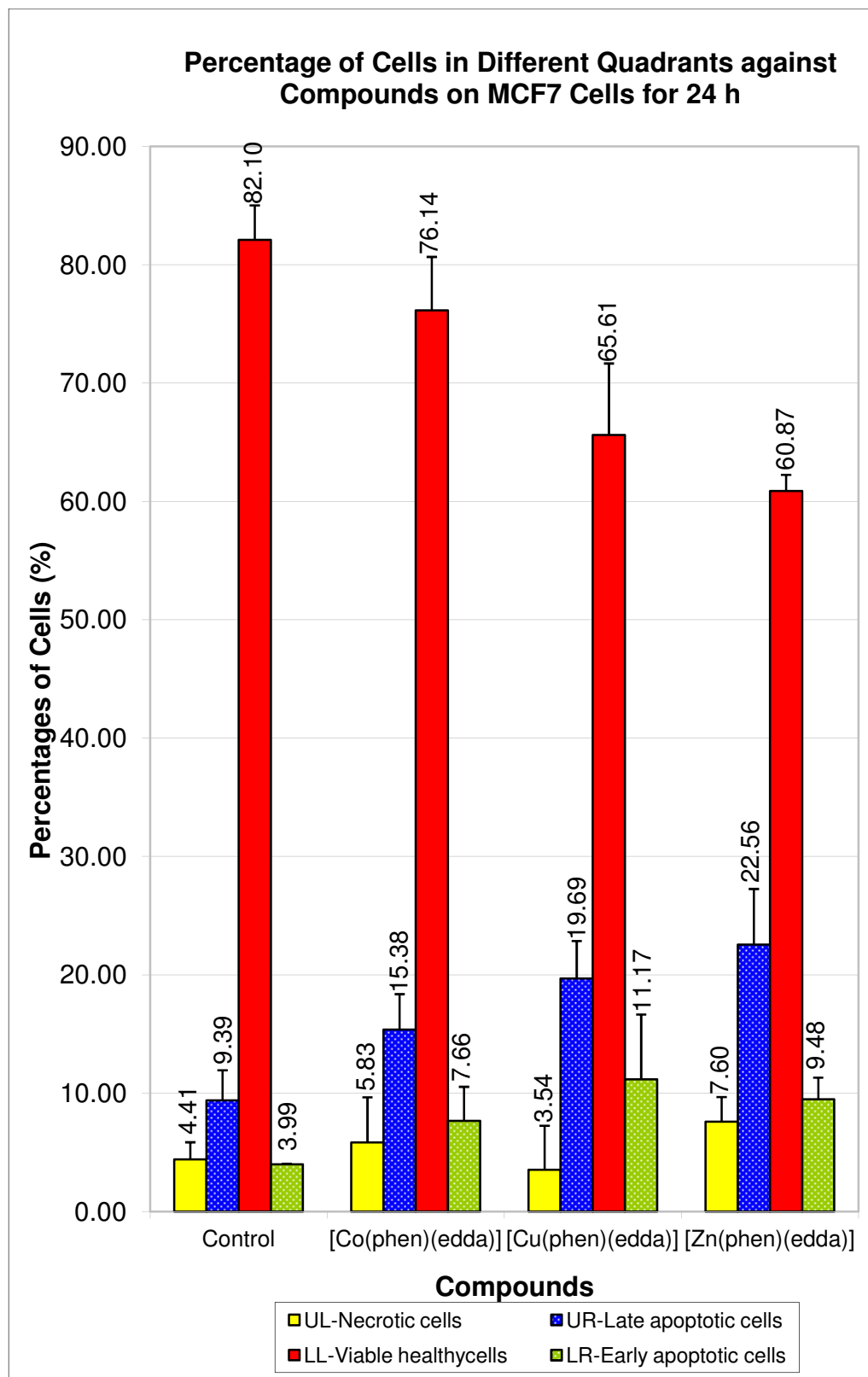
Figure 4.19: Histogram of Percentages of Cells in Different Quadrants in MCF7 Cultures with Treatment and Without Treatment for 24 h. Histogram showing the percentages of cells at viable healthy stage (LL), necrosis (UL), early apoptosis (LR) and late apoptosis (UR). Data were means of three independent experiments ± S.E. (bars).
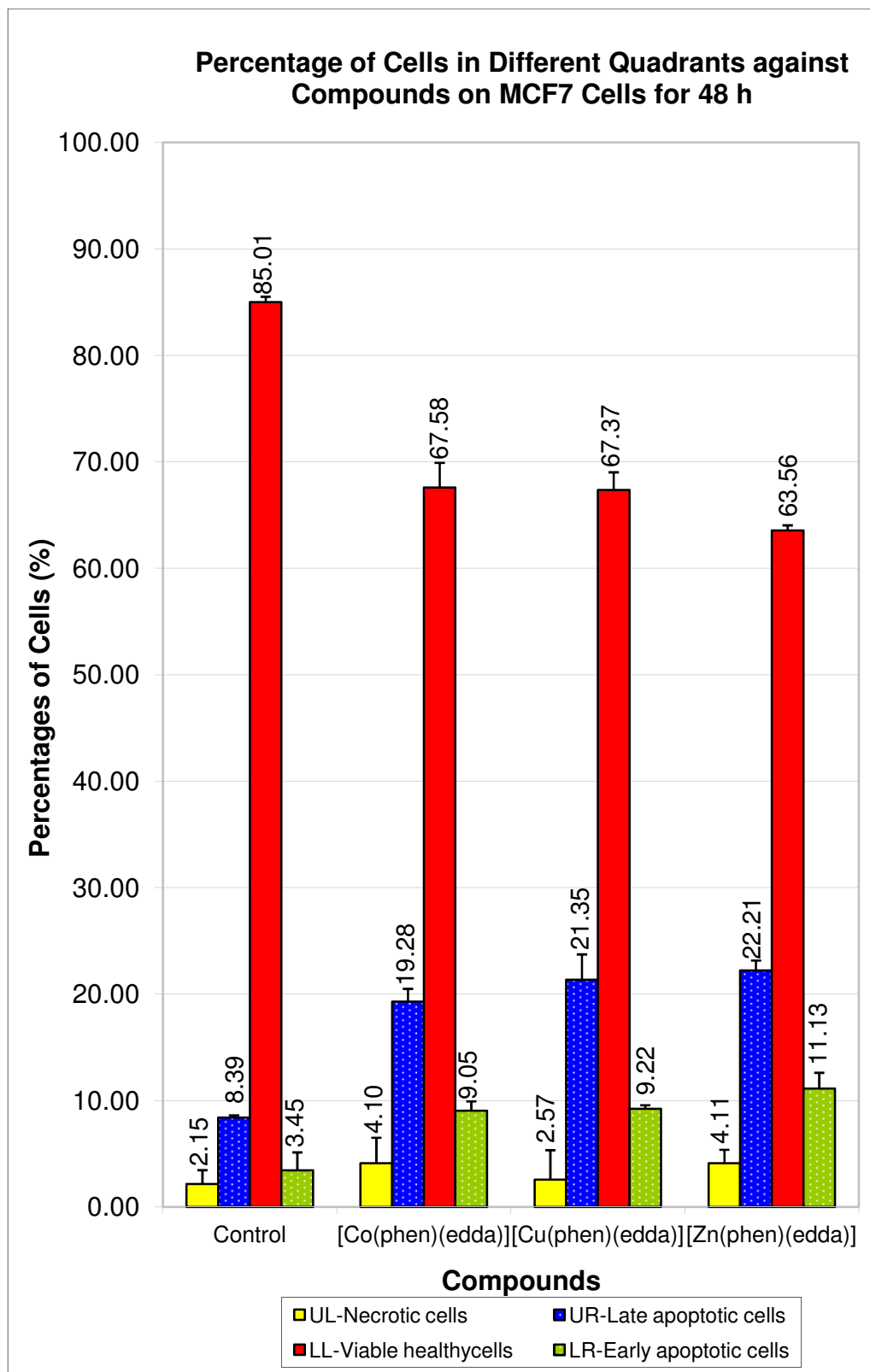
Figure 4.20: Histogram of Percentages of Cells in Different Quadrants in MCF7 Cultures with Treatment and Without Treatment for 48 h. Histogram showing the percentages of cells at viable healthy stage (LL), necrosis (UL), early apoptosis (LR) and late apoptosis (UR). Data were means of three independent experiments ± S.E. (bars).
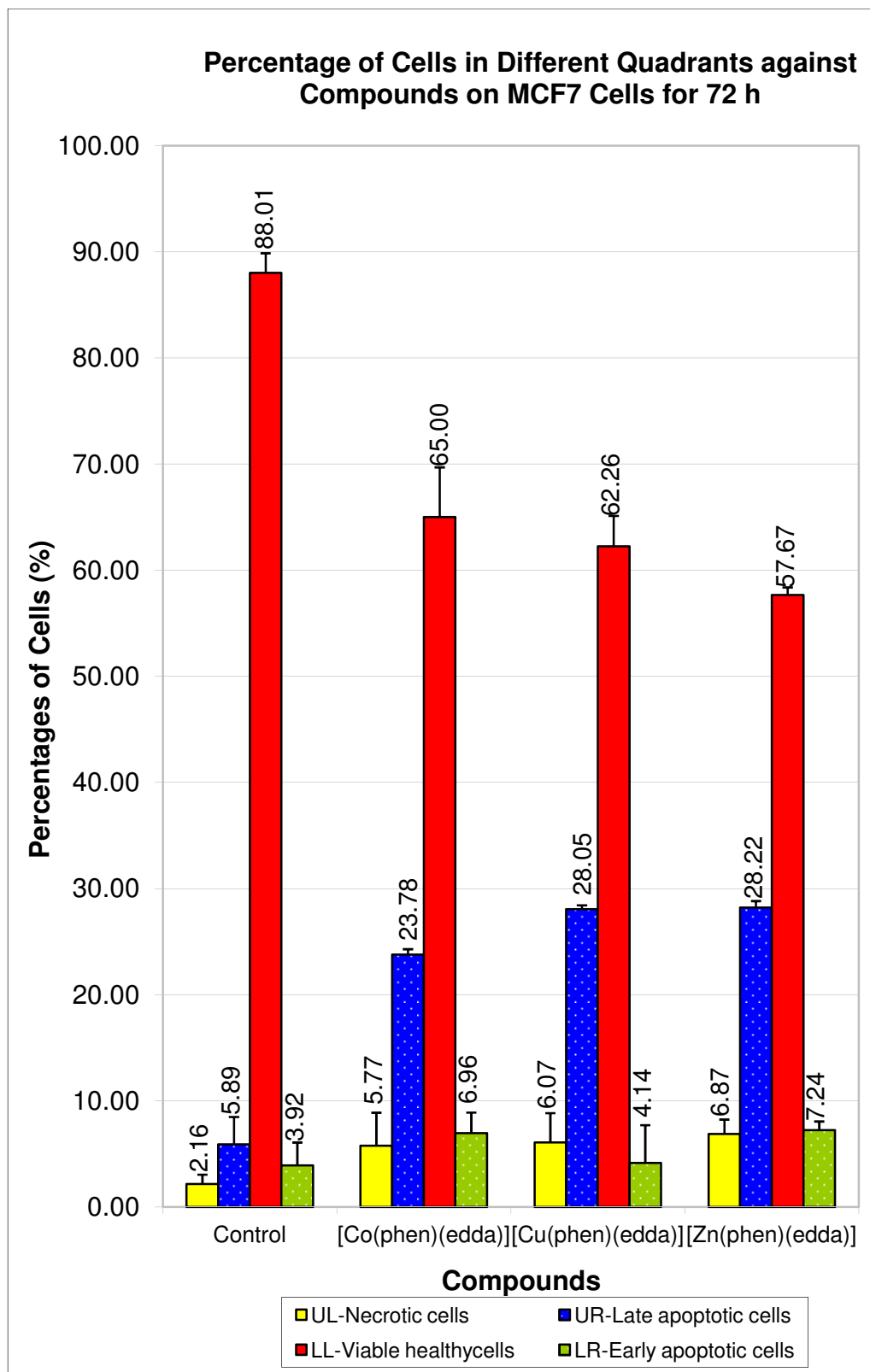
Figure 4.21: Histogram of Percentages of Cells in Different Quadrants in MCF7 Cultures with Treatment and Without Treatment for 72 h. Histogram showing the percentages of cells at viable healthy stage (LL), necrosis (UL), early apoptosis (LR) and late apoptosis (UR). Data were means of three independent experiments ± S.E. (bars).

4.5 Analysis of Cell Cycle Arrest in MCF7 Cells

MCF7 cells were treated with [Co(phen)(edda)], [Cu(phen)(edda)] and [Zn(phen)(edda)] for 24, 48 and 72 h for cell cycle analysis. Fluorescence activated cell sorting (FACS) was used for this purpose. In FACS analysis, cells are sampled from a growing cell culture and the total fraction of cells with different DNA contents is determined. FACS analysis will then give the fraction of cells in sub G_0/G_1, G_0/G_1, S and G_2/M phase with their characteristic amount of DNA. Briefly, MCF7 cells were seeded and allowed to adhere for 70% confluence. Cells were collected 24 h after seeding and treated with [Co(phen)(edda)], [Cu(phen)(edda)] and [Zn(phen)(edda)] for varying time periods. Cells were harvested, fixed and stained with propidium iodide before proceeding to cell sorting and cell cycle analysis. Untreated cells were used as a control and nocodazole was used as a positive control. Nocodazole is an inhibitor of mitosis that acts by preventing the microtubule assembly and cause arrest in G_2/M phase of the cell cycle (Cooper *et al.*, 2006). Each result was obtained from three independent experiments. The percentage increase or decrease in the number of cells in each phase of the cell cycle compared to that in the control was determined (Figures 4.26-4.28).

Untreated MCF7 cells exhibited an asynchronous cell cycle profile following 24, 48 and 72 h in culture [Figures 4.22-4.25, (1)]. The majority of the cells were at the G_0/G_1 phase (24 h, 57.04%; 48 h, 58.40%; 72 h, 60.23%), while only 27.51% (in 24 h), 29.66% (in 48 h) and 26.07% (in 72 h) of cells were found to be at the G_2/M phase of the cell cycle respectively.

Morphologically, untreated cells appeared flat with few floaters. In comparison, 0.2 µg/ml nocodazole-treated cells showed cells accumulating at sub G_0/G_1 phase (28.29% in 24 h, 33.04% in 48 h and 40.73% in 72 h) and at G_2/M phase (36.22% in 24 h, 37.20% in 48 h and 42.44% in 72 h) [Figure 4.22(2)]. PI DNA staining showed increase in percentages distribution of cells at sub G_0/G_1 phase which is a hallmark of apoptosis and induced cell cycle arrest at G_2/M phase when treated with nocodazole. Morphologically, nocodazole-treated cells appeared rounded and shiny.

By contrast, MCF7 cells exposed to 13.5 µM [Co(phen)(edda)] for 24 h showed a similar cell cycle profile (G_0/G_1, S and G_2/M) to untreated cells except that there was a small increase in percentages of cells in sub G_0/G_1 phase [(Figure 4.23, (A)]. The proportion of cells with hypodiploid DNA in this sub G_0/G_1 phase was slightly increased from 5.78% to 11.42% at 24 h. As there was no significant increase in the population of MCF7 cells in G_0/G_1, S and G_2/M phases compared to those of untreated cells when they were treated with cobalt compound for 24 h, cell cycle arrest did not occur. The percentages of cells were 56.09% in G_0/G_1 phase, 8.51% in S phase and 24.31% in G_2/M phase (Figure 4.26). MCF7 cells exposed to 2.8 µM [Cu(phen)(edda)] for 24 h showed a similar cell cycle profile to untreated cells except that there was a significant increase in percentages of cells in sub G_0/G_1 phase [(Figure 4.24, (A)]. Here, cells in sub G_0/G_1 phase with hypodiploid DNA content were slightly increased from 5.78% to 13.97% at 24 h incubation. As there was no obvious increase in the population of cells in G_0/G_1, S and G_2/M phase when cells were treated with copper compound for 24 h, no cell cycle occurred. The

percentages of cells in G_0/G_1 phase were 54.09%, 8.18% in S phase and 23.67% in G_2/M phase (Figure 4.26). While, MCF7 cells exposed to 5 µM [Zn(phen)(edda)] for 24 h showed a similar cell cycle profile to untreated cells but displayed a slight increase in percentages of cells in sub G_0/G_1 phase [(Figure 4.25, (A)]. The composition of cells with hypodiploid DNA in sub G_0/G_1 phase were slightly increased from 5.78% to 13.90% at 24 h. Treatment of MCF7 cells with this zinc compound did not induce cell cycle arrest at 24 h because there was no significant difference in distribution of cells in G_0/G_1, S and G_2/M phases as compared to untreated MCF7 cells. The percentages of cells in G_0/G_1 phase were 52.54%, 11.29% in S phase and 22.82% in G_2/M phase (Figure 4.26). In summary, all [M(phen)(edda)] complexes exhibited increase of population of cells in sub G_0/G_1 phase due to apoptosis but did not induce cell cycle arrest at G_0/G_1, S or G_2/M phases.

After 48 h of incubation, MCF7 cells treated with 13.5 µM [Co(phen)(edda)] still showed a similar cell cycle profile to untreated cells [(Figure 4.23, (B)]. Again the population of cells in sub G_0/G_1 phase (i.e. with hypodiploid DNA) was slightly increased from 5.80% to 12.51% at 48 h. The percentages of cells were 61.17% in G_0/G_1 phase, 5.20% in S phase and 21.45% in G_2/M phase (Figure 4.27). Thus, there was no significant increase in the population of cells in G_0/G_1, S and G_2/M phase when treated with cobalt compound at 48 h, showing no cell cycle arrest at these phases. MCF7 cells exposed to 2.8 µM [Cu(phen)(edda)] for 48 h showed increase in percentage of cells in sub G_0/G_1 phase compared to untreated cells [(Figure 4.24, (B)]. Here, cells in sub G_0/G_1 phase with hypodiploid DNA content were increased from

5.80% to 17.74% at 24 h. The percentages of cells in G_0/G_1 phase were 53.68%, 5.99% in S phase and 22.83% in G_2/M phase (Figure 4.27). There was no obvious increase in population of cells in G_0/G_1, S and G_2/M phases when treated with copper compound at 48 h, and no cell cycle arrest activity was observed at these phases. However, MCF7 cells treated with 5 μM [Zn(phen)(edda)] for 48 h showed a little different cell cycle profile as compared to untreated cells [(Figure 4.25, (B)]. The percentage of cells sub G_0/G_1 phase (i.e. with hypodiploid DNA content) increased from 5.80% to 15.70%, which was similar to the results of other complexes. [Zn(phen)(edda)]-treated cells were slightly blocked in the S phase (from 8.98% to 12.50%) at 48 h. The percentages of cells in two other phases, G_0/G_1 and G_2/M were 51.54% and 20.71% (Figure 4.27). Notably, [Co(phen)(edda)] and [Cu(phen)(edda)] complexes exhibited the same effects for the incubation time of 48 h with only increase of population of cells in sub G_0/G_1 phase due to apoptosis but did not induce cell cycle arrest at G_0/G_1, S and G_2/M phase. On the other hand, treatment of MCF7 cells with [Zn(phen)(edda)] complex showed that a small increase of population of cells in S phase, showing cell cycle arrest of cancer cells at this phase.

After 72 h of incubation, MCF7 cells treated with 13.5 μM [Co(phen)(edda)] showed a similar cell cycle profile to untreated cells but there was a further increase in percentages of cells in sub G_0/G_1 phase [(Figure 4.23, (C)]. The content of hypodiploid DNA in sub G_0/G_1 phase was slightly increased from 7.40% to 15.55% at 72 h. The percentages of cells were 55.45% in G_0/G_1 phase, 8.11% in S phase and 22.67% in G_2/M phase (Figure 4.28).

There was no distinct increase in the population of cells in G_0/G_1, S and G_2/M phase when cells were treated with cobalt compound for 72 h. Thus the cobalt compound did not induce any cell cycle arrest. MCF7 cells treated with 2.8 µM [Cu(phen)(edda)] for 72 h showed a similar cell cycle profile to that of untreated cells but showed a large increase in percentage of cells in sub G_0/G_1 phase [(Figure 4.24, (C)]. The increase in percentage of apoptotic cells, as shown by sub G_0/G_1 peak increasing from 7.40% to 30.44%, due to [Cu(phen)(edda)] is the highest when compared to those due to the other [M(phen)(edda)] complexes. The percentages of cells in G_0/G_1, S and G_2/M phases were 46.52%, 6.77% and 20.84%, respectively (Figure 4.28). There was no obvious increase in population of cells in G_0/G_1, S and G_2/M phases when treated with copper compound at 72 h. This meant that there was no cell cycle arrest induced by [Cu(phen)(edda)]. However, MCF7 cells treated with 5 µM [Zn(phen)(edda)] for 72 h showed a different cell cycle profile as compared to untreated cells [(Figure 4.25, (C)]. There was a marked decrease in the proportion of cells in G_2/M phase (from 26.07 to 9.25%) and significant increase in the proportion of cells in S phase (from 9.43% to 16.96%). This meant there was cell cycle arrest at S phase. Appearance of sub G_0/G_1 cells with a distinct peak (from 7.40% to 25.26%) usually indicate apoptosis induced by tested drugs. Increase in sub G_0/G_1 phase was apparent at 48 until 72 h (Figure 4.28). In contrast, MCF7 cells treated with [Co(phen)(edda)] and [Cu(phen)(edda)] showed no obvious cell cycle arrest at S phase, but more cells were present in the sub G_0/G_1 phase, as compared to untreated MCF7 cells. At 72 h, treatment of MCF7 cells with [Co(phen)(edda)] and [Cu(phen)(edda)] underwent apoptosis as evidenced by 15.55% and 30.44% of

cells at sub G_0/G_1 phase, respectively (Figure 4.28). Interestingly, prolonged treatment resulted in an increase in the number of apoptotic cells in [M(phen)(edda)]-treated MCF7 cells at 72 h. The results presented here indicated that [Zn(phen)(edda)] induced cell growth inhibition through apoptosis and induction of cell cycle arrest while [Co(phen)(edda)] and [Cu(phen)(edda)] only induced apoptosis in MCF7 cells. The apoptosis of [M(phen)(edda)]-treated MCF7 cells as inferred from cell cycle data was in agreement with the previous findings from morphology studies and the apoptosis study using Annexin V/PI staining.

(1) Untreated Control   **(2) Nocodazole**
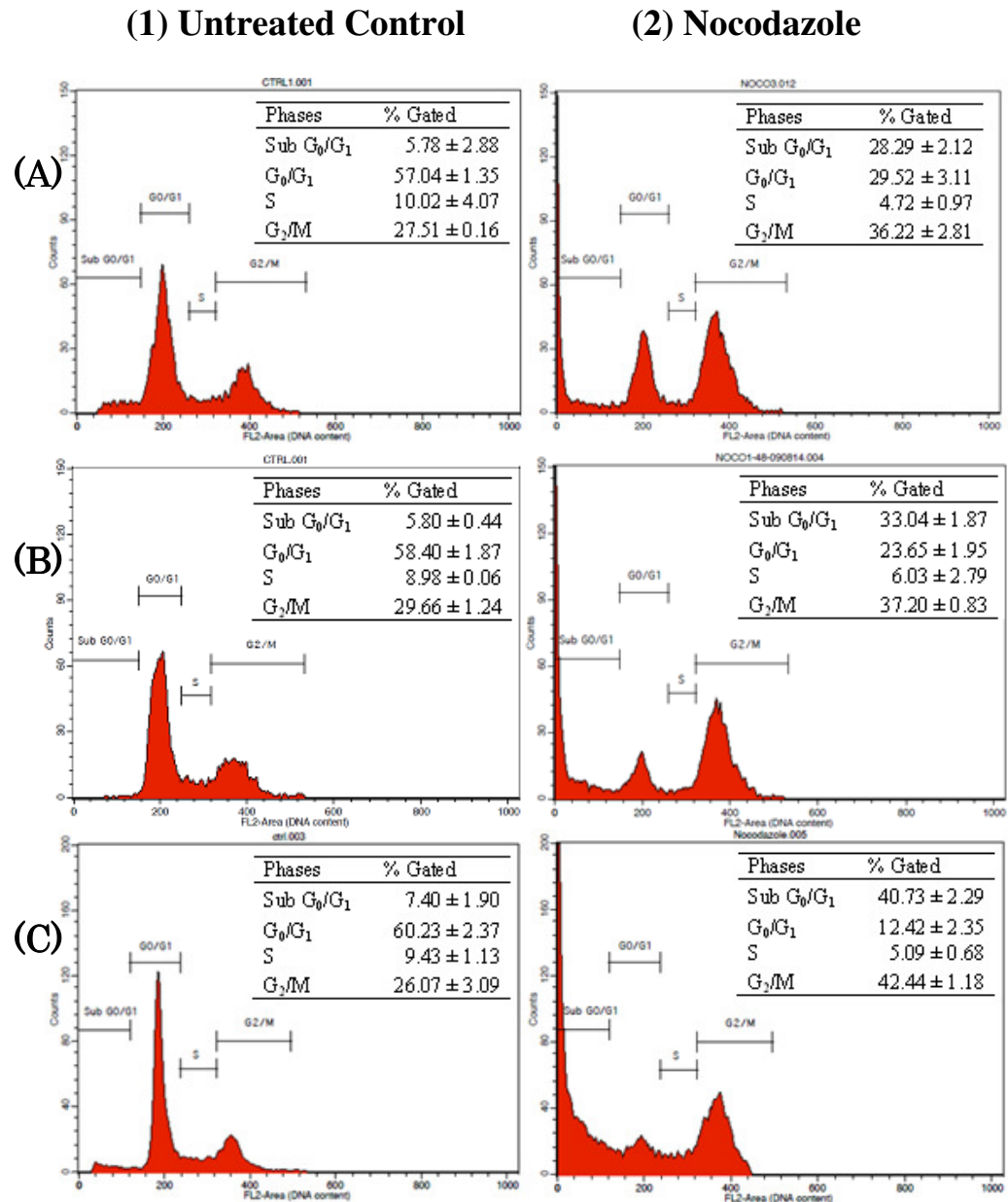
Figure 4.22: FACS Analysis of Cell Cycle Arrest of Untreated MCF7 Cells versus Nocodazole-treated MCF7 Cells for 24, 48 and 72 h. Cells were fixed and stained with PI. Percentages of the sub G_0/G_1, G_0/G_1, S and G_2/M phase were determined by Cell Quest analysis software on the basis of DNA content of the histogram. Data represented mean values of three independent experiments and same as the following figures.

(1) Untreated MCF7 cells exhibited asynchronous cell cycle profile following 24(A), 48(B) and 72(C) h in culture. (2) In contrast, MCF7 cells treated with 0.2 µg/ml of nocodazole for three separate days arrested G_2/M phase. Nocodazole was used as a positive control.

(1) Untreated Control   (3)[Co(phen)(edda)]

(A)

Phases	% Gated
Sub G_0/G_1	5.78 ± 2.88
G_0/G_1	57.04 ± 1.35
S	10.02 ± 4.07
G_2/M	27.51 ± 0.16

Phases	% Gated
Sub G_0/G_1	11.42 ± 1.34
G_0/G_1	56.09 ± 3.90
S	8.51 ± 3.15
G_2/M	24.31 ± 0.79

(B)

Phases	% Gated
Sub G_0/G_1	5.80 ± 0.44
G_0/G_1	58.40 ± 1.87
S	8.98 ± 0.06
G_2/M	29.66 ± 1.24

Phases	% Gated
Sub G_0/G_1	12.51 ± 4.00
G_0/G_1	61.17 ± 3.00
S	5.20 ± 1.01
G_2/M	21.45 ± 0.01

(C)

Phases	% Gated
Sub G_0/G_1	7.40 ± 1.90
G_0/G_1	60.23 ± 2.37
S	9.43 ± 1.13
G_2/M	26.07 ± 3.09

Phases	% Gated
Sub G_0/G_1	15.55 ± 1.86
G_0/G_1	55.45 ± 4.94
S	8.11 ± 0.75
G_2/M	22.67 ± 1.54

Figure 4.23: FACS Analysis of Cell Cycle Arrest of Untreated MCF7 Cells versus [Co(phen)(edda)]-treated MCF7 Cells for 24, 48 and 72 h.

(1) Untreated MCF7 cells exhibited asynchronous cell cycle profile following 24(A), 48(B) and 72(C) h in culture. (3) MCF7 cells treated with 13.5 µM of [Co(phen)(edda)] for three separate days showed a similar cell cycle profile to untreated cells but an increased in percentage of cells in sub G_0/G_1 phase.
.

(1) Untreated Control   **(4) [Cu(phen)(edda)]**
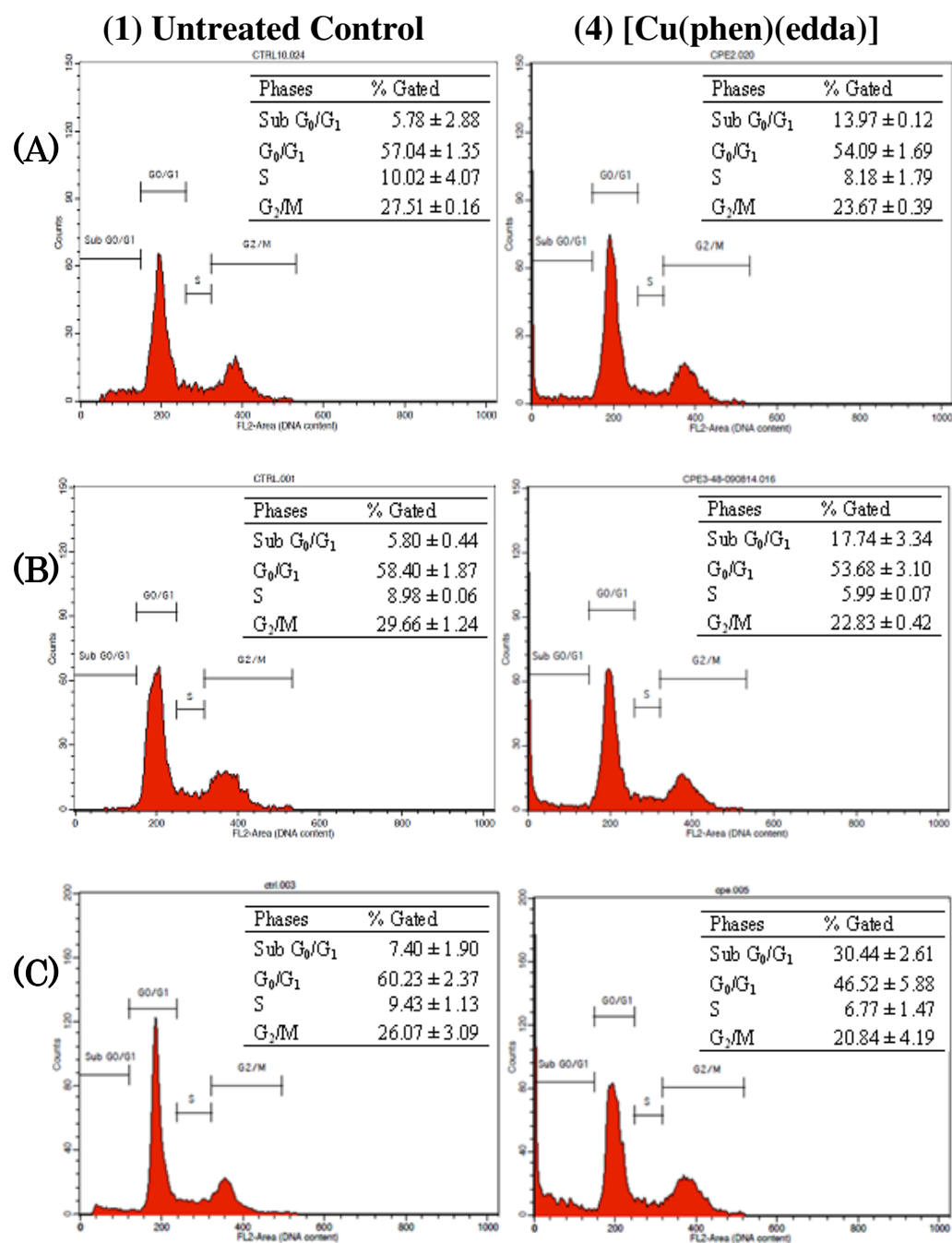
Figure 4.24: FACS Analysis of Cell Cycle Arrest of Untreated MCF7 Cells versus [Cu(phen)(edda)]-treated MCF7 Cells For 24, 48 and 72 h.

(1) Untreated MCF7 cells exhibited asynchronous cell cycle profile following 24(A), 48(B) and 72(C) h in culture. (4) MCF7 cells treated with 2.8 μM of [Cu(phen)(edda)] for three separate days showed a similar cell cycle profile to untreated cells but an increased in percentage of cells in sub G_0/G_1 phase.

(1) Untreated Control   **(5) [Zn(phen)(edda)]**

Phases	% Gated
Sub G_0/G_1	5.78 ± 2.88
G_0/G_1	57.04 ± 1.35
S	10.02 ± 4.07
G_2/M	27.51 ± 0.16

Phases	% Gated
Sub G_0/G_1	13.90 ± 1.05
G_0/G_1	52.54 ± 0.08
S	11.29 ± 2.59
G_2/M	22.82 ± 1.39

Phases	% Gated
Sub G_0/G_1	5.80 ± 0.44
G_0/G_1	58.40 ± 1.87
S	8.98 ± 0.06
G_2/M	29.66 ± 1.24

Phases	% Gated
Sub G_0/G_1	15.70 ± 1.62
G_0/G_1	51.54 ± 0.91
S	12.50 ± 1.03
G_2/M	20.71 ± 0.20

Phases	% Gated
Sub G_0/G_1	7.40 ± 1.90
G_0/G_1	60.23 ± 2.37
S	9.43 ± 1.13
G_2/M	26.07 ± 3.09

Phases	% Gated
Sub G_0/G_1	25.26 ± 2.19
G_0/G_1	51.78 ± 3.62
S	16.96 ± 1.74
G_2/M	9.25 ± 2.56
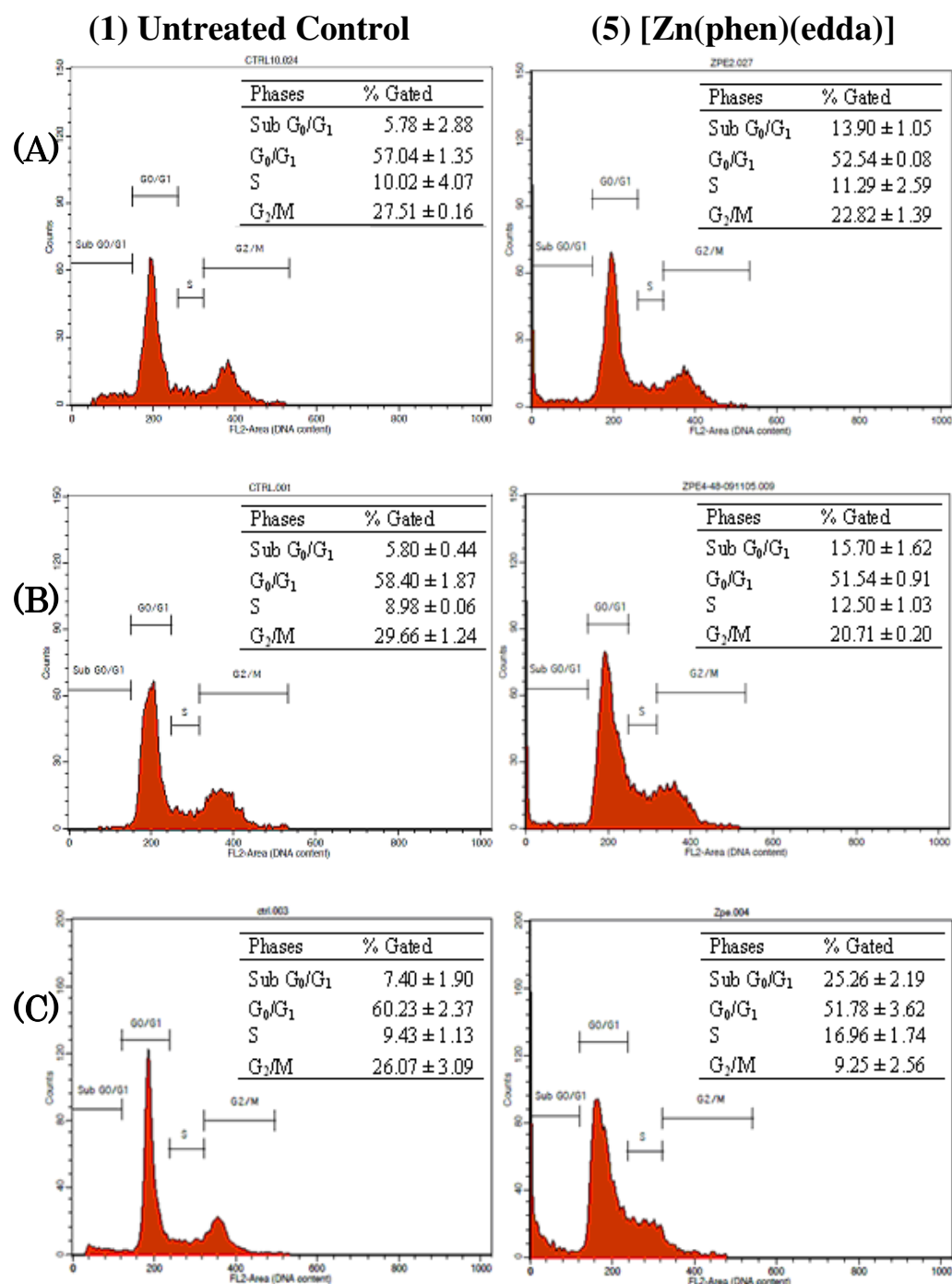
Figure 4.25: FACS Analysis of Cell Cycle Arrest of Untreated MCF7 Cells versus [Zn(phen)(edda)]-treated MCF7 Cells For 24, 48 and 72 h.

(a) Untreated MCF7 cells exhibited asynchronous cell cycle profile following 24(A), 48(B) and 72(C) h in culture. (e) In contrast, MCF7 cells treated with 5 µM of [Zn(phen)(edda)] for three separate days showed an increased of cells in sub G_0/G_1 phase and S phase block can be seen in the cell cycle profile.
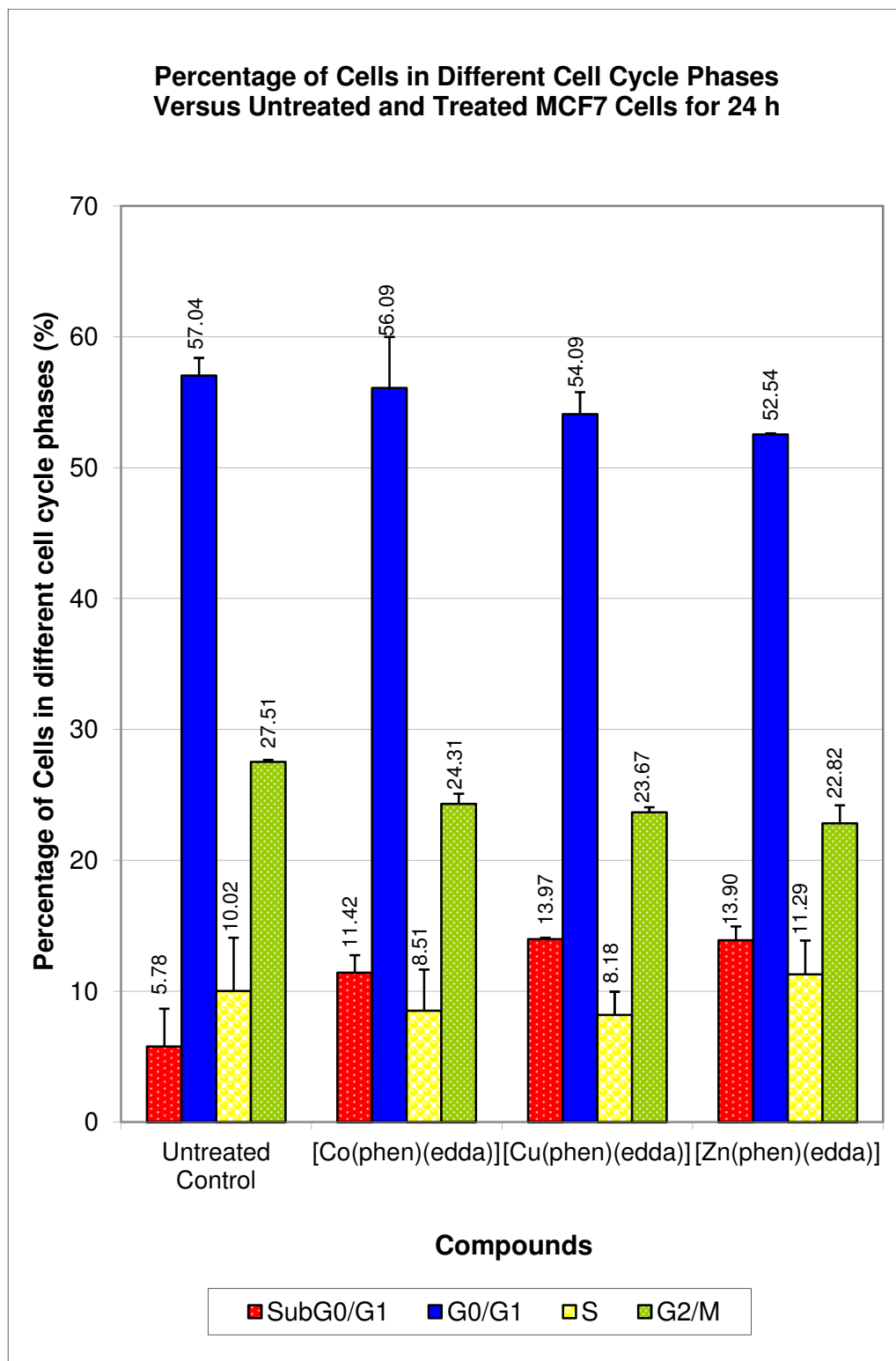
Figure 4.26: Histogram of Cell Cycle Distribution in MCF7 Cultures With Treatment and Without Treatment for 24 h. Histogram showing the percentages of cells at sub G_0/G_1, G_0/G_1, S and G_2/M phase of cell cycle. Data were means of three independent experiments ± S.E. (bars).
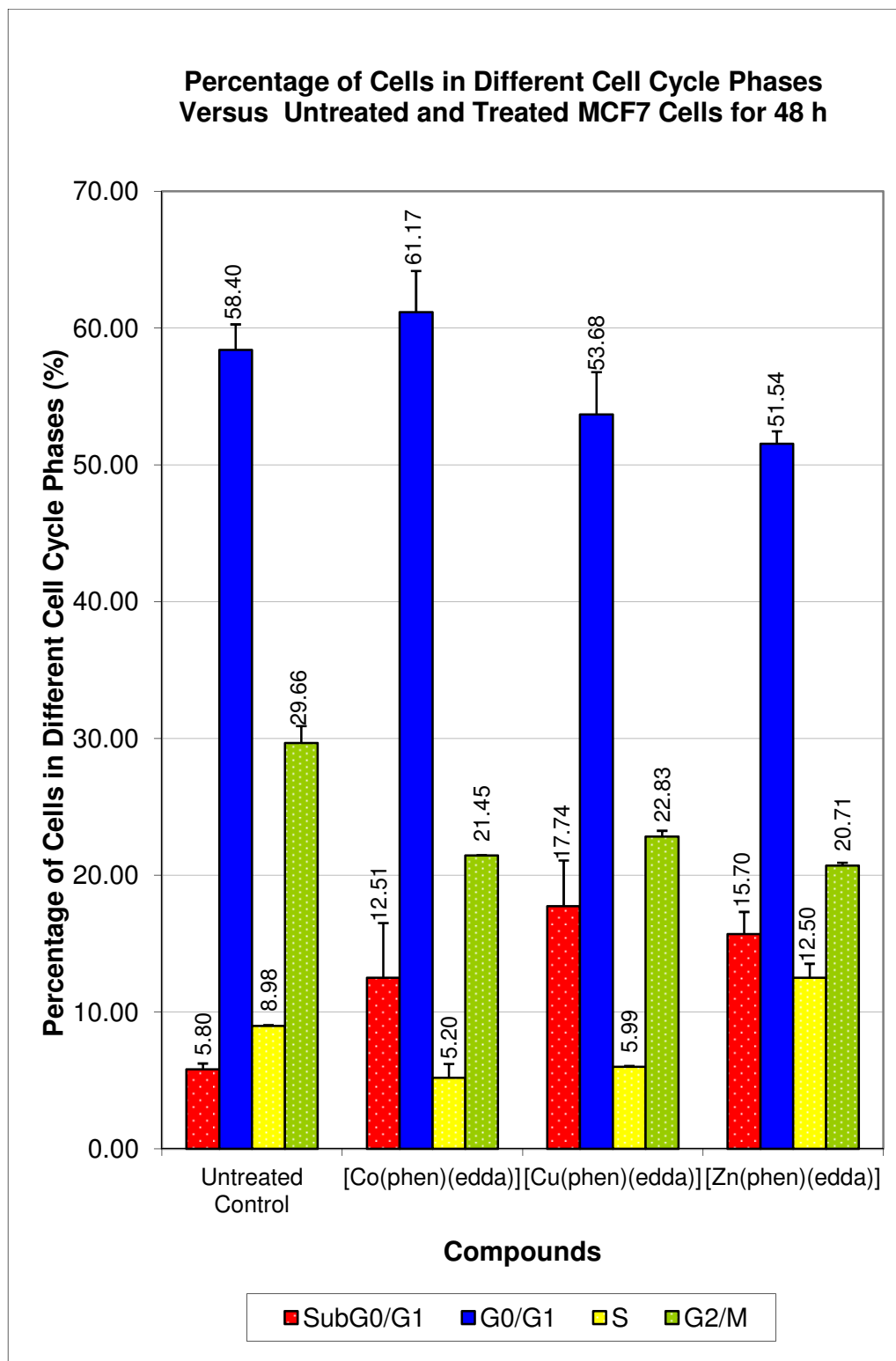
Figure 4.27: Histogram of Cell Cycle Distribution in MCF7 Cultures With Treatment and Without Treatment for 48 h. Histogram showing the percentages of cells at sub G_0/G_1, G_0/G_1, S and G_2/M phase of cell cycle. Data were means of three independent experiments ± S.E. (bars).
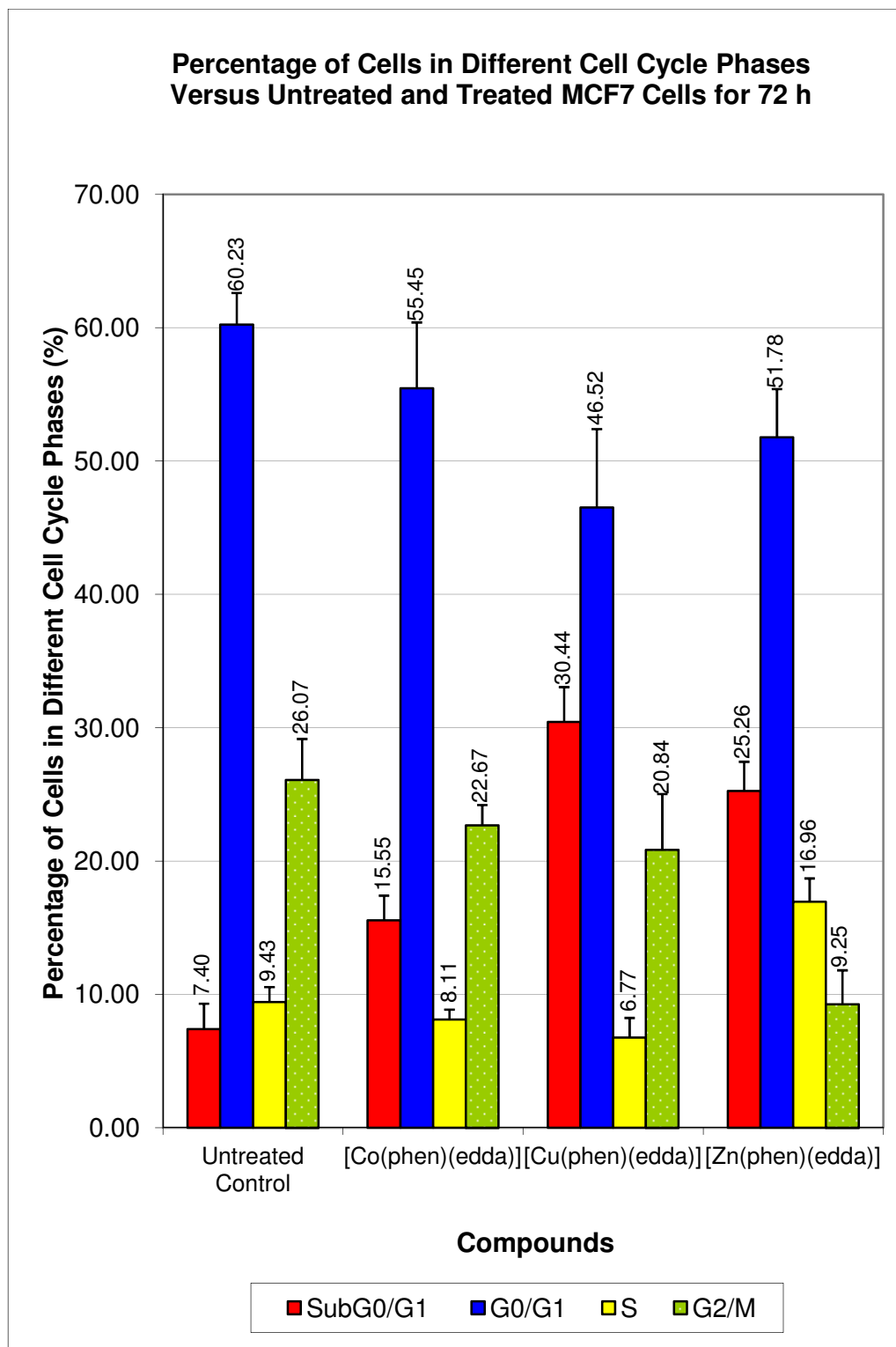
Figure 4.28: Histogram of Cell Cycle Distribution in MCF7 Cultures With Treatment and Without Treatment for 72 h. Histogram showing the percentages of cells at sub G_0/G_1, G_0/G_1, S and G_2/M phase of cell cycle. Exposure of cells to [Zn(phen)(edda)] showed different pattern in distribution of cell cycle compared to untreated control. Data were means of three independent experiments ± S.E. (bars).

4.6 Mitochondrial Fluorescent Intensity by Flow Cytofluorimetric Analysis in MCF7 Cells

To assess if [Co(phen)(edda)], [Cu(phen)(edda)] and [Zn(phen)(edda)] contributed to the initiation of apoptosis *via* a mitochondrial-regulated mechanism, the $\Delta\psi_m$ of the cells was determined with and without treatment with [M(phen)(edda)] complexes by using FACS analysis. MCF7 cell line was used as a model in this study as described. MCF7 cells were seeded and allowed to reach 70% confluence. Cells were collected after seeding and treated with 13.5 µM [Co(phen)(edda)], 2.8 µM [Cu(phen)(edda)] and 5 µM [Zn(phen)(edda)] for 24, 48 and 72 h incubation time. Unfixed MCF7 cells were labeled with JC-1 stain and then analyzed on flow cytometer. The results were obtained from four independent experiments. In healthy non-apoptotic cells, the dye accumulates and aggregates within the mitochondria, resulting in bright red staining. It is known that JC-1 forms red emitting fluorescent 'J-aggregates' at a high membrane potential while the dye emits a monomeric green fluorescence at a lower membrane potential. Cells stained with JC-1 were then subjected to cytofluorimetric analyses to quantify the red and green fluorescent. In apoptotic cells, due to the collapse of the membrane potential, JC-1 cannot accumulate within the mitochondria and remains in the cytoplasm in its green-fluorescent monomeric form. During the experiments, R2 was labeled as the gated region of cells with intact michondrial membranes; and R3 was labeled as the gated region of cells with indication of a change in the $\Delta\psi_m$. These gated regions have been determined appropriately using the control and

[M(phen)(edda)]-treated MCF7 cells for each particular incubation time (24, 48 and 72 h).

Importantly, the fluorescence emission spectrum of JC-1 or uptake of the dye into mitochondria is dependent on its concentration which, in turn, is determined by the status of the $\Delta\psi_m$. In this study, untreated MCF7 cells showed red spectral shift resulting in higher levels of red fluorescence emission and formed JC-1 aggregates following 24, 48 and 72 h in culture [Figures 4.29-4.32, (a)]. The proportion of untreated control cells in high red fluorescence FL-2 (R2) gated channel were 80.86%, 87.88% and 89.74% for 24, 48 and 72 h incubation, respectively [Figures 4.29-4.32, (a)]. There were only small percentages of cells in monomeric form which emitted green fluoresence and these were captured in FL-1 (R3) gated channel. Here, the $\Delta\psi_m$ of normal healthy mitochondria were polarized and JC-1 was rapidly taken up by such mitochondria. This uptake increased the concentration gradient of JC-1 leading to the formation of J-aggregates within the mitochondria. In comparison, MCF7 cells treated with 10 µg/ml of cisplatin showed reduced red fluorescence in the R2 gated channel and increased green fluorescence in the R3 gated channel. The percentages of cisplatin-treated cells with red fluorescence (JC-1 aggregates) were 74.74%, 67.26% and 35.59% for 24, 48 and 72 h incubation, respectively [Figure 4.29, (b)]. The corresponding percentages of cisplatin-treated cells with green fluorescence (JC-1 monomers) were 25.30%, 32.78% and 64.38% for 24, 48 and 72 h incubation, respectively [Figure 4.29(b)]. Cisplatin was used as a positive control in this analysis. Cisplatin acts as an

agent that has been shown to induce mitochondrial dysfunction and cytotoxicity in cancer cells (Meijer *et al.*, 2001; Lewis *et al.*, 2001).

At 24 h, MCF7 cells treated with 13.5 µM [Co(phen)(edda)] and 2.8 µM [Cu(phen)(edda)] showed no significant difference in the level of R2 gated red fluorescence emission and level of R3 gated green fluorescence emission [(Figures 4.30-4.31, (A)] compared with those of untreated cells. There were 80.77% and 78.09% of population of cells with J-aggregates (red fluorescence) for cells treated with [Co(phen)(edda)] and [Cu(phen)(edda)] complexes respectively while the corresponding percentages of cells in monomeric form (green fluorescence) were 19.07% and 21.75%, respectively (Figure 4.33). The treatment of 5 µM [Zn(phen)(edda)] on MCF7 cells showed a small decrease in the level of R2 gated region (red emission) and a small increase in the level R3 gated region (green emission) [(Figure 4.32, (A)]. Here, the population of cells with J-aggregates (red emission) decreased from 80.86% to 76.94% while that of cells with J-monomers (green emission) increased from 18.97% to 22.14% (Figure 4.33). Apoptosis is frequently associated with depolarization of the $\Delta\psi_m$ (Cossarizza *et al.*, 1993; Kroemer *et al.*, 1999), resulting in increased number of cells with reduced red fluorescence in the FL-2 channel. In other words, the apoptotic population frequently presents lower red fluorescence signal intensity (FL-2 channel) than the untreated control population.

MCF7 cells treated with [Co(phen)(edda)] and [Cu(phen)(edda)] complexes for 48 h resulted in significant reduction of red fluorescence in the R2 gated channel and noticeable increase in green fluorescence in the R3 gated

channel [(Figures 4.30-4.31, (B)]. Treatment with [Co(phen)(edda)] showed population of cells with red-emitting J-aggregates decreased from 87.88% to 64.64% and population of cells with green-emitting J-monomers increased from 11.29% to 35.37% (Figure 4.34). In comparison, treatment of cells with [Cu(phen)(edda)] resulted in decrease in population of cells with J-aggregates from 87.88% to 68.56% and corresponding increase in population of cells with J-monomers from 11.29% to 31.29% (Figure 4.34). Interestingly, a large percentage of cells with reduced red fluorescence in the R2 gated channel and a large percentage of cells with increased green fluorescence in the R3 gated channel were observed with [Zn(phen)(edda)] treatment for 48 h incubation [(Figures 4.32, (B)]. In this [Zn(phen)(edda)]-treated cells, the population of cells with red J-aggregates was reduced from 87.88% to 52.96% while that of cells with green J-monomers increased from 11.29% to 46.26%, indicating that the cells were dying and in a mode of cell death referred to as apoptosis (Figure 4.34). JC-1 that fluoresces (red emission) in the FL-1 (R3) channel and lacks fluorescence (green emission) in the FL-2 (R2) channel is indicative of depolarized $\Delta\psi_m$. Thus, membrane potential of the mitochondria was undergoing a transition from polarized to depolarized form.

The shifting of the emission spectra from red to green that separated by fluorescence channels were evident after treatment MCF7 cells with [Co(phen)(edda)] and [Cu(phen)(edda)] complexes for 72 h exposure [(Figures 4.30-4.31, (C)]. Treatment with [Co(phen)(edda)] resulted in population of cells with red J-aggregates decreased from 89.74% to 63.49% while that of cells with green J-monomers increased from 9.69% to 35.64% (Figure 4.35).

On the other hand, treatment of MCF 7 cells with [Cu(phen)(edda)] resulted population of cells with red J-aggregates decreased from 89.74% to 70.95% while that of cells with green J-monomers increased from 9.69% to 28.32% (Figure 4.35). Interestingly, [Zn(phen)(edda)]-treated MCF7 cells for 72 h resulted in dramatic decrease in red J-aggregates to 28.81% while formation of green J-monomers were markedly increased to 70.77% (Figure 4.35). A time-dependent reduction in $\Delta\psi_m$ was observed for cells treated with [M(phen)(edda)]. At 72 h, [Zn(phen)(edda)] induced more reduction in $\Delta\psi_m$ compared to cisplatin. These results are consistent with cells undergoing apoptosis which is normally accompanied by a transition from polarized to depolarized $\Delta\psi_m$. Depolarization of mitochondria occurred for cells treated with [M(phen)(edda)], indicating altered mitochondrial function which may be a cause of or be associated with apoptosis.

Mitochondria in untreated control MCF7 cells are primarily healthy and functioning normally. Only small percentage of the control population of cells had depolarized $\Delta\psi_m$ which may reflect a basal level of apoptosis or presence of other cellular processes that are associated with depolarized $\Delta\psi_m$. In contrast, huge percentage of control population of cells with reduced red fluorescence in FL-2 channel may indicate the untreated cells are unhealthy (e.g. deterioration or contamination).

The $\Delta\psi_m$ is indicated by a change in the red/green fluorescence intensity ratio ($I_{590\ nm}/I_{527\ nm}$). The ratio of red fluorescence intensity divided by green fluorescence intensity was calculated for untreated cells and those treated

with [M(phen)(edda)] for 24, 48 and 72 h incubation. A decrease in this ratio indicates a decrease in $\Delta\psi_m$. In Figure 4.36, the effect of treating MCF7 cells with 13.5 μM [Co(phen)(edda)], 2.8 μM [Cu(phen)(edda)] and 5 μM [Zn(phen)(edda)] on the $\Delta\psi_m$ are shown. Except for [Co(phen)(edda)], the other [M(phen)(edda)] complexes statistically decreased in $\Delta\psi_m$ only after more than 24 h. Decrease of $\Delta\psi_m$ caused by [M(phen)(edda)] was time-dependent (48 and 72 h). Following 24 to 72 h incubation, treatment of MCF7 cells with [Zn(phen)(edda)] resulted in the greatest reduction with the ratios of red to green fluorescence, indicating a large-scale mitochondrial depolarization (Figure 4.36).

(a) Untreated Control **(b) Cisplatin**
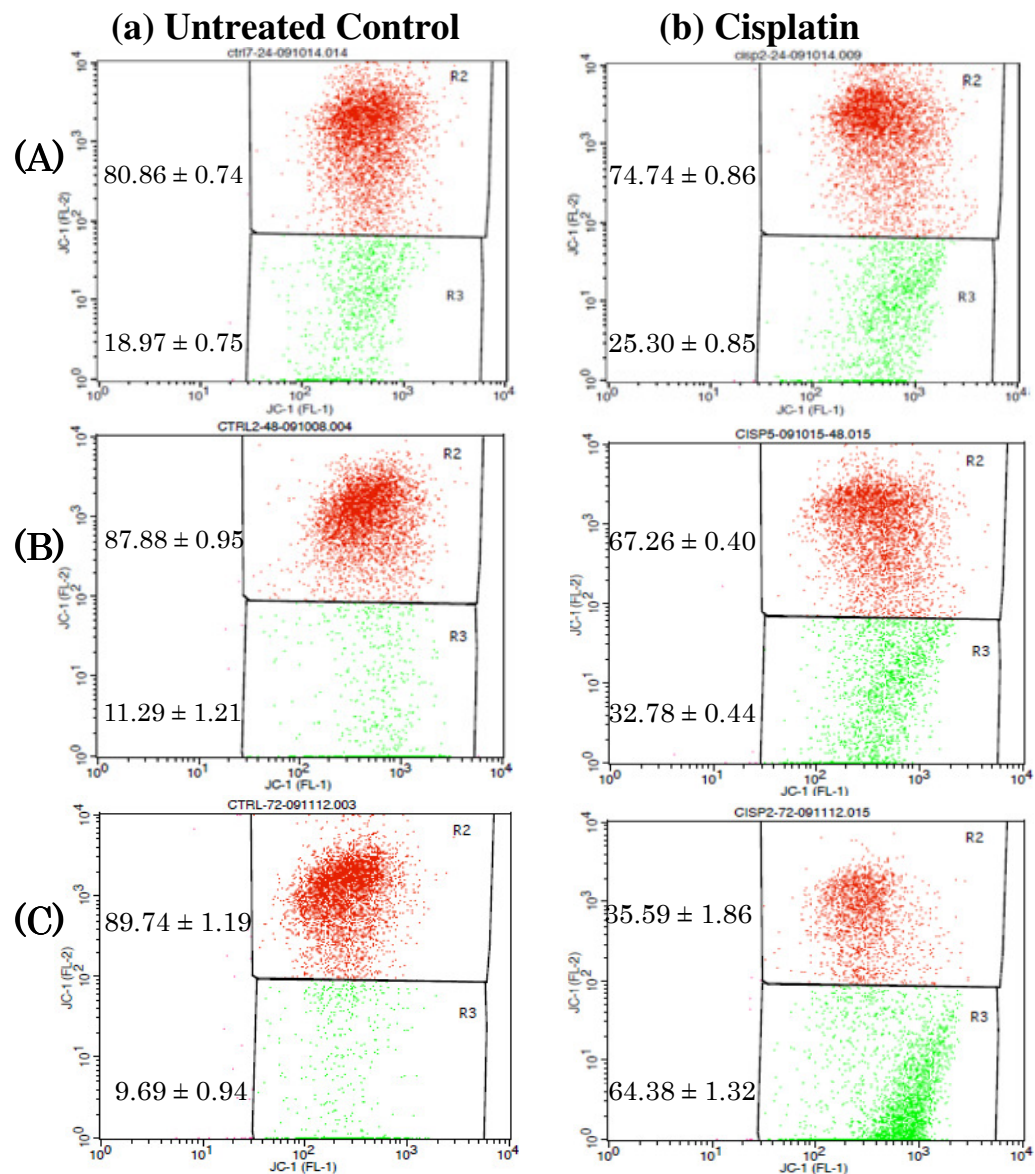
Figure 4.29: Flow Cytometric Analysis of Cisplatin Causes Mitochondrial Depolarization in MCF7 Cells with JC-1 Staining for 24 h (A), 48 h (B) and 72h (C). Data are expressed in dot plots of the FL-1 channel (JC-1 green fluorescence) versus the FL-2 channel (JC-1 red fluorescence). Gated region R2 (red) includes cells with intact mitochondrial membranes and gated region R3 (green) depicts cells has depolarized. Data represented mean values of four independent experiments and same as the following figures.

(a) Untreated MCF7 cells showed red spectral shift resulting in higher levels of red fluorescence emission formed JC-1 aggregates following 24, 48 and 72 h in culture. (b) In contrast, cisplatin treated MCF7 cells showed JC-1 remained in the cytoplasm as monomers exhibited fluorescence in the green end spectrum is indicative of change in mitochondrial membrane potential ($\Delta\psi_m$). Cisplatin was used as a positive control.

(a) Untreated Control

(c) [Co(phen)(edda)]

(A) 80.86 ± 0.74 | 80.77 ± 0.41

18.97 ± 0.75 | 19.07 ± 0.40

(B) 87.88 ± 0.95 | 64.64 ± 1.82

11.29 ± 1.21 | 35.37 ± 1.93

(C) 89.74 ± 1.19 | 63.49 ± 0.89

9.69 ± 0.94 | 35.64 ± 0.87
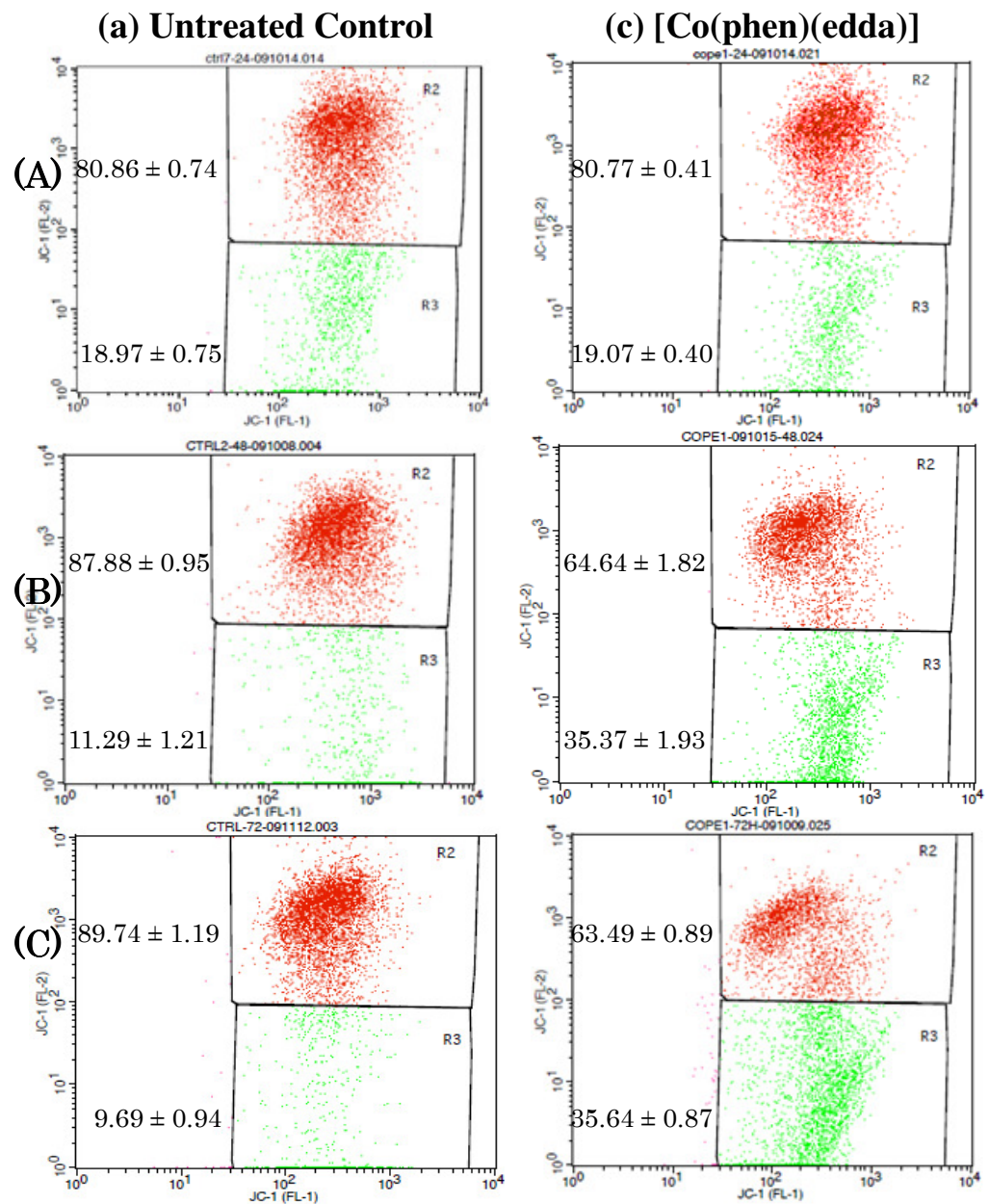
Figure 4.30: Flow Cytometric Analysis of [Co(phen)(edda)] Causes Mitochondrial Depolarization in MCF7 Cells with JC-1 staining for 24 h (A), 48 h (B) and 72 h (C).

(a) Untreated MCF7 cells showed red spectral shift resulting in higher levels of red fluorescence emission formed JC-1 aggregates following 24 h (A), 48 h (B) and 72 h (C) in culture. (c) In contrast, MCF7 cells treated with 13.5 μM [Co(phen)(edda)] for three separate days showed increasing levels of green fluorescence emission. Thus, mitochondria were undergoing a transition from polarized to depolarized $\Delta\psi_m$. JC-1 leaks out of the mitochondria into the cytoplasm as monomers resulting in a decrease of red fluorescence.
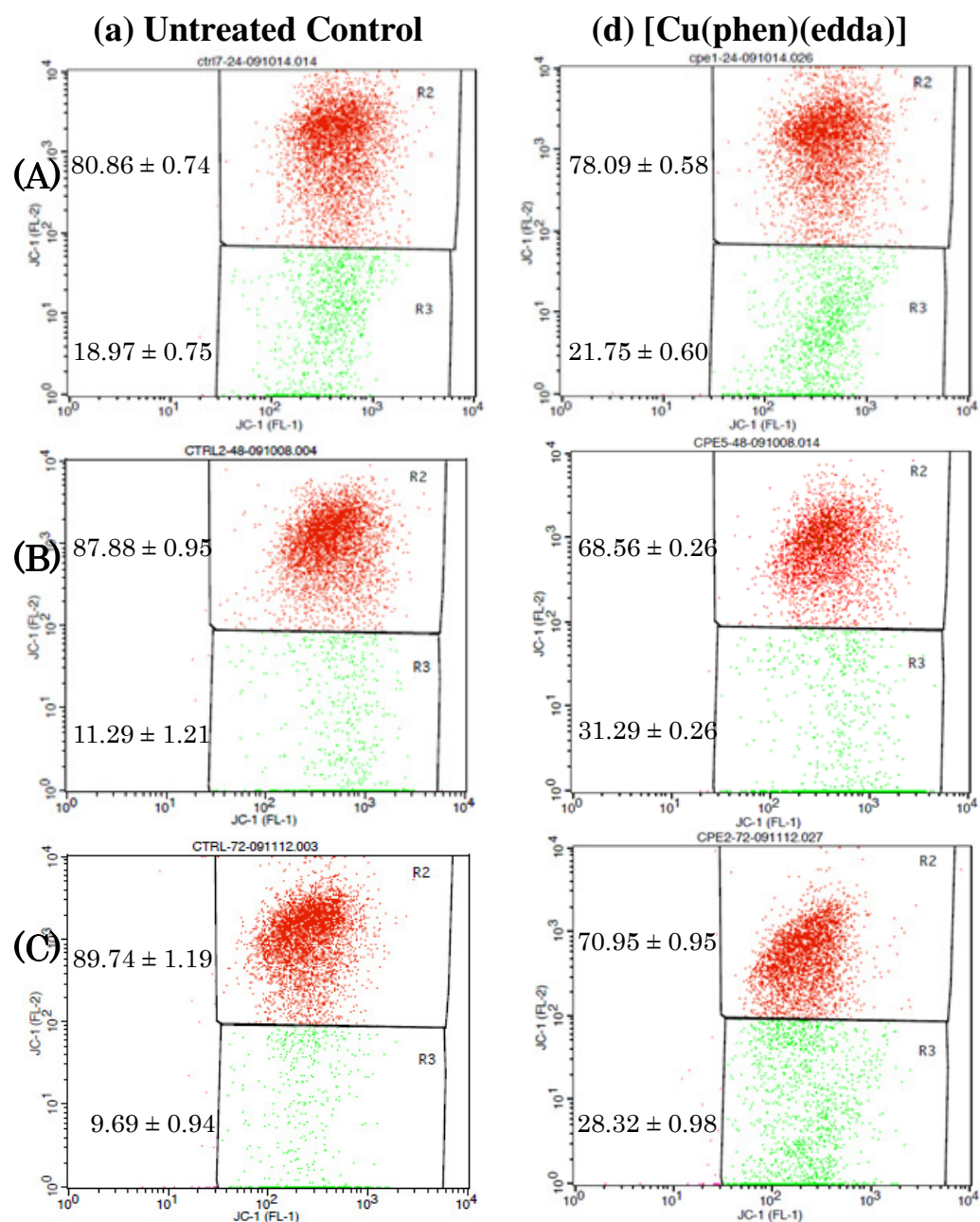
Figure 4.31: Flow Cytometric Analysis of [Cu(phen)(edda)] Causes Mitochondrial Depolarization in MCF7 Cells with JC-1 staining for 24 h (A), 48 h (B) and 72 h (C).

(a) Untreated MCF7 cells showed red spectral shift resulting in higher levels of red fluorescence emission formed JC-1 aggregates following 24 h (A), 48 h (B) and 72 h (C) in culture. (d) In contrast, MCF7 cells treated with 2.8 μM [Cu(phen)(edda)] for three separate days showed increasing levels of green fluorescence emission. Thus, mitochondria were undergoing a transition from polarized to depolarized $\Delta\psi_m$. JC-1 leaks out of the mitochondria into the cytoplasm as monomers resulting in a decrease of red fluorescence.
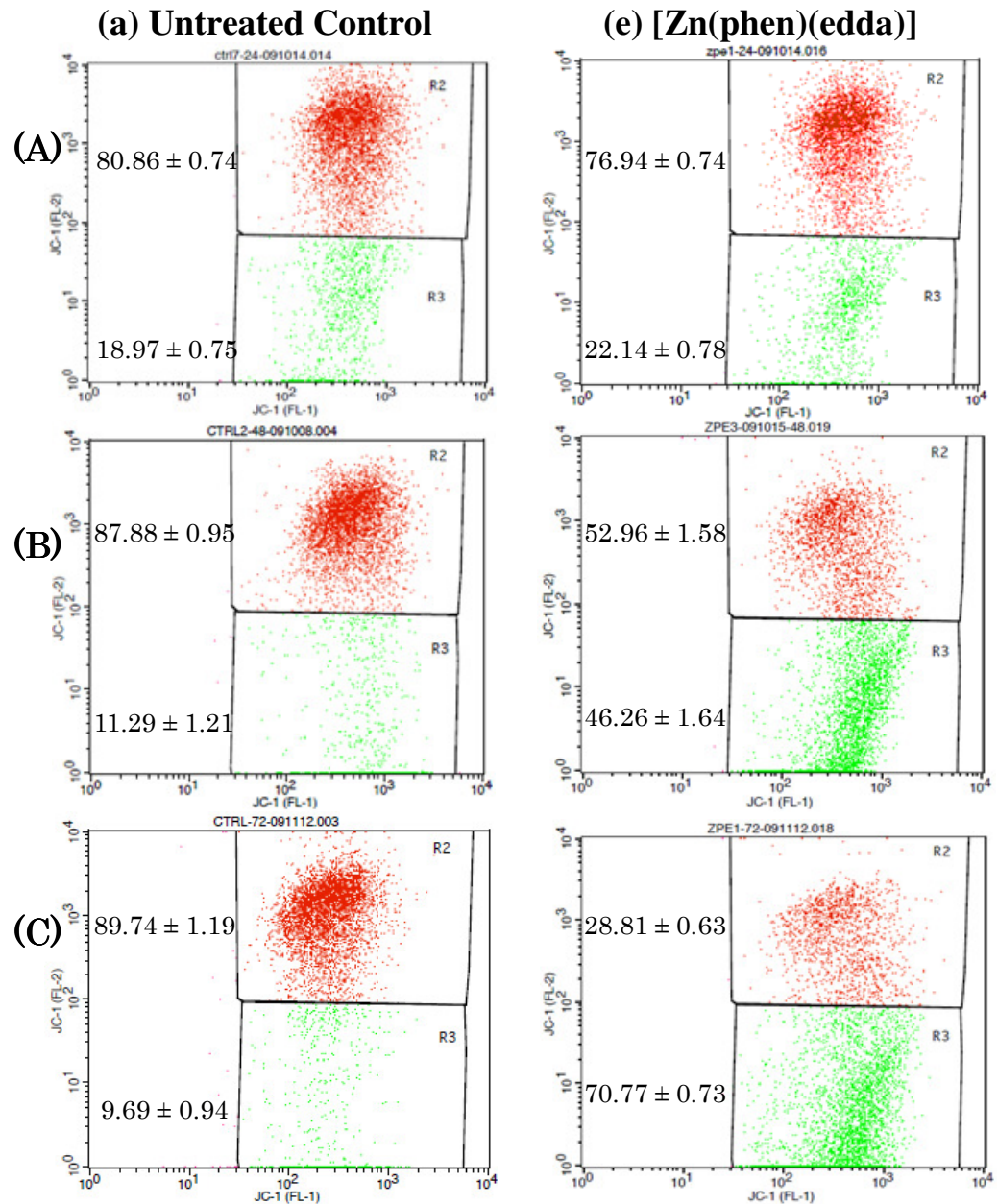
Figure 4.32: Flow Cytometric Analysis of [Zn(phen)(edda)] Causes Mitochondrial Depolarization in MCF7 Cells with JC-1 staining for 24 h (A), 48 h (B) and 72 h (C).

(a) Untreated MCF7 cells showed red spectral shift resulting in higher levels of red fluorescence emission formed JC-1 aggregates following 24 h (A), 48 h (B) and 72 h (C) in culture. (e) In contrast, MCF7 cells treated with 5 μM [Zn(phen)(edda)] for three separate days showed increasing levels of green fluorescence emission. Thus, mitochondria were undergoing a transition from polarized to depolarized $\Delta\psi_m$. JC-1 leaks out of the mitochondria into the cytoplasm as monomers resulting in significantly reduced of red fluorescence.
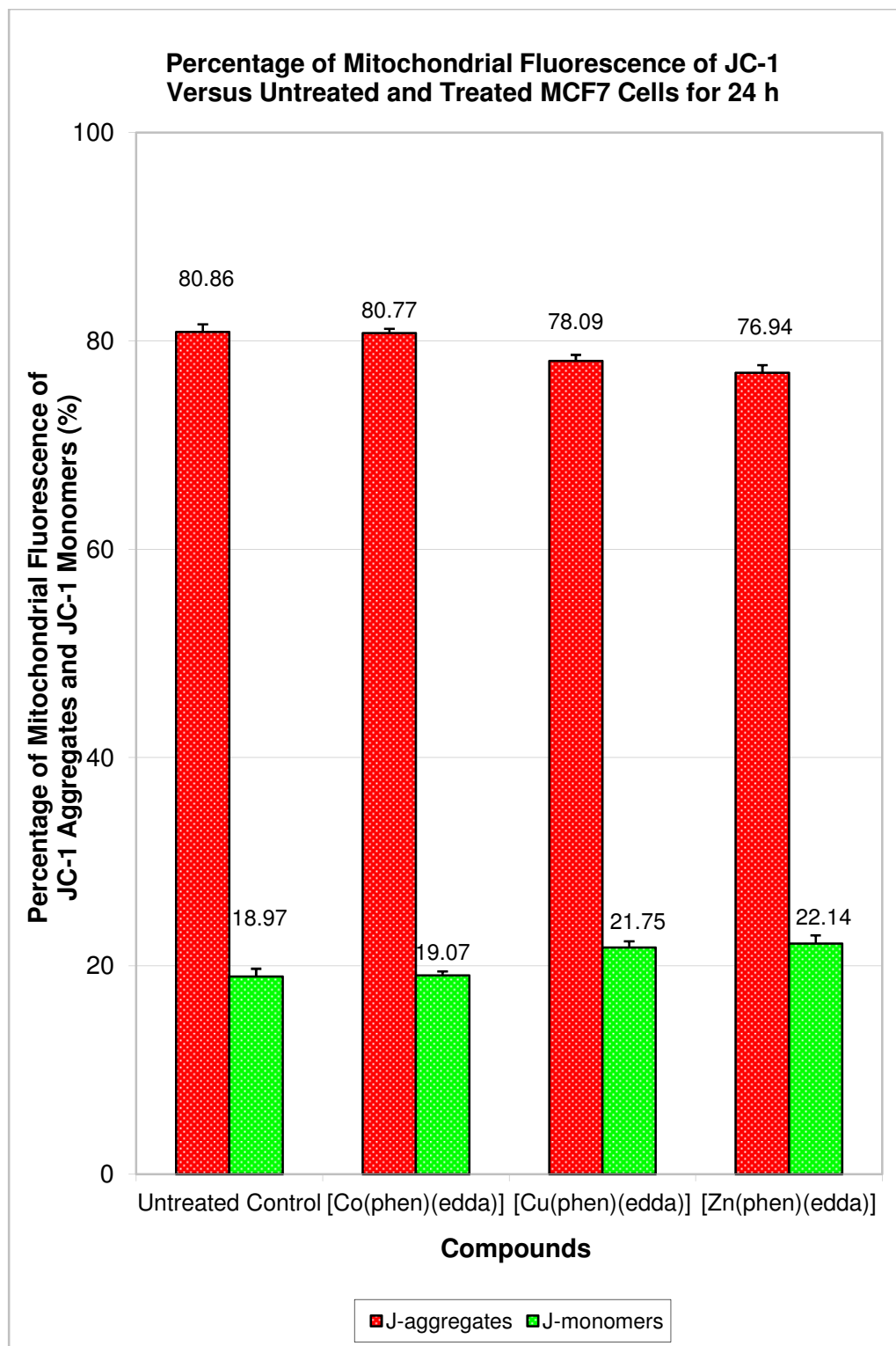
Figure 4.33: Percentage of Cells at Red Fluorescence Aggregates and Green Fluorescence Monomers of JC-1 Staining in Untreated and [Co(phen)(edda)], [Cu(phen)(edda)] as well as [Zn(phen)(edda)]-treated MCF7 Cells for 24 h.
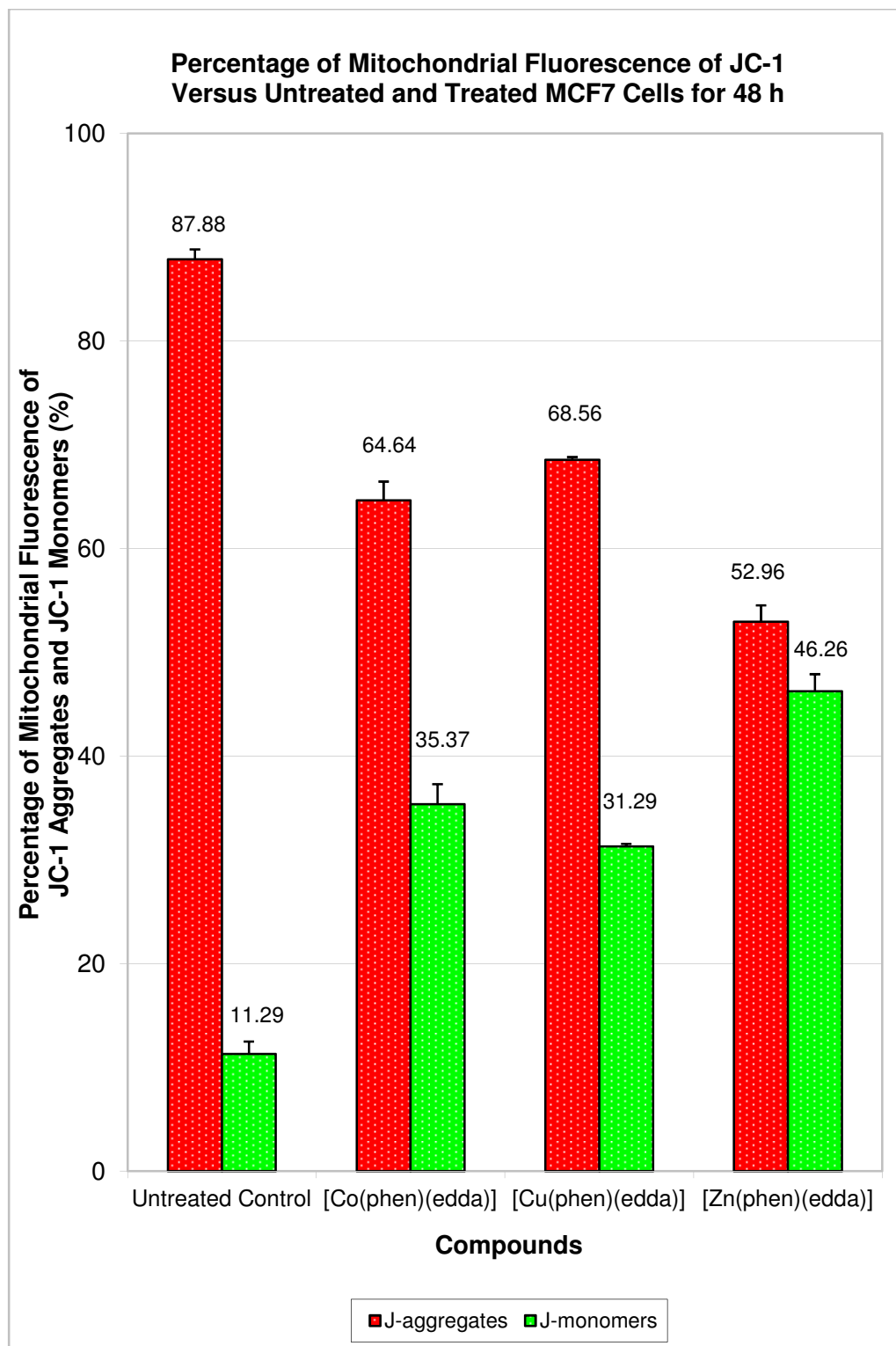
Figure 4.34: Percentage of Cells at Red Fluorescence Aggregates and Green Fluorescence Monomers of JC-1 Staining in Untreated and [Co(phen)(edda)], [Cu(phen)(edda)] as well as [Zn(phen)(edda)]-treated MCF7 Cells for 48 h.
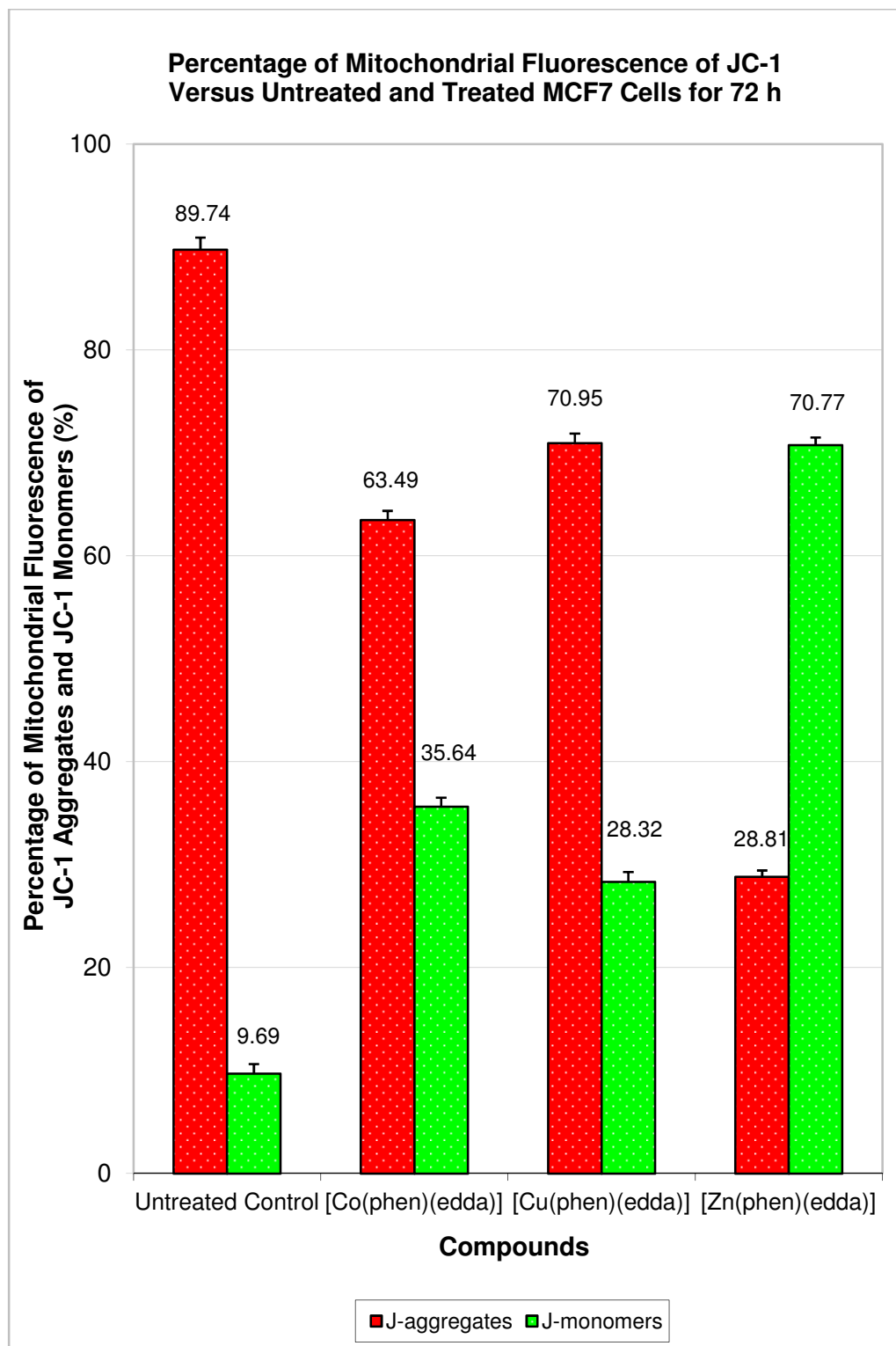
Figure 4.35: Percentage of Cells at Red Fluorescence Aggregates and Green Fluorescence Monomers of JC-1 Staining in Untreated and [Co(phen)(edda)], [Cu(phen)(edda)] as well as [Zn(phen)(edda)]-treated MCF7 Cells for 72 h.
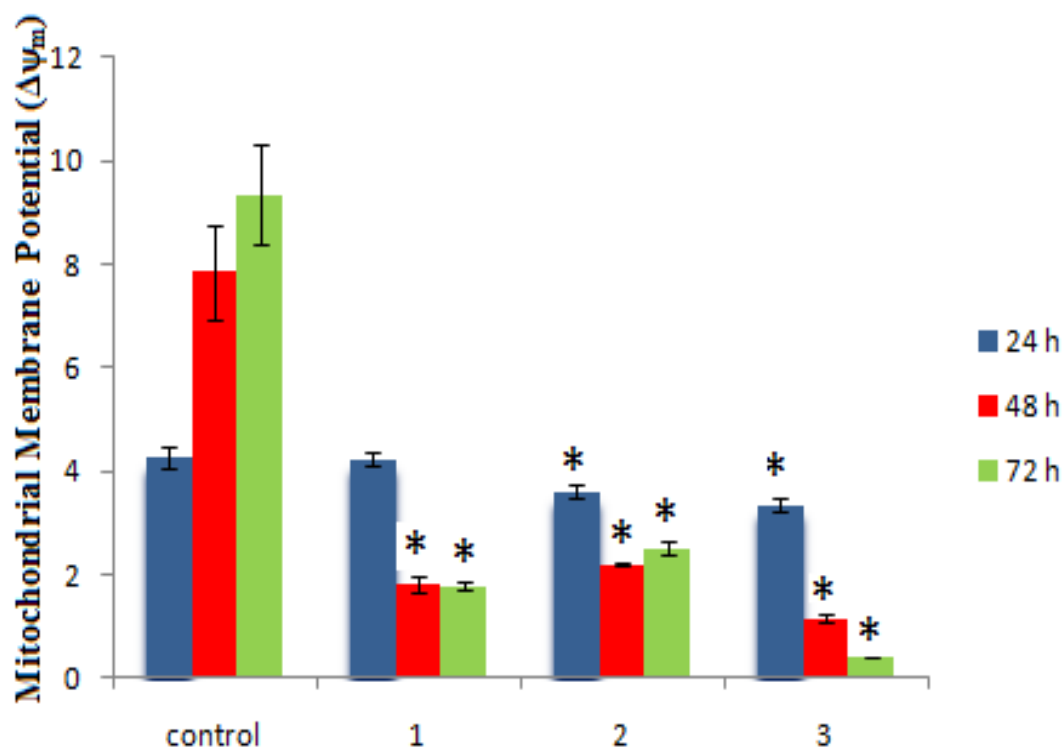
Figure 4.36: Effect of [M(phen)(edda)] Complexes (Co, 1; Cu, 2; Zn, 3) on the Mitochondrial Membrane Potential ($\Delta\psi_m$). Control (blank). Cells were treated with IC_{50} concentration of respective metal complexes for 24 h (blue), 48 h (red) and 72 h (green) respectively. Data are mean for four independent experiments. *$p < 0.05$ compared to control.

4.7   Topoisomerase I Inhibition Assay

Topoisomerase I (Topo I) manipulates coiling by unwinding duplex DNA, resulting in a more relaxed structure. It binds to the duplex DNA, cleaves a phosphodiester bond of one strand, passes the other strand through the nick and then religates the nick. Human topo I can relax both positive and negative supercoils. Supercoiled plasmid DNA pBR322 is suitable substrate for study with topoisomerase I, which is one strand DNA cutter. The supercoiled pBR322 is very compact and moves faster in the gel during electrophoresis. When one strand of the supercoiled DNA is cut, the resultant unwinded, more relaxed open circular pBR322 is formed and this nicked DNA moves slower. When two strands of the supercoiled DNA are cut, the linear DNA is formed and it moves at intermediate speed. The commercial pBR322 (4.4 kb) has a small amount of both more relaxed nicked and linear forms of DNA (Figures 4.37-4.43, L2-3). As for the topoisomers (relaxed DNA), the more relaxed ones will move slower than the less relaxed ones (Webb and Ebeler, 2008).

In this DNA relaxation assay, one unit of human topo I can completely convert all the supercoiled plasmid pBR322 (4.4 kb) to fully relaxed topoisomer, which is the completely unwound covalently bonded closed circular DNA (Figures 4.37-4.43, L4). Incubating the pBR322 with the highest concentration of test compounds (metal salts, phen, metal(II) complexes) from 5-40 μM, no cleavage or unwinding of the DNA was observed as the banding pattern was the same as the control without any added test compounds (Figures 4.37-4.43, L3). As can be seen from Figures 4.38-4.40 (L6-9), the CoCl$_2$,

ZnCl$_2$ and phen did not inhibit the activity of the topo I as the DNA bands are the same as those observed for DNA incubated with topo I alone. However, CuCl$_2$ caused some inhibition of topo I at 40 μM (Figure 4.37, L9).

Interestingly, incubating the pBR322 with human topo I and increasing concentration from the [Co(phen)(edda)], [Cu(phen)(edda)] and [Zn(phen)(edda)] complexes from 5 to 40 μM gave rise to the reduction of the nicked band (containing nicked and fully relaxed DNA) and formation of various faster moving bands of topoisomers with different degree of relaxation. Furthermore, the appearance of slower moving bands of less relaxed topoisomers is observed with increasing concentration of the metal(II) complexes (Figures 4.41-4.43, L6-9). These results showed [Co(phen)(edda)], [Cu(phen)(edda)] and [Zn(phen)(edda)] inhibited the activity of topo I activity. An examination of the gel images presented in Figures 4.41-4.43 showed that at 40 μM of [Zn(phen)(edda)] had the highest inhibitory effect on topo I activity as the amount of observably slower moving bands of less relaxed topoisomers was visibly more than those in the presence of 40 μM of [Co(phen)(edda)] and [Cu(phen)(edda)] complexes (Figure 4.41-4.43, L10). The degree of inhibition of topo I by [M(phen)(edda)] was concentration dependent. However, no total inhibition of human topo I activity by [M(phen)(edda)] was observed in the complex concentration range used.

An initial preliminary mechanistic study of inhibition of topo I was also conducted by different sequential mixing of the three components, *viz.* DNA, [M(phen)(edda)] compounds and topo I (Figure 4.44). In the first case, all the

reaction components mixed simultaneously [Figure 4.44, Panel (a)]; in the second case, [M(phen)(edda)] compounds and topo I were mixed first before adding DNA [Figure 4.44, Panel (b)]; and in the third case, DNA and [M(phen)(edda)] compounds were mixed before adding topo I [Figure 4.44, Panel (c)]. Figure 4.44 (Lanes 3-5) showed the gel patterns of pBR322 incubated with 50 μM of [M(phen)(edda)] compounds. No cleavage or unwinding of the DNA was observed for DNA with [M(phen)(edda)] complex alone (Figure 4.44, Lanes 3-5) as the banding patterns were the same as the control (Figure 4.44, Lane 2), i.e. DNA alone. Inhibition of topo I seemed to increase from [Cu(phen)(edda)] to [Co(phen)(edda)] to [Zn(phen)(edda)] when all three reaction components were mixed simultaneously at the same time [Panel (a), Lanes 7-9]. For the prior mixing of [M(phen)(edda)] compounds with topo I, significant band of supercoiled DNA (Form I) was observed in Panel (b), Lane 10. In this case, [Cu(phen)(edda)] inhibited the action of topo I the most, while Co(II) and Zn(II) complexes inhibited topo I less, as evidenced by presence of less relaxed topoisomers in Panel (b) in Lanes 11-12. For the third case involving prior mixing of DNA with [M(phen)(edda)] compounds, the gel patterns in Panel c for all [M(phen)(edda)] compounds were the same, i.e. two bands (Form II and Form III) were observed with the Form II bands been stained more intensely.
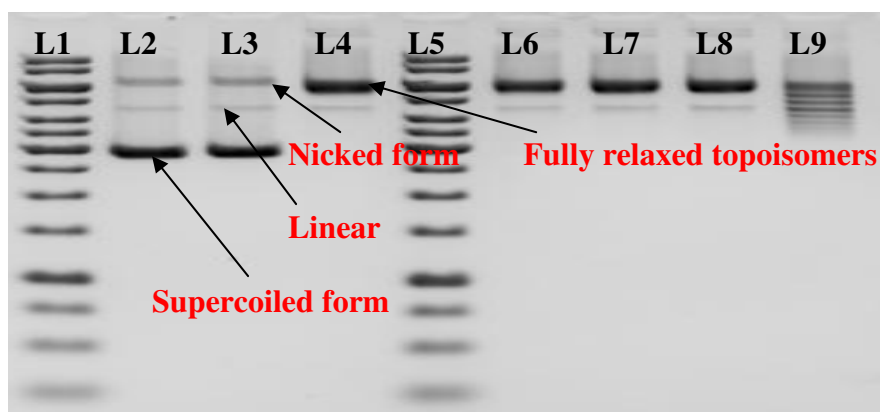
Figure 4.37: Effect of Metal salt CuCl₂ in Human Topoisomerase I (Topo I) Inhibition Assay by Gel Electrophoresis. Electrophoresis results of incubating human topo I (1 unit/21μL) with pBR322 (0.25 μg) in the absence or presence of 5-40 μM of metal salt, CuCl₂: Lane 1 & 5, gene ruler 1 Kb DNA ladder; Lane 2, DNA alone; Lane 3, DNA + 40 μM CuCl₂ (control); Lane 4, DNA + 1unit Human Topo I (control); Lane 6, DNA + 5 μM CuCl₂+ 1unit Human Topo I; Lane 7, DNA + 10 μM CuCl₂ + 1unit Human Topo I; Lane 8, DNA + 20 μM CuCl₂ + 1unit Human Topo I; Lane 9, DNA + 40 μM CuCl₂+ 1unit Human Topo I.
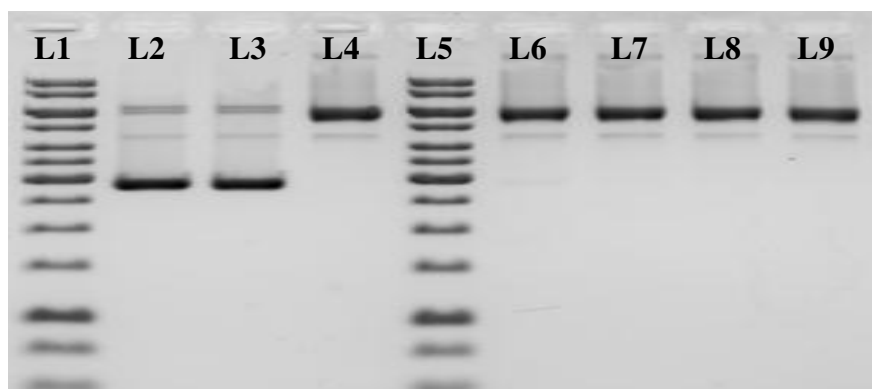
Figure 4.38: Effect of Metal Salt CoCl₂ in Human Topoisomerase I (Topo I) Inhibition Assay by Gel Electrophoresis. Electrophoresis results of incubating human topo I (1 unit/21μL) with pBR322 (0.25 μg) in the absence or presence of 5-40 μM of metal salt, CoCl₂: Lane 1 & 5, gene ruler 1 Kb DNA ladder; Lane 2, DNA alone; Lane 3, DNA + 40 μM CoCl₂ (control); Lane 4, DNA + 1unit Human Topo I (control); Lane 6, DNA + 5 μM CoCl₂+ 1unit Human Topo I; Lane 7, DNA + 10 μM CoCl₂+ 1unit Human Topo I; Lane 8, DNA + 20 μM CoCl₂+ 1unit Human Topo I; Lane 9, DNA + 40 μM CoCl₂+ 1unit Human Topo I.
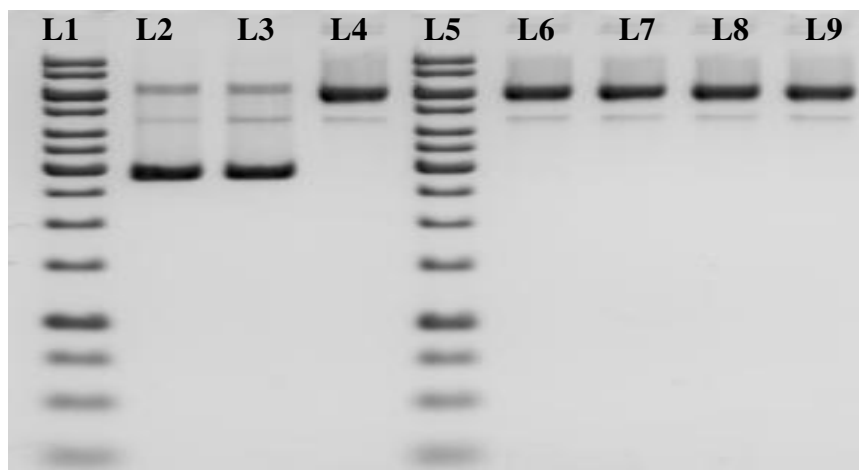
Figure 4.39: Effect of Metal Salt ZnCl₂ in Human Topoisomerase I (Topo I) Inhibition Assay by Gel Electrophoresis. Electrophoresis results of incubating human topo I (1 unit/21μL) with pBR322 (0.25 μg) in the absence or presence of 5-40 μM of metal salt, ZnCl₂: Lane 1 & 5, gene ruler 1 Kb DNA ladder; Lane 2, DNA alone; Lane 3, DNA + 40 μM ZnCl₂ (control); Lane 4, DNA + 1unit Human Topo I (control); Lane 6, DNA + 5 μM ZnCl₂ + 1unit Human Topo I; Lane 7, DNA + 10 μM ZnCl₂+ 1unit Human Topo I; Lane 8, DNA + 20 μM ZnCl₂ + 1unit Human Topo I; Lane 9, DNA + 40 μM ZnCl₂+ 1unit Human Topo I.
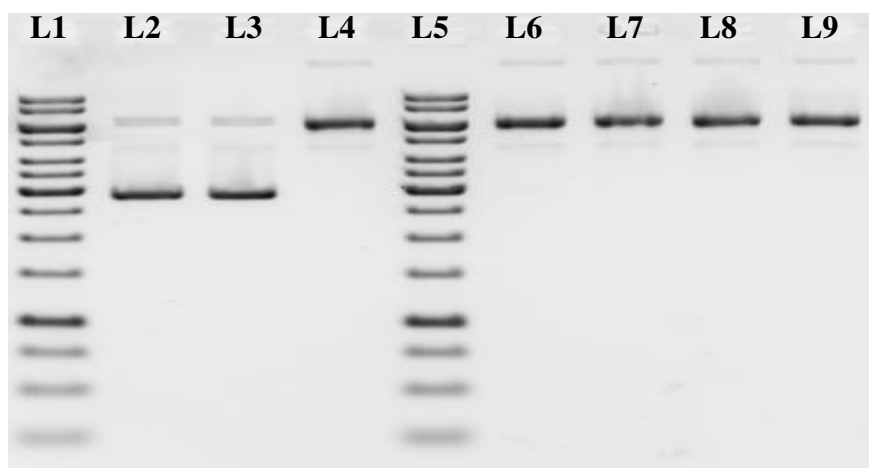
Figure 4.40: Effect of 1,10-phenanthroline (phen) in Human Topoisomerase I (Topo I) Inhibition Assay by Gel Electrophoresis. Electrophoresis results of incubating human topo I (1 unit/21μL) with pBR322 (0.25 μg) in the absence or presence of 5-40 μM of phen: Lane 1 & 5, gene ruler 1 Kb DNA ladder; Lane 2, DNA alone; Lane 3, DNA + 40 μM phen (control); Lane 4, DNA + 1unit Human Topo I (control); Lane 6, DNA + 5 μM phen + 1unit Human Topo I; Lane 7, DNA + 10 μM phen + 1unit Human Topo I; Lane 8, DNA + 20 μM phen + 1unit Human Topo I; Lane 9, DNA + 40 μM phen + 1unit Human Topo I.
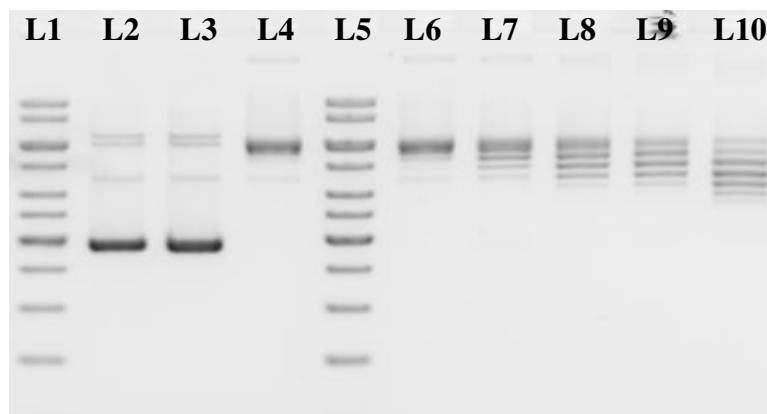
Figure 4.41: Effect of [Co(phen)(edda)] in Human Topoisomerase I (Topo I) Inhibition Assay by Gel Electrophoresis. Electrophoresis results of incubating human topo I (1 unit/21μL) with pBR322 (0.25 μg) in the absence or presence of 5-40 μM of complex, [Co(phen)(edda)]: Lane 1 & 5, gene ruler 1 Kb DNA ladder; Lane 2, DNA alone; Lane 3, DNA + 40 μM complex (control); Lane 4, DNA + 1unit Human Topo I (control); Lane 6, DNA + 5 μM complex + 1unit Human Topo I; Lane 7, DNA + 10 μM complex + 1unit Human Topo I; Lane 8, DNA + 20 μM complex + 1unit Human Topo I; Lane 9, DNA + 30 μM complex + 1unit Human Topo I; Lane 10, DNA + 40 μM complex + 1unit Human Topo I.
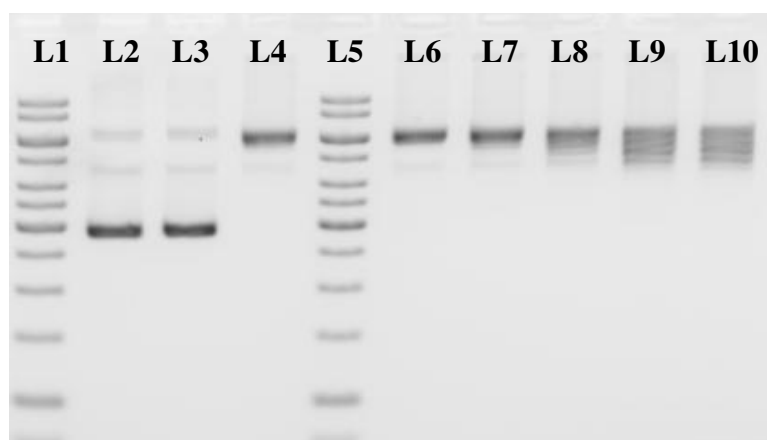
Figure 4.42: Effect of [Cu(phen)(edda)] in Human Topoisomerase I (Topo I) Inhibition Assay by Gel Electrophoresis. Electrophoresis results of incubating human topo I (1 unit/21μL) with pBR322 (0.25 μg) in the absence or presence of 5-40 μM of complex, [Cu(phen)(edda)]: Lane 1 & 5, gene ruler 1 Kb DNA ladder; Lane 2, DNA alone; Lane 3, DNA + 40 μM complex (control); Lane 4, DNA + 1unit Human Topo I (control); Lane 6, DNA + 5 μM complex + 1unit Human Topo I; Lane 7, DNA + 10 μM complex + 1unit Human Topo I; Lane 8, DNA + 20 μM complex + 1unit Human Topo I; Lane 9, DNA + 30 μM complex + 1unit Human Topo I; Lane 10, DNA + 40 μM complex + 1unit Human Topo I.
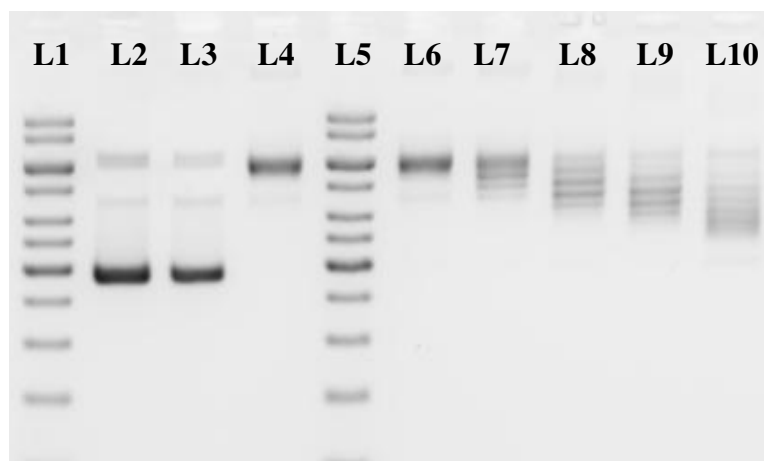
Figure 4.43: Effect of [Zn(phen)(edda)] in Human Topoisomerase I (Topo I) Inhibition Assay by Gel Electrophoresis. Electrophoresis results of incubating human topo I (1 unit/21μL) with pBR322 (0.25 μg) in the absence or presence of 5-40 μM of complex, [Zn(phen)(edda)]: Lane 1 & 5, gene ruler 1 Kb DNA ladder; Lane 2, DNA alone; Lane 3, DNA + 40 μM complex (control); Lane 4, DNA + 1unit Human Topo I (control); Lane 6, DNA + 5 μM complex + 1unit Human Topo I; Lane 7, DNA + 10 μM complex + 1unit Human Topo I; Lane 8, DNA + 20 μM complex + 1unit Human Topo I; Lane 9, DNA + 30 μM complex + 1unit Human Topo I; Lane 10, DNA + 40 μM complex + 1unit Human Topo I.
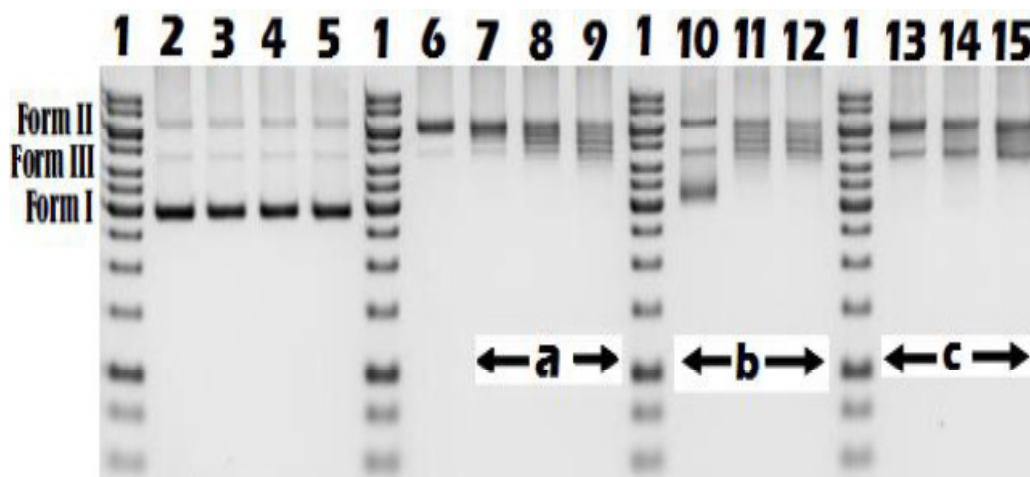
Figure 4.44: Electrophoresis Results of Sequential Incubation of Human Topo I (1 unit/21μL) with pBR322 (0.25 μg) in the Presence of 50 μM of [M(phen)(edda)] (M = Cu: lanes 7,10,13; Co: lanes 8, 11, 14; Zn: lanes 9, 12, 15). For all panels: Lanes 1, gene ruler 1 Kb DNA ladder; Lane 2, DNA alone; Lanes 3-5, DNA + 50 μM [Cu(phen)(edda)], [Co(phen)(edda)] and [Zn(phen)(edda)] respectively (control); Lane 6, DNA + 1unit Human Topo I (control). For panels (a)-(c), DNA + Topo I + [M(phen)(edda)]: (a), mix all components together at the same time; (b), mixing [M(phen)(edda)] and topo I first; (c), mixing DNA and M(phen)(edda) first. Form I, supercoiled pBR322 DNA; Form III, linear DNA; Form II, nicked open circular DNA.

CHAPTER 5.0

DISCUSSION

This section describes the results showing [Co(phen)(edda)], [Cu(phen)(edda)] and [Zn(phen)(edda)] compounds exert their cytotoxic effect and possess selectivity towards breast cancer cells, MCF7 over breast normal cells, MCF10A. Besides, the tested compounds have good drug-like property based on Lipinski's Rule of Five. Lipophilicity makes the compounds have tendency to permeate cell membrane. The results indicate that all [M(phen)(edda)] compounds induce apoptosis in breast cancer cells but only Zn analogue can induce cell cycle arrest at S phase. Moreover, treatment with [M(phen)(edda)] compounds increased depolarization of mitochondrial membrane potential and was able to inhibit the function of topo I in relaxing the supercoiled pBR322. Therefore, treatment with [M(phen)(edda)] compounds suggest that cell death involves multiple targets.

5.1   Anticancer Property and Selectivity of [M(phen)(edda)] on Human Breast Cell Lines

5.1.1   *In Vitro* Anticancer Property of [M(phen)(edda)]

Many intercalating ligand 1,10-phen complexes, including Cu(II)-phen and Zn(II)-phen complexes but less in Co(II)-phen complexes have been

reported to have potent anticancer activities (Tripathi *et al.*, 2007; Ng *et al.*, 2008). Instead of binary complexes, ternary transition metal complexes are receiving more and more attention as it presented potential applications in pharmacology and cancer therapy. In this study, an amino acid, edda, is bound together with an intercalating ligand to a metal(II) cation and formed the [M(phen)(edda)] compound. The balance between therapeutic potential and toxic effect of a compound is very important when evaluating its usefulness as a pharmacological drug.

In this investigation, *in vitro* cytotoxicities of [Co(phen)(edda)], [Cu(phen)(edda)] and [Zn(phen)(edda)] towards human cancer cells, MCF7 and normal cells, MCF10A for 24, 48 and 72 h incubation time were compared. The origin of MCF7 cell line is representative of the most frequent cancer types worldwide (Ferlay *et al.*, 2004). Established cell lines are often employed as biosensors because the cells can be used in all experiments to achieve high repeatability (Freshney, 1989). Concentrations of [M(phen)(edda)] and incubation time were tested to optimize the assay for MCF7 and MCF10A cells in obtaining the measurement of absorbance on viable cells which quantified and presented in percentage with reference to non-treated cells.

In vitro antiproliferative effect was measured by using MTT assay, a rapid assay for growth and survival of mammalian cells based on the transformation and colorimetric quantification which detect the level of succinate dehydrogenase (a reductase enzyme) within mitochondria (Kregiel *et*

al., 2008). Briefly, MTT, a yellow tetrazole, is reduced to non-water-soluble crystalline purple formazan crystal within the cell. This reduction takes place only when reductase enzyme is active. DMSO acts as a solubilizing agent added to dissolve the insoluble purple formazan product into pinkish-purple solution. The absorbance of this colored solution can be quantified by measuring at 560 nm wavelength by a microplate reader. Microscopical viewing of cell cultures before and after performing the assay is an essential step to ensure a reliable performance of the MTT assay. The assumption of this assay is that the succinate dehydrogenase activity is proportional to the number of living cells and the signal generated is dependent on the degree of activation of the cells. In other words, the amount of the crystals can be determined spectrophotometrically and serves as an estimate for the number of mitochondria and hence the number of living cells in the sample. When the amount of purple formazan produced by the cells treated with [M(phen)(edda)] is compared with the amount of formazan produced by untreated control cells, the effectiveness of [M(phen)(edda)] in causing death can be deduced through the production of a dose-response graph. Thus, the percent of cell survival relative to the control cells were plotted as a function of concentration of the [M(phen)(edda)] compounds (Figures 4.2-4.10). Throughout this study, the [M(phen)(edda)] compounds were able to damage and destroy cells, and thus decreased the reduction of MTT to formazan. The results showed that 13.5 μM of [Co(phen)(edda)], 2.8 μM of [Cu(phen)(edda)] and of 5 μM [Zn(phen)(edda)] are potential anticancer agent with inhibitory activities against MCF7 cancer cells which preferably incubation time in 72 h (Table 4.1). Reliably, MTT assay can be used to measure cytotoxicity and

proliferation, and show a high degree of precision at the same time (Mosmann, 1983).

It is clear that [M(phen)(edda)] compounds inhibited the proliferation of MCF7 breast cancer cells in a time and dose-dependent manner. For 72 h incubation, the order of compounds with increasing antiproliferative properties are [Co(phen)(edda)] (IC$_{50}$, 13.5 µM) < [Zn(phen)(edda)] (IC$_{50}$, 5 µM) < [Cu(phen)(edda)] (IC$_{50}$, 2.8 µM). Interestingly, these IC$_{50}$ values were better than cisplatin (IC$_{50}$, 10.9 µM) and oxaliplatin (IC$_{50}$, 18.2 µM) (Starha *et al.*, 2009). The metal(II) chlorides were not cytotoxic to MCF7 even at 72 h incubation, as reported by others for the same cell line (IC$_{50}$ values: CoCl$_2$, >100 µM; ZnCl$_2$, 130 µM; CuCl$_2$, >200 µM) (Trávníček *et al.*, 2005; Kovala-Demertzi *et al.*, 2006; Maloň *et al.*, 2002). Initial study reported that the IC$_{50}$ value of 1,10-phen was also determined for MCF7 in 72 h and it was 74.3 µM (Ng *et al.*, 2008).

The enhanced IC$_{50}$ values for the metal complexes suggest that there is synergy between the cytotoxic phen ligand with these metal cations. In other words, chelation of the phen ligand to these metal cations enhanced its cytotoxicity. Such cytotoxic enhancement resulting from chelation of phen to metal cation in binary or ternary complexes is seldom investigated, as far as we know. One such reported synergy involves the octahedral [La(phen)]$^{3+}$ complex (Heffeter *et al.*, 2006). Ranford *et al.* (1993) also found that incorparating phen into the copper(II) complexes of 3,5-disubstituted salicylates enhanced their *in vitro* antitumor properties. A similar synergic

metal–ligand combination is also reported for a set of dicopper(II) complexes where the IC_{50} values of the complexes for MCF7 are in the range 24 – 54 µM while both the copper(II) chloride and the various non-polypyridyl proligands have IC_{50} >100 µM (Trávníček *et al.*, 2001). In contrast, almost all the nine square planar ternary platinum(II) complexes of phen and various amino acids, [Pt(phen)(aa)]NO$_3$ tested (except [Pt(phen)(pro)]NO$_3$), are found to be not cytotoxic towards a human leukemia cell line (Jin and Ranford, 2000). Complex geometry may be a significant contributing factor in ensuring a synergic effect in the rational design of anticancer ternary metal complexes.

5.1.2   *In Vitro* Anticancer Selectivity towards Human Breast Cancer Cell Line over Normal Breast Cell Line

The common occurrence of drug-resistant tumor cells and the lack of selectivity of cancer drugs in differentiating between tumor cells and normal cells are two overriding problems in cancer treatments (Mahepal *et al.*, 2008). In an attempt to combat this lack of selectivity, three new complexes [Co(phen)(edda)], [Cu(phen)(edda)] and [Zn(phen)(edda)] were investigated on human breast cell lines.

Despite the high cytotoxicity to cancer cells [Co(phen)(edda)], [Cu(phen)(edda)] and [Zn(phen)(edda)] are much less toxic to normal human MCF10A. Interestingly, the analysis of the IC_{50} values (72 h) of these compounds showed significant selectivity towards breast cancer cells, MCF7 over non-malignant breast epithelial cells, MCF10A by a factor of

approximately twofold to sixfold (Table 4.1). Notably, the findings suggest that the compounds possess selectivity between cancer and normal cells. When one compares the relative cytotoxicity towards both cell lines in the lower concentration range, the selectivity of these compounds is more prominent (Figures 4.8-4.10). For example, 13.5 µM [Co(phen)(edda)] reduced cell viability of MCF7 cancer cells by 50%, while it reduced that of MCF10A normal cells at about 20%. In addition, 2.8 µM [Cu(phen)(edda)] reduced cell viability of MCF7 cancer cells by 50%, whereas it reduced that of MCF10A normal cells by only about 5%. Moreover, 5 µM [Zn(phen)(edda)] reduced cell viability of MCF7 cancer cells by 50% while it reduced that of MCF10A normal cells at about 12.5%.

MCF7 cells may be more sensitive than MCF10A cells to the antiproliferative effect of [M(phen)(edda)] because of the faster growth rate (i.e., lower doubling time) (Grem *et al.*, 2001; Boyd, 2004). However, this factor may have been minimized in our MTT assay, which used a shorter incubation period (1 – 3 days) and higher cell density per well (about 25,000 cells) (Boyd, 2004). Consequently, the selectivity shown by [M(phen)(edda)] towards MCF7 cells may not be due to the higher growth rate of MCF7 cells.

The results therefore certainly demonstrate that 50% viability of MCF7 cancer cells may be due to apoptosis and/or cell cycle arrest as it is considered to be one of the main mechanisms of inhibition of cell growth by the complexes. Indeed, all these [M(phen)(edda)] compounds were found to induce apoptosis in the MCF7 cells, while only the Zn(II) analogue was also able to

induce cell cycle arrest in S phase (Ng *et al.*, 2008). In addition, the cytotoxicity of the complexes may be partly due to their ability to bind to nuclear DNA and cause conformational changes and/or DNA damage *via* production of ROS (Ng *et al.*, 2008; Seng *et al.*, 2008). The much higher cytotoxicity of [Cu(phen)(edda)], compared with the Co(II) and Zn(II) analogues, may be attributed to its higher nucleolytic property and greater ability to generate ROS (Seng *et al.*, 2008). Most chemotherapeutic agents decrease tumor cell proliferation by induction of an apoptotic response (Kerr *et al.*, 1994). Besides, induction of apoptotic cell death can also be partly attributed to inhibition of topo I as reported for other anticancer compounds (Arjmand and Muddassir, 2010; Chashoo *et al.*, 2011). Thus, it is reasonable to attribute the cytotoxicity of these complexes towards cancer cells as due their action on multiple targets.

The above selectivity may be, in part, be attributed to inhibition of topo I which is over-expressed in MCF7 cells. The importance of this tumor selectivity has been highlighted and the severe toxicities of many clinical anticancer drugs are attributed to the lack of this factor (Carter, 1984; Sleijfer *et al.*, 1989). Although cisplatin is a highly effective anticancer agent, it is noted for dose-limiting side effects including hematologic toxicity, renal toxicity, gastrointestinal toxicity, nephrotoxicity, ototoxicity, and optic neuropathy which restrict its use in the clinic (Zisman *et al.*, 2011). Both alkylating agents such as busulfan, cisplatin and cyclophosphamide, and chemotherapy drugs such as 5-flurouracil, vinblastine, bleomycin and doxorubicin, can cause irreversible damage to the ovaries, which leads to

premature menopause, or to the testes, resulting in abnormal or reduced sperm production (Sonmezer and Oktay, 2004). Therefore, it is essential to develop more tumor selective drugs which are taken up more uniformly and/or selectively activated in the tumor environment, particularly in the hypoxic regions of solid tumors. Exposure of other organs to the toxicity of anticancer drugs, which is also encountered with newer clinically used oxaliplatin, remains an ongoing clinical and research problem (El-Ghannam *et al.*, 2010; Meyer *et al.*, 2011). Their preferential toxicities toward cancer cells over non-cancer cells suggest a strong potential of [Co(phen)(edda)], [Cu(phen)(edda)] and [Zn(phen)(edda)] towards safe antitumor application. Thus, animal studies involving the [M(phen)(edda)] complexes are been planned and this issue will be addressed in future.

5.2   Partition Coefficient Determination

The core properties required to estimate absorption, distribution, and transport of metal complexes in the body are solubility, lipophilicity, stability, and affinity towards transport proteins (Rudnev *et al.*, 2006). Determination of these properties are important in anticancer metallodrug research as they help to select a potential drug candidate to reach preclinical and clinical trial and also to design more active and/or less toxic compounds. Nowadays, most of the metal complexes are deficient in such screening assays and this seems to be an obstacle in their discovery process. Lipophilicity means the tendency of the compound to partition between lipophilic organic phase (immiscible with water) and polar aqueous phase; and the value of lipophilicity most commonly

refers to logarithm of partition coefficient, P (log P) between these two phases. An appropriate hydrophilic/lipophilic balance contributes the drug-likeness rule that ensure sufficient plasma concentration of the drug after oral administration. Characterization of novel metal coordination compounds in terms of relevant chemical and biochemical properties, preferably determined using rapid and inexpensive analytical methods so as to contribute to a better and more detailed understanding of chemotherapeutic significance of these [Co(phen)(edda)], [Cu(phen)(edda)] and [Zn(phen)(edda)] compounds. In this study, such assay has been conducted in parallel with MTT assay and implemented before much more expensive and labor intensive *in vitro* and *in vivo* studies in future. If the compounds are poor in their physicochemical properties such as lipophilicity in this case, they would have been largely removed by late stage clinical trial in development and it may bring about significant burdens in timelines and huge expenditures between discovery and clinical development. Besides, Ghadimi *et al.* (2011) have reported that lipophilicity has great influence on biological activity of IC_{50} in its structure-activity relationship. It is also important to consider the expensive and highly demanding and time-consuming clinical trials if a researcher is determined in developing a novel therapeutic drug for cancer.

Here, lipophilicity of the compounds was investigated. [Co(phen)(edda)], [Cu(phen)(edda)] and [Zn(phen)(edda)] was found to dissolve easily in deionized distilled water. From the analysis of log P data (Table 4.2) in this study, one can conclude that [Zn(phen)(edda)] possesses the most striking features with respect to its bioconcentration and membrane

permeability. Merluzzi *et al.* (1989) have reported that lipophilic zinc complexes easily penetrate the cell plasma membrane and were found to be cytotoxic in direct relationship to their lipophilicity. Notably, [Co(phen)(edda)], [Cu(phen)(edda)] and [Zn(phen)(edda)] lipophilicity might permit their passage through the cell membrane because of their respective good log P values of 0.30, 0.33 and 0.70, respectively. Thus, these compounds show promise as valid oral drug nominees. In order for a drug to be orally absorbed, it must first travel across lipid bilayers in the intestinal epithelium. For efficient transport, the drug must be hydrophobic enough to partition into the lipid bilayer, but not so hydrophobic, that once it is in the bilayer, it will not partition out again (Kubinyi, 1979). Lipid solubility, expressed as a partition coefficient, is determined by factors other than simply how easily the molecule dissolves in lipid (Scott, 1993). It gives an indication of the ability of a molecule to cross the plasma membrane of a cell by diffusion. Since the membrane is highly lipid in nature, the ability of the drugs to diffuse across the membrane will be dependent on the lipophilic properties of the drugs (Zedeck, 2004). In this analysis, [Co(phen)(edda)], [Cu(phen)(edda)] and [Zn(phen)(edda)] with higher concentration in the octanol phase as compared to the water phase is indicative of a greater likelihood that the compounds will pass through the cell membrane. The compounds must pass through a complex system of living cell membranes before it can enter the bloodstream. Moreover, the positive value of partition coefficient observed for the complexes which contain the aromatic phenanthroline ligand, indicate that these molecules are lipophilic in nature.

Ng *et al.* (2008) have reported that all [M(phen)(edda)] complexes are neutral molecules. Instead, most anticancer metal complexes containing 1,10-phen are cationic (D'Cruz *et al.*, 1999; Narla *et al.*, 2001; Roy *et al.*, 2010). The permeability of a membrane is the ease of molecules to pass through it. Permeability depends mainly on the electric charge of the molecule and to a lesser extent the molecular weight of the molecule. Therefore, electrically neutral and small molecules cross the membrane easier than charged, large ones. As predicted, [Co(phen)(edda)] presents the lowest lipophilicity (log P = 0.30) and it is the least cytotoxic and selective (IC$_{50}$, 13.5 µM) compound among the three compounds. The complexes [Cu(phen)(edda)] and [Zn(phen)(edda)] with log P = 0.33 and 0.70, respectively are more lipophilic than [Co(phen)(edda)] and at the same time more sensitive against the MCF7 cancer cells (Table 4.2). [Zn(phen)(edda)] has the highest octanol/water partition coefficient but does not exhibit the most selective cytotoxic activity against MCF7 cancer cells. On the other hand, [Cu(phen)(edda)] possess an intermediate partition coefficient compared to [Co(phen)(edda)] and [Zn(phen)(edda)], which plays an important role in their uptake by both normal and cancer cells due to copper compound exhibited the most cytotoxic and selective against MCF7 cancer cells. It is therefore necessary to retain the lipophilicity of the compound within a certain octanol-water partition coefficient range in order to facilitate the uptake of a drug, and determine the degree of selectivity and cytotoxic potency of drug (Mahepal *et al.*, 2008). Interestingly, there are approximately twofold increase in log P and IC$_{50}$ values of [Zn(phen)(edda)] (IC$_{50}$, 5 µM) as compared with [Cu(phen)(edda)] (IC$_{50}$, 2.8 µM), indicates that [Zn(phen)(edda)] has greater permeability potency to cross

the cell membrane passively (*via* its molecular weight and neutral charge) and also exerts its effectiveness in killing cancer cells. In this study, zinc compound has shown the best activities among the results of all [M(phen)(edda)] complexes when observed in apoptosis analysis, $\Delta\psi_m$ detection, topo I inihibition assay and only this compound can arrest cell cycle arrest. Furthermore, neutral metal complexes should be more lipophilic than the corresponding ionic metal complexes and their greater uptake by cells can lead to increased cytotoxicity with effective lower IC_{50} value. The delivery of the drugs that combine high cytotoxicity and selectivity to the target cancer cells or tissues, as well as limited toxicity in normal cells or tissues remains a challenge, although some very promising examples have emerged recently. A poor therapeutic ratio (efficacy/toxicity) is generally unacceptable in a drug (Lajiness *et al.*, 2004); however, it may be a workable finding through an early drug discovery of hits-to-lead phase prior to lead optimization phase to allow for the best chance of discovering a candidate that combines all of the qualities of a successful drug product. Therefore, believing in incorporating toxicological properties into a definition of drug-likeness is important since they are always associated with activity against a specific target.

Some examples of hydrophilic drugs are cisplatin, doxorubicin, 5-fluorouracil and others. These drugs are still facing difficulties in drug delivery formulations to treat cancer (Birnbaum and Brannon-Peppas, 2003). Screnci *et al.* (2000) have reported that log *P* values of platinum-based derivatives of cisplatin, carboplatin and oxaliplatin are -2.53, -2.30, and -1.65, respectively. Another researchers, Platts *et al.* (2006) have reported that cisplatin and

carboplatin have log P values of -2.16 and -1.63, respectively. Their poor lipophilicity makes them not to be very bioavailable after oral intake and hence is to be applied *via* intravenous route. Besides, Ghose and research colleagues (1999) had tested for more than 80% of the known compounds and reported the qualifying range of the calculated log P is between -0.4 and 5.6. In addition, Kerns and Di (2008) have reported that an optimal gastrointestinal absorption by passive diffusion permeability after orally intake of drug is to have a moderate log P within the range from 0 to 3. Compounds with a lower log P are more polar and have poorer lipid bilayer permeability. While, compounds with a higher log P are more non-polar and have poor aqueous solubility. Therefore, a good balance of permeability and solubility has to be achieved. As within the limits proposed for drugs, Ng *et al.* (2008) have reported that the molecular weight of [Co(phen)(edda)].3H$_2$O, [Cu(phen)(edda)].5H$_2$O and [Zn(phen)(edda)].3^1/$_2$H$_2$O are 467.34, 507.98 and 482.81, respectively (Table 4.2).

When these compounds dissolved in water, the lattice water molecules are released. In the solution, the Co(II), Cu(II) and Zn(II) complex molecules have molecular weights of 413.30, 417.91 and 419.75, respectively. Thus, these compounds have molecular weight less than 500. Besides, each of the compounds contains two hydrogen bond donors (2 amino nitrogen N-H of edda) and eight hydrogen bond acceptors (8 lone pairs of electrons from the 4 carboxylate oxygen atoms of edda) (Figure 1.1). From the partition coefficient in water-octanol mixture, the calculated log P value for [Co(phen)(edda)], [Cu(phen)(edda)] and [Zn(phen)(edda)] are 0.30, 0.33 and 0.70, respectively.

Therefore, the properties of the compounds are in accord with Lipinski's rule-of-five, i.e (1) molecular weight is less than 500; (2) less than 5 hydrogen bond donors; (3) less than 10 hydrogen bond acceptors; and (4) log P value less than 5 (Lipinski *et al.*, 2001). Lipinski's Rule of Five is a rule of thumb to evaluate drug-likeness or to determine if a chemical compound with a certain pharmacological or biology activity has properties that would make it a likely orally active drug in humans. Lipinski's Rule of Five is still useful to screen the drug-like property of a potential drug because of the exorbitant cost of clinical trial (Lipinski *et al.*, 2001). In fact, a recent analysis of the top 69 pharmaceutical drugs in 2007 found that 56 drugs obey this rule (Giménez *et al.*, 2010).

Compounds with poorer physical and chemical properties, including those which are insoluble and non-permeable could be filtered out at an earlier stage. As the [Co(phen)(edda)], [Cu(phen)(edda)] and [Zn(phen)(edda)] complexes have good lipophilic and good antiproliferative properties, these compounds can be recommended for moving into the next development stage, i.e. enter preclinical and clinical investigation. Thus, these compounds have the potential to be developed into oral drugs.

5.3 Compounds Affected Cell Morphology of MCF7 Cells

5.3.1 Compounds Induce Surface Morphology Changes Characteristic of Apoptosis

The historical recognition has shown that apoptotic cell death involved a unique series of events and was initially based on morphological evidence of changes in cell structures. Other studies have shown that cells with treatment of metal-based drugs-induced apoptosis in tissue culture usually go through a unique series of surface morphological changes (Cohen *et al.*, 1999; Hossain and Kleve, 2011), as shown in Figures 4.11-4.13. These include the following: (a) a loss of adhesion to substratum, resulting in cell rounding; (b) a flurry of surface zeiotic blebbing, which may last for only a few hours; (c) shrinkage of the cell, with cessation of blebbing and other movements (e.g. translocation of phosphatidylserine from the inside of the cell to the outer surface) to package themselves into a form that allows for their removal by macrophages; (d) the slow protrusion of elongated "echinoid spikes" from the cell surface; and (e) after a long delay of several hours, the "blistering" of the cell surface membrane with eventual lysis (Willingham, 1999). It was also found that at a later step of apoptosis, condensation of chromatin is more advanced and cytoplasmic organelles are loosing their structure (Erkkilä *et al.*, 2003). In this morphological study, a series of pattern of treated MCF7 cells undergoing apoptosis was observed; cell rounding > cell blebbing > echinoid spikes > cell blisters > cell lysis. It is noted that the morphological changes on cell surface with the treatment of the [M(phen)(edda)] compounds have occurred. The usual sequences of morphological changes in untreated adherent cultured cells are also shown in Figures 4.11-4.13. Untreated control MCF7 cells retained their normal size and shape while neighboring cells were closely connected to each other. In comparison with control conditions, when the incubation time was increased from 24 h to 48 h and 72 h, the number of apoptotic MCF7 cells

and cell debris increased as evident by morphological observation when treated with all [M(phen)(edda)] compounds. Thus, they are said to be time-dependent.

5.3.2 Compounds Induce Nuclear Changes Characteristic of Apoptosis

The field of cell death research has undergone an explosion of new knowledge over the past decade. The realization that apoptosis or programmed cell death involves highly conserved mechanisms in cells and that the accompanying events are important in most pathologic field, has attracted many people to do cell death research. The need for histochemical and cytochemical methods to evaluate death of cells, especially in intact tissues, has led to the development of several techniques (Mark, 1999). In this morphological study, DAPI fluorescent dye was used due to its main advantages, *viz.* the cells can be stained quickly, simple protocol, relatively straightforward and inexpensive. This technique does not require complex staining procedures as is found in TUNEL assay, and DAPI is a robust nuclear dye (DeCoster, 2007). An evidence of apoptosis can be observed that is linked to individual cell responses as reflected by morphological changes based on fluorescent staining of the cell nucleus using DAPI.

DAPI can pass through an intact cell membrane and it can be used to stain both live and fixed cells. In this morphological study, the cells were fixed because DAPI can pass through the membrane more efficiently as compared to live cells and therefore the effectiveness of the stain is higher (Yasujima *et al.*, 2010). Here, MCF7 cells that were treated with 13.5 µM [Co(phen)(edda)], 2.8

144

μM [Cu(phen)(edda)] and 5 μM [Zn(phen)(edda)] (and 10μg/ml cisplatin) for 24, 48 and 72 h followed by staining the cell nuclei with DAPI showed changes of nuclear features. During apoptosis, DAPI can pass through the membranes of cells to stain the nuclei and the blue fluorescence of the DAPI dye can be observed by fluorescent microscopy. The dye in the apoptotic cells will emit an intense blue fluorescence. For untreated MCF7 control cells, their round nuclei are stained uniformity and their margins are clear. But, for apoptotic MCF7 cells, the margins of their nuclei are abnormal and the condensed chromosomes are easily stained.

When cells were stained with DAPI and observed under the microscope, not many apoptotic cells were seen in 24 h incubation. However, after 48 and 72 h, marked morphological changes were seen in the detached cells. In parallel with these morphological changes, some cells had nuclei that were condensed or probably fragmented and these were termed apoptotic, while others appeared to have normal morphology. The condensed nuclei of apoptotic cells are clearly visible as they are stained by DAPI more intensely (Figure 4.14). At 72 h, almost all cells have entered apoptosis with treatment of [Co(phen)(edda)], [Cu(phen)(edda)] and [Zn(phen)(edda)]. As the time of the cells incubating with the compounds increased, cells with brightly stained nuclei increased. Therefore, the intense fluorescence intensity shown in nuclear condensations indicate that [M(phen)(edda)] complexes induced apoptotic cell death in MCF7 cells. This nuclear shape change occurs at an early point in the series of apoptotic morphological events, usually soon after the beginning of surface blebbing (Collins *et al.*, 1997). Furthermore, AIF and endonuclease G

are released from mitochondria upon outer mitochondrial membrane permeabilization and translocate into the nucleus to contribute to nuclear chromatin condensation and large-scale DNA fragmentation (Fulda and Debatin, 2006). However, it is still not exactly clear how AIF contributes to nuclear DNA fragmentation. In mammalian cells, cyclophilin A, a peptidyl-prolyl *cis–trans* isomerase, cooperates with AIF to induce breakdown of DNA (Fulda and Debatin, 2006).

5.4   Analysis of Induction of Apoptosis

Many researchers have studied the application of apoptosis mechanisms relevant to cancer therapy (Ferreira *et al.*, 2002; Gerl and Vaux, 2005; Ghobrial *et al.*, 2005). One outcome from these studies was the discovery of various kinds of apoptosis-inducing chemicals and those actually has reached preclinical and clinical investigation. Moreover, some clinically used anticancer drugs, such as cisplatin (Stordal and Davey, 2007), doxorubicin (Laginha *et al.*, 2005), etoposide (Lin and Yao, 1994) are known to induce apoptosis in carcinoma. Apoptosis is especially relevant to cancer regulation. Additionally, most cancers actually disable apoptosis. That is, they disable the signals so that the body cannot recognize the cell as cancer. As one can imagine, the study of apoptosis has all kinds of implications for cancer treatments. If one could find a way to induce apoptosis in cancerous cells, it will potentially force cancer cells to kill themselves. Therefore, apoptosis is an active, energy-dependent process in which the cell participates in its own destruction.

In this study, at 24 h, with [Co(phen)(edda)], [Cu(phen)(edda)] and [Zn(phen)(edda)] treatment, the percentages of the apoptotic cells (early apoptotic cells + late apoptotic cells) are 23.04%, 30.86% and 32.04%, respectively. For [Co(phen)(edda)], [Cu(phen)(edda)] and [Zn(phen)(edda)] treatment at 48 h, the percentages of the apoptotic cells are 28.33%, 30.57% and 33.34%, respectively. Finally for 72 h treatment with [Co(phen)(edda)], [Cu(phen)(edda)] and [Zn(phen)(edda)] , the percentages of the apoptotic cells are of 30.74%, 32.19% and 35.46%, respectively. Therefore, the percentages of the apoptotic cells increased with increase in the incubation time. In early-stage apoptosis, the plasma membrane excludes PI. These cells stained with Annexin V-FITC but not PI, thus distinguishing cells in early apoptosis. However, in late-stage apoptosis, the cell membrane lost integrity thereby allowing Annexin V-FITC to also access PS in the interior of the treated MCF7 cells. PI used to resolve these late-stage apoptotic (Annexin V-FITC$^+$/PI$^+$) and necrotic cells (Annexin V-FITC$^-$/PI$^+$) from the early-stage apoptotic cells (Annexin V-FITC$^+$/PI$^-$). By observing each panels of the quadrant, the flow cytometry results showed that some population of cells from early stage of apoptosis gradually progressed to the late stage of apoptosis with treatment of [Co(phen)(edda)], [Cu(phen)(edda)] and [Zn(phen)(edda)] [Figures 4.16-4.18, (c), (d), (e)]. This is because PS externalization is an early feature of apoptosis and can be detected by the binding of Annexin V to PS on the cell surface (van Engeland *et al.*, 1996).

In addition to apoptosis induction, another common effect shared by many anticancer drugs is the introduction of cell cycle arrest. Perturbation of

cell cycle progression can cause severe damage to cells and may trigger apoptosis. In this project, [Co(phen)(edda)], [Cu(phen)(edda)] and [Zn(phen)(edda)] treatment progressively generated particles with hypodiploid DNA content (Figures 4.23-4.25). Apoptotic cells with hypodiploid DNA content were measured by quantifying the sub G_0/G_1 peak in the cell cycle pattern (Li *et al.*, 2007). Flow cytometric studies revealed that exposure of MCF7 cells to IC_{50} concentrations of [Co(phen)(edda)], [Cu(phen)(edda)] and [Zn(phen)(edda)] resulted in marked time-dependent increases in the proportion of apoptotic cells as reflected by the sub-hypodiploid peaks. The signal transduction pathway leading to apoptosis is a highly organized physiological mechanism for destroying injured and abnormal cells that may play an important role in some cellular processes of cell cycle (Xia *et al.*, 1999). Some anticancer drugs, when applied *in vivo*, are able to intercalate with DNA in cancer cells and do arrest cancer cells in the cell cycle (Bachur *et al.*, 1978). However, there are many literature reports which established cell death associated with S phase arrest and apoptosis (Iguchi *et al.*, 2007; Chen and Wong, 2008; N'cho and Brahmi, 2001). Characterization of apoptosis mainly derives from morphological and ultrastructural observations (Kerr *et al.*, 1972). Observed features in microscopic work include decreased cell size, membrane blebbing, chromatin condensation, spike and blister formation and ultimately cell lysis act as strong evidence in apoptosis. In addition, apoptosis is initiated by the release of mitochondrial pro-apoptotic proteins into the cytosol (Gulbins *et al.*, 2003). Therefore, the collapsed of the percentage of $\Delta\psi_m$ also contribute to the evidence of apoptosis.

Ng *et al.* (2008) have reported that cell death induced by metal complexes Co^{2+}, Cu^{2+} and Zn^{2+} is mainly *via* apoptosis. These data are in agreement with results in this project where [M(phen)(edda)] induced apoptosis caused morphological changes such as formation of blebs, spikes and chromatin condensation (Figures 4.11-4.14), shown by a significant cell populations in sub G_0/G_1 phase (Figures 4.26-4.28) and evidence of lowering $\Delta\psi_m$ by JC-1 staining (Figures 4.36). Some researchers had reported that increase in cell population at sub G_0/G_1 phase had been taken as evidence of cells entering apoptosis (Sprenger *et al.*, 2002; Wang *et al.*, 2005; Heffeter *et al.*, 2006). Among all the 60 cell lines, the MCF7 cell line is often used in apoptosis studies because it is well known to have a genetically defective form of caspase 3, an important apoptosis-inducing effector molecule (Jänicke *et al.*, 1998). AIF might be released during the cascade events as it does not use caspases and normally located in the intermembrane space of mitochondria. It might be released from the mitochondria and migrates into the nucleus, eventually binds to DNA and exhibit nuclease activity in the presence of reducing agents which triggers the destruction of the DNA and leads to cell death (Ostrakhovitch and Cherian, 2005; Fulda and Debatin, 2006). This study presumes that [M(phen)(edda)] complexes may involve in mitochondrial mediators of caspase-independent apoptosis and also signaling through the intrinsic pathway of apoptosis. Continuous work in this project has to be done to further confirm the mechanism of action of [M(phen)(edda)] complex.

5.5   Analysis of Cell Cycle Arrest

According to literature, cell cycle arrest may be a prerequisite step for initiating terminal differentiation (Bernhard *et al.*, 2000). Although, G_0/G_1 arrest has been the center of attention in differentiation, some reports are concerned with the involvement of G_2/M and S phase arrest in this event (Rapaport, 1983; Gorin *et al.*, 2000). Inhibition of DNA synthesis was accompanied by the cell differentiation suggesting that duplication of the cellular genome during the S phase of cell cycle is a critical event during which the cells are highly susceptible to the induction of differentiation (Plagemenn *et al.*, 1975; Rapaport, 1983; Bernhard *et al.*, 2000; Huang *et al.*, 2002). In this investigation, an S phase arrest was observed on [Zn(phen)(edda)]-treated MCF7 cells in 72 h. Figures 4.26-4.28 summarizes the results of the assessment of possible cell cycle perturbations after 24, 48 and 72 h of exposure to [Co(phen)(edda)], [Cu(phen)(edda)] and [Zn(phen)(edda)].

On treatment with 13.5 µM [Co(phen)(edda)] for 24 h, there was a 5.42% increase in the number of MCF7 cells in the sub G_0/G_1 phase [Figure 4.23(3)] while there was a 0.95%, 1.51% and 3.20% decrease in the number of cells entering the G_0/G_1, S and G_2/M phase of the cell cycle, respectively. This indicated that the [Co(phen)(edda)]-treated cells showed no obvious cell cycle arrest. When the treatment period was increased to 48 h, [Co(phen)(edda)] induced a transient G_0/G_1 arrest with increase of 2.77% of cells. However, after 48 until 72 h treatment with [Co(phen)(edda)], treated MCF7 cells showed a significant decline in G_0/G_1 phase while pushing these fractions into

sub G_0/G_1 phase. Significant rise in apoptotic fraction was observed after 24 h of drugs treatment which increased with the incubation time. Sprenger *et al.* (2002), Wang *et al.* (2005) and Heffeter *et al.* (2006) have reported that increase in cell population at sub G_0/G_1 phase had been taken as evidence of cells entering apoptosis.

FACS analysis of MCF7 cells treated with 2.8 µM [Cu(phen)(edda)] for 24 h showed a 8.19% increase in the number of cells in sub G_0/G_1 phase and there was 2.95%, 1.84% and 3.84% decrease in the number of cells in the G_0/G_1, S and G_2/M phase of the cell cycle, when compared to the control cells. At 48 h, there was a 11.94% increase in the number of MCF7 cells in sub G_0/G_1 phase [Figure 4.24(4)] while there was a 4.72%, 2.99% and 6.83% decrease in the number of cells entering the G_0/G_1, S and G_2/M phase of the cell cycle, respectively. With the treatment of [Cu(phen)(edda)] on MCF7 cells in 72 h, a massive increase in population of cells (from 7.40% to 30.44%) in sub G_0/G_1 phase with approximately increased by fourfold. It is the highest percentages of apoptotic cells along with the presence of prominent sub G_0/G_1 peak that compared among [M(phen)(edda)] treatments and thus it is likely to contribute to the antiproliferative effect on cancer cells due to its ability to induce apoptosis. However, there were a decrease in the number of cells in G_0/G_1, S and G_2/M phases of the cell cycle in 72 h incubation. This indicated that after a prolonged exposure to the compound, more cells were dying. Moreover, detection of hypodiploid sub G_0/G_1 population of cells confirms its role as an inducer of apoptosis (Schwartz and Shah, 2005).

After treatment of MCF7 cells with 5 μM [Zn(phen)(edda)] for 24 h, a significant increase in percentages of cells with hypodiploid DNA content from 5.78% to 13.90% in sub G_0/G_1 phase due to apoptosis. The number of apoptotic cells increased with time, reaching about 15.70% after 48 h and 25.26% until 72 h. However, longer exposures to [Zn(phen)(edda)] resulted an increase in percentages of MCF7 cells in S phase (24 h, 11.29%; 48 h, 12.50% and 72 h, 16.96% compared to about 1.2-7.5% variation in control cells). In other words, after a period of exposure (after 24 until 72 h), the S phase arrested MCF7 cells were unable to proceed into the G_2/M phase [Figure 4.25(5)]. A time-dependent increase in early S phase cell population along with a compensated decrease of cells in G_0/G_1 and G_2/M phases were observed for 72 h of treatment. It therefore appears that the cell death promoting effect of [Zn(phen)(edda)] is partially due to blocking the cells in S phase, preventing progression to the G_2/M phase. The ability of [Zn(phen)(edda)] to abolish cells in the G_2/M phase may contribute to its ability to function as a tumor growth inhibitor and is highly comparable to other potent antitumor agents. It is known that tumor cells are dependent on the G_2/M checkpoint (Schwartz and Shah, 2005). Therefore, cell cycle G_2/M checkpoint abrogation by [Zn(phen)(edda)] may impact on cell death or proliferation. Similar to the effect of [Zn(phen)(edda)], some other well-known antitumor agents such as cisplatin, irofulven, okadaic acid and topotecan also arrest cells in S phase thereby inhibiting tumor proliferation (Albertella *et al.*, 2005; Serova *et al.*, 2006; Traore *et al.*, 2001; Redkar *et al.*, 2004). Besides, Joe *et al.* (2002) have reported that resveratrol caused a dose-dependent cancer cell growth inhibition,

and this antiproliferative effect appears to be due to its ability to induce S phase arrest and apoptotic cell death.

In this study, the data presented here show that [Zn(phen)(edda)] induced an S phase arrest at concentration based on IC_{50} value for 24, 48 and 72h (Figures 4.26-4.28). During S phase, cells are continuously checking the integrity of their DNA to ensure the accuracy of the copying process. If any alteration is found, there are two safety mechanisms (i.e. DNA damage and DNA replication checkpoints) that stop S-phase progression and coordinate the repair of damaged DNA (Zhou and Elledge, 2000; Hakem, 2008). Thus, the data suggested that DNA damage induced by [Zn(phen)(edda)] arrests cells in S phase and activates the DNA replication checkpoints. This scenario is different from that obtained with treatment of [Co(phen)(edda)] and [Cu(phen)(edda)] where both complexes did not observe any cell cycle arrest following 24 - 72 h incubation. Whether these effects are metal- or ligand-dependent is presently not known. In these experiments, the S phase accumulation was the highest at 72 h with exposure of the cells to [Zn(phen)(edda)]. [Zn(phen)(edda)]-treated MCF7 cells would probably stop in the cell cycle progression as they could not proceed to the stage of mitosis, due to the high amount of DNA damage that they endured during cell cycle arrest at S phase, and consequently, they would die.

The ability of a compound to affect specific phases of the cell cycle may indicate its cytotoxic mechanism of action. Transit of normal cells through G_0/G_1 and into S phase typically requires the action of mitogens, and is

controlled by the cyclin dependent kinases (Cdks) that are sequentially activated by cyclins D, E and A (Morgan, 1995). Further experiments need to be done to confirm this hypothesis. Because D-type cyclins and Cdks are required for the progression of cells from the G_0/G_1 phase to the S phase of the cell cycle, cyclin D1 expression has to be found out. Further work is being carried out to investigate further the molecular mechanism of cell death of the [M(phen)(edda)] complexes, and confirm the above preliminary observations.

5.6   Detection of the Mitochondrial Membrane Potential ($\Delta\psi_m$)

Apoptosis is a complex process that can be induced by many different factors, which, in turn, act through various cell death signaling pathways. The role of the mitochondria could potentially vary and may be dependent on a variety of factors including mode of apoptosis induction, cell type, or cell status with respect to the cell cycle, state of differentiation, development, normalcy or pathology (Cossarizza *et al.*, 1993). More recently, it has been shown that mitochondria are integrally involved in apoptosis or programmed cell death (Zamzami *et al.*, 1996). One of the earliest events in the progression of apoptosis is the dissipation of the $\Delta\psi_m$ (Xiao *et al.*, 2011).

Particular focus has recently been given to this assay which was designed to study the $\Delta\psi_m$ during apoptosis (Salvioli *et al.*, 1997). To study the $\Delta\psi_m$ changes in human cell line, it was found that JC-1 is a more reliable fluorescent probe than 3,3'-dihexiloxocarbocyanine iodide (DiOC6) and rhodamine-123 (Salvioli *et al.*, 1997). JC-1, a lipophilic cation, is being used in

a new cytofluorimetric technique to detect variation in membrane electrical potential at the single cell level (Cossarizza *et al.*, 1993). JC-1 is more advantageous than rhodamines and other carbocyanines because it can enter selectively into mitochondria and reversibly change its color from green to reddish orange as membrane potentials changes.

Cytofluorimetric analysis by FACS with $\Delta\psi_m$-specific fluorescent JC-1 staining has been carried out to investigate the effect of [Co(phen)(edda)], [Cu(phen)(edda)] and [Zn(phen)(edda)] at IC_{50} concentration on the changes in the $\Delta\psi_m$. In this study, cisplatin was used as a positive control. The results showed that cisplatin-treated MCF7 cells exhibited increase in green fluorescence in monomeric forms following 24, 48 and 72 h in culture, compared to untreated control (Figure 4.29). At 24 h incubation, there is no noticeable change in green fluorescence. Exposure of MCF7 cells to 13.5 μM [Co(phen)(edda)] and 2.8 μM [Cu(phen)(edda)] showed a distinct increase in green fluorescence intensity only after 48 h (Figure 4.34). From 48 to 72 h incubation with Co(II) and Cu(II) complexes, the increase in green fluorescence seems to level off. However, incubation of MCF7 cells with 5 μM [Zn(phen)(edda)] compound for 24, 48 and 72 h caused greatest shifting of JC-1 fluorescence intensity from red to green. The results showed that percentages of population of cells in monomeric form increased from 18.97% to 22.14% (in 24 h), from 11.29% to 46.26% (in 48 h), and from 9.69% to 70.77% (in 72 h), respectively. As a result, a time-dependent reduction in $\Delta\psi_m$ was detected in the groups treated with [M(phen)(edda)].

$\Delta\psi_m$ can be calculated from the ratio ($I_{590\ nm}/I_{527\ nm}$) between red fluorescence (590 nm) intensity and green fluorescence (527 nm) intensity using JC-1 (Chen *et al.*, 2010). The measurement of the ratio of the red to green JC-1 fluorescence in cells by flow cytometry is a sensitive and specific method for monitoring changes in $\Delta\psi_m$ in living cells during induction of apoptosis by various agents (Cossarizza, 2000). In Figure 4.36, the effect of 13.5 µM [Co(phen)(edda)], 2.8 µM [Cu(phen)(edda)] and 5 µM [Zn(phen)(edda)] on $\Delta\psi_m$ in MCF7 is shown. It is clearly seen that they significantly decrease the $\Delta\psi_m$ only after more than 24 h and the decrease is time-dependent (48 and 72 h). At 72 h, [Zn(phen)(edda)] induced the greatest reduction in $\Delta\psi_m$. After 72 h of [M(phen)(edda)] treatments, the magnitude of the $\Delta\psi_m$ lost in the treated cells were almost 3 to 22 times compared to that of control, with Zn(II) compound reduced $\Delta\psi_m$ the most and even reduced more than cisplatin. Interestingly, [Zn(phen)(edda)] showed a strong decrease in $\Delta\psi_m$ which could damage the function and integrity of mitochondrial membrane. The above decrease in $I_{590\ nm}/I_{527\ nm}$ in response to [M(phen)(edda)] complexes emphasize on their mitochondrial role in apoptosis that reflect increase of JC-1 monomers outside the mitochondria while imply depolarization of the mitochondrial membrane. This is because normal cells have high $\Delta\psi_m$ values and their membranes are polarized but cells that are undergoing apoptosis have low $\Delta\psi_m$ values and their membranes are said to be depolarized. Collapse of the $\Delta\psi_m$ results in a depolarized $\Delta\psi_m$ is often observed to occur early during apoptosis (Xiao *et al.*, 2011). Taken together, the results suggest that decrease in $\Delta\psi_m$, these [M(phen)(edda)] compounds can interact with the mitochondria. This lowering of $\Delta\psi_m$ can initiate apoptotic intrinsic pathway (Debatin, 2000).

Therefore, apoptosis induced by [M(phen)(edda)] complexes is by intrinsic pathway which involved decrease in $\Delta\psi_m$. The order of loss of $\Delta\psi_m$ by JC-1 staining of [M(phen)(edda)] series of complexes is [Zn(phen)(edda)] > [Cu(phen)(edda)] > [Co(phen)(edda)]. The results have linked dissipation of the $\Delta\psi_m$ to the initiation of apoptosis and decreased $\Delta\psi_m$ enhanced the initiation of apoptosis.

In fact, ruthenium complexes reportedly induced loss of $\Delta\psi_m$ and concomitant intrinsic pathway of cell death (Meggers *et al.*, 2009; Mulcahy *et al.*, 2010). An anticancer manganese(II) complex also caused lowering of $\Delta\psi_m$ (Chen *et al.*, 2010). Many researchers had reported that there are a number of studies about collapse of the mitochondrial membrane potential during apoptosis, leading to a generalization that depolarization of the mitochondria is one of the first events occurring during apoptosis and may even be a prerequisite for cytochrome c or AIF release (Ostrakhovitch and Cherian, 2005; Roy *et al.*, 2008). During the past decade, the most significant research in mitochondrial biology may be the discovery that mitochondria play an important role in apoptosis, a fundamental biological process by which cells die in a well-controlled or programmed manner. Given the complexity of apoptosis, it is likely that there are a number of mechanisms available to the cell for carrying out the process of apoptosis (Petit *et al.*, 1995). It has been reported that several nDNA-encoded (nDNA, nuclear deoxyribonucleic acid) pro-apoptotic proteins including cytochrome c, AIF, endonuclease G, and smac/DIABLO (smac, second mitochondria-derived activator of caspase; DIABLO, direct inhibitor of apoptosis-binding protein with low isoelectric

point) normally reside in the mitochondria in caspase-dependent and caspase-independent apoptosis pathways where they perform known or yet unidentified physiological functions (Kroemer, 2007). However, once these protein factors are released from mitochondria, they trigger a series of biochemical events leading to activation of apoptotic signaling cascades. Perhaps, the most well characterized apoptotic cascade is the activation of caspases (a class of proteases) by cytochrome c and apaf-1 in the presence of adenosine triphosphate (ATP) or deoxyadenosine triphosphate (dATP) (Boatright and Salvesen, 2003). In contrast, translocation of AIF from mitochondria to the nucleus appears to cause apoptosis in a caspase-independent manner (Kroemer, 2007). Therefore, dysfunction of mitochondrial membrane causes increase of the permeability of the mitochondrial membrane and subsequently promotes the release of apoptogenic factors, including cytochrome c (caspase-dependent) and AIF (caspase-independent). Subsequently, they may activate the caspases enzyme system, which further act upon cell nucleus and cell keratinoprotein to induce irreversible apoptotic changes (Budihardjo *et al.*, 1999; Kroemer, 2007). The functional changes of mitochondria may be accompanied with decreasing the formation of ATP, reducing the activity of dehydrogenase, thus influencing cell respiration, cell metabolism, energy supply and even the cell death (Brand and Nicholls, 2011). According to Ostrakhovitch and Cherian (2005), Cu^{2+} induces apoptosis through depolarization of $\Delta\psi_m$ with release of AIF.

Using flow cytometry, initial publication work has established that [M(phen)(edda)] induced apoptosis in MCF7 and there was no necrosis (Ng *et*

al., 2008). These data are in agreement with previous results where [M(phen)(edda)] induced apoptosis caused morphological changes such as formation of blebs, spikes, blisters and condensation of chromatin (Figures 4.11-4.14), shown by a significant cell populations in sub G_0/G_1 (Figures 4.26-4.28) and evidence of mode of cell death of apoptosis in Annexin V-FITC/PI staining analysis (Figures 4.19-4.21). Loss of $\Delta\psi_m$ induced by [M(phen)(edda)] suggests mitochondria-mediated apoptosis. However, studies into cell death induced by metal(II) ions showed that decrease in $\Delta\psi_m$ may involve different pathways of apoptosis or different mode of cell death. For example, $CoCl_2$ induced apoptosis in rat PC12 cells through both mitochondria-mediated pathway accompanied by loss in $\Delta\psi_m$ and death receptor-mediated pathway (Jung and Kim, 2004). Killing of rat neurons by excess Zn^{2+} ions involved loss of $\Delta\psi_m$ and inhibition of oxygen utilization in the mitochondria (Dineley *et al.*, 2005). Micromolar concentration of Cu^{2+} could induce both apoptosis and necrosis of trout hepatocytes (Krumschnabel *et al.*, 2005). Besides strong production of ROS, Cu^{2+} induced decrease in $\Delta\psi_m$ and induced mitochondrial permeability transition (Krumschnabel *et al.*, 2005). It was also found that Cu^{2+} and Zn^{2+} could induced apoptosis in MCF7 cells, and the cell death involved decrease in $\Delta\psi_m$, elevated ROS production and activation of p53 (Krumschnabel *et al.*, 2005). The role of p53 in apoptosis is crucial, and depolarization of mitochondrial membrane caused release of AIF and its translocation into the nucleus (Krumschnabel *et al.*, 2005). Unlike the present results from [M(phen)(edda)] study for 72 h incubation, the Cu^{2+} ions induced greater decrease in $\Delta\psi_m$ than Zn^{2+} ions in MCF7 cells (Ostrakhovitch and Cherian, 2005). In fact, one of the most important organelles involved in

apoptosis regulation is the mitochondrion and there is always association between the changes of $\Delta\psi_m$ and apoptosis.

Recently, [Cu(4,7-dimethyl-phenanthroline)(glycinate)NO$_3$] was reported to induce overproduction of ROS leading to loss of ψ_m and cell death in human lung cancer cells (Kachadourian *et al.*, 2010). Besides, Wang *et al.* (2003) have reported that the decrease in $\Delta\psi_m$ is correlated with ROS production and may be one of the earlier steps occurring before nuclear DNA damage. Such a relationship could be due to two mutually interconnected phenomena, *viz.* (i) ROS causing damage to the mitochondrial membrane, and (ii) the damaged mitochondrial membrane causing increased ROS production. This is because $\Delta\psi_m$ is the driving force for mitochondrial ATP synthesis, loss of $\Delta\psi_m$ results in depletion of cellular ATP level. The loss of $\Delta\psi_m$ causes the cellular ROS generation and in turn leads to the oxidative DNA lesions followed by DNA fragmentation (Roy *et al.*, 2008). Therefore, a consequence of mitochondria function is the production ROS. Besides, Seng *et al.* (2008) have reported that [M(phen)(edda)] complexes have nucleolytic properties and are able to generate ROS. This study presumes that the [M(phen)(edda)] complexes induced free radicals such as ROS, and may be correlated in the decrease of $\Delta\psi_m$. AIF translocation may be initiated from mitochondria to the nucleus in MCF7 cells, which are depleted in caspase 3 (Jänicke *et al.*, 1998). Hence, it is deduced that the participation of mitochondria-related mechanism is one of the factors resulting in [M(phen)(edda)]-induced apoptosis.

5.7   Human DNA Topoisomerase I (Topo I) Inhibition Study

DNA topo I is an enzyme that plays vital role in releasing the topological stress of DNA generated by cellular metabolic processes such as replication, transcription repair, and chromatin assembly by introducing temporary single-strand breaks in the DNA (Carey *et al.*, 2003). This enzyme has been identified as important targets in cancer chemotherapy and microbial infections (Singh *et al.*, 2007). However, very few metal complexes have been reported to inhibit topoisomerases and even fewer Zn(II) complexes have been reported to inhibit topo I and II (Chuang *et al.*, 1996).

In this study, it was found that one unit of topo I could completely convert all the plasmid pBR322 to fully relaxed DNA or topoisomers (Figures 4.37-4.43, L4) while the phen, $CoCl_2$, $CuCl_2$ and $ZnCl_2$ could not inhibit topo I in the concentration range 5-40 μM except $CuCl_2$ at 40 μM (Figures 4.37-4.40). The present negative results for the salts $CoCl_2$ and $ZnCl_2$ is in agreement with previous findings which found that its concentration needed to be above 80 μM to significantly inhibit topo I and presence of high excess of $MgCl_2$ was needed (Douvas *et al.*, 1991). Very high concentration of $ZnCl_2$ (mM levels) has been also reportedly needed to inhibit topo I isolated from shrimp *Penaeus japonicas* (Chuang *et al.*, 1996). In the presence of 10 or 20 μM [M(phen)(edda)] complexes, faster moving bands of less relaxed topoisomers are formed which resulted from partial inhibition of the topo I by the complexes (Figures 4.41-4.43, L6-10). With further increase of [Co(phen)(edda)], [Cu(phen)(edda)] and [Zn(phen)(edda)] complex

concentration from 5 to 40 μM, new bands of faster moving and lesser relaxed topoisomers are formed. In the complex concentration range used, it is not clear whether there is a limiting concentration of complex above which there is no further increase in inhibition of topo I. The order of inhibitory effect on topo I activity of [M(phen)(edda)] series of complexes is [Zn(phen)(edda)] > [Co(phen)(edda)] > [Cu(phen)(edda)]. This implies that metal ion is a factor that should take into consideration in designing topo I inhibitor. [Zn(phen)(edda)] complex has a great potential as anticancer drug as it can efficiently inhibit the function of topo I in relaxing the plasmid DNA and it is also found that [Zn(phen)(edda)] complex induced cell cycle arrest in the present study and in a previous work (Ng *et al.*, 2008).

Inhibition of topo I by [M(phen)(edda)] can occur *via* two mechanistic possibilities: (i) binding of [M(phen)(edda)] to DNA and thereby blocking the action of the topo I, and (ii) binding of [M(phen)(edda)] to the topo I and preventing its ability to relax the DNA. To investigate this, three types of mixing the three components were used, *viz.* (i) simultaneous mixing of all components [Figure 4.44, (a)], (ii) mixing [M(phen)(edda)] and topo I first before adding DNA [Figure 4.44, (b)], and (iii) mixing DNA and [M(phen)(edda)] before adding topo I [Figure 4.44, (c)]. Simultaneous mixing gave results which showed that inhibition of topo I seemed to increase from [Cu(phen)(edda)] to [Co(phen)(edda)] to [Zn(phen)(edda)] [Panel (a), Lanes 7-9]. Among the complexes, [Cu(phen)(edda)] gave the greatest inhibition for prior mixing of topo I with complex [Panel (b)] as a lot of supercoiled DNA is observed (DNA Form I; Lane 10). For the prior mixing of DNA with

[M(phen)(edda)], the gel pattern (panel c) was different from those which were obtained from the previous two mode of mixing. Here, two similar bands (Form III and Form II) were observed for all the complexes and the presence of quite intense Form II bands suggests substantial amount of fully relaxed topoisomers whose formation where not inhibited by the [M(phen)(edda)] complexes [Panel (c); Lanes 13-15]. No observation of supercoiled band (Form I) and more intense Form II bands suggests that inhibition of topo I arising from prior mixing of DNA with complex (panel c) is less than that from prior mixing of topo I with complex [Panel (b)]. In this third mode of mixing, there may be unconfirmed presence of some nicked DNA (band Form II) and linear DNA (band Form III) which arose from single and double strand cleavage respectively. These differences indicate that inhibition of topo I by [M(phen)(edda)] could occur by both mechanism.

The anticancer mechanism of [M(phen)(edda)] complexes may also involve inhibition of topo I, which catalyzes topological changes in DNA by forming transient DNA single strand breaks. Compounds that inhibit topo I are reported to have a wide range of antitumor activities and such topo I inhibitors are among the most widely used anticancer drugs (Rothenberg, 1997; Pommier, 2006; Beretta *et al.*, 2008; Teicher, 2008; Sunani *et al.*, 2009). Among the 60 National Cancer Institute's cell lines, MCF7 and HCT116 colon cancer cells 440 have the highest levels of topo I expression (Reinhold *et al.*, 2010). In fact, some anticancer gold(III) tetraarylporphyrins were able to induce topo I inhibition (Sun *et al.*, 2010).

CHAPTER 6.0

CONCLUSION

Here, [M(phen)(edda)] compounds were experimented under physiological conditions and also illucidated their reactivity in the biological systems. [Co(phen)(edda)], [Cu(phen)(edda)] and [Zn(phen)(edda)] are found to have significantly inhibited the proliferation of MCF7 breast cancer cells after an incubation period of 72 h where the growth inhibition suggests their cytotoxicity. The growth inhibitory effect of [M(phen)(edda)] is time- and dose-dependent. This manifested us that decrease in the percentage of cell viability and the IC_{50} values (72 h) are 13.5 µM for [Co(phen)(edda)], 2.8 µM for [Cu(phen)(edda)] and 5 µM for [Zn(phen)(edda)]. Additionally, they may have potential application for other drug-resistant cancer types as MCF7 cells are cisplatin-resistant (Jänicke, 2008) and exert greater efficacy by their ability to act against multiple biological targets. The enhanced cytotoxicity of the [M(phen)(edda)] complexes towards MCF7 cancer cells, as evidenced by their IC_{50} values and in comparison with the IC_{50} values of unchelated 1,10-phen and free metal(II) ions, suggests synergic combination of the two types of ligand and metal ion used. Besides such synergic effect, the type of metal ion can affect the mode of cell death of these anticancer metal complexes as exemplified by the ability of only the zinc complex to induce cell cycle arrest. As an added advantage, MTT assay shows that they are more cytotoxic to MCF7 breast cancer cells than to MCF10A normal breast cells. Their

cytotoxicity towards MCF7 is comparable or better than that of the metal(II) chlorides, cisplatin and oxaliplatin (Trávníček *et al.*, 2005; Kovala-Demertzi *et al.*, 2006; Maloň *et al.*, 2002; Starha *et al.*, 2009). When comparing the relative cytotoxicity towards both cell lines in the lower concentration range, the selectivity of these compounds is more significant. These [M(phen)(edda)] complexes reduced cell viability of MCF7 cancer cells by 50% while that of MCF10A normal cells is by about 5% to 20%. This suggests that [M(phen)(edda)] compounds are much less or not so harmful to normal cells.

All of the compounds have good drug-like property based on Lipinski's Rule of Five with log of n-octanol:water partition coefficient of 0.30, 0.33 and 0.70, respectively. They have good ability to penetrate biological membranes. Their greater uptake by cells can lead to increase cytotoxicity with effective lower IC_{50} values, unlike cisplatin and many anticancer drugs which have poor uptake by cells (Screnci *et al.*, 2000; Platts *et al.*, 2006; Birnbaum and Brannon-Peppas, 2003). The morphological and biochemical (Annexin V-FITC/PI analysis, cell cycle analysis and $\Delta\psi_m$ detection) evidences indicated that the type of cell death caused by [M(phen)(edda)] in MCF7 cells is apoptosis. In addition, it is concluded that [Co(phen)(edda)], [Cu(phen)(edda)] and [Zn(phen)(edda)] induce cancer cell apoptosis based on quantifying the sub G_0/G_1 peak in the cell cycle progression, depolarization $\Delta\psi_m$, externalization of phosphotidylserine as well as observation of different stages of the apoptotic cells characterized by specific changes in cell surface and nuclear staining/morphology. The full mechanism by which apoptosis is executed remains to be determined. Further research to determine the complete

molecular mechanism of action is warranted. Growth inhibitory effect of [Co(phen)(edda)] and [Cu(phen)(edda)] complexes on MCF7 cell proliferation accompanied with the induction of apoptosis, while only [Zn(phen)(edda)] compound can induce both apoptosis and cell cycle arrest at S phase.

Furthermore, [M(phen)(edda)] decreased the level of $\Delta\psi_m$ and this effect was time-dependent manner. Decrease in the $\Delta\psi_m$ in this study suggests that [M(phen)(edda)] complexes involved mitochondrial dependent apoptosis pathway. These complexes have the ability to generate ROS and can cause DNA damage (DNA cleavage) (Seng *et al.*, 2008). Previous *in vitro* study by Seng *et al.* (2008) have shown that these [M(phen)(edda)] can bind to DNA and cause DNA damage under appropriate conditions. Therefore, DNA can be a target of these metal complexes. Unlike cisplatin, these complexes are neutral and bind to DNA by intercalation (Andrews and Howell, 1990). The mode of action of these anticancer [M(phen)(edda)] complexes is thus probably different from cisplatin.

Many anticancer drugs are topo I inhibitors (Rothenberg, 1997; Pommier, 2006; Beretta *et al.*, 2008; Teicher, 2008; Sunani *et al.*, 2009). Since the [M(phen)(edda)] complxes can efficiently inhibit the activity of human topo I in relaxing the plasmid DNA and topo I inhibition has been found to lead to apoptosis, topo I may be another target of these metal complexes. This sounds reasonable as MCF7 cells and many other types of cancer have elevated expression levels of topo I (Lynch *et al.*, 2001). Based on known action of

anticancer compounds against the above individual targets, the mode of action of the present complexes could involve multiple targets, *viz.* DNA, mitochondria and topo I. So it is concluded from this study that these ternary metal complexes with the ligands, 1,10-phen and edda, have significant potential to be developed as new metal-based anticancer drugs for treating breast and possibly other forms of cancer.

The exact mechanism of action in apoptotic process is not clear. Many researchers have reported that $\Delta\psi_m$ was measured as an early event in the initiation of apoptosis, since a decrease of $\Delta\psi_m$ preceeds leakage of pro-apoptotic proteins involved in caspase-dependent and -independent apoptosis from mitochondria into the cytosol (Ostrakhovitch and Cherian, 2005; Kroemer, 2007; Roy *et al.*, 2008). This study presumes that [M(phen)(edda)] complexes induced free radicals such as ROS, and may be correlated in the decrease of $\Delta\psi_m$. MCF7 cells which are depleted in caspase 3 (Jänicke *et al.*, 1998) with the mechanism of AIF translocation may be initiated from mitochondria *via* cytosol to the nucleus, where it bind to DNA, trigger destruction of DNA and lead to cell death. Further study can be done to determine the involvement of AIF in the caspase-independent pathway. To assess whether apoptosis is caspase-dependent or -independent, assays measuring the release of mitochondrial cell death factors, *viz.* caspase-3, cytochrome c and AIF can be performed (Cande *et al.*, 2002; Zhang *et al.*, 2012). Besides, determination of intracellular ROS production can be done by using two probes, viz. (i) 2',7'-dichlorodihydrofluorescein diacetate (H2DCFDA), specific for hydrogen peroxide (H_2O_2) detection, and (ii)

dihydroethidium (DHE), specific for superoxide (O_2^-) detection. Mitochondria and cytosol fractions are isolated from the same MCF7-treated cells and ROS from the isolated fractions can be measured (Heerdt, *et al.*, 2000; Sohaebuddin *et al.*, 2010). Therefore, the ability to determine $\Delta\psi_m$ and ROS can provide important clues about the physiological status of the cell and the function of the mitochondria. Other than that, the finding of the mitochondrial-to-nuclear translocation of cell death factor AIF participates in the apoptotic process *in vitro* and *in vivo* can also be done (Daugas *et al.*, 2000; Cregan *et al.*, 2002; Chen *et al.*, 2004; Choudhury; *et al.*, 2011). A protein that kills cancer cells, p53 involved in all types of human cancer and its activation can lead to apoptosis and cell cycle arrest (Amundson *et al.*, 1998; Arbor, 2011). Many traditional cancer drugs also activate p53 but they cause DNA damage in both tumor and normal cells causing toxic side effects (Arbor, 2011). In this study, [M(phen)(edda)] have potential to develop into anticancer drugs as they are more selectively cytotoxic to cancer cells than normal cells, induce apoptotic cell death and only Zn(II) compound arrest cell cycle at S phase. In future, known targets of p53 include genes associated with growth control and cell cycle checkpoints [e.g. cyclin-dependent kinase inhibitor (CIP1/WAF1), growth arrest and DNA damage protein (GADD45), wild-type p53-induced phosphatase 1 (WIP1), murine double minute 2 (MDM2), epidermal growth factor receptor (EGFR), proliferating cell nuclear antigen (PCNA), Cyclin D1, Cyclin G, transforming growth factor α (TGFα) and putative tumor suppressor 14-3-3σ], DNA repair (GADD45, PCNA, and CIP1/WAF1), and apoptosis [Bcl-2–associated X protein (BAX), B-cell lymphoma-extra large (BCL-XL), tumor necrosis factor receptor superfamily member 6 isoform 1 (FAS1), FASL,

insulin-like growth factor-binding protein-3 (IGF-BP3), PAG608 encodes nuclear zinc-finger protein and death receptor 5 (DR5)] can be investigated (Amundson *et al.*, 1998). It is clear that more research is needed in the chemistry and biology of the [M(phen)(edda)] compounds. Unfortunately this is not always possible, because most of the studies are life-time experimental projects. To reach this purpose, stronger collaboration among chemists, biochemists and physicians is needed.

LIST OF REFERENCES

Albertella, M. R., Green, C. M., Lehmann, A. R. and O'Connor, M. J. (2005). A role for polymerase eta in the cellular tolerance to cisplatin-induced damage, *Cancer Research*, 65, 9799–9806.

American Cancer Society. (2010). *Leukemia-chronic lymphocytic*. URL: http://documents.cancer.org/acs/groups/cid/documents/webcontent/003 111-pdf.pdf. Accessed on 1st October 2010.

Andrews, P. A. and Howell, S. B. (1990). Cellular pharmacology of cisplatin: perspectives on mechanisms of acquired resistance. *Cancer Cells*, 2, 35–43.

Ansari, K. I., Grant, J. D., Kasiri, S., Woldemariam, G., Shrestha, B. and Mandal, S. S. (2009). Manganese (III)-salens induce tumor selective apoptosis in human cells. *Journal of Inorganic Biochemistry*, 103 (5), 818-826.

Arjmand, F. and Muddassir, M. (2010). Design and synthesis of heterobimetallic topoisomerase I and II inhibitor complexes: in vitro DNA binding, interaction with 5'-GMP and 5'-TMP and cleavage studies. *Journal of Photochemistry and Photobiology B: Biology*, 101, 37-46.

Arjmand, F., Muddassir, M. and Khan, R. H. (2010). Chiral preference of L-tryptophan derived metal-based antitumor agent of late 3d-metal ions (Co(II), Cu(II) and Zn(II)) in comparison to D- and DL-tryptophan analogues: their in vitro reactivity towards CT DNA, 5'-GMP and 5'-TMP. *European Journal of Medicinal Chemistry* 45, 3549-57.

Au, L., Zheng, D., Zhou, F., Li, Z. Y., Li, X. and Xia, Y. (2008). A quantitative study on the photothermal effect of immuno gold nanocages targeted to breast cancer cells. *ACS Nano*, 2 (8), 1645-1652.

Bachur, N. R., Gordon, S. L. and Gee, M. V. (1978). A general mechanism for microsomal activation of quinone anticancer agents for free radicals. *Cancer Research*, 38, 1745– 1750.

Bailly C. (2003). Homocamptothecins: potent topoisomerase I inhibitors and promising anticancer drugs. *Critical Reviews in Oncology/Hematology*, 45, 91-108.

Bandi, P., Brinton, L., Buchert, S., Cokkinides, V., Cowens-Alavarado, R., Elk, R., Gansler, T., Gapstur, S., Harris, L., Kramer, J., McGinnis, L., McNeal, B., Murray, T., Newman, L., Richards, C., Runowicz, C., Saslow, D., Shah, M., Smith, R., Smith, R., Sullivan, K., Thun, M., Wagner, D., Ward, E. and Xu, J. (2009). Breast Cancer facts and figures 2009-2010. In: *American Cancer Society*. (pp. 1-36). Atlanta: American Cancer Society, Inc.

Banerjee, R. and Ragsdale, S. W. (2003). The many faces of vitamin B12: catalysis by cobalamin-dependent enzymes. *Annual Review of Biochemistry*, 72, 209-247.

Barceló-Oliver, M., García-Raso, A., Terrón, A., Molins, E., Prieto, M. J., Moreno, V., Martínez, J., Lladó, V., López, I., Gutiérrez, A. and Escribá, P.V. (2007). Synthesis and mass spectroscopy kinetics of a novel ternary copper(II) complex with cytotoxic activity against cancer cells. *Journal of Inorganic Biochemistry*, 101, 649-659.

Bartkowiak, D., Stempfhuber, M., Wiegel, T. and Bottke, D. (2009). Radiation and chemoinduced multidrug resistance in colon carcinoma cells. *Strahlentherapie und Onkologie*, 185 (12), 815-820.

Beretta, G. L., Perego, P. and Zunino, F. (2008). Targeting topoisomerase I: molecular mechanisms and cellular determinants of response to topoisomerase I inhibitors. *Expert Opinion on Therapeutic Targets*, 12, 1243-1256.

Bernhard, D., Tinhofer, I., Tonko, M., Hubl, H., Ausserlechner, M. J., Greil, R., Kofler, R. and Csordas, A. (2000). Resveratrol causes arrest in the S-phase prior to Fas-independent apoptosis in CEM-C7H2 acute leukemia cells. *Cell Death and Differentiation*, 7, 834-842.

Beyersmann, D. and Haase, H. (2001). Functions of zinc in signaling, proliferation and differentiation of mammalian cells. *Biometals*, 14, 331–341.

Birnbaum, D. T. and Brannon-Peppas, L. (2003). Microparticle drug delivery system. In: Brown, D. M. (Eds.), *Drug delivery systems in cancer therapy*. (pp 117-136). New Jersey: Humana Press, Inc.

Bizik, J., Kankuri, E., Ristimäki, A., Taïeb, A., Vapaatalo, H., Lubitz, W. and Vaheri, A. (2004). Cell–cell contacts trigger programmed necrosis and induce cyclooxygenase-2 expression. *Cell Death and Differentiation*, 11, 183–195.

Boatright, K. M. and Salvesen, G. S. (2003). Mechanisms of caspase activation. *Current Opinion in Cell Biology*, 15, 725–731.

Bodor, N., Gabanyi, Z. and Wong, C. K. (1989). A new method for the estimation of partition coefficient. *Journal of the American Chemical Society*, 111, 3783-3786.

Boutaleb-Charki, S., Marín, C., Maldonado, C. R., Rosales, M. J., Urbano, J., Guitierrez-Sánchez, R., Quirós, M., Salas, J. M. and Sánchez-Moreno, M. (2009). Copper (II) complexes of [1,2,4]triazolo [1,5-a]pyrimidine derivatives as potential anti-parasitic agents. *Drug Metabolism Letters*, 3, 35-44.

Bowman, G., Bonneau, R. H., Chinchilli, V. M., Tracey, K. J. and Cockroft, K. M. (2006). A novel inhibitor of inflammatory cytokine production (CNI-1493) reduces rodent post-hemorrhagic vasospasm. *Neurocritical Care*, 5, 222-229.

Boyd M. R. (2004). The NCI human tumor cell line (60 cell) screen. In: Teicher, B. and Andrews, P. A. (Eds.), *Drug development guide: preclinical screening, clinical trials, and approval*. 2nd edition (pp 41-61). New Jersey: Humana Press, Inc.

Brabec, V., Kasparkova, J., Vrana, O., Novakova, O., Cox, J. W., Qu, Y. and Farrell, N. (1999). DNA modifications by a novel bifunctional trinuclear platinum phase I anticancer agent. *Biochemistry*, 38, 6781–6790.

Brand, M. D. and Nicholls, D. G. (2011). Assessing mitochondrial dysfunction in cells. *Biochemical Journal*, 435, 297–312.

Brow, J. M., Pleatman, C. R. and Bierbach, U. (2002). Cytotoxic acridinylthiourea and its platinum conjugate produce enzyme-mediated DNA strand breaks. *Bioorganic and Medicinal Chemistry Letters*, 12, 2953 -2955.

Brown, A. M., Kristal, B. S., Effron, M. S., Shestopalov, A. I., Ullucci, P. A., Sheu, K. F., Blass, J. P. and Cooper, A. J. (2000). Zn^{2+} inhibits alpha-ketoglutarate-stimulated mitochondrial respiration and the isolated alpha-ketoglutarate dehydrogenase complex. *Journal of Biological Chemistry*, 275, 13441-13447.

Brubaker, G. R., Schaefer, D. P. and Worrell, J. H. (1971). Complexes of cobalt(III) with flexible tetradentate ligands. *Coordination Chemistry Reviews*, 7, 161-195.

Budihardjo, I., Oliver, H., Lutter, M., Luo, X. and Wang, X. (1999) Biochemical pathways of caspase activation during apoptosis. *Annual Review of Cell and Development Biology*, 15, 269-290.

Cabrera, A., Alonzo, E., Sauble, E., Chu, Y. L., Linder, M. C., Sato, D. S. and Mason, A. Z. (2008). Copper binding components of blood plasma and organs, and their responses to influx of large doses of ^{65}Cu, in the mouse. *Biometals*. 21, 525–543.

Carey, J. F., Schultz, S. J., Sisson, L., Fazzio, T. G. and Champoux, J. (2003). DNA relaxation by human topoisomerase I occurs in the closed clamp conformation of the protein. *Proceedings of the National Academy of Sciences*, 100, 5640–5645.

Carter, S. K. (1984). Cisplatin - past, present and future. In: Hacker, M. P., Douple, E. B. and Krakoff, I., H. (Eds.), *Platinum Coordination Complexes in Cancer Chemotherapy*. (pp 359-365). Boston: Martinus Nijhoff Press.

Center, M., Jemal, A. and Siegel, R. L. (2011). Global cancer facts & figures 2nd edition. (pp 1-60). Atlanta: American Cancer Society.

Chashoo, G., Singh, S. K., Sharma, P. R., Mondhe, D. M., Hamid, A., Saxena, A., Andotra, S. S., Shah, B. A., Qazi, N. A., Taneja, S. C. and Saxena, A. K. (2011). A propionyloxy derivative of 11-keto-β-boswellic acid induces apoptosis in HL-60 cells mediated through topoisomerase I & II inhibition. *Chemistry-Biology Interactions*, 189, 60-71.

Chaviara, A. T., Christidis, P. C., Papageorgiou, A., Chrysogelou, E., Hadjipavlou-Litina, D. J. and Bolos, C. A. (2005). In vivo anticancer, anti-inflammatory, and toxicity studies of mixed-ligand Cu(II) complexes of dien and its Schiff dibases with heterocyclic aldehydes and 2-amino-2-thiazoline. Crystal structure of [Cu(dien)(Br)(2a-2tzn)](Br)(H$_2$O). *Journal of Inorganic Biochemistry*, 99, 2102-2109.

Chen, T. F. and Wong, Y. S. (2008). Selenocystine induces s-phase arrest and apoptosis in human breast adenocarcinoma MCF-7 cells by modulating ERK and Akt phosphorylation. *Journal of Agricultural and Food Chemistry*, 56, 10574–10581.

Chen, D., Milacic, V., Frezza, M. and Dou, Q. P. (2009). Metal complexes, their cellular targets and potential for cancer therapy. *Current Pharmaceutical Design*, 15, 777-791.

Chen, Q. Y., Zhou, D. F., Guo, W. J. and Gao, J. (2010). Synthesis, anticancer activities, interaction with DNA and mitochondria of manganese complexes. *Journal of Inorganic Biochemistry*, 104, 1141-1147.

Chiou, S. H. and Ohtsu, N. (1985). Antiproliferative and DNA-scission activities of L-ascorbic acid in the presence of copper chelates. *Proceedings of the National Science Council, Republic of China*, 9, 275-280.

Chohan, Z. H., Pervez, H., Rauf, A., Khan, K. M. and Supuran, C. T. (2004). Isatin-derived antibacterial and antifungal compounds and their transition metal complexes. *Journal of Enzyme Inhibition and Medicinal Chemistry*, 19, 417-423.

Chohan, Z. H., Shaikh, A. U. and Supuran, C. T. (2006). *In-vitro* antibacterial, antifungal and cytotoxic activity of cobalt (II), copper (II), nickel (II) and zinc (II) complexes with furanylmethyl- and thienylmethyl-dithiolenes: [1,3-dithiole-2-one and 1,3-dithiole-2-thione]. *Journal of Enzyme Inhibition and Medicinal Chemistry*, 21, 733-740.

Choi, J. H., Oh, J. C., Kim, K. H., Chong, S. Y., Kang, M. S. and Oh D. Y. (2002). Successful treatment of cisplatin overdose with plasma exchange. *Yonsei Medical Journal*, 43 (1), 128–132.

Chuang, N. N., Lin, C. L. and Chen, H. K. (1996). Modification of DNA topoisomerase I enzymatic activity with phosphotyrosyl protein phosphatase and alkaline phosphatase from the hepatopancreas of the shrimp *Penaeus japonicus* (Crustacea: Decapoda). *Comparative Biochemistry and Physiology Part B: Biochemistry* and *Molecular Biology*, 114, 145-151.

Christodoulou, C. V., Eliopoulos, A. G., Young, L. S., Hodgkins, L., Ferry, D. R. and Kerr, D. J. (1998). Antiproliferative activity and mechanism of action of titanocene dichloride. *British Journal of Cancer* 77, 2088-2097.

Chu, G., Mantin, R., Shen, Y. M., Baskett, G. and Sussman, H. (1993). Massive cisplatin overdose by accidental substitution for carboplatin. Toxicity and management. *Cancer*, 72, 12, 3707–3714.

Chu, G. (1994). Cellular responses to cisplatin: the roles of DNA binding proteins and DNA repairs. *Journal of Biological Chemistry*, 269, 787-790.

Chuprina, A., Lukin, O., Demoiseaux, R., Buzko, A. and Shivanyuk, A. (2010). Drug- and lead-likeness, target class, and molecular diversity analysis of 7.9 million commercially available organic compounds provided by 29 suppliers. *Journal of Chemical Information and Modeling*, 50, 470-479.

Clark, J. D., Shi, X. Y., Li, X. Q., Qiao, Y. L., Liang, D. Y., Angst, M. S. and Yeomans, D. C. (2007). Morphine reduces local cytokine expression and neutrophil infiltration after incision. *Molecular Pain*, 3, 28.

Cohen, E., Ophir, I. and Shaul, Y. B. (1999). Induced differentiation in HT29, a human colon adenocarcinoma cell line. *Journal of Cell Science*, 112, 2657-2666.

Cohen, S. M. and Lippard, S. J. (2001). Cisplatin : from DNA damage to cancer chemotherapy. *Progress in Nucleic Acid Research and Molecular Biology*, 67, 93-130.

Colditz, G. A., Sellers, T. A. and Trapido, E. (2006). Epidemiology – identifying the causes and preventability of cancer? *Nature Reviews*, 6, 75-83.

Coleman, L. W., Rohr, L. R., Bronstein, I. B. and Holden J. A. (2002). Human DNA topoisomerase I: An anticancer drug target present in human sarcomas. *Human Pathology*, 33, 599-607.

Collins, J. A., Schandl, C. A., Young, K. K., Vesely, J. and Willingham, M. C. (1997). Major DNA fragmentation is a late event in apoptosis. *Journal of Histochemistry &* Cytochemistry, 45, 923–934.

Cooper, S., Iyer, G., Tarquini, M. and Bissett, P. (2006). Nocodazole does not synchronize cells: implications for cell-cycle control and whole-culture synchronization. *Cell Tissue Research*, 324, 237-242.

Cossarizza, A., Baccarani-Contri, M., Kalashnikova, G. and Franceschi, C. (1993). A new method for the cytofluorimetric analysis of mitochondrial membrane potential using the J-aggregate forming lipophilic cation 5,5′,6,6′-tetrachloro-1,1′,3,3′-tetraethylbenzimidazolcarbocyanine iodide (JC-1). *Biochemical and Biophysical Research Communications*, 197, 40-45.

Cossarizza, A. (2000). Mitochondria and apoptosis: functional studies on membrane potential (Delta Psi). *Minerva Biotecnologica*, 12, 57-61.

D'Cruz, O. J., Dong, Y. H. and Uckun F. M. (1999). Spermicidal activity of oxovanadium(IV) complexes of 1,10-phenanthroline, 2,2′-bipyridyl, 5′-bromo-2′-hydroxyacetophenone and derivatives in humans. *Biology of Reproduction*, 60, 435-444.

Dangoor, N. E. (2011). How many different types of cancer are there? URL: http://cancerhelp.cancerresearchuk.org/about-cancer/cancer-questions/how-many-different-types-of-cancer-are-there   Accessed on 1st December 2011.

Darzynkiewicz, Z., Bruno, S., Del Bino, G., Gorczyca, W., Hotz, M. A., Lassota, P. and Traganos, F. (1992). Features of apoptotic cells measured by flow cytometry. *Cytometry*, 13, 795-808.

Debatin, K. M. (2000). Activation of apoptosis pathways by anticancer treatment. *Toxicology Lett*ers, 112-113, 41-48.

De Boeck, M., Lison, D. and Kirsch-Volders, M. (1998). Evaluation of the *in vitro* direct and indirect genotoxic effects of cobalt compounds using the alkaline comet assay. Influence of inter donor and inter experimental variability. *Carcinogenesis*, 19, 2021–2029.

De Boeck, M., Kirsch-Volders, M. and Lison, D. (2003). Cobalt and antimony: genotoxicity and carcinogenicity. *Mutation Research*, 533, 135–152.

DeCoster, M. A. (2007). The nuclear area factor (NAF): a measure for cell apoptosis using microscopy and image analysis. In: Méndez-Vilas A. and Díaz, J. (Eds.), *Modern research and educational topics in microscopy*. (pp 378-384). Badajoz , Spain: Formatex.

De Vizcaya-Ruiz, A., Rivero-Muller, A., Ruiz-Ramirez, L., Kass, G. E., Kelland, L. R., Orr, R. M. and Dobrota, M. (2000). Induction of apoptosis by a novel copper-based anticancer compound, casiopeina II, in L1210 murine leukaemia and CH1 human ovarian carcinoma cells. *Toxicology In Vitro*, 14, 1-5.

Deegan, C., Coyle, B., McCanna, M., Devereux, M. and Egan, D. A. (2006). *In vitro* anti-tumour effect of 1,10-phenanthroline-5,6-dione (phendione), $[Cu(phendione)_3](ClO_4)_2 \cdot 4H_2O$ and $[Ag(phendione)2]ClO_4$ using human epithelial cell lines. *Chemico-Biological Interactions*, 164, 115–125.

DiMasi, J. A., Hansen, R. W. and Grabowski, H. G. (2003). The price of innovation: new estimates of drug development costs. *Journal* of *Health Economics*, 22, 151-185.

Dineley, K. E., Richards, L. L., Votyakova, T. V. and Reynolds, J. J. (2005). Zinc causes loss of membrane potential and alters production of reactive oxygen species in isolated brain mitochondria. *Mitochondrion*, 5, 55-65.

Dock, L. and Vahter, M. (1999). Metal toxicology. In: Ballantyne, B., Marrs, T. and Syversen, T. (Eds.), *General and Applied Toxicology*. 2nd edition. (vol. 3, pp 2049–2078). London: Macmillan Reference Ltd.

Dong, Y. H., Narla, R. K., Sudbeck, E. and Uckun, F. M. (2000). Synthesis, X-ray structure, and anti-leukemic activity of oxovanadium(IV) complexes. *Journal of Inorganic Biochemistry*, 78, 321–330.

Douvas, A., Lambie, P. B., Turman, M. A., Nitahara, K. S. and Hammond, L. (1991). Negative regulation of Scl-70/topoisomerase I by zinc and an endogenous macromolecule. *Biochemical and Biophysical* Research *Communications*, 178, 414-421.

Edge, S. B., Byrd, D. R., Compton, C. C., Fritz, A. G., Greene, F. L. and Trotti, A. (2010). Purposes and Principles of Cancer Staging. In: *AJCC Cancer Staging Handbook: From the AJCC Cancer Staging Manual*. 7th Edition. (pp. 1-12). New York: Springer Science Business Media.

Eide, D. and Guerinot, M. L. (1997). Metal ion uptake in eukaryotes. *American Society for Microbiology News*, 63, 199-205.

El-Ghannam, A., Ricci, K., Malkawi, A., Jahed, K., Vedantham, K., Wyan, H., Allen, L. D. and Dre´au, D. (2010). A ceramic-based anticancer drug delivery system to treat breast cancer. *Journal of Materials Science: Materials of Medicine*, 21, 2701–2710.

Elmore, S. (2007). Apoptosis: a review of programmed cell death. *Toxicologic Pathology*, 35, 495-516.

Elo, H. (2004). Uniform potent activity of the antiproliferative metal chelate transbis (resorcylaldoximato) copper (II) against a large panel of human tumor cell lines *in vitro*. *Chemotherapy*, 50, 229-233.

Enoch, T. and Nurse, P. (1990). Mutation of fission yeast cell cycle control genes abolishes dependence of mitosis on DNA replication. *Cell*, 60, 665–673.

Erdlenbruch, B., Pekrun, A., Schiffmann, H., Witt, O. and Lakomek, M. (2002). Topical topic: accidental cisplatin overdose in a child: reversal of acute renal failure with sodium thiosulfate. *Medical and Pediatric Oncology*, 38 (5), 349–352.

Erkkilä, K., Suomalainen, L., Wikström, M., Parvinen, M. and Dunkel, L. (2003). Chemical anoxia delays germ cell apoptosis in the human testis. *Biology of Reproduction*, 69, 617–626.

Essbauer, S. and Ahne, W. (2002). The epizootic haematopoietic necrosis virus (Iridoviridae) induces apoptosis *in vitro*. *Journal* of *Veterinary Medicine Series B- Infectious Diseases and Veterinary Public Health*, 49, 25-30.

Evans, N. (2006). State of the evidence: What is the connection between the environment and breast cancer? In: *Breast Cancer Fund and Breast Cancer Action*. 4th edition. (pp 4-84). San Francisco: Bruce Printing, Inc.

Farber E. (1982). Chemical carcinogenesis: a biological perspective. *American Journal of Pathology*, 106, 271–296.

Farrell, N., Kelland, L. R, Roberts, J. D. and Van Beusichem, M. (1992). Activation of the trans geometry in platinum antitumor complexes: a survey of the cytotoxicity of trans complexes containing planar ligands in murine L1210 and human tumor panels and studies on their mechanism of action. *Cancer Research*, 52 (18), 5065–5072.

Ferlay, J., Bray, F. and Pisani, P. (2002). Globocan 2002: Cancer incidence, mortality and prevalence worldwide. IARC CancerBase No. 5, version 2.0., Lyon, France: IARC Press, 2004.

Ferreira, C. G., Epping, M., Kruyt, F. A. and Giaccone, G. (2002). Apoptosis: target of cancer therapy. *Clinical Cancer Research*, 8, 2024–2034.

Ferry, G., Boutin, J. A., Hennig, P., Genton, A., Desmet, C., Fauchère, J. L., Atassi, G. and Tucker, G.C. (1998). A zinc chelator inhibiting gelatinases exerts potent *in vitro* anti-invasive effects. *European Journal of Pharmacology*, 351, 225-233.

Fink, S. L. and Cookson, B. T. (2005). Apoptosis, Pyroptosis, and Necrosis: Mechanistic Description of Dead and Dying Eukaryotic Cells. *Infection and Immunity*, 73, 1907-1916.

Ford, J. M. and Hait, W. N. (1990). Pharmacology of drugs that alter multidrug resistance in cancer. *Pharmacological Reviews*, 42, 155–199.

Formigari, A., Alberton, P., Cantale, V., Nadal, V. D., Feltrin, M., Ferronato, S., Santon, A., Schiavon, L. and Irato, P. (2008). Relationship between metal transcription factor-1 and zinc in resistance to metals producing free radicals. *Current Chemical Biology*, 2, 256-266.

Fraga, C. G. (2005). Relevance, essentiality and toxicity of trace elements in human health. *Molecular Aspects of Medicine*, 26, 235–244.

Franke, A., Lante, W., Fackeldey, V., Becker, H. P., Kurig, E., Zöller, L. G., Weinhold, C. and Markewitz, A. (2005). Pro-inflammatory cytokines after different kinds of cardio-thoracic surgical procedures: is what we see what we know? *European Journal of Cardio-Thoracic Surgery*, 28, 569-575.

Frazzini, V., Rockabrand, E., Mocchegiani, E. and Sensi, S. L. (2006). Oxidative stress and brain aging: is zinc the link? *Biogerontology*, 7, 307–314.

Freshney, R. I. (1989). Culture of Animal Cells: A Manual of Basic Technique (2nd Ed.). New York: John Wiley & Sons, Inc.

Fu, O. Y., Hou, M. F., Yang, S. F., Huang, S. C. and Lee, W. Y. (2009). Cobalt chloride-induced hypoxia modulates the invasive potential and matrix metalloproteinases of primary and metastatic breast cancer cells. *Anticancer Research*, 29, 3131-3138.

Fukuda, M., Nishio, K., Kanzawa, F., Ogasawara, H., Ishida, T., Arioka, H., Bojanowski, K., Oka, M. and Saijo, N. (1996). Synergism between cisplatin and topoisomerase I inhibitors, NB-506 and SN-38, in human small cell lung cancer cells. *Cancer Research*, 56, 789-793.

Fulda, S. and Debatin, K. M. (2006). Extrinsic versus intrinsic apoptosis pathways in anticancer chemotherapy. *Oncogene*, 25, 4798–4811.

Gately, D. P. and Howell, S. B. (1993). Cellular accumulation of the anticancer agent cisplatin: a review. *British Journal of Cancer*, 67, 1171–1176.

Gerl, R. and Vaux, D. L. (2005). Apoptosis in the development and treatment of cancer. *Carcinogenesis*, 26,.263-270.

Gewies, A. (2003). Introduction to apoptosis. *ApoReview*, 1-26.

Ghadimi, S., Asad-Samani, K. and Ebrahimi-Valmoozi, A. A. (2011). Synthesis, spectroscopic characterization and structure-activity relationship of some phosphoramidothioate pesticides. *Journal of the Iranian Chemical Society*, 8, 717-726.

Ghobrial, I. M., Witzig, T. E. and Adjei, A. A. (2005). Targeting apoptosis pathways in cancer therapy. *CA: A Cancer Journal for Clinicians*, 55, 178-194.

Ghose, A. K., Viswanadhan, V. N. and Wendoloski, J. J. (1999). A knowledge-based approach in designing combinatorial or medicinal chemistry libraries for drug discovery. 1. A qualitative and quantitative characterization of known drug databases. *Journal of Combinatorial Chemistry*, 1, 55-68.

Giménez, B. G., Santos, M. S., Ferrarini, M. and Fernandes, J. P. (2010). Evaluation of blockbuster drugs under the rule-of-five. *Pharmazie*, 65, 148-152.

Grabrick, D. M., Hartmann, L. C., Cerhan, J. R., Vierkant, R. A., Therneau, T. M., Vachon, C. M., Olson, J. E., Couch, F. J., Anderson, K. E., Pankratz, V. S. and Sellers, T. A. (2000). Risk of breast cancer with oral contraceptive use in women with a family history of breast cancer. *Journal Of the American Medical Association*, 284, 1791-1798.

Godard, T., Deslandes, E., Lebailly, P., Vigreux, C., Poulain, L. and Sichel, F. (1999). Comet assay and DNA flow cytometry analysis of staurosporine-induced apoptosis. *Cytometry*, 36, 117–122.

Goodgame, D. M. L., Page, C. J. and Stratford, I. J. (1991). Metal complexes of ligands containing intercalating units. Synthesis of nickel(II), copper(II), rhodium(II), and platinum(II) complexes with diamine-substituted acridines and quinolines, and with mitonafide [*N*-(2,2-dimethylaminoethyl)-3-nitro-1, 8-naphthalimide] and related ligands. *Transition Metal Chemistry*, 16, 2223-2229.

Gorin, N. C., Estey, E., Jones, R. J., Levitsky, H. I., Borrello, I. and Slavin, S. (2000). New developments in the therapy of acute myelocytic leukemia. *Hematology (Am Soc Hematol Educ Program)*, 69-89.

Grem, J. L., Danenberg, K. D., Behan, K., Parr, A., Young, L., Danenberg, P. V., Nguyen, D., Drake, J., Monks, A. and Allegra, C. J. (2001) Thymidine kinase, thymidylate synthase, and dihydropyrimidine dehydrogenase profiles of cell lines of the national cancer institute's anticancer drug screen. *Clinical Cancer Research*, 7, 999–1009.

Gulbins, E., Dreschers, S. and Bock, J. (2003). Role of mitochondria in apoptosis. *Experimental Physiology*, 88, 85-90.

Gust, R., Ott, I., Posselt, D. and Sommer, K. (2004). Development of cobalt(3,4-diarylsalen) complexes as tumor therapeutics *Journal of Medicinal Chemistry*, 47, 5837–5846.

Guthrie, T. H. and Gynther, L. (1985). Acute deafness. A complication of high-dose cisplatin. *Archives of Otolaryngology*, 111, 5, 344–345.

Guo, Z. and Sadler, P. J. (1999). Metals in medicine. *Angewandte Chemie International Edition*, 38, 1512-1531.

Hada, H., Honda, C. and Tanemura, H. (1977). Spectroscopic study on the J-aggregate of cyanine dyes. I. Spectral changes of UV bands concerned with J-aggregate formation. *Photographic Science and Engineering*, 21, 83-91.

Hakem, R. (2008). DNA-damage repair: the good, the bad, and the ugly. *EMBO Journal*, 27, 589–605.

Halyard, M. Y., Jatoi, A., Sloan, J. A., Bearden, J. D. 3rd, Vora, S. A., Atherton, P. J., Perez, E. A., Soori, G., Zalduendo, A. C., Zhu, A., Stella, P. J. and Loprinzi, C. L. (2007). Does zinc sulfate prevent therapy-induced taste alterations in head and neck cancer patients? Results of phase III double-blind, placebo-controlled trial from the North Central Cancer Treatment Group (N01C4). *International Journal of Radiation Oncology, Biology and Physics*, 67, 1318-1322.

Hambley, T. W. (2007). Developing new metal-based therapeutics: challenges and opportunities. *Dalton Transactions*, 2007, 4929-4937.

Hamilton, I. M., Gilmore, W. S. and Strain, J. J. (2000). Marginal copper deficiency and atherosclerosis. *Biological Trace Element Research*, 78, 179–189.

Harris, E. D. (1991). Copper transport: an overview. *Proceedings of the Society for Experimental Biology and Medicine*, 196, 130–140.

Harrison, D. O., Thomas, R., Underhill, A. E., Everall, F. A., Gomm, P. S. and Low, G. D. (1985). Metal complexes of anti-inflammatory drugs. Part II. Azapropazone complexes of iron(III), cobalt(II), nickel(II), copper(II) and zinc(II). *Journal of Coordination Chemistry*, 14, 107 – 112.

Hartwell, L. H. and Kastan, M.B. (1994). Cell cycle control and cancer. *Science*, 266, 1821–1828.

He, Q., Liang, C. H. and Lippard, S. J. (2000). Steroid hormones induce HMG 1 over expression and sensitized breast cancer cells to cisplatin and carboplatin. *Proceedings of the National Academy of Sciences USA*, 97, 5768-5772.

Healy, E., Dempsey, M., Lally, C. and Ryan, M. P. (1998). Apoptosis and necrosis: Mechanisms of cell death induced by cyclosporine A in a renal proximal tubular cell line. *Kidney International*, 54, 1955-1966.

Heffeter, P., Jakupec, M. A., Körner, W., Wild, S., von Keyserlingk, N. G., Elbling, L., Zorbas, H., Korynevska, A., Knasmüller, S., Sutterlüty, H., Micksche, M., Keppler, B. K. and Berger, W. (2006). Anticancer activity of the lanthanum compound [tris(1,10-phenanthroline)lanthanum(III)]trithiocyanate (KP772; FFC24). *Biochemical Pharmacology*, 71, 426-440.

Hines, M. D. and Allen-Hoffmann, B. L. (1996). Analysis of DNA fragmentation in epidermal keratinocytes using the apoptosis detection system, fluorescein. *Promega Notes*, 1996, 59, 30-37.

Hingorani, R., Deng, J., Elia, J., McIntyre, C. and Mittar, D. (2011). Detection of apoptosis Using the BD annexin V FITC assay on the BD FACSVerse™ system, *Beckton Dickinson Bioscience*, 1-12.

Hisham, A. N. and Yip, C. H. (2003). Spectrum of breast cancer in Malaysian women. *World Journal of Surgery*, 27, 921-923.

Hofmann, G., Bauernhofer, T., Krippl, P., Lang-Loidolt, D., Horn, S., Goessler, W., Schippinger, W., Ploner, F., Stoeger, H. and Samonigg, H. (2006). Plasmapheresis reverses all side-effects of a cisplatin overdose–a case report and treatment recommendation. *BMC Cancer*, 6 (1), 1-7.

Hossain, M. Z. and Kleve, M. G. (2011). Nickel nanowires induced and reactive oxygen species mediated apoptosis in human pancreatic adenocarcinoma cells. *International Journal of Nanomedicine*, 6, 1475-1485.

Howell, A. and Dowsett, M. (2004). Endocrinology and hormone therapy in breast cancer: Aromatase inhibitors versus antioestrogens. *Breast Cancer Research*, 6, 269–274.

Huang, M., Wang, Y., Collins, M., Mitchell, B. S. and Graves, L. M. (2002). A77 1726 induces differentiation of human myeloid leukemia K562 cells by depletion of intracellular CTP pool. *Molecular Pharmacology*, 62, 463-472.

Huang, J., Yu, G., Zhang, Z. L., Wang, Y. L., Zhu, W. H. and Wu, G. S. (2004). Application of TLSER method in predicting the aqueous solubility and n-octanol/ water partition coefficient of PCBs, PCDDs and PCDFs. *Journal of Environmental Science*, 16, 21-29.

Humer, J., Ferko, B., Waltenberger, A., Rapberger, R., Pehamberger, H. and Muster, T. (2008). Azidothymidine inhibits melanoma cell growth *in vitro* and *in vivo*. *Melanoma Research*, 18, 314-321.

Igene, H. (2008). Global health inequalities and breast cancer: an impending public health problem for developing countries. *Breast Journal*, 14, 428-434.

Iguchi, T., Miyakawa, Y., Saito, K., Nakabayashi, C., Nakanishi, M., Saya, H., Ikeda, Y. and Kizaki M. (2007). Zoledronate-induced S phase arrest and apoptosis accompanied by DNA damage and activation of the ATM/Chk1/cdc25 pathway in human osteosarcoma cells. *International Journal of Oncology*, 31, 285-291.

Jackson, A., Davis, J., Pither, R. J., Rodger, A. and Hannon, M. J. (2001). Estrogenderived steroidal metal complexes: agents for cellular delivery of metal centers to estrogen receptor-positive cells. *Inorganic Chemistry*, 40, 3964-3973.

Jamieson, E. R. and Lippard, S. J. (1999). Structure, Recognition and processing of cisplatin DNA adducts. *Chemical Reviews*, 99, 2467-2498.

Jänicke, R. U., Sprengart, M. L., Wati, M. R. and Porter, A. G. (1998). Caspase-3 is required for DNA fragmentation and morphological changes associated with apoptosis. *Journal of Biological Chemistry*, 273, 9357-9360.

Jänicke, R. U. (2008). MCF-7 breast carcinoma cells do not express caspase-3. *Breast Cancer Research and Treatment*, 117, 219-221.

Jemal, A., Bray, F., Center, M. M., Ferlay, J., Ward, E. and Forman, D. (2011). Global Cancer Statistics. *CA: A Cancer Journal for Clinicians*, 61, 69–90.

Jiang, J., Tang, X. L., Dou, W., Zhang, H. H., Liu, W. S., Wang, C. X. and Zheng, J. R. (2010). Synthesis and characterization of the ligand based on benzoxazole and its transition metal complexes: DNA-binding and antitumor activity. *Journal of Inorganic Biochemistry*, 104, 583–591.

Jin, V. X. and Ranford, J. D. (2000). Complexes of platinum(II) or palladium(II) with 1,10-phenanthroline and amino acids. *Inorganica Chimica Acta*, 304, 38-44.

Joe, A. K., Liu, H., Zuzui, M., Vural, M. E., Ziao, D. and Weinstein, I. B. (2002). Resveratrol induces growth inhibition, S-phase arrest, apoptosis and changes in biomarker expression in human cancer cell lines. *Clinical Cancer Research*, 8, 893–903.

Johnson, D. G. and Walker, C. L. (1999). Cyclins and Cell Cycle Checkpoints. *Annual Review of Pharmacology and Toxicology*, 39, 295–312.

Jung, H. K., Lee, J. and Lee, S. N. (1995). A case of massive cisplatin overdose managed by plasmapheresis. *The Korean Journal of Internal Medicine*, 10 (2), 150–154.

Jung, J. Y. and Kim, W. J. (2004). Involvement of mitochondrial- and Fas-mediated dual mechanism in $CoCl_2$-induced apoptosis of rat PC12 cells. *Neuroscience Letters*, 371, 85-90.

Jung, Y. and Lippard, S. J. (2007). Direct cellular responses to platinum-induced DNA damage. *Chemical Reviews*, 107, 1387-1407.

Jungwirth, U., Kowol, C. R., Keppler, B. K., Hartinger, C. G., Berger, W. and Heffeter, P. (2011). Anticancer activity of metal complexes: involvement of redox processes. *Antioxidants and Redox Signalling*, 15, 1085-1127.

Kachadourian, R., Brechbuhl, H. M., Ruiz-Azuara, L., Gracia-Mora, I. and Day, B. J. (2010). Casiopeina IIgly-induced oxidative stress and mitochondrial dysfunction in human lung cancer A549 and H157 cells. *Toxicology*, 268, 176-183.

Kamangar, F., Dores, G. and Anderson, W. (2006). Patterns of cancer incidence, mortality, and prevalence across five continents: Defining priorities to reduce cancer disparities in different geographic regions of the world. *Journal of Clinical Oncology*, 24(14), 2137-2150.

Kalia, S. B., Kaushal, G., Kumar, M., Cameotra, S. S., Sharma, A., Verma, M. L. and Kanwar, S. S. (2009). Antimicrobial and toxicological studies of some metal complexes of 4-methylpiperazine-1-carbodithioate and phenanthroline mixed ligands. *Brazilian Journal of Microbiology*, 40, 916-922.

Kapoor, S. (2009). Lanthanum and its rapidly emerging role as an anticarcinogenic agent. *Journal of Cellular Biochemistry*, 106 (2), 193.

Keidan, J. (2007). Sucked into the Herceptin maelstrom. *British Medical Journal*, 334(7583), 16-18.

Kerr, J. F. R., Wyllie, A. H. and Currie, A. R. (1972). Apoptosis: a basic biological phenomenon with wide-ranging implications in tissue kinetics. *British Journal of Cancer*, 26, 239-257.

Kerr, J. F. R., Winterford, C. M. and Harmon, B. V. (1994). Apoptosis: its clinical significance in cancer and cancer therapy. *Cancer of Philadelphia*, 73, 2013–2026.

Kerns, E. H. and Di, L. (2008). Drug-like properties: concepts, structure design and methods: from ADME to toxicity optimization. In: *Lipophilicity*. 1st edition. (pp. 45-47). Amsterdam: Academic Press, Inc.

Khursheed, J. (2009). Zinc: An Essential Trace Element for Parenteral Nutrition. *Gastroenterology*,137, S7-S12.

Kim, R., Emi, M. and Tanabe, K. (2006). Role of mitochondria as the gardens of cell death. *Cancer Chemotherapy* and *Pharmacology*, 57, 545-553.

Kihlmark, M., Imreh, G. and Hallberg, E. (2001). Sequential degradation of proteins from the nuclear envelope during apoptosis. *Journal of Cell Science*, 114, 3643–3653.

Kimura, E. and Kikuta, E. (2000). Why zinc in zinc enzymes?—from biological roles to DNA base-selective recognition. *Journal of Biological Inorganic Chemistry*; 5, 139 –155.

Kobayashi, M. and Shimizu, S. (1999). Cobalt proteins. *European Journal of Biochemistry*, 261, 1-9.

Komen S. G. (2009). *Facts For Life: What is Breast Cancer?* URL: http://ww5.komen.org/uploadedFiles/Content_Binaries/806-368a.pdf. Accessed on 28th January 2010.

Köpf-Maier, P. (1994). Complexes of metals other than platinum as antitumour agents. *European Journal of Clinical Pharmacology*, 47, 1-16.

Korichneva, I. (2005). Redox regulation of cardiac protein kinase C. *Experimental and Clinical Cardiology*, 10, 256–261.

Kovala-Demertzi, D., Yadav, P. N., Wiecek, J., Skoulika, S., Varadinova, T. and Demertzis, M. A. (2006). Zinc(II) complexes derived from pyridine-2-carbaldehyde thiosemicarbazone and (1E)-1-pyridin-2-ylethan-1-one thiosemicarbazone. Synthesis, crystal structures and antiproliferative activity of zinc(II) complexes. *Journal of Inorganic Biochemistry*, 100, 1558-1567.

Kregiel, D., Berlowska, J. and Ambroziak, W. (2008). Succinate dehydrogenase activity assay *in situ* with blue tetrazolium salt in crabtree-positive *Saccharomyces cerevisiae* strain. *Food Technology and Biotechnology*, 46, 376–380.

Kristal, A. R., Stanford, J. L., Cohen, J. H., Wicklund, K. and Patterson, R. E. (1999). Vitamin and mineral supplement use is associated with reduced risk of prostate cancer. *Cancer Epidemiology*, *Biomarkers and Prevention*, 8, 887-892.

Kroemer G. (1999). Mitochondrial control of apoptosis: an overview. *Biochemical Society Sympodia*, 66, 1-15.

Kroemer, G., Galluzzi, L. and Brenner, C. (2007). Mitochondrial membrane permeabilization in cell death. *Physiological Reviews*, 87, 99–163.

Krumschnabel, G., Manzl, C., Berger, C., and Hofer, B. (2005). Oxidative stress, mitochondrial permeability transition, and cell death in Cu-exposed trout hepatocytes. *Toxicology and Applied Pharmacology*, 209, 62-73.

Kubinyi, H. (1979). *Nonlinear dependence of biological activity on hydrophobic character: the bilinear model*. URL: http://en.wikipedia.org/wiki/Partition_coefficient. Accessed on 10th March 2011.

Lacroix, M. and Leclercq, G. (2004). Relevance of breast cancer cell lines as models for breast tumors: an update. *Breast Cancer Research and Treatment*, 83, 249–289.

Laginha, K. M., Verwoert, S., Charrois, G. J. and Allen, T. M. (2005). Determination of doxorubicin levels in whole tumor and tumor nuclei in murine breast cancer tumors. *Clinical Cancer Research*, 11, 6944-6949.

Lagrange, J. L., Cassuto-Viguier, E., Barbé, V., Fischel, J. L., Mondain, J. R., Etienne, M. C., Ferréro, J. M., Creisson-Ducray, A., Formento, P. and Milano, G. (1994). Cytotoxic effects of long-term circulating ultrafiltrable platinum species and limited efficacy of haemodialysis in clearing them. *European Journal of Cancer*, 30A(14), 2057–2060.

Lajiness, M. S., Vieth, M. and Erickson, J. (2004). Molecular properties that influence oral drug-like behavior. *Current Opinion in Drug Discovery and Development*, 7, 470-477.

Lange, T. S., Kim, K. K., Singh, R. K., Strongin, R. M., McCourt, C. K. and Brard, L. (2008). Iron (III)-salophene: an organometallic compound with selective cytotoxic and anti-proliferative properties in platinum-resistant ovarian cancer cells. *PLoS One*, 3 (5), e2303.

Lee, K. B., Wang, D., Lippard, S. J. and Sharp, P. A. (2002). Transcription-coupled and DNA damage-dependent ubiqitinition of RNA polymerase II *in vitro. Proceedings of the National Academy of Sciences USA*, 99, 4239-4244.

Lemasters, J. J. and Ramshesh, V. K. (2007). Imaging of mitochondrial polarization and depolarization with cationic fluorophores. *Methods in Cell Biology*, 80, 283-95.

Lewis, W., Copeland, W. C. and Day, B. J. (2001). Mitochondrial DNA depletion, oxidative stress and mutation: mechanisms of dysfunction from nucleoside reverse transcriptase inhibitors. *Laboratory Investigation*, 81, 777–789.

Li, J. M. and Brooks, G. (1999). Cell cycle regulatory molecules (cyclins, cyclin-dependent kinases and cyclin-dependent kinase inhibitors) and the cardiovascular system; potential targets for therapy? *European Heart Journal*, 20, 406-420.

Li, M. O., Sarkisian, M. R., Mehal, W. Z., Rakic, P. and Flavell, R. A. (2003). Phosphatidylserine receptor is required for clearance of apoptotic cells. *Science*, 302, 1560–1563.

Li, A. P. (2005). Preclinical in vitro screening assays for drug-like properties. *Drug Discovery Today: Technologies*, 2 , 179–185.

Li, W. Y., Chiu, L. C., Lam, W. S., Wong, W. Y., Chan, Y. T. and Ho, Y. P (2007). Ethyl acetate extract of Chinese medicinal herb *Sarcandra glabra* induces growth inhibition on human leukemia HL60 cells, associated with cell cycle arrest and up-regulation of pro-apoptotic Bax/Bcl-2 ratio. *Oncology Reports*, 17, 425-431.

Li, F. H., Zhao, G. H., Wu, H. X., Lin, H., Wu, X. X., Zhu, S. R. and Lin. H. K. (2006). Synthesis, characterization and biological activity of lanthanum(III) complexes containing 2-methylene–1,10-phenanthroline units bridged by aliphatic diamines. *Journal of Inorganic Biochemistry*, 100, 36–43.

Liang, X. J., Chen, C., Zhao, Y. and Wang, P. C. (2010). Circumventing tumor resistance to chemotherapy by nanotechnology methods. *Molecular Biology*, 596, 467-488.

Light, D. O. and Warbuton R. (2011). Demythologizing the high costs of pharmaceutical research. *BioSocieties*, 6, 34-50.

Lim, G. C. C., Rampal, S. and Halimah, Y. (2008). Cancer incidence in peninsular Malaysia, 2003-2005. In: *National Cancer Registry, Ministry of Health Malaysia.* (pp 1-179). Kuala Lumpur: National Cancer Registry.

Lin, F. R. and Yao, E. G. (1994). Etoposide-based combination chemotherapy in malignant histiocytosis. *Journal of Tongji Medical Universiti*, 14, 227-229.

Linder, M. C. (2001). Copper and genomic stability in mammals. *Mutation Research*, 475, 141–152.

Lipinski, C. A., Lombardo, F., Dominy, B. W. and Feeney, P. J. (2001). Experimental and computational approaches to estimate solubility and permeability in drug discovery and development settings. *Advanced Drug Delivery Reviews*, 46, 3-26.

Locksley, R. M., Killeen, N., and Lenardo, M. J. (2001). The TNF and TNF receptor superfamilies: integrating mammalian biology. *Cell*, 104, 487-501.

Lottner, C., Bart, K. C., Bernhart, G. and Brunner, H. (2002). Hematoporphyrin derived soluble porphyrin-platinum conjugates with combined cytotoxic and phototoxic antitumour activity. *Journal of Medicinal Chemistry*, 45, 2064-2078.

Louie, A. Y. and Meade, T. J. (1999). Metal complexes as enzymetic inhibitors. *Chemical Reviews*, 99, 2711-2734.

Lovec, H., Grzeschiczek, A., Kowalski, M. B. and Moroy, T. (1994). Cyclin D1/*bcl*-1 cooperates with myc genes in the generation of B-cell lymphoma in transgenic mice. *EMBO Journal*, 13, 3487–3495.

Lynch, B. J., Bronstein, I. B. and Holden, J. A. (2001). Elevations of DNA topoisomerase I in invasive carcinoma of the breast. *Breast Journal*, 7, 176-180.

MacLachlan, T. K., Sang, N. and Giordano, A. (1995). Cyclins, cyclin-dependent kinases and cdk inhibitors: implications in cell cycle control and cancer. *Critical Reviews in Eukaryotic Gene Expression*, 5, 127–156.

Magda, D., Lecane, P., Wang, Z., Hu, W., Thiemann, P., Ma, X., Dranchak, P. K., Wang, X., Lynch, V., Wei, W., Csokai, V., Hacia, J. G. and Sessler, J. L. (2008). Synthesis and Anticancer Properties of Water-Soluble Zinc Ionophores. *Cancer Research*, 68, 5318-5325.

Majno, G. and Joris, I. (1995) Review: apoptosis, oncosis and necrosis. An overview of cell death. *American Journal of Pathology*, 146, 3–15.

Mahepal, S., Bowen, R., Mamo, M. A., Layh, M. and Jansen van Rensburg, C. E. (2008). The *in vitro* antitumour activity of novel, mitochondrial-interactive, gold-based lipophilic cations. *Metal-Based Drugs*, 2008, 1-5.

Maki, N. and Sakuraba, S. (1969). New methods of preparing the mixed cyano cobalt(II) complexes. *Bulletin of the Chemical Society of Japan*, 42, 1908-1915.

Maloň, M., Trávníček, Z., Maryško, M., Marek, J., Doležal, K., Rolčík, J. and Strnad, M. (2002). Synthesis, characterization and antitumour activity of copper(II) 6-(4-chlorobenzylamino)purine complexes. X-ray structure of 6-(4-chloro-benzylamino)purinium perchlorate. *Transition Metal Chemistry*, 27, 580–586.

Marcon, G., Carotti, S., Coronnello, M., Messori, L., Mini, E., Orioli, P., Mazzie, T., Cinellu, M. A. and Minghetti, G. (2002). Gold (III) complexes with bipyridyl ligands: solution chemistry, cytotoxicity, and DNA binding properties. *Journal of Medicinal Chemistry*, 45, 1672-1677.

Martins, E. T., Baruah, H., Kramarczyk, J., Saluta, G., Day, C. S., Kucera, G. L. and Bierbach, U. (2001). Design, synthesis, and biological activity of novel non-cisplatin type platinum–acridine pharmacophores. *Journal of Medicinal Chemistry*, 44, 4492-4496.

Marzano, C., Pellei, M., Tisato, F. and Santini, C. (2009). Copper complexes as anticancer agents. *Anticancer Agents in Medicinal Chemistry*, 9, 185-211.

Matsushime, H., Roussel, M. F., Ashmun, R. A. and Sherr, C. J. (1991). Colony-stimulating factor 1 regulates novel cyclins during the G1 phase of the cell cycle. *Cell*, 65, 701–713.

McCann, M., Santos, A., da Silva, B., Romanos, M., Pyrrho, A., Devereux, M., Kavanagh, K., Fichtner, I. and Kellett, A. (2012). In vitro and in vivo studies into the biological activities of 1,10-phenanthroline, 1,10-phenanthroline-5,6-dione and its copper(II) and silver(I) complexes. *Toxicology Research*, 1, 47-54.

McCutcheon, I. E. (2006). The problem of the aggressive pituitary tumor. URL: http://www.touchbriefings.com/pdf/2403/mccutcheon.pdf Accessed on 1st December 2010.

McKay, B. C., Becerril, C. and Ljungman, M. (2001). P53 plays a protective role against UV- and cisplatin-induced apoptosis in transcription-coupled repair proficient fibroblasts. *Oncogene*. 20 (46), 6805-6808.

McKeage, M. J., Maharaj, L. and Berners-Price, S. J. (2002). Mechanisms of cytotoxicity and antitumor activity of gold(I) phosphine complexes: the possible role of mitochondria. *Coordination Chemistry Reviews*, 232, 127-135.

Meggers, E., Atilla-Gokcumen, G. E., Gründler, K., Frias, C. and Prokop, A. (2009). Inert ruthenium half-sandwich complexes with anticancer activity. *Dalton Transactions*, 38, 10882-10888.

Meijer, C., van Luyn, M. J., Nienhuis, E. F., Blom, N., Mulder, N. H. and de Vries, E. G. (2001). Ultrastructural morphology and localization of cisplatin-induced platinum–DNA adducts in a cisplatin-sensitive and - resistant human small cell lung cancer cell line using electron microscopy. *Biochemical Pharmacology*, 61, 573–578.

Merluzzi, V. J., Cipriano, D., McNeil, D., Fuchs, V., Supeau, C., Rosenthal, A. S. and Skiles, J. W. (1989). Evaluation of zinc complexes on the replication of rhinovirus 2 *in vitro*. *Research Communications in Chemical Pathology and Pharmacology*, 66, 425-440.

Messori, L., Abbate, F., Marcon, G., Orioli, P., Fontani, M., Mini, E. and Carroti, S. (2000). Gold (III) complexes as potential anti tumor agents: solution chemistry, cytotoxicity and DNA binding properties. *Journal of Medicinal Chemistry*, 43, 3541-3548.

Meyer, F., Galan, P., Douville, P., Bairati, I., Kegle, P., Bertrais, S., Estaquio, C. and Hercberg, S.. (2005). Antioxidant vitamin and mineral supplementation and prostate cancer prevention in the SU.VI.MAX trial. *International Journal of Cancer*, 116, 182-186.

Meyer, L., Patte-Mensah, C., Taleb, O. and Mensah-Nyagan, A. G. (2011). Allopregnanolone prevents and suppresses oxaliplatin-evoked painful neuropathy: multi-parametric assessment and direct evidence. *Pain*, 152, 170–181.

Miesel, R. and Weser U. (2006). Anticarcinogenic reactivity of copper-di-schiff bases with superoxide dismutase-like activity. *Free Radical Research Communication*, 11, 39-51.

Monti, E., Paracchini, L., Piccinini, F., Malatesta, V., Morazzoni, F. and Supino, R. (1990). Cardiotoxicity and antitumor activity of a copper (II)-doxorubicin chelate. *Cancer Chemotherapy and Pharmacology*, 25, 333-336.

Morgan, D. O. (1995). Principles of CDK regulation. *Nature,* 374, 131-134.

Mosmann, T. (1983). Rapid colorimetric assay for cellular growth and survival: Application to proliferation and cytotoxicity assays. *Journal of Immunological Methods*, 65, 55-63.

Mower, D. A., Peckham, D. W., Illera, V. A., Fishbaugh, J. K., Stunz, L. L. and Ashman, R. F. (1994). Decreased membrane phosphohpid packing and decreased cell size precede DNA cleavage in mature mouse B cell apoptosis. *Journal of Immunology*, 152, 4832-4842.

Mozaffar, A., Elham, S., Bijan, R. and Leila, H. (2004). Thermodynamic and spectroscopic study on the binding of cationic Zn(II) and Co(II) tetrapyridinoporphyrazines to calf thymus DNA: the role of the central metal in binding parameters. *New Journal of Chemistry*, 28, 1227-1234.

Mulcahy, S. P., Gründler, K., Frias, G., Wagner, L., Prokop, A. and Meggers, E. (2010). Discovery of a strongly apoptotic ruthenium complex through combinatorial coordination chemistry. *Dalton Transactions*, 39, 8177-8182.

Nagata, S. (2000). Apoptotic DNA fragmentation. *Experimental of Cell Research*, 256, 12–18.

Najajreh, Y., Perez, J. M., Navarroo-Ranninger, C. and Gibsin, D. (2002). Novel soluble cationic trans-diaminedichloroplatinum (II) complexes that are active against cisplatin resistant ovarian cancer cell lines. *Journal of Medicinal Chemistry*, 45, 5189-5195.

Narimah, A., Rugayah, H. B., Tahir, A. and Maimunah, A. H. (1999). Breast examination, national health and morbidity survey 1996. Vol. 20. Kuala Lumpur: Public Health Institute, Ministry of Health, Malaysia.

Narla, R. K., Chen, C. L., Dong, Y. H. and Uckun, F. M. (2001). *In vivo* antitumor activity of bis(4,7-dimethyl-1,10-phenanthroline) Sulfatooxovanadium(IV) {METVAN [VO(SO4)(Me2-Phen)2]}. *Clinical Cancer Research*, 7, 2124-2133.

N'cho, M. and Brahmi, Z. (2001). Evidence that Fas-induced apoptosis leads to S phase arrest. *Human Immunology*, 62, 310-319.

Ng, C. H., Kong, K. C., Von, S. T., Balraj, P., Jensen, P., Thirthagiri, E., Hamada, H. and Chikira, M. (2008). Synthesis, characterization, DNA-binding study and anticancer properties of ternary metal(II) complexes of edda and an intercalating ligand. *Dalton Transactions*, 4, 447-454.

Noonan, E. J., Place, R. F., Giardina, C. and Hightower, L. E. (2007). Hsp70B' regulation and function. *Cell Stress and Chaperones*, 12, 219-229.

Noureini, S. K. and Wink, M. (2009). Transcriptional down regulation of hTERT and senescence induction in HepG2 cells by chelidonine. *World Journal of Gastroenterology*,15, 3603-3610.

O'Connor, K., Gill, C., Tacke, M., Rehmann, F. J., Strohfeldt, K., Sweeney, N., Fitzpatrick, J. M. and Watson, R. W. (2006). Novel titanocene anti-cancer drugs and their effect on apoptosis and the apoptotic pathway in prostate cancer cells. *Apoptosis*. 11, 1205-1214.

Ohtsubo, M., Theodoras, A. M., Schumacher, J., Roberts, J. M. and Pagano, M. (1995). Human cyclin E, a nuclear protein essential for the G1-to-S phase transition. *Molecular Cell Biology*, 15, 2612–2624.

Orvig, C. and Abrams, M. J. (1999). Medicinal inorganic chemistry: introduction. *Chemical Reviews*, 99, 2201-2203.

Ostrakhovitch, E. A. and Cherian, M. G. (2005). Role of p53 and reactive oxygen species in apoptotic response to copper and zinc in epithelial breast cancer cells. *Apoptosis*, 10, 111-121.

Ott, I. and Gust, R. (2007). Non platinum metal complexes as anti-cancer drugs. *Archiv der Pharmazie (Weinheim)*, 340, 117-126.

Pedada, S. R., Bathula, S., Vasa, S. S. R., Charla, K. S. and Gollapalli, N. R. (2009). Micellar effect on metal-ligand complexes of Co*(*II*),* Ni(II*),* Cu*(*II) and Zn*(*II) with citric acid. *Bulletin of the Chemical Society of Ethiopia*, 23, 347-358.

Pereira, R. M., Andrades, N. E., Paulino, N., Sawaya, A. C., Eberlin, M. N., Marcucci, M. C., Favero, G. M., Novak, E. M. and Bydlowski, S. P. (2007). Synthesis and characterization of a metal complex containing naringin and Cu, and its antioxidant, antimicrobial, antiinflammatory and tumor cell cytotoxicity. *Molecules*, 12, 1352-1366.

Pereira, G. C. and Oliveira, P. J. (2010). Pharmacological strategies to counteract doxorubicin-induced cardiotoxicity: the role of mitochondria. *Journal of Theoretical and Experimental Pharmacology*, 1(2), 39-53.

Pillaire, M. J., Hoffmann, J. S., Defais, M. and Villani, G. (1995). Replication of DNA containing cisplatin lesions and its mutagenic consequences. *Biochimie*, 77(10), 803-807.

Piulats, J. M., Jiménez, L., García del Muro, X., Villanueva, A., Viñals, F. and Germà-Lluch, J. R. (2009). Molecular mechanisms behind the resistance of cisplatin in germ cell tumours. *Clinical and Translational Oncology*, 12, 780-786.

Plagemenn, P. G., Richey, D. P., Zylka, J. M. and Erbe, J. (1975). Cell cycle and growth stage-dependent changes in the transport of nucleosides, hypoxanthine, choline, and deoxyglucose in cultured Novikoff rat hepatoma cells. *Journal of Cell Biology*, 64, 29-41.

Platts, J. A., Oldfield, S. P., Reif, M. M., Palmucci, A., Gabano, E., Osella, D. (2006). The rp-hplc measurement and qspr analysis of logp(o/w) values of several pt(ii) complexes. *Journal of Inorganic Biochemistry*, 100, 1199-1207.

Pommier, Y. (2006). Topoisomerase I inhibitors: camptothecins and beyond. *Nature Reviews Cancer*, 18, 789-802.

Pommier, Y. and Cushman, M. (2009). The indenoisoquinoline noncamptothecin topoisomerase I inhibitors: update and perspectives. *Molecular Cancer Therapeutics*, 8, 1008-1014.

Porter, P. L. (2009). Global trends in breast cancer incidence and mortality. *Salud Pública* de *México*, 51, 141-146.

Pucci, B., Kasten, M. and Giordano, A. (2000). Cell cycle and apoptosis. *Neoplasia*, 2, 291–299.

Qutob, S. S., Multani, A. S., Pathak, S., Feng, Y., Kendal, W. S. and Ng, C. E. (2004). Comparison of the X-radiation, drug and ultraviolet-radiation responses of clones isolated from a human colorectal tumor cell line. *Radiation Research*, 161 (3), 326-334.

Radanović, D. J. (1984). Optical activity of cobalt(III), chromium(III) and rhodium(III) complexes with aminopolycarboxylate EDTA-type and related ligands. *Coordination Chemistry Reviews*, 54, 159-261.

Raikwar, M. K., Kumar, P., Singh, M. and Singh, A. (2008). Toxic effect of heavy metals in livestock health. *Veterinary World*, 1, 28-30.

Rajendiran, V., Karthik, R., Palaniandavar, M., Stoeckli-Evans, H., Periasamy, V. S., Akbarsha, M. A., Srinag, B. S. and Krishnamurthy, H. (2007). Mixed-ligand copper(II)-phenolate complexes: effect of coligand on enhanced DNA and protein binding, DNA cleavage, and anticancer activity. *Inorganic Chemistry*, 46, 8208–8221.

Ranford, J. D., Sadler, P. J., Tocher, D. A. (1993). Cytotoxicity and antiviral activity of transition-metal salicylato complexes and crystal structure of Bis(diisopropylsalicylato)(1,10-phenanthroline)copper(II). *Journal of the Chemical Society Dalton Transactions*, 22, 3393-3399.

Rapaport, E. (1983). Treatment of human tumor cells with ADP or ATP yields arrest of growth in the S phase of the cell cycle. *Journal of Cellular Physiology*, 114, 279-283.

Rastogi, R. P., Sinha, R. and Sinha R. P. (2009). Apoptosis: molecular mechanisms and pathogenicity. *Experimental and Clinical Sciences, International Online Journal*, 8, 155-181.

Ray, R. S., Rana, B., Swami, B., Venu, V. and Chatterjee, M. (2006). Vanadium mediated apoptosis and cell cycle arrest in MCF7 cell line. *Chemico-Biological Interactions*, 163, 239–247.

Ray, S., Mohan, R., Singh, J. K., Samantaray, M. K., Shaikh, M. M., Panda, D. and Ghosh, P. (2007). Anticancer and antimicrobial metallopharmaceutical agents based on palladium, gold, and silver N-heterocyclic carbene complexes. *Journal of the American Chemical Society*, 129 (48), 15042-15053.

Redkar, A., Mixter, P. and Daoud, S. S. (2004). Implications of p53 in growth arrest and apoptosis on combined treatment of human mammary epithelial cells with topotecan and UCN-01. *Journal of Experimental Therapeutics and Oncology*, 4, 213–222.

Reedijk, J. and Teuben, J. M. (1999). Cisplatin: Chemistry and biochemistry of a leading anticancer drug. In: Lippert, B. (Ed.). (pp 339–362). Weinheim, Germany: Wiley-VCH.

Reedijk, J. (2003). New clues for platinum antitumor chemistry: Kinetically controlled metal binding to DNA. *Proceedings of the National Academy of Sciences*, 100(7), 3611–3616.

Reers, M., Smith, T. W. and Chen, L. B. (1991). J-aggregate formation of a carbocyanine as a quantitative fluorescent indicator of membrane potential. *Biochemistry*, 30, 4480-4486.

Reinhold, W. C., Mergny, J. L., Liu, H., Ryan, M., Pfister, T. D., Kinders, R., Parchment, R., Doroshow, J., Weinstein, J. N. and Pommier, Y. (2010) Exon array analyses across the NCI-60 reveals potential regulation of TOP1 by transcription pausing at guanosine quartets in the first intron. *Cancer Research*, 70, 2191-2203.

Rieger, A. M., Nelson, K. L., Konowalchuk, J. D., Barreda, D. R. (2011). Modified annexin V/propidium iodide apoptosis assay for accurate assessment of cell death. *Journal of Visualized Experiments*, 50, 2597.

Roberts, C. G., Gurisik, E., Biden, T. J., Sutherland, R. L. and Butt, A. J. (2007). Synergistic cytotoxicity between tamoxifen and the plant toxin persin in human breast cancer cells is dependent on Bim expression and mediated by modulation of ceramide metabolism. *Molecular Cancer Therapeutics*, 6, 2777-2785.

Rosenberg, B., Van Camp, L. and Krigas, T. (1965). Inhibition of cell division in *Escherichia coli* by electrolysis products from a platinum electrode. *Nature*, 205, 698–699.

Rothenberg, M. L. (1997). Topoisomerase I inhibitors: review and update. *Annals of Oncology*, 8, 837-855.

Roy, A., Ganguly, A., BoseDasgupta, S., Das, B. B., Pal, C., Jaisankar, P. and Majumder, H. K. (2008). Mitochondria-dependent reactive oxygen species-mediated programmed cell death induced by 3,3'-diindolylmethane through inhibition of F0F1-ATP synthase in unicellular protozoan parasite Leishmania donovani. *Molecular Pharmacology*, 74, 1292-1307.

Roy, S., Saha, S., Majumdar, R., Dighe, R. R. and Chakravarty, A. R. (2010). DNA photocleavage and anticancer activity of terpyridine copper(II) complexes having phenanthroline bases. *Polyhedron*, 29, 2787-2794.

Rudnev, A. V., Foteeva, L. S., Kowol, C., Berger, R., Jakupec, M. A., Arion, V. B., Timerbaev, A. R. and Keppler, B. K. (2006). Preclinical characterization of anticancer gallium(III) complexes: solubility, stability, lipophilicity and binding to serum proteins. *Journal of Inorganic Biochemistry*, 100, 1819-1826.

Ruelle, P. (2000). The n-octanol and n-hexane/water partition coefficient of environmentally relevant chemicals predicted from the mobile order and disorder (MOD) thermodynamics. *Chemosphere*, 40, 457-512.

Sabo, T. J., Grgurić-Šipka, S. R. and Trifunović, S. R. (2002). Transition metal complexes with EDDA-type ligands - A review. *Synthesis and Reactivity in Inorganic and Metal-Organic Chemistry*, 32, 1661-1717.

Salido, M., Gonzalez, J. L. and Vilches, J. (2007). Loss of mitochondrial membrane potential is inhibited by bombesin in etoposide-induced apoptosis in PC-3 prostate carcinoma cells. *Molecular Cancer Therapeutics*, 6, 1292-1299.

Salvioli, S., Ardizzoni, A., Franceschi, C. and Cossarizza, A. (1997). JC-1, but not DiOC6(3) or rhodamine 123, is a reliable fluorescent probe to assess DY changes in intact cells: implications for studies on mitochondrial functionality during apoptosis. *FEBS Letters*, 411, 77-82.

Santos, A. S., Daugas, E., Ravagnan, L., Samejima, K., Zamzami, N., Loeffler, M., Costantini, P. and Ferri, K. F. (2000). Two Distinct Pathways Leading to Nuclear Apoptosis. *Journal of Experimental Medicine*, 192, 571–580.

Santos, A., Calvet, L., Terrier-Lacombe, M. J., Larsen, A., Benard, J., Pondarre, C., Aubert, G., Morizet, J., Lavelle, F. and Vassal G. (2004). *In Vivo* Treatment with CPT-11 leads to differentiation of neuroblastoma xenografts and topoisomerase I alterations. *Cancer Research*, 64, 3223-3229.

Sasco, A. J. (2001). Epidemiology of breast cancer: an environmental disease? *Acta Pathologica, Microbiologica et Immunologica Scandinavica*, 109, 321–332.

Schiller, J. H., Rozental, J., Tutsch, K. D. and Trump, D. L. (1989). Inadvertent administration of 480 mg/m2 of cisplatin. *American Journal of Medicine*, 86, (5), 624–625.

Schlenk, M., Ott, I. and Gust, R. (2008). Cobalt−alkyne complexes with imidazoline ligands as estrogenic carriers: synthesis and pharmacological investigations, *Journal of Medicinal Chemistry*, 51, 7318–7322.

Schwartz, G. K. and Shah, M. A. (2005). Targeting the cell cycle: a new approach to cancer therapy. *Journal of Clinical Oncology*, 23, 9408–9412.

Screnci, D., McKeage, M. J., Galettis, P., Hambley, T. W., Palmer, B. D. and Baguley, B. C. (2000). Relationships between hydrophobicity, reactivity, accumulation and peripheral nerve toxicity of a series of platinum drugs. *British Journal of Cancer*, 82, 966–972.

Seng, H. L., Alan Ong, H. K., Raja Abd Rahman, R. N. Z., Yasmin, B. M., Tiekink, E. R. T., Tan, K. W., Maah, M. J., Caracelli, I. and Ng, C. H. (2008). Factors affecting nucleolytic efficiency of some ternary metal complexes with DNA binding and recognition domains. Crystal and molecular structure of Zn(phen)(edda). *Journal of Inorganic Biochemistry*, 102 , 1997–2011.

Seng, H. L., Von, S. T., Tan, K. W., Maah, M. J., Ng, S. W., Rahman, R. N., Caracelli, I. and Ng, C. H. (2010). Crystal structure, DNA binding studies, nucleolytic property and topoisomerase I inhibition of zinc complex with 1,10-phenanthroline and 3-methyl-picolinic acid. *Biometals*, 23 (1), 99-118.

Sensi, S. L., Yin, H. Z. and Weiss, J. H. (2000). AMPA/kainate receptor-triggered Zn^{2+} entry into cortical neurons induces mitochondrial Zn^{2+} uptake and persistent mitochondrial dysfunction. *European Journal of Neuroscience*, 12, 3813-3818.

Serova, M., Calvo, F., Lokiec, F., Koeppel, F., Poindessous, V., Larsen, A. K., Laar, E. S., Waters, S. J., Cvitkovic, E. and Raymond, E. (2006). Characterizations of irofulven cytotoxicity in combination with cisplatin and oxaliplatin in human colon, breast, and ovarian cancer cells, *Cancer Chemotherapy and Pharmacology*, 57, 491–499.

Sherr, C. J. (1994). G1 Phase progression cycling on cue. *Cell*, 79, 551–555.

Simstein, R., Burow, M., Parker, A., Weldon, C. and Beckman, B. (2003). Apoptosis, chemoresistance and breast cancer: insights from the MCF-7 cell model system. *Experimental Biology and Medicine*, 228, 995–1003.

Singh, S. K., Joshi, S., Singh, A. R., Saxena, J. K. and Pandey D. S. (2007). DNA binding and topoisomerase II inhibitory activity of water-soluble Ruthenium(II) and Rhodium(III) Complexes. *Inorganic Chemistry*, 46, 10869-10876.

Singh, N., Nigam, M., Ranjan, V., Sharma, R., Balapure, A. K. and Rath, S. K. (2009). Caspase mediated enhanced apoptotic action of cyclophosphamide- and resveratrol-treated MCF-7 cells. *Journal of Pharmacological Sciences*, 109, 473-485.

Sleijfer, D. T., Smit, E. F., Meijer, S., Mulder, N. H. and Postmus, P. E. (1989). Acute and cumulative effects of carboplatin on renal function. *British Journal of Cancer*, 60, 116–120.

Smiley, S. T., Reers, M., Mottola-Hartshorn, C., Lin, M., Chen, A., Smith, T. W., Steele, G. D. and Chen, L. B. (1991). Intracellular heterogeneity in mitochondrial membrane potential revealed by a J-aggregate-forming lipophilic cation JC-1. *Proceedings of the National Academy of Science of the United States of America*, 88, 3671-3675.

Smith, R., Sullivan, K., Thun, M., Wagner, D., Ward, E. and Xu, J. (2009). Breast cancer facts and figures 2009-2010. *American Cancer Society*, 1-40.

Sonmezer, M. and Oktay, K. (2004). Fertility preservation in female patients. *Human Reproduction Update*, 10, 251-266.

Smith, J. (2011). U.K. *Committee calls fulvestrant unwise use of resources*. URL: http://www.oncologypractice.com/oncologyreport/specialty-focus/breast/single-article-age.html?tx_ttnews%5Btt_news%5D=62321 Accessed on 1st March 2012.

Sprenger, K. B., Bundschu, D., Lewis, K., Spohn, B., Schmitz, J. and Franz, H. E. (1983). Improvement of uremic neuropathy and hypogeusia by dialysate zinc supplementation: A double-blind study. *Kidney International Supplement*, 16, S315–S318.

Sprenger, C. C., Vail, M. E., Evans, K., Simurdak, J. and Plymate, S. R., (2002). Over-expression of insulin-like growth factor binding protein-related protein-1(IGFBP-rP1/mac25) in the M12 prostate cancer cell line alters tumor growth by a delay in G1 and cyclin A associated apoptosis, *Oncogene*, 21, 140-147.

Starha, P., Trávnícek, Z. and Popa I. (2009). Synthesis, characterization and *in vitro* cytotoxicity of the first palladium(II) oxalato complexes involving adenine-based ligands. *Journal of Inorganic Biochemistry*, 103, 978-988.

Stewart, D. J. (2007). Mechanisms of resistance to cisplatin and carboplatin. *Critical Reviews in Oncology/Hematology*, 63, 12–31.

Stordal, B. and Davey, M. (2007). Understanding cisplatin resistance using cellular models. *IUBMB Life*, 59, 696–699.

Strumberg, D., Brügge, S., Korn, M. W., Koeppen, S., Ranft, J., Scheiber, G., Reiners, C., Möckel, C., Seeber, S. and Scheulen, M. E. (2002). Evaluation of long-term toxicity in patients after cisplatin-based chemotherapy for non-seminomatous testicular cancer. *Annals of Oncology*, 13, 229–236.

Storr, T., Thompsona, K. H. and Orvig, C. (2006). Design of targeting ligands in medicinal inorganic chemistry. *Chemical Society Reviews*, 35, 534-544.

Stryer, L. (1995). *Principles of biochemistry*. 4th edition. (pp 147-153). New York: W. H. Freeman and Company.

Sullivan, K.,Thun, M., Wagner, D., Ward, E. and Xu, J. Q. (2009). Breast Cancer facts and figures 2009-2010. *American Cancer Society*, 1-36.

Sun, R. W. Y., Li, C. K. L., Ma, D. L., Yan, J. J., Lok, C. N., Leung, C. H., Zhu, N. and Che, C. M. (2010). Stable anticancer gold(III)-porphyrin complexes: effects of porphyrin structure. *Chemistry-A European Journal*, 16, 3097-3113.

Sun, Q., van Dam, R. M., Willett, W. C. and Hu F. B. (2009). Prospective study of zinc intake and risk of type 2 diabetes in women. *Diabetes Care*, 32 (4), 629-634.

Sunani, S., Nishimura, T., Nishimura, I., Ito, S., Arakawa, H. and Ohkubo, M. (2009). Synthesis and biological activities of topoisomerase I inhibitors, 6-arylmethylamino analogues of edotecarin. *Journal of Medicinal Chemistry*, 52, 3225-3237.

Susin, S. A., Lorenzo, H. K., Zamzami, N., Marzo, I., Snow, B. E., Brothers, G. M., Mangion, J., Jacotot, E., Costantini, P., Loeffler, M., Larochette, N., Goodlett, D. R., Aebersold, R., Siderovski, D. P., Penninger, J. M. and Kroemer, G. (1999). Molecular characterization of mitochondrial apoptosis-inducing factor. *Nature*, 397(6718), 441-446.

Tan-Chiu, E., Yothers, G., Romond, E., Geyer, C. E. Jr., Ewer, M., Keefe, D., Shannon, R. P., Swain, S. M., Brown, A., Fehrenbacher, L., Vogel, V. G., Seay, T. E., Rastogi, P., Mamounas, E. P., Wolmark, N., Bryant, J. (2005). Assessment of cardiac dysfunction in a randomized trial comparing doxorubicin and cyclophosphamide followed by paclitaxel, with or without trastuzumab as adjuvant therapy in node-positive, human epidermal growth factor receptor 2-overexpressing breast cancer: NSABP B-31. *Journal of Clinical Oncology*, 23(31), 7811-7819.

Teicher, B. A. (2008). Next generation topoisomerase I inhibitors: Rationale and biomarker strategies. *Biochemical Pharmacology*, 75, 1262-1271.

Temmink, O. H., Hoebe, E. K., Van Der Born, K., Ackland, S. P., Fukushima, M. and Peters, G. J. (2007). Mechanism of trifluorothymidine potentiation of oxaliplatin-induced cytotoxicity to colorectal cancer cells. *British Journal of Cancer*, 96, 231-240.

Thati, B., Noble, A., Creaven, B. S., Walsh, M., Kavanagh, K. and Egan, D. A. (2007). Apoptotic cell death: A possible key event in mediating the *in vitro* anti-proliferative effect of a novel copper(II) complex, [Cu(4-Mecdoa)(phen)2] (phen=phenanthroline, 4-Mecdoa=4-methylcoumarin-6, 7-dioxactetate), in human malignant cancer cells. *European Journal of Pharmacology*, 569, 16–28.

Thompson, K. H. and Orvig, C. (2006). Metal complexes in medicinal chemistry: new vistas and challenges in drug design. *Dalton Transactions*, 6, 761-764.

Tipton, I. H. and Cook, M. J. (1963). Trace elements in human tissue. II. Adult subjects from the United States. *Health Physics*, 9, 103–145.

Traore, A., Baudrimont, I., Ambaliou, S., Dano, S. D. and Creppy, E. E. (2001). DNA breaks and cell cycle arrest induced by okadaic acid in Caco-2 cells a human colonic epithelial cell line. *Archives of Toxicology*, 75, 110–117.

Trávníček, Z., Malon, M., Šindelář, Z., Doležal, K., Rolčík, J., Kryštof, V., Strnad, M. and Marek, M. (2001). Preparation, physicochemical properties and biological activity of copper(II) complexes with 6-(2-chlorobenzylamino) purine (HL1) or 6-(3-chlorobenzylamino) purine (HL2).The single-crystal X-ray structure of [Cu(H$^+$L$_2$)Cl$_3$]Cl.2H$_2$O. *Journal of Inorganic Biochemistry*, 84, 23–32.

Trávníček, Z., Klanicová, A., Popa, I. & Rolčík, J. (2005). Synthetic, spectral, magnetic and in vitro cytotoxic activity studies of cobalt(II) complexes with cytokinin derivatives: X-ray structure of 6-(3-methoxybenzylamino)purinium chloride monohydrate. *Journal of Inorganic Biochemistry*, 99, 776–786.

Tripathi, L., Kumar, P. and Singhai A. K. (2007). Role of chelates in treatment of cancer. *Indian Journal of Cancer*, 44, 62-71.

Tsang, S. Y., Tam, S. C., Bremner, L. and Burkitt, M. J. (1996). Copper-1,10-phenanthroline induces internucleosomal DNA fragmentation in HepG2 cells, resulting from direct oxidation by the hydroxyl radical, *Biochemistry Journals*, 317, 13–16.

Tsang, R. Y., Al-Fayea, T. and Au, H. J. (2009). Cisplatin overdose: toxicities and management. *Drug Safety*, 32, 1109-1122.

Toumi, H. (2010). *Cancer kills more people than AIDS, tuberculosis and malaria combined.* URL: http://www.habibtoumi.com/2010/04/22/cancer-kills-more-people-than-aids-tuberculosis-and-malaria-combined. Accessed on 18th June 2010.

Underwood, E. J. (1977). Trace Elements in Human and Animal Nutrition. 4th Edition. (pp 1). New York: Academic Press.

Vaidyanathan, V. G. and Nair, B. U. (2003). Photooxidation of DNA by a cobalt(II) tridentate complex. *Journal of Inorganic Biochemistry*, 94, 121–126.

Valko, M., Leibfritz, D., Moncol, J., Cronin, M. T. D., Mazur, M. and Telser, J. (2007). Free radicals and antioxidants in normal physiological functions and human disease. *The International Journal of Biochemistry and Cell Biology*, 39, 44–84.

Vallee, B. L. and Falchuk, K. H. (1981). Zinc and gene expression. *Philosophical Transactions of the Royal Society of London B: Biological Sciences*, 294, 185–197.

Van Engeland, M., Nieland, L. J., Ramaekers, F. C., Schutte, B. and Reutelingsperger, C. P. (1998). Annexin V-affinity assay: a review on an apoptosis detection system based on phosphatidylserine exposure. *Cytometry*, 31, 1-9.

Van Engeland, M., Ramaekers, F. C., Schutte, B. and Reutelingsperger, C. P. (1996). A novel assay to measure loss of plasma membrane asymmetry during apoptosis of adherent cells in culture. *Cytometry*, 24, 131–139.

Van Zutphen, S. and Reedijk, J. (2005). Targeting platinum anti-tumour drugs: overview of strategies employed to reduce systemic toxicity. *Coordination Chemistry Reviews*, 249, 2845-2853.

Verhaegh, G. W., Richard, M. J. and Hainaut, P. (1997). Regulation of p53 by metal ions and by antioxidants: dithiocarbamate down regulates p53 DNA-binding activity by increasing the intracellular levels of copper. *Molecular and Cellular Biology*, 17, 5699–5706.

Vermeulen, K., Van Bockstaele, D. R. and Berneman, Z. N. (2003). The cell cycle: a review of regulation, deregulation and therapeutic targets in cancer. *Cell Proliferation*, 36, 131-149.

Volkter, W. A. and Hoffman, T. J. (1999). Therapeutic radiopharmaceuticals. *Chemical Reviews*, 99, 2269-2292.

Von, S. T., Seng, H. L., Lee, H. B., Ng, S. W., Kitamura, Y., Chikira, M. and Ng, C. H. (2011). DNA molecular recognition and cellular selectivity of anticancer metal(II) complexes of ethylenediaminediacetate and phenanthroline: multiple targets. *Journal of Biological Inorganic Chemistry*. (Epub ahead of print).

Wahid, M. I. (1999). *Breast Cancer*. URL: http://www.malaysiaoncology.org/article.php?aid=114. Accessed on 12th December 2009.

Waldman, T., Lengauer, C., Kinzler, K.W., and Vogelstein, B. (1996). Uncoupling of S phase and mitosis induced by anticancer agents in cells lacking p21. *Nature*, 381, 713–716.

Wang, T. C., Cardiff, R. D., Zukerberg, L., Lees, E., Arnold, A. and Schmidt, E. V. (1994). Mammary hyperplasia and carcioma in MMTV-cyclin D1 transgenic mice. *Nature*, 369, 669–671.

Wang, X., Sharma, R. K., Gupta, A., George, V., Thomas, A. J., Falcone, T. and Agarwal, A. (2003). Alterations in mitochondria membrane potential and oxidative stress in infertile men: a prospective observational study. *Fertility and Sterility*, 80, 844-850.

Wang, X. L., Chao, H., Li, H., Hong, X. L., Liu, Y. J., Tan, L. F. and Ji, L. N. (2004). DNA interactions of cobalt (III) mixed-polypridyl complexes containing asymmetric ligands. *Journal of Inorganic Biochemistry*, 98, 1143-1150.

Wang, T. C., Chen, I. L., Lu, P. J., Wong, C. H., Liao, C. H., Tsiao, K. C., Chang, K. M., Chen, Y. L. and Tzeng, C. C. (2005). Synthesis, antiproliferative, and antiplatelet activities of oxime- and methyloxime-containing flavone and isoflavone derivatives. *Bioorganic and Medicinal Chemistry*, 13, 6045-6053.

Wapnir, R. A. (1998). Copper absorption and bioavailability. *American Journal of Clinical Nutrition*, 67(suppl), 1054S–1060S.

Webb, M. R and Ebeler, S. E. (2008). Comparative analysis of topoisomerase IB inhibition and DNA intercalation by flavonoids and similar compounds: structural determinates of activity. *Journal of Food Biochemistry*, 32, 576–596.

Willingham, M. C. (1999). Cytochemical methods for the detection of apoptosis. *The Journal of Histochemistry & Cytochemistry*, 47, 1101–1109.

Wong, B., Masse, J. E., Yen, Y. M., Giannikoupolous, P., Feigon, J. and Johnson, R. C. (2002). Binding of cisplatin modified DNA by *Saccharomyces cerevisiae* HMGB Protien Nhp6A. *Biochemistry*, 41, 5404-5414.

Wong E. and Giandomenico, C. M. (1999). Current status of platinum-based antitumor drugs. *Chemical Reviews*, 99, 2451–2466.

Wylhe, A. H., Kerr, J. F. R. and Cume, A. R. (1980). Cell death: the significance of apoptosis. *International* Review of *Cytology*, 68, 251-306.

Xia, Z., Bergstrand, A., Depierre, J. W. and Nassberger, L. (1999). The antidepressants imipramine, clomipramine and citalopram induce apoptosis in human acute myeloid leukemia HL-60 cells via caspase-3 activation. *Journal of Biochemical and Molecular Toxicology*, 13, 338–347.

Xiao, R., Ferry, A. L. and Dupont-Versteegden, E. E. (2011). Cell death-resistance of differentiated myotubes is associated with enhanced anti-apoptotic mechanisms compared to myoblasts. *Apoptosis*, 16, 221-234.

Yang, D., van Boom, S. S. G. E., Reedijk, J., van Boom, J. H., Farrell, N. and Wang, A. H.-J. (1995). A novel DNA structure induced by the anticancer bisplatinum compound cross-linked to a GpG site in DNA. *Nature Structural Biology*, 2, 577–586.

Yasujima, T., Ohta, K. Y., Inoue, K., Ishimaru, M. and Yuasa, H. (2010). Evaluation of 4',6-diamidino-2-phenylindole as a fluorescent probe substrate for rapid assays of the functionality of human multidrug and toxin extrusion proteins. *Drug Metabolism and Disposition*, 38, 715-721.

Yasumatsu, N., Adachi, Y. Y. Y. and Sakurai, H. (2007). Antidiabetic copper(II)-picolinate: Impact of the first transition metal in the metallopicolinate complexes. *Bioorganic and Medicinal Chemistry*, 15, 4917-4922.

Yip, C. H., Taib, N. A. and Mohamed, I. (2006). Epidemiology of breast cancer in Malaysia. *Asian Pacific Journal of Cancer Prevention*, 7, 369-374.

Yu, Y., Wong, J., Lovejoy, D. B., Kalinowski, D. S. and Richardson, D. R. (2006). Chelators at the cancer coalface: desferrioxamine to triapine and beyond. *Clinical Cancer Ressearch,* 12, 6876-6883.

Zamble, D. B. and Lippard, S. J. (1995). Cisplatin and DNA repair in cancer chemotherapy. *Trends in Biochemical Sciences*, 20, 435-439.

Zamble, D. B., Jacks, T., and Lippard, S. J. (1998). P53-dependent and – independent responses to cisplatin in mouse testicular teratocarcinoma cells. *Cell biology*, 95, 6163-6168.

Zamzami, N., Marchetti, P., Castedo, M., Decaudin, D., Macho, A., Hirsch, T., Susin, S. A., Petit, P. X., Mignotte, B. and Kroemer G. (1995). Sequential reduction of mitochondrial transmembrane potential and generation of reactive oxygen species in early programmed cell death. *Journal of Experimental Medicine*, 182, 367-377.

Zamzami, N., Susin, S. A., Marchetti, P., Hirsch, T., Gómez-Monterrey, I., Castedo, M. and Kroemer, G. (1996). Mitochondrial control of nuclear apoptosis. *Journal of Experimental Medicine*, 183, 1533-1544.

Zedeck, M. S. (2004). *Absorption, Distribution and Storage of Chemicals*. URL:http://www.visionlearning.com/library/module_viewer.php?mid= 106. Accessed on 1st October 2010.

Zhang, S. C., Zhu, Y. G., Tu, C., Wei, H. Y., Yang, Z., Lin, L. P., Ding, J., Zhang, J. F. and Guo Z. J. (2004). A novel cytotoxic ternary copper(II) complex of 1,10-phenanthroline and L-threonine with DNA nuclease activity. *Journal of Inorganic Biochemistry*, 98, 2099–2106.

Zhang, Y., Rodionov, D. A., Gelfand, M. S. and Gladyshev, V. N. (2009). Comparative genomic analyses of nickel, cobalt and vitamin B12 utilization. *BMC Genomics*, 10, 78.

Zhou, B. B. and Elledge, S. J. (2000). The DNA damage response: putting checkpoints in perspective. *Nature*, 408, 433–439.

Zisman, M., Santos, N. D., Johnstone, S., Tsang, A., Bermudes, D., Mayer, L. and Tardi, P. (2011). Optimizing liposomal cisplatin efficacy through membrane composition manipulations. *Chemotherapy Research and Practice*, 2011, 1-7.

Zou, M. H., Shi, C. and Cohen, R. A. (2002). Oxidation of the zinc-thiolate complex and uncoupling of endothelial nitric oxide synthase by peroxynitrite. *Journal of Clinical Investigation*, 109, 817-826.

DNA molecular recognition and cellular selectivity of anticancer metal(II) complexes of ethylenediaminediacetate and phenanthroline: multiple targets

Sze-Tin Von, Hoi-Ling Seng, Hong-Boon Lee, Seik-Weng Ng, Yusuke Kitamura, Makoto Chikira & Chew-Hee Ng

Volume 16 · Number 1 · January 2011

A Publication of the Society of Biological Inorganic Chemistry
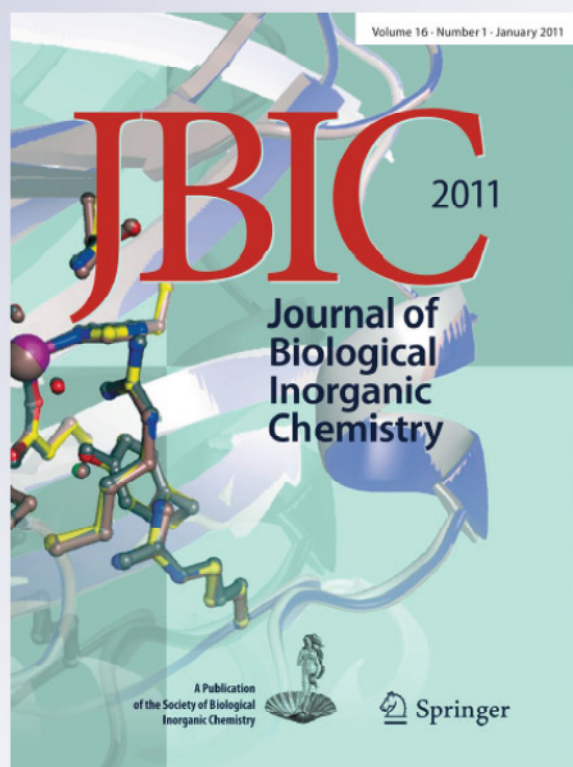
Springer

ORIGINAL PAPER

DNA molecular recognition and cellular selectivity of anticancer metal(II) complexes of ethylenediaminediacetate and phenanthroline: multiple targets

Sze-Tin Von · Hoi-Ling Seng · Hong-Boon Lee ·
Seik-Weng Ng · Yusuke Kitamura ·
Makoto Chikira · Chew-Hee Ng

Abstract By inhibiting only two or three of 12 restriction enzymes, the series of [M(phen)(edda)] complexes [M(II) is Cu, Co, Zn; phen is 1,10-phenanthroline; edda is N,N'-ethylenediaminediacetate] exhibit DNA binding specificity. The Cu(II) and Zn(II) complexes could differentiate the palindromic sequences 5′-CATATG-3′ and 5′-GTATAC-3′, whereas the Co(II) analogue could not. This and other differences in their biological properties may arise from distinct differences in their octahedral structures. The complexes could inhibit topoisomerase I, stabilize or destabilize G-quadruplex, and lower the mitochondrial membrane potential of MCF7 breast cells. The pronounced stabilization of G-quadruplex by the Zn(II) complex may account for the additional ability of only the Zn(II) complex to induce cell cycle arrest in S phase. On the basis of the known action of anticancer compounds against the above-mentioned individual targets, we suggest the mode of action of the present complexes could involve multiple targets. Cytotoxicity studies with MCF10A and cisplatin-resistant MCF7 suggest that these complexes exhibit selectivity towards breast cancer cells over normal ones.

S.-T. Von · C.-H. Ng (✉)
Faculty of Science,
Universiti Tunku Abdul Rahman,
3190 Kampar, Malaysia
e-mail: ngch@utar.edu.my

H.-L. Seng
Unit GL33, Malaysia University of Science and Technology,
47301 Petaling Jaya,
Selangor, Malaysia

H.-B. Lee
Cancer Research Initiatives Foundation,
47500 Selangor, Malaysia

S.-W. Ng
Chemistry Department,
University of Malaya,
50603 Kuala Lumpur, Malaysia

Y. Kitamura · M. Chikira
Department of Applied Chemistry,
Chuo University,
Kasuga 1-13-27, Bunkyo-ku,
Tokyo 112-8551, Japan

Introduction

Resistance to cisplatin and its toxic side effects have prompted a search for new metal-based anticancer agents [1]. Cisplatin's mode of action involves forming coordinate bonds to two adjacent guanine bases to form a DNA adduct, deforming the DNA at the binding site and thereby initiating apoptosis. Some new non-platinum anticancer metallodrugs can bind to DNA by intercalation [2–5]. Another approach involves shifting from DNA as a target to proteins and enzymes [6–14]. Among these are those anticancer metal complexes which inhibit topoisomerases [12–14]. Recently, some Mn(II) complexes, which bind weakly to DNA, have been found to exhibit cytotoxicity towards cancer cells via targeting of mitochondria by reduction of the mitochondrial membrane potential [15]. Lipophilic Ru(II) complexes showing significant cytotoxicity were found to preferentially accumulate in mitochondria [16]. Chen et al. [17] reported

🖄 Springer

ruthenium polypyridyl complexes that induce mitochondrial-mediated apoptosis in cancer cells. In addition, G-quadruplex, a non-B-form DNA structure, is now being targeted by anticancer metal complexes [18, 19].

In our preliminary anticancer investigation, we found that a series of neutral metal(II) complexes with 1,10-phenanthroline (phen) and *N,N'*-ethylenediaminedicarboxylate (edda), [M(phen)(edda)] (M is Cu, Co, Zn), are antiproliferative towards MCF7 breast cancer cells at micromolar levels and could induce apoptosis with or without cell cycle arrest, depending on the metal(II) ion [20]. These complexes bind to the DNA by intercalation. As a continuation, we obtained the crystal structure of [Co(phen)(edda)] to complement earlier structures of the copper and zinc analogues. Their DNA binding selectivity was further investigated with restriction enzyme inhibition. To elucidate the mechanism of their anticancer activity, the interaction of [M(phen)(edda)] with human G-quadruplex and topoisomerase I was investigated in vitro. A mitochondrial membrane potential detection kit was also used. 3-(4,5-Dimethylthiazol-2-yl)-2,5-diphenyltetrazolium bromide (MTT) assay was used to screen the complexes on MCF7 and MCF10A cells to assess for their cytotoxic selectivity for cancer cells over normal ones.

Materials and methods

Materials and instruments

Phen, H_2edda, and other chemicals were purchased and used as such. The chemicals used were of analytical grade. Elemental analysis (C, H, N) was conducted with a PerkinElmer 2400 CHN analyzer. UV–vis spectroscopic measurements were recorded with a PerkinElmer Lambda 40 spectrometer. Fluorescence measurements were performed using a PerkinElmer LS55 photoluminescence spectrometer. Circular dichroism (CD) spectra of the G-quadruplex alone and with metal complexes were obtained with a 1.0-mm quartz cell using a JASCO J-820 spectropolarimeter. A CON 700 benchtop conductivity meter from EUTECH Instruments was used to measure the conductivity of deionized water and 1×10^{-3} M solutions of each [M(phen)(edda)] complex in deionized water at room temperature, using KCl standard solution (1,413 µS) as a calibrant.

Synthesis of [Co(phen)(edda)]·$3H_2O$

A mixture of $CoCl_2$·$6H_2O$ (0.25 g, 0.001 mol) and phen (0.21 g, 0.001 mol) was dissolved in a water–ethanol mixture (4:6 v/v) to give a light-orange solution. H_2edda (0.18 g, 1 mmol) was then added and then ammonia solution was added to dissolve the H_2edda. The resultant mixture was continuously stirred and heated on a hot plate.

Slow evaporation of the resultant solution yielded orange crystalline needles suitable for X-ray determination. Yield, 65%. Calcd. for $C_{18}H_{24}N_4O_7Co$: C 46.26, H 5.18, N 11.99. Found: C 45.79, H 4.67, N 11.78%.

X-ray crystallography

The unit cell parameters and the intensity data of the [Co(phen)(edda)]·$3H_2O$ complex were collected with a Bruker SMART APEX CCD diffractometer, equipped with a graphite monochromated Mo K_α X-ray source ($\lambda = 0.71073$ Å). The APEX2 software program was used for data acquisition and the SAINT software program was used for cell refinement and data reduction [21]. Absorption corrections to the data were made using SADABS [22]. SHELXL97 was used for solving and refinement of the structure [23, 24]. The structure was solved by direct methods and refined by a full-matrix least-squares procedure on F^2 with anisotropic displacement parameters for non-hydrogen atoms. Hydrogen atoms in their calculated positions were refined using a riding model. The molecular structure was plotted using ORTEP-3 for Windows [25]. The crystal data details are summarized in Table 1 and selected bond lengths and angles are given in Table 2. Crystallographic data for the Co(II) complex have been deposited with the Cambridge Crystallographic Data Centre (CCDC) as supplementary publication no. CCDC-774860. Copies of the data can be obtained free of charge from the CCDC (12 Union Road, Cambridge CB2 1EZ, UK; Tel: +44-1223-336408; Fax: +44-1223-336003; e-mail: deposit@ccdc.cam.ac.uk).

Restriction enzyme inhibition assay

Each reaction mixture contained 0.25 µg of λ DNA, 2 µL of 10× restriction enzyme reaction buffer, 50 µM [M(phen)(edda)] complex, 5 U of restriction enzyme, and sterile deionized water. The total volume of each reaction mixture was 20 µL. Initially, λ DNA was incubated with metal(II) complex at 37 °C for 60 min. Then, restriction enzyme was added and the reaction mixture was incubated for another 2 h at the same temperature. Each reaction was terminated by the addition of 2 µL of 10% sodium dodecyl sulfate (SDS), and this was followed by addition of 3 µL of dye solution comprising 0.02% bromophenol blue and 50% glycerol. SDS is required to denature the restriction enzyme, preventing further functional enzymatic activity. The mixtures were applied to a 2.0% agarose gel and electrophoresed for 2 h at 80 V with a running buffer of tris(hydroxymethyl)aminomethane (Tris)–acetate–EDTA. The gel was stained, destained, and photographed under UV light using a Syngene bioimaging system and the digital image was viewed with the GeneFlash software program.

J Biol Inorg Chem

Table 1 Crystal data and refinement for [Co(phen)(edda)]·3H₂O (phen is 1,10-phenanthroline, edda is *N,N*-ethylenediaminedicarboxylate)

Empirical formula	$C_{18}H_{24}N_4O_7Co$
Formula weight	467.34
Temperature (K)	100(2)
Wavelength (Å)	0.71073
Crystal system	Monoclinic
Space group	$C2/c$
Unit cell dimensions (Å, °)	$a = 14.273(5)$
	$b = 9.947(3)$
	$c = 28.532(9)$
	$\alpha = 90$
	$\beta = 102.979(5)$
	$\gamma = 90$
Volume (Å³)	3,947(2)
Z	8
Density (calculated) (g cm³)	1.573
μ/mm	0.920
F (000)	1,944
Crystal size (mm)	$0.24 \times 0.20 \times 0.06$
θ range (°)	0.73 to 27.50
Limiting indices	$-17 \leq h \leq 18$
	$-12 \leq k \leq 12$
	$-37 \leq l \leq 35$
Reflections collected/unique reflections	4,511/3,907 [$R_{int} = 0.0466$]
Maximum and minimum transmission	0.9469 and 0.8095
Refinement method	Full-matrix least squares on F^2
Data/restraints/parameters	4,511/0/276
Goodness of fit on F^2	1.121
Final R indices [$I > 2\sigma(I)$]	$R1 = 0.0772$, $wR2 = 0.1869$
R indices (all data)	$R1 = 0.0882$, $wR2 = 0.1938$
Largest diffraction peak and hole (e^- Å⁻³)	1.106 and −0.737

DNA binding constant and interaction with G-quadruplex

The apparent binding constant of each [M(phen)(edda)] complex for ds(CGCGAATTCGCG)₂ (where "ds" means "double-stranded") and ds(CGCGATATCGCG)₂ was determined by ethidium bromide quenching assay, as described previously [26]. High performance liquid chromatography grade G-quadruplex 22-mer oligonucleotide 5′-AGGGTTAGGGTTAGGGTTAGGG-3′ was obtained from Eurogentec Ait and was annealed according to a previously reported procedure [26]. The CD spectra were obtained by scanning Tris–NaCl-buffered solutions of the G-quadruplex without and with [M(phen)(edda)]. CD spectral bands of the DNA alone and with the [M(phen)(edda)] complexes were obtained.

Human DNA topoisomerase I inhibition assay

The human DNA topoisomerase I inhibitory activity was determined by measuring the relaxation of supercoiled plasmid DNA pBR322. Each reaction mixture contained 10 mM Tris–HCl, pH 7.5, 100 mM NaCl, 1 mM phenylmethylsulfonyl fluoride, α-toluenesulfonyl fluoride, 1 mM 2-mercaptoethanol, 0.25 µg plasmid DNA pBR322, 1 U of human DNA topoisomerase I, and the complexes at a specified concentration. The total volume of each reaction mixture was 20 µL and these mixtures were prepared on ice. Upon enzyme addition, reaction mixtures were incubated at 37 °C for 30 min. The reactions were terminated by the addition of 2 µL of 10% SDS, and this was followed by addition of 3 µL of dye solution comprising 0.02% bromophenol blue and 50% glycerol. SDS is required to denature topoisomerase I, preventing further functional enzymatic activity. The mixtures were applied to 1.2% agarose gel and electrophoresed for 5 h at 33 V with a running buffer of Tris–acetate EDTA. The gel was stained, destained, and photographed under UV light using a Syngene bioimaging system and the digital image was viewed with GeneFlash. In a preliminary investigation into the mechanism of topoisomerase I inhibition, differential mixing of DNA, [M(phen)(edda)], and topoisomerase I was performed. The inhibition assay procedure described above was repeated to obtain three sets of results from three types of sequential mixing, viz., (1) all three components were mixed simultaneously, (2) topoisomerase I was incubated with [M(phen)(edda)] for 30 min before DNA was added, followed by a further incubation of 30 min, and (3) DNA was incubated with [M(phen)(edda)] for 30 min before topoisomerase I was added, followed by incubation for another 30 min.

Flow cytometry mitochondrial membrane potential detection

For this purpose, a mitochondrial membrane potential detection kit (Becton, Dickinson, USA) was used following the manufacturer's instructions. Briefly, 7.0×10^5 MCF7 cells were seeded in 100-mm Petri dishes, allowed to recover for 24 h, and then treated with 13.5 µM [Co(phen)(edda)], 2.8 µM [Cu(phen)(edda)], and 5 µM [Zn(phen)(edda)] (concentrations required to inhibit cell proliferation by 50%, IC₅₀) and cells were collected after 24, 48, and 72 h incubation. Adhering and floating cells were included in this analysis, respectively, and poured together into the centrifuge tube. The cells were washed with

207

Table 2 Selected bond distances (Å) and angles (°) of [M(phen)(edda)]

	[Co(phen)(edda)]	[Zn(phen)(edda)]	[Cu(phen)(edda)]
M–X(edda)			
M(1)–O(1)	2.057(4)	2.086(2)	2.314(11)
M(1)–O(3)	2.064(4)	2.113(2)	2.3957(12)
M(1)–N(1)	2.167(5)	2.174(2)	2.0263(13)
M(1)–N(2)	2.153(5)	2.164(2)	2.0328(13)
M–Y(phen)			
M(1)–N(3)	2.142(5)	2.165(2)	2.0328(13)
M(1)–N(4)	2.112(5)	2.149(2)	2.0369(13)
O(1)–M(1)–O(3)	171.83(16)	171.45(8)	174.02(4)
N(1)–M(1)–N(2)	83.12(18)	84.21(9)	86.03(5)
N(3)–M(1)–N(4)	78.65(19)	77.41(9)	81.85(5)

phosphate-buffered saline, trypsinized, and resuspended in RPMI 1640 medium. After centrifugation for 5 min at 1,500 rpm, each pellet was transferred into a sterile 15-ml round-bottom polystyrene tube (Becton, Dickinson, Germany) and resuspended gently in 0.5 ml of freshly prepared $5,5',6,6'$-tetrachloro-$1,1',3,3'$-tetraethylbenzimidazol-carbocyanine iodide (JC-1) working solution at 37 °C in a CO_2 incubator and incubated for 15 min. Spare dye was removed by washing twice in $1\times$ assay buffer and centrifugation. Then, 2 ml of $1\times$ assay buffer was added to each pellet in the first wash and 1 mL of $1\times$ assay buffer was added to each pellet in the second wash. Finally, each pellet was resuspended gently in 0.5 mL of $1\times$ assay buffer and cell-associated fluorescence was measured via an FACS-Calibur flow cytometer (Becton, Dickinson, Germany). Breakdown of the mitochondrial membrane potential ($\Delta\Psi_m$) was determined by fluorescence-activated cell sorting analysis using JC-1, which allows detection of changes of the mitochondrial membrane potential. The excitation peak of JC-1 is at 488 nm. The approximate emission peaks of monomeric and aggregate forms of JC-1 are at 527 and 590 nm, respectively. A total of 10,000 events were acquired and the cells were properly gated for analysis. The cell populations were displayed as a dot plot divided into two quadrants with green fluorescence monomers (x-axis) versus red fluorescence aggregates (y-axis). The experiment was repeated at least three times with two replicates each time. For the $\Delta\Psi_m$ data, the Wilcoxon rank-sum test was used to evaluate p values.

Cell culture and reagents

MCF7 breast carcinoma cells were purchased from ATCC (no. HTB-22). MCF10A breast epithelial cells were generously provided by Alan Khoo Soo Beng (IMR, Malaysia). MCF7 cells were cultured in RPMI 1640 medium (Sigma-Aldrich, Germany) supplemented with 10% fetal bovine serum (Sigma-Aldrich, Germany) and subcultured using trypsin–EDTA (0.25%) solution (Sigma-Aldrich, Germany). MCF10A cells were cultured in Dulbecco's modified Eagle's medium (GIBCO®, USA) supplemented with F12 nutrient mixture (GIBCO®, USA), 100 μg of water-soluble hydrocortisone (Sigma-Aldrich, Germany), epidermal growth factor, recombinant human (Invitrogen, USA), minimal essential medium nonessential amino acids solution (GIBCO®, USA), horse serum donor herd (GIBCO®, USA), insulin (Sigma-Aldrich, Germany), L-glutamine (GIBCO®, USA), and penicillin/streptomycin (GIBCO®, USA) and were subcultured using trypsin–EDTA (0.05%) solution (Mediatech, Germany). All cell lines were maintained in a CO_2 water-jacketed incubator (NuAire, USA) with an atmosphere of 95 and 5% CO_2 at 37 °C. On the next day, the medium was removed and fresh medium containing serum as described earlier was added. After the cultures had been allowed to grow to 70% confluence (achieved 3–4 days after subculture) with a change in the medium on alternate days, they were trypsinized and passaged.

Cytotoxicity assay

Cells were plated at 2.5×10^5 cells/mL for MCF7 cells and at 2.5×10^5 cells/mL for MCF10A cells in 100 μL per well in 96-well microtiter plates and allowed to recover for 24 h. Then, the cells were incubated at 37 °C for 24, 48, and 72 h as different sets. The medium was withdrawn after specified times and fresh growth medium with a different concentration of [Co(phen)(edda)], [Cu(phen)(edda)], and [Zn(phen)(edda)] was added to each well. Each test with a specified concentration of metal(II) complex was done in triplicate. Cytotoxicity was expressed as IC_{50} values calculated from full dose–response curves (drug concentrations inducing a 50% reduction of cell survival in comparison with the control cultured in parallel

Fig. 1 ORTEP plot of [Co(phen)(edda)] (phen is 1,10-phenanthroline, edda is *N,N'*-ethylenediaminedicarboxylate) at 40% ellipsoid probability with atomic labeling scheme. Lattice water molecules are not shown
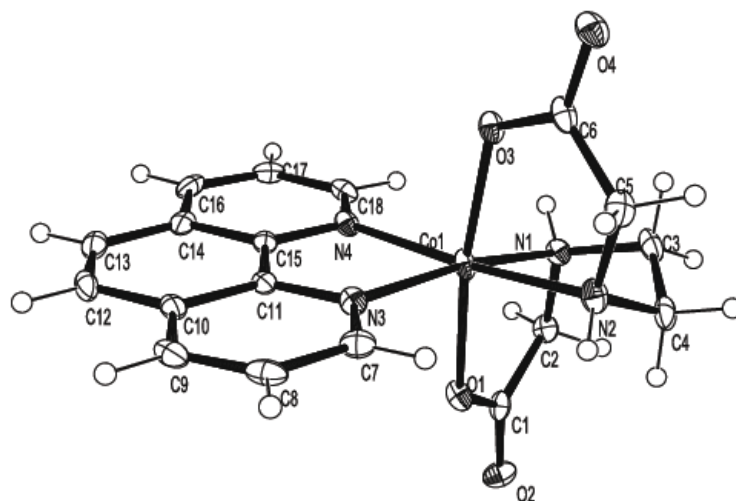
without drugs). In brief, for the MTT assay, 20 μL of MTT (5 mg/mL stock in phosphate-buffered saline) was added to each well and the mixture was incubated for 3–4 h under normal growth conditions to allow the viable cells to convert MTT to formazan. Then the medium was discarded and formazan crystals were dissolved by adding 100 μL of dimethyl sulfoxide. For complete dissolution, the plate was shaken gently for 5 min. The assay is based on cleavage of the tetrazolium salt MTT by mitochondrial dehydrogenase to form a pinkish purple soluble formazan complex, which was quantified by a microplate reader. The color intensity of the lysates, which reflects the cell growth conditions, was directly measured at 560 nm using a model 680 microplate reader (Bio-Rad, Japan). The percentage of viable cells (calculated on the basis of absorbance of the control untreated sample) was plotted as a function of concentration of [M(phen)(edda)]. For comparison, the above procedure was repeated for MCl_2 salts (M is Cu, Co, Zn; aqueous solutions). The IC_{50} values were estimated from the graphs. The doubling time for MCF7 is about 25 h [27], whereas that of MCF10A is about 48 h [28].

Results and discussion

Crystal structure of [Co(phen)(edda)]

The single-crystal structure analysis of the [Co(phen)(edda)]·$3H_2O$ complex shows two enantiomers (Λ and Δ) in the racemic crystal (monoclinic *C2/c* space group) and that it has an octahedral structure similar to the structures of the Cu(II) and Zn(II) racemic analogues (*P*-1 space group) [20, 29]. Crystal data and structure refinement details are summarized in Table 1. Selected bond distances

and angles together with those of the analogues are given in Table 2 for comparison. The Co(II) complex has a *syn–cis* configuration (Fig. 1), the same configuration as the other complexes. In each structure, the metal(II) ion exists within a *trans*-N_4O_2 donor set contributed by the tetradentate edda dianion and the phen molecule. In contrast to the Jahn–Teller distortion in [Cu(phen)(edda)], both [Co(phen)(edda)] and [Zn(phen)(edda)] complexes have a tetragonally compressed octahedral environment, i.e., two shorter axial bonds [M–O (carboxylate oxygen)] and four longer equatorial bonds (Table 2). However, the axial bonds of [Co(phen)(edda)] (average, 2.0605 Å; high spin, $t_{2g}^5 e_g^2$) are significantly shorter than those of [Zn(phen)(edda)] (average, 2.0995 Å) with $t_{2g}^6 e_g^4$ electronic configuration and consequently [Co(phen)(edda)] has much lesser distortion. This differential length of the axial bonds can conceivably moderate the depth of intercalation of the phen moiety of [M(phen)(edda)] as it was previously proven that the mode of binding to duplex DNA is intercalation [20].

Both the orientation of the three-bladed propeller chirality (Λ and Δ configuration) and changes in the dimension of the octahedral parameters of [M(phen)(edda)] can affect the mode of intercalation of the phen moiety (including the nature of base–base insertion or base pair–base pair insertion), and the proximity and orientation of the hydrogen-donor/hydrogen-acceptor sites of the edda moiety during binding with the chiral, helical duplex DNA.

Molar conductivity

Conductivity measurement is useful for studying the stability of the metal complexes in solution and analyzing the

Table 3 Molar conductivity of 1 mM [M(phen)(edda)] and KCl (Ω^{-1} cm^2 mol^{-1}) in deionized water at 25 °C

	0 h	24 h	36 h	72 h
[Cu(phen)(edda)]	16.80	19.23	20.00	21.37
[Zn(phen)(edda)]	11.29	16.84	18.27	20.08
[Co(phen)(edda)]	13.50	28.47	40.09	49.97
KCl	145.35	144.40	146.53	147.20
KCl standard	1,415	1,413	1,413	1,412

Table 4 Apparent binding constant, K_{app}, for binding of [M(phen)(edda)] to 10 μM ds(CGCGAATTCGCG)$_2$ (where "ds" means "double-stranded") and ds(CGCGATATCGCG)$_2$ oligonucleotides

	K_{app} (K_{AATT}) for ds(CGCGA ATTCGCG)$_2$ (M^{-1})	K_{app} (K_{ATAT}) for ds(CGCGA TATCGCG)$_2$ (M^{-1})	K_{ATAT}/ K_{AATT}
[Zn(phen)(edda)]	$9.55 \pm 0.13 \times 10^3$	$1.12 \pm 0.07 \times 10^4$	1.17
[Cu(phen)(edda)]	$1.83 \pm 0.11 \times 10^4$	$1.92 \pm 0.09 \times 10^4$	1.05
[Co(phen)(edda)]	$1.12 \pm 0.08 \times 10^4$	$1.38 \pm 0.12 \times 10^4$	1.23

species in solution. The conductivity of the aqueous solution of [M(phen)(edda)] complexes was monitored at 0, 24, 48, and 72 h, and the results were expressed as molar conductivity (Table 3). The initial molar conductivities (at 0 h) of all three [M(phen)(edda)] complexes were in the range 11–17 S cm^2 mol^{-1}, indicating their nonelectrolyte nature and their existence as undissociated species [30, 31]. In the time range 24–72 h, the molar conductivities of the Cu(II) and Zn(II) complexes increase slightly (17–21 S cm^2 mol^{-1}), but these values were within the range for neutral, nonelectrolytic metal complexes. This suggests the stability of these two complexes or insignificant ionization. The molar conductivities of the Co(II) complex at 0, 24, 48, and 72 h were 13, 28, 40, and 50 S cm^2 mol^{-1}, respectively. Undissociated neutral Co(II) and other metal(II) complexes have molar conductivities in the range 10–24 Ω^{-1} cm^2 mol^{-1}, whereas 1:1 electrolytic unicationic metal(II) complexes have values within the range 59–73 S cm^2 mol^{-1} [30]. The increasing molar conductivity suggested increasing oxidation of [Co^{II}(phen)(edda)] to [Co^{III}(phen)(edda)]$^+$ by dissolved oxygen.

Restriction enzyme inhibition

Previously, CD study results showed that the [M(phen)(edda)] complexes bind preferentially to ds(AT)$_6$ rather than to ds(CG)$_6$ [20]. To further investigate the binding specificity of the [M(phen)(edda)] complexes, a restriction enzyme inhibition assay was used. Twelve restriction enzymes (with the binding site given in parentheses), viz., *Tsp* 5091 (5′-↓AATT-3′), *Mun*I (5′-C↓AATTG-3′), *Bst* 11071 (5′-GTA↓TAC-3′), *Nde*I (5′-CA↓TATG-3′), *Eco*RI (5′-G↓AATTC-3′), *Ase*I (5′-AT↓TAAT-3′), *Sca*I (5′-AGT↓ACT-3′), *Pvu*II (5′-CAG↓C TG-3′), *Sal*I (5′-G↓TCGAC-3′), *Pst*I (5′-CTGCA↓G-3′), *Hae*III (5′-GG↓CC-3′), and *Ssp*I (5′-AAT↓ATT-3′), were used. (Figs. S1–S3). [Cu(phen)(edda)] and [Zn(phen)(edda)], both at 50 μM, could only totally inhibit *Ase*I and *Nde*I, and the other restriction enzymes were not affected. [Co(phen)(edda)] could totally inhibit another additional restriction enzyme, *Bst* 11071. As a comparison, the intercalating dye thiazole orange could totally inhibit all the restriction enzymes, which suggests its random DNA binding (data not shown). These results suggest that the octahedral

[M(phen)(edda)] complexes bind not randomly but specifically at the two or three of the binding sequences of *Ase*I (5′-ATTAAT-3′), *Nde*I (5′-CATATG-3′), and *Bst* 11071 (5′-GTATAC-3′). Interestingly, [Co(phen)(edda)] inhibits all three restriction enzymes (*Ase*I, *Nde*I, and *Bst* 1071) and seems to be less selective as it cannot differentiate the 5′-CATATG-3′ sequence from the 3′-CATATG-5′ sequence. However, the Cu(II) and Zn(II) complexes seem to be able to differentiate this pair of palindromic sequences as they can inhibit *Nde*I (5′-CATATG-3′) but not *Bst* 11071 (5′-GTATAC-3′).

Another relevant observation is that *Eco*RI (5′-G↓AATTC-3′) is not inhibited by any of the [M(phen)(edda)] complexes, suggesting no binding of complex at the AATT sequence. *Tsp* 5091(5′-↓AATT-3′), *Mun*I (5′-C↓AATTG-3′), and *Ssp*I (5′-AAT↓ATT-3′) are also not inhibited. *Ase*I, *Nde*I, and *Bst* 1071 have a continuous sequential AT unit alone or a TA unit between two AT units. This comparison suggests that the assumed binding of [M(phen)(edda)] complexes to ds(CGCGATATCGCG)$_2$ and ds(CGCGAATTCGCG)$_2$ at the underlined sequences is only correct for the former duplex. There are no significant differences in the apparent binding constants of [M(phen)(edda)] complexes for these two duplexes (Table 4). NMR studies on the interaction of [Zn(phen)(edda)] with these duplexes are in progress to determine the binding sites.

Interaction with G-quadruplex

The interaction of the [M(phen)(edda)] complexes with G-quadruplex derived from a 23-mer oligonucleotide, 5′-AG$_3$(T$_2$AG$_3$)$_3$-3′, was investigated by CD spectroscopy. As expected, the racemic [M(phen)(edda)] complexes did not show any CD spectra (data not shown). On the other hand, the CD spectrum of the G-quadruplex alone shows two maxima at approximately 295 nm (ascribed to G–G base stacking) and at approximately 250 nm, and a minimum at approximately 267 nm (Fig. 2, spectra I). We have previously established it to be an antiparallel G-quadruplex with basket strand orientation [26]. G-quadruplex (20 μM)
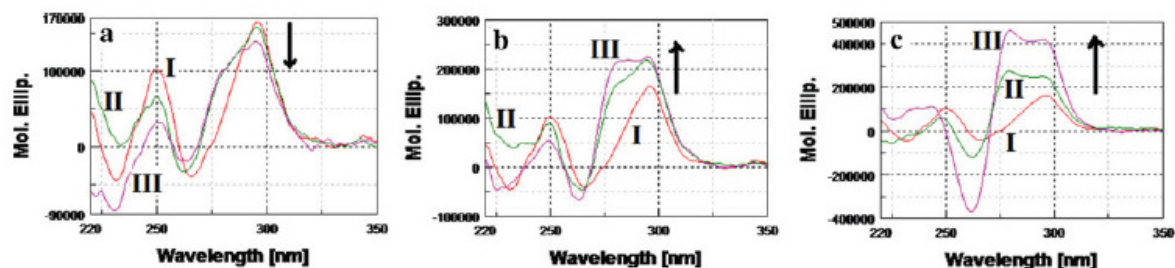
Fig. 2 Circular dichroism spectra of 20 μM G-quadruplex 5'-AG$_3$(T$_2$AG$_3$)$_3$-3' in the absence and presence of M(phen)(edda) (**a** Co, **b** Cu, **c** Zn). *I* G-quadruplex alone (*red*), *II* G-quadruplex with 60 μM complex (*green*), *III* G-quadruplex with 120 μM complex (*purple*) in 5 mM tris(hydroxymethyl)aminomethane, 50 mM NaCl buffer at pH 7.5

was incubated with [M(phen)(edda)] at two different concentrations, viz., 60 and 120 μM, and the CD spectra were obtained (Fig. 2). The three peaks remain practically unchanged, suggesting retention of antiparallel structure.

However, there seemed to be a distinct induced positive peak at approximately 280 nm when Cu(II) and Zn(II) complexes were added to the G-quadruplex. Although this induced peak has also been observed to be induced by bis(3-methylpicolinato-$\kappa^2 N,O$)$_2$(1,10-phenanthroline-$\kappa^2 N,N$)zinc(II) pentahydrate, its formation was not explained [26]. It may arise as a result of the preferential binding of one enantiomer of [M(phen)(edda)] on the G-quadruplex. How the existence of the chiral Δ and Λ enantiomers in the racemic octahedral [M(phen)(edda)] complexes affects their individual interaction with G-quadruplex needs further investigation by other techniques. There may or may not be significant differences. As far as we know, there is no precedence for such investigation involving Δ and Λ isomers except that involving a different kind of chiral enantiomes of a metallo-supramolecular cylinder where one of its enantiomers (*P* form) can selectively stabilize the chiral G-quadruplex [32].

With respect to the changes of the G-quadruplex maximum at 295 nm, the Co(II) complex induces increasing reduction in band intensity, whereas the Cu(II) and Zn(II) complexes induce an increasing enhancement in band intensity. The presence of enantiomeric pairs of [M(phen)(edda)] may complicate interpretation of CD spectral differences. Nevertheless, we tentatively ascribe the respective increase and decrease in the band intensity of the peak at 295 nm to corresponding stabilization and destabilization of the G-quadruplex, as was observed for other compounds [26, 33–35]. When the complex concentration is increased from 60 to 120 μM, the Cu(II) complex does not seem to further amplify the intensity of the 295-nm peak. Interestingly, the Zn(II) complex causes nearly doubling of the intensity of the 295-nm peak, suggesting much greater stabilization of the G-quadruplex. Such modulation of the binding effect by changes in the

geometrical dimension of the octahedral [M(phen)(edda)] complexes is unknown, and this is the first of its kind ever reported. Besides stabilizing G-quadruplex, G-quadruplex stabilizers are known to exhibit cytotoxicity against tumor cell lines [36–39]. Unlike a hexaoxazole macrocycle compound (HXDV) which stabilizes G-quadruplex and induces cell cycle arrest in M phase, the [Zn(phen)(edda)] complex is an S-phase blocker [20, 40].

Topoisomerase I inhibition

It was found that 1 U of topoisomerase I could completely convert all plasmid pBR322 to fully relaxed DNA or topoisomers (Fig. 3, lane 4), whereas phen (data not shown), CoCl$_2$, CuCl$_2$ (except at 40 μM), and ZnCl$_2$ could not inhibit topoisomerase I in the concentration range 5–40 μM (Fig 2). In the presence of 10 or 20 μM [M(phen)(edda)] complexes, faster moving bands of less relaxed topoisomers are formed which resulted from partial inhibition of topoisomerase I by the complexes (Fig. 3d–f, lanes 6–10). With further increase of complex concentration, new bands of faster moving and less relaxed topoisomers are formed. In the complex concentration range used, it is not clear whether there is a limiting concentration of complex above which there is no further increase in inhibition of topoisomerase I.

Inhibition of topoisomerase I by [M(phen)(edda)] can occur via two mechanistic possibilities: (1) binding of [M(phen)(edda)] to DNA, thereby blocking the action of topoisomerase I, and (2) binding of [M(phen)(edda)] to topoisomerase I, thereby preventing its ability to relax the DNA. To investigate this, three types of mixing of the three components were used: (1) simultaneous mixing of all components (Fig. 4, panel a); (2) mixing [M(phen)(edda)] and topoisomerase I first before adding DNA (Fig. 4, panel b); and (3) mixing DNA and [M(phen)(edda)] before adding topoisomerase I (Fig. 4, panel c). Simultaneous mixing gave results which showed that inhibition of topoisomerase I seemed to increase from [Cu(phen)(edda)]
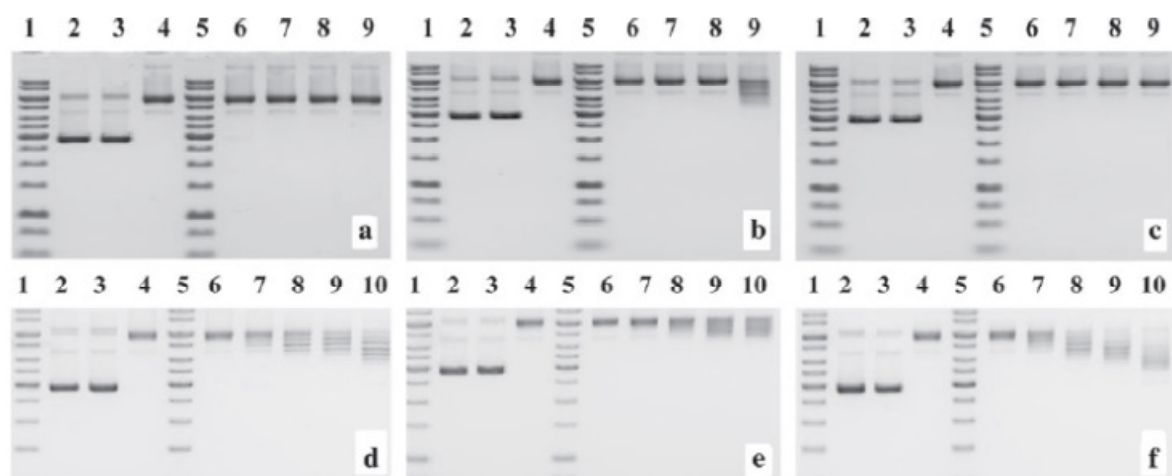
Fig. 3 Human topoisomerase I inhibition assay by gel electrophoresis. Electrophoresis results of incubating human topoisomerase I (1 U/21 μL) with pBR322 (0.25 μg) in the absence or presence of 5–40 μM metal salt (**a** CoCl₂, **b** CuCl₂, **c** ZnCl₂, *lanes 1–9*) or [M(phen)(edda)] [**d** Co(II), **e** Cu(II), **f** Zn(II), *lanes 1–10*). **a–f** *Lane 1* and *5* GeneRuler 1-kb DNA ladder, *lane 2* DNA alone, *lane 3* DNA + 40 μM compound (control), *lane 4* DNA + 1 U human topoisomerase I (control) **a–c** Topoisomerase I with increasing concentration of MCl₂: *lane 6* 5 μM, *lane 7* 10 μM, *lane 8* 20 μM, *lane 9* 40 μM. **d–f** Topoisomerase I with increasing concentration of [M(phen)(edda)]: *lane 6* 5 μM, *lane 7* 10 μM, *lane 8* 20 μM, *lane 9* 30 μM, *lane 10* 40 μM
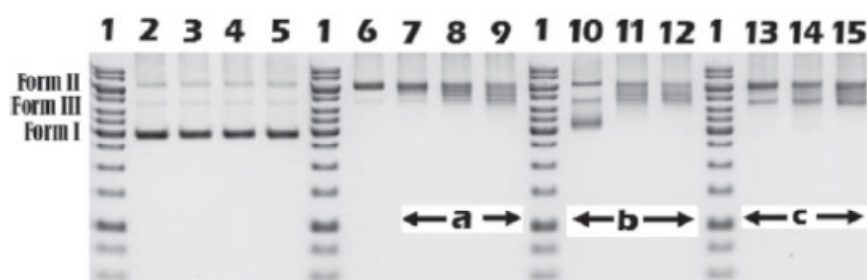

Fig. 4 Electrophoresis results of sequential incubation of human topoisomerase I (1 U/21 μL) with pBR322 (0.25 μg) in the presence of 50 μM [M(phen)(edda)] (M is Cu *lanes 7, 10,* and *13*; Co *lanes 8, 11,* and *14*; Zn: *lanes 9, 12, 15*). For all panels, *lane 1* GeneRuler 1-kb DNA ladder, *lane 2* DNA alone, *lanes 3–5* DNA + 50 μM [Cu(phen)(edda)], [Co(phen)(edda)], and [Zn(phen)(edda)], respectively (control), *lane 6* DNA + 1 U human topoisomerase I (control). For panels *a–c*, DNA + topoisomerase I + [M(phen)(edda)]: *a* mixing all components together at the same time, *b* mixing [M(phen)(edda)] and topoisomerase I first, *c* mixing DNA and M(phen)(edda) first. *Form I* supercoiled pBR322 DNA, *form II* nicked open circular DNA, *form III* linear DNA

to [Co(phen)(edda)] to [Zn(phen)(edda)] (Fig. 4, panel a, lanes 7–9). Among the complexes, [Cu(phen)(edda)] gave the greatest inhibition for prior mixing of topoisomerase I with complex (Fig. 4, panel b) as a lot of supercoiled DNA is observed (DNA form I; lane 10). For the prior mixing of DNA with [M(phen)(edda)], the gel pattern (Fig. 4, panel c) was different from the gel patterns which were obtained from the previous two modes of mixing. Here, two similar bands (form III and form II) were observed for all the complexes, and the presence of quite intense form II bands suggests a substantial amount of fully relaxed topoisomers whose formation was not inhibited by the [M(phen)(edda)] complexes (Fig. 4, panel c; lanes 13–15). No observation of a supercoiled band (form I) and more

intense form II bands suggests that inhibition of topoisomerase I arising from prior mixing of DNA with the complex (Fig. 4, panel c) is less than that from prior mixing of topoisomerase I with the complex (Fig. 4, panel b). In this third mode of mixing, there may be unconfirmed presence of some nicked DNA (band form II) and linear DNA (band form III) which arose from single-strand and double-strand cleavage, respectively. These differences indicate that inhibition of topoisomerase I by [M(phen)(edda)] could occur by both mechanisms.

The anticancer mechanism of [M(phen)(edda)] complexes may also involve inhibition of topoisomerase I, which catalyzes topological changes in DNA by forming transient DNA single-strand breaks. Compounds that

Table 5 Mitochondrial fluorescence showing the percentage of 5,5',6,6'-tetrachloro-1,1',3,3'-tetraethylbenzimidazol-carbocyanine iodide (*JC-1*) monomers and JC-1 aggregates in untreated cells and those treated with compounds

	Period (h)	Untreated control	[Co(phen)(edda)]	[Cu(phen)(edda)]	[Zn(phen)(edda)]
JC-1 aggregates (580 nm)	24	80.86 ± 0.74	80.77 ± 0.41	78.09 ± 0.58	76.94 ± 0.74
	48	87.88 ± 0.95	64.64 ± 1.82	68.56 ± 0.26	52.96 ± 1.58
	72	89.74 ± 1.19	63.49 ± 0.89	70.95 ± 0.95	28.81 ± 0.63
JC-1 monomers (527 nm)	24	18.97 ± 0.75	19.07 ± 0.40	21.75 ± 0.60	22.14 ± 0.78
	48	11.29 ± 1.21	35.37 ± 1.93	31.29 ± 0.26	46.26 ± 1.64
	72	9.69 ± 0.94	35.64 ± 0.87	28.32 ± 0.98	70.77 ± 0.73

inhibit topoisomerase I are reported to have a wide range of antitumor activities, and such topoisomerase I inhibitors are among the most widely used anticancer drugs [41–45]. Among the 60 National Cancer Institute's cell lines, MCF7 and HCT116 colon cancer cells have the highest levels of topoisomerase I expression [46]. Human topoisomerase I also promotes formation of G-quadruplex and binds to preformed G-quadruplex [47, 48]. In fact, some anticancer gold(III) tetraarylporphyrins were able to induce topoisomerase I inhibition [49].

Mitochondrial membrane potential

For the study of mitochondrial membrane potential changes ($\Delta\Psi_m$) in human cell lines, it was found that JC-1 is a more reliable fluorescent probe than 3,3'-dihexyloxocarbocyanine iodide and rhodamine 123 [50]. JC-1, a lipophilic cation, is a cytofluorimetric compound used to detect variation in membrane electrical potential at the single-cell level [51]. JC-1 is more advantageous than rhodamines and other carbocyanines because it can enter selectively into mitochondria and reversibly change its color from green to reddish orange as the membrane potential changes. This property is due to the reversible formation of JC-1 aggregates upon membrane polarization that causes shifts in emitted light from 527 nm (i.e., emission of JC-1 monomeric form) to 590 nm (i.e., emission of JC-1 aggregates) when JC-1 is excited at 490 nm [52, 53]. Thus, the color of the dye changes reversibly from green to reddish orange as the mitochondrial membrane becomes more polarized [54]. Both colors can be detected using the filters commonly mounted in all flow cytometers, so the green emission can be analyzed in the FL-1 channel (*x* axis) and the reddish-orange emission can be analyzed in the FL-2 channel (*y* axis). The main advantage of the use of JC-1 is that it can be both qualitative, considering the shift from green to reddish-orange fluorescence, and quantitative, considering the pure fluorescence intensity, which can be detected in both FL-1 and FL-2 channels.

Cytofluorimetric analysis by fluorescence-activated cell sorting with mitochondrial-membrane-potential-specific fluorescent JC-1 staining was conducted to investigate the effect of [Co(phen)(edda)], [Cu(phen)(edda)], and [Zn(phen)(edda)] at IC$_{50}$ on the changes in the mitochondrial membrane potential. Cisplatin was used as a positive control and the result showed cisplatin-treated MCF7 cells exhibited increase in green fluorescence in monomeric forms as expected following 24, 48, and 72 h in culture compared with an untreated control (Fig. S4). Exposure of MCF7 cells to 13.5 μM [Co(phen)(edda)] and 2.8 μM [Cu(phen)(edda)] showed a distinct increase in green fluorescence intensity only after 48 h (Table 5). At 24 h incubation, there is no significant change in green fluorescence. From 48 to 72 h incubation with Co(II) and Cu(II) complexes, the increase in green fluorescence seems to level off. However, incubation of MCF7 cells with 5 μM Zn(II) complex for 24, 48, and 72 h caused the greatest shift of JC-1 fluorescence intensity from red to green, with values of 22.14, 46.26, and 70.77%, respectively.

The above-mentioned increase in green fluorescence intensity reflects the increase in the number of JC-1 monomers outside the mitochondria and implies depolarization of the mitochondrial membrane in the presence of the [M(phen)(edda)] complexes. Normal cells have a polarized mitochondrial membrane potential and this is indicated by high numbers of JC-1 aggregates (red fluorescence) and low numbers of JC-1 monomers (green fluorescence) (Table 5, untreated control). Collapse of the mitochondrial membrane potential results in a depolarized mitochondrial membrane potential, and is often observed to occur early during apoptosis. Obviously, the cationic JC-1 worked by going to negative sites inside the mitochondria to form the red JC-1 aggregates, and it is released to form the green JC-1 monomers when the charge changes. In other words, the red emission signal decreases (with concomitant increase in the green emission signal) when the membrane potential of mitochondria is lost. The fluorescence intensity detected by the flow cytometer reflects the function of mitochondria [55].

Mitochondrial membrane potentials ($\Delta\Psi_m$) can be calculated from the ratio ($I_{590\ nm}/I_{527\ nm}$) between red fluorescence (590 nm) intensity and green fluorescence
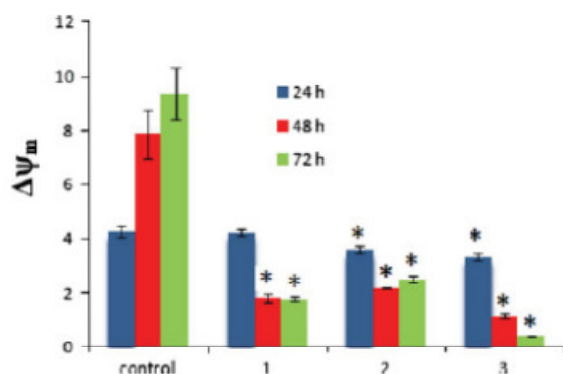
Fig. 5 Effect of [M(phen)(edda)] complexes (*1* Co, *2* Cu, *3* Zn) on the mitochondrial membrane potential ($\Delta\Psi_m$). Cells were treated with the concentration required to inhibit cell proliferation by 50% of respective metal complexes for 24, 48, and 72 h, respectively. The data are mean for four or more experiments. *$p < 0.05$ compared with the control

(527 nm) intensity using JC-1 [15]. The effect of [M(phen)(edda)] complexes on $\Delta\Psi_m$ in MCF7 cells is shown in Fig. 5. It is clearly seen that they significantly decrease $\Delta\Psi_m$ only after more than 24 h and the decrease is time-dependent (48 and 72 h). At 72 h, [Zn(phen)(edda)] induced the greatest reduction in $\Delta\Psi_m$. The decrease of $\Delta\Psi_m$ suggests that these compounds interact with the mitochondria [15]. This lowering of the mitochondrial membrane potential can initiate the apoptotic intrinsic pathway [56]. In fact, ruthenium complexes reportedly induced loss of mitochondrial membrane potential and the concomitant intrinsic pathway of cell death [57, 58]. Recently, [Cu(4,7-dimethyl-phenanthroline)(glycinate)NO$_3$] was reported to induce overproduction of reactive oxygen species (ROS), leading to loss of mitochondrial membrane potential and cell death in human lung cancer cells [59]. An anticancer Mn(II) complex also caused lowering of $\Delta\Psi_m$ [15].

Using flow cytometry, we have previously established that [M(phen)(edda)] induced apoptosis in MCF7 and there was no necrosis [20]. Loss of mitochondrial membrane potential induced by [M(phen)(edda)] suggests an intrinsic pathway of apoptosis. However, studies of cell death induced by metal(II) ions showed that decrease in mitochondrial membrane potential may involve different pathways of apoptosis or a different mode of cell death. For example, CoCl$_2$ induced apoptosis in rat PC12 cells through both a mitochondria-mediated pathway accompanied by loss of mitochondrial membrane potential and a death-receptor-mediated pathway [60]. Killing of rat neurons by excess Zn^{2+} ions involved loss of mitochondrial membrane potential and inhibition of oxygen utilization in the mitochondria [61]. Micromolar concentration of Cu^{2+}

could induce both apoptosis and necrosis of trout hepatocytes [62]. Besides strong production of ROS, Cu^{2+} induced a decrease in $\Delta\Psi_m$ and induced mitochondrial permeability transition [62]. It was also found that Cu^{2+} and Zn^{2+} could induced apoptosis in MCF7 cells, and the cell death involved a decrease in $\Delta\Psi_m$, elevated ROS production, and activation of p53 [62]. The role of p53 in apoptosis is crucial, and depolarization of the mitochondrial membrane caused release of apoptosis-inducing factor and its translocation into the nucleus [62]. Unlike the present results from the study of [M(phen)(edda)] for 72 h incubation, the Cu^{2+} ions induced greater decrease than Zn^{2+} ions of $\Delta\Psi_m$ in MCF7 cells [63].

Anticancer selectivity

The [Co(phen)(edda)], [Cu(phen)(edda)], and [Zn(phen) (edda)] complexes were evaluated for cytotoxic activity in vitro against human breast normal and cancer cell lines (MCF10A and MCF7, respectively). MTT antiproliferative assay was used to screen the compounds on MCF10A and MCF7 cell lines for 24, 48, and 72 h. Cells were incubated with increasing concentration of each compound. The viable cells were quantified and the numbers were presented as a percentage with reference to nontreated cells. The IC$_{50}$ (the concentration of the metal complexes at which the conversion of MTT to formazan by viable cells is reduced by 50% compared with control cells) values for different compounds are summarized in Table 6. It is clear that the compounds inhibit the proliferation of MCF7 breast cancer cells in a time- and dose-dependent manner. For 72 h incubation, the order of increasing cytotoxicity is [Co(phen)(edda)] (IC$_{50}$ 13.5 μM), [Zn(phen)(edda)] (IC$_{50}$ 5.0 μM), [Cu(phen)(edda)] (IC$_{50}$ 2.8 μM). These IC$_{50}$ values were comparable to those or better than those for cisplatin (IC$_{50}$ 10.9 μM) and oxaliplatin (IC$_{50}$ 18.2 μM) [64]. The metal(II) chlorides were not cytotoxic to MCF7 even at 72 h incubation, as was found by others for the same cell line (CoCl$_2$, IC$_{50}$ > 100 μM; ZnCl$_2$, IC$_{50}$ 130 μM; CuCl$_2$, IC$_{50}$ > 200 μM) [65–67]. Previously, we reported the IC$_{50}$ of phen for MCF7 as 74 μM [20].

All these [M(phen)(edda)] compounds were found to induce apoptosis in the cancer cells, while only the Zn(II) analogue was also able to induce cell cycle arrest in S phase [20]. The cytotoxicity of the complexes may be partly due to their ability to bind to nuclear DNA and cause conformational changes and/or DNA damage via production of ROS [20, 29]. The much higher cytotoxicity of [Cu(phen)(edda)], compared with the Co(II) and Zn(II) analogues, may be attributed to its higher nucleolytic property and greater ability to generate ROS [29]. Induction of apoptotic cell death can also be partly attributed to

Table 6 Cytotoxicity (IC$_{50}$ values, µM) of [Co(phen)(edda)], [Cu(phen)(edda)], and [Zn(phen)(edda)] towards human cancer and normal cell lines

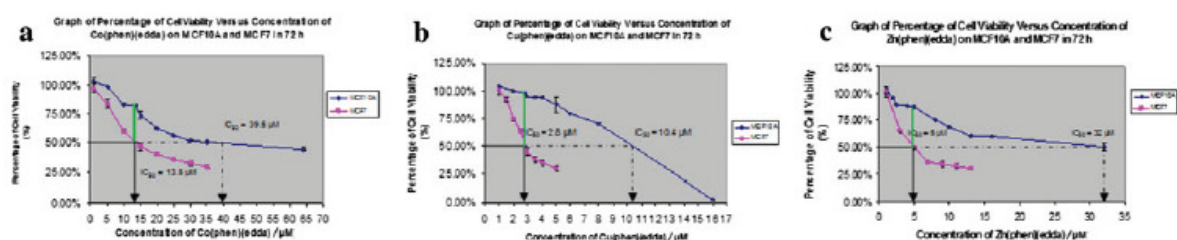|	Cell line					
	MCF7			MCF10A		
	24 h	48 h	72 h	24 h	48 h	72 h
[Co(phen)(edda)]	>160.0	58.0	13.5	>140.0	128.0	39.5
[Cu(phen)(edda)]	25.0	5.5	2.8	30.0	15.0	10.4
[Zn(phen)(edda)]	>140.0	15.0	5.0	>140.0	50.0	32.0
ZnCl$_2$	>100	>100	>100			
CuCl$_2$	>100	>100	>100			
CoCl$_2$	>100	>100	>100			

Fig. 6 Percentage cell viability versus concentration of [M(phen)(edda)] [**a** Co(II), **b** Cu(II), **c** Zn(II)] for MCF7 (*pink*) and MCF10A (*blue*) cells incubated for 72 h

inhibition of topoisomerase I as reported for other anticancer compounds [68, 69]. Anticancer activity of the [M(phen)(edda)] complexes can also work through targeting the G-quadruplex. In fact, G-quadruplex is now accepted as a new therapeutic target in human cancer [70]. Thus, it is reasonable to attribute the cytotoxicity of these complexes towards cancer cells as due their action on multiple targets.

However, analysis of the IC$_{50}$ values of these compounds shows that they are less cytotoxic to the MCF10A normal cells by a factor of approximately twofold to threefold. When one compares the relative cytotoxicity towards both cell lines in the lower concentration range, the selectivity of these compounds is more significant (Fig. 6). For example, 2.8 µM [Cu(phen)(edda)] reduced cell viability of MCF7 cancer cells by 50%, whereas it reduced that of MCF10 normal cells by only about 5%. MCF7 cells may be more sensitive than MCF10A cells to the antiproliferative effect of [M(phen)(edda)] because of the faster growth rate (i.e., lower doubling time) [71, 72]. However, this factor may have been minimized in our MTT assay, which used a shorter incubation period (1–3 days) and higher cell density per well (about 25,000 cells) [72]. Consequently, the selectivity shown by [M(phen)(edda)] towards MCF7 cells may not be due to the higher growth rate of MCF7 cells.

This selectivity may, in part, be attributed to inhibition of topoisomerase I, which is overexpressed in MCF7 cells. The importance of this tumor selectivity has been highlighted and the severe toxicities of many clinical anticancer drugs are attributed to this factor [73–75]. Exposure of other organs to the toxicity of anticancer drugs, which is also encountered with newer clinically used oxaliplatin, remains an ongoing clinical and research problem [76, 77]. Thus, animal studies involving the [M(phen)(edda)] complexes are been planned and this issue will be addressed.

Conclusion

Analysis of the crystal structures of the neutral [M(phen)(edda)] complexes shows distinct differences in their distorted octahedral geometries. Besides the constraint imposed by the tetradentate edda ligand, the geometrical dimension and distortion are affected by the electronic configuration ($t_{2g}^x e_g^y$). This difference in the octahedral structure, in the absence of a better alternative explanation, seems to account for the differences in binding interaction of the complexes with duplex and G-quadruplex DNA via modulation of intercalative and other binding interactions. Restriction enzyme inhibition assay results show that these complexes show specificity in their binding to DNA. The Cu(II) and Zn(II) complexes seem to be able to differentiate a pair of palindromic sequences (5′-CATATG-3′ and 5′-GTATAC-3′), whereas the Co(II) analogue cannot. Besides targeting the duplex and G-quadruplex DNA, these metal complexes can inhibit topoisomerase I and interact

with mitochondria to lower the mitochondrial membrane potential. Inhibition of topoisomerase I and DNA sequence specificity by [M(phen)(edda)] may be related to the fact that organic anticancer compounds also possess DNA sequence-selective binding [78–80]. Taken together, the data suggest [M(phen)(edda)] complexes induce apoptosis via involvement of multiple targets. As an added advantage, MTT assay shows that they are more cytotoxic to MCF7 breast cancer cells than to MCF10A normal breast cells. Their cytotoxicity towards MCF7 cells is comparable to or better than that of cisplatin and oxaliplatin. Additionally, they may have potential application for other drug-resistant cancer types as MCF7 cells are cisplatin-resistant [81].

References

1. Gao EJ, Wang KH, Zhu MC, Liu L (2010) Eur J Med Chem 45:2784–2790
2. Klajner M, Hebraud P, Sirlin C, Gaiddon C, Harlepp S (2010) J Phys Chem B 114:14041–14047
3. Chen CY, Chen QZ, Wang XF, Liu MS, Chen YF (2009) Trans Met Chem 34:757–763
4. Wang P, Tang N (2009) J Fluoresc 19:1073–1082
5. Tan M, Zhu J, Pan Y, Chen Z, Liang H, Liu H, Wang H (2009) Bioinorg Chem Appl 2009:1–9
6. Casini A, Hartinger CG, Nazarov AA, Dyson PJ (2010) Topics Organomet Chem 32:57–80
7. Cinellu MA, Maiore L, Manassero M, Casini A, Arca M, Fiebig HH, Kelter G, Michelucci E, Pieraccini G, Gabbiani C, Messori L (2007) ACS Med Chem Lett 1:336–339
8. Pizarro AM, Habtemariam A, Sadler PJ (2010) Top Organomet Chem 32:21–56
9. Filak LK, Mühlgassner G, Jakupec MA, Heffeter P, Berger W, Arion VB, Keppler BK (2010) J Biol Inorg Chem 15:903–918
10. Tisato F, Marzano C, Porchia M, Pellei M, Santini C (2010) Med Res Rev 20:708–749
11. Xiao Y, Chen D, Zhang X, Cui Q, Fan Y, Bi C, Dou QP (2010) Int J Oncol 37:81–87
12. Olszewski U, Claffey J, Hogan M, Tacke M, Zeillinger R, Bednarski PJ, Hamilton G (2010) Invest New Drugs. doi: 10.1007/s10637-010-9395-5
13. Bielawska A, Poplawska B, Surazyński A, Czarnomysy R, Bielawski K (2010) Eur J Pharmacol 643:34–41
14. Lo YC, Ko TP, Su WC, Su TL, Andrew Wang HJ (2008) J Inorg Biochem 103:1082–1092
15. Chen QY, Zhou DF, Huang J, Guo WJ, Gao J (2010) J Inorg Biochem 104:1141–1147
16. Pisani MJ, Weber DK, Heimann K, Collins JG, Keene FR (2010) Metallomics 2:393–396
17. Chen T, Liu Y, Zheng WJ, Liu J, Wong YS (2010) Inorg Chem 49:6366–6368
18. Jiang YL, Liu ZP (2010) Mini Rev Med Chem 10:726–736
19. Che CM, Siu FM (2010) Curr Opin Chem Biol 14:255–261
20. Ng CH, Kong KC, Von ST, Balraj P, Jensen P, Thirthagiri E, Hamada H, Chikira M (2008) Dalton Trans 36:447–454
21. Bruker (2007) APEX2 and SAINT. Bruker AXS, Madison
22. Sheldrick GM (1996) SADABS. University of Göttingen, Germany
23. Sheldrick GM (1997) SHELXS 97 program for crystal structure solution. University of Göttingen, Germany
24. Sheldrick GM (1997) SHELXL-97 program for crystal structure refinement. University of Göttingen
25. Farrugia LJ (1997) J Appl Crystallogr 30:565
26. Seng HL, Von ST, Tan KW, Maah MJ, Ng SW, Raja Abd Rahman RNZ, Caracelli I, Ng CH (2010) Biometals 23:99–118
27. Shi LM, Fan Yi, Lee JK, Waltham M, Andrews DT, Scherf U, Paull KD, Weinstein JN (2000) J Chem Inf Comput Sci 40:367–379
28. Gajewski E, Gaur S, Akman SA, Matsumoto L, van Balgooy JNA, Doroshow JH (2007) Biochem Pharm 73:1947–1956
29. Seng HL, Alan Ong HK, Raja Abd Rahman RNZ, Yamin BM, Tiekink ERT, Tan KW, Maah MJ, Caracelli I, Ng CH (2008) J Inorg Biochem 102:1997–2011
30. Chin LF, Kong SM, Seng HL, Kong KhooKS, Vikneswaran R, Teoh SG, Ahmad M, Alan Khoo SB, Maah MJ, Ng CH (2011) J Inorg Biochem 105:221–229
31. Tasa E, Kilic A, Durgun M, Kupecik L, Yilmaz I, Arslan S (2010) Spectrochim Acta A 75:811–818
32. Yu H, Wang X, Fu M, Ren J, Qu X (2008) Nucleic Acids Res 36:5695–5703
33. Agarwal T, Roy S, Chakraborty TK, Maiti S (2010) Biochemistry 49:8388–8397
34. Nagesh N, Krishnaiah A (2003) J Biochem Biophys Methods 57:65–74
35. Talib J, Green C, Davis KJ, Urathamakul T, Beck JL, Aldrich-Wright JR, Ralph SF (2008) Dalton Trans 37:1018–1026
36. Gomez D, Wenner T, Brassart B, Douarre C, O'Donohue MF, El Khoury V, Shin-Ya K, Morjani H, Trentesaux C, Riou JF (2006) J Biol Chem 281:38721–38729
37. Tauchi T, Shin-ya K, Sashida G, Sumi M, Okabe S, Ohyashiki JH, Ohyashiki K (2006) Oncogene 25:5719–5725
38. Phatak P, Cookson JC, Dai F, Smith V, Gartenhaus RB, Stevens MF, Burger AM (2007) Br J Cancer 96:1223–1233
39. Gowan SM, Harrison JR, Patterson L, Valenti M, Read MA, Neidle S, Kelland LR (2002) Mol Pharmacol 61:1154–1162
40. Tsai YC, Qi H, Lin CP, Lin RK, Kerrigan JE, Rzuczek SG, Lavoie EJ, Rice JE, Pilch DS, Lisa Lyu Y, Liu LF (2009) J Biol Chem 34:22535–22543
41. Sunani S, Nishimura T, Nishimura I, Ito S, Arakawa H, Ohkubo M (2009) J Med Chem 52:3225–3237
42. Rothenberg ML (1997) Ann Oncol 8:837–855
43. Beretta GL, Perego P, Zunino F (2008) Expert Opin Ther Targets 12:1243–1256
44. Teicher BA (2008) Biochem Pharmacol 75:1262–1271
45. Pommier Y (2008) Nat Rev Cancer 18:789–802
46. Reinhold WC, Mergny J-L, Liu H, Ryan M, Pfister TD, Kinders R, Parchment R, Doroshow J, Weinstein JN, Pommier Y (2010) Cancer Res 70:2191–2203
47. Arimondo PB, Riou JF, Mergny JL (2000) Nucl Acids Res 28:4832–4838
48. Marchand C, Pourquier P, Laco GS, Jing N, Pommier Y (2002) J Biol Chem 277:8906–8911
49. Sun RWY, Li CKL, Ma DL, Yan JJ, Lok C-N, Leung CH, Zhu N, Che CM (2010) Chem Eur J 16:3097–3113
50. Salvioli S, Ardizzoni A, Cossarizza A, Franceschi C (1997) FEBS Lett 411:72–82
51. Cossarizza A, Baccarani CM, Kalashnikova G, Franceschi C (1993) Biochem Biophs Res Commun 197:40–45
52. Hada H, Honda C, Tanemura H (1977) Photogr Sci Eng 21:83–91
53. Reers M, Smith TW, Chen LB (1991) Biochemistry 30:4480–4486

54. Smiley ST, Reers M, Hartshorn CM, Lin M, Chen A, Smith TW, Steele GD, Chen LB (1991) Proc Natl Acad Sci USA 88:3671–3675
55. Cossarizza A (2000) Miner Biotechnol 12:57–61
56. Debatin K-M (2000) Toxicol Lett 112–113:41–48
57. Meggers E, Atilla-Gokcumen GE, Gründler K, Frias C, Prokop A (2009) Dalton Trans 38:10882–10888
58. Mulcahy SP, Gründler K, Frias G, Wagner L, Prokop A, Meggers E (2010) Dalton Trans 39:8177–8182
59. Kachadourian R, Brechbuhl HM, Ruiz-Azuara L, Gracia-Mora I, Day BJ (2010) Toxicology 268:176–183
60. Jung J-Y, Kim W-J (2004) Neurosci Lett 371:85–90
61. Dineley KE, Richards LL, Votyakova TV, Reynolds JJ (2005) Mitochondria 5:55–65
62. Krumschnabel G, Manzl C, Berger C, Hofer B (2005) Toxicol Appl Pharmacol 209:62–73
63. Ostrakhovitch EA, Cherian MG (2005) Apoptosis 10:111–121
64. Štarha P, Trávníček Z, Popa I (2009) J Inorg Biochem 103:978–988
65. Trávníček Z, Klanicová A, Popa I, Rolčik J (2005) J Inorg Biochem 99:776–786
66. Kovala-Demertzi D, Yadav PN, Wiecek J, Skoulika S, Varadinova T, Demertzis MA (2006) J Inorg Biochem 100:1558–1567
67. Maloň M, Trávníček Z (2002) Trans Met Chem 27:580–586
68. Arjmand F, Muddassir M (2010) J Photochem Photobiol B Biol 101:37–46
69. Chashoo G, Singh SK, Sharma PR, Mondhe DM, Hamid A, Saxena A, Andotra SS, Shah BA, Qazi NA, Taneja SC, Saxena AK (2011) Chem Biol Interact 189:60–71
70. Neidle S (2010) FEBS J 277:1118–1125
71. Grem JL, Danenberg KD, Behan K, Parr A, Young L, Danenberg PV, Nguyen D, Drake J, Monks A, Allegra CJ (2001) Clin Cancer Res 7:999–1009
72. Boyd MR (2004) In: Teicher B, Andrews PA (eds) Drug development guide: preclinical screening, clinical trials, and approval. 2nd edn. Humana, New Jersey, pp 41–61
73. Carter SK (1984) In: Hacker MP (eds) Platinum coordination complexes in cancer chemotherapy. Martinus Nijhoff Press, Boston pp 359–365
74. Keppler BK (1993) Metal complexes in cancer therapy. VCH, Weinheim, pp 1–15
75. von Hoff DD, Schilsky R, Reichert CM, Reddick RL, Rozencweig M, Young RC, Muggia FM (1979) Cancer Treat Rep 63:1527–1535
76. El-Ghannam A, Ricci K, Malkawi A, Jahed K, Vedantham K, Wyan H, Allen LD, Dréau D (2010) J Mater Sci Mater Med 21:2701–2710
77. Meyer L, Patte-Mensah C, Taleb O, Mensah-Nyagan AG (2011) Pain 152:170–181
78. Capranico G, Binaschi M, Borgnetto ME, Zunino F, Palumbo M (1997) Trends Pharmacol Sci 18:323–329
79. Rao VA, Agama K, Holbeck S, Pommier Y (2007) Cancer Res 67:9971–9979
80. Arimondo PB, Thomas CJ, Oussedik K, Baldeyrou B, Mahieu C, Halby L, Guianvarc'h D, Lansiaux A, Hecht SM, Bailly C, Giovannangeli C (2006) Mol Cell Biol 26:324–333
81. Jänicke RU (2008) Breast Cancer Res Treat 117:219–221

Synthesis, characterization, DNA-binding study and anticancer properties of ternary metal(II) complexes of edda and an intercalating ligand†‡

Chew Hee Ng,*[a] King Chow Kong,[a] Sze Tin Von,[a] Pauline Balraj,[b] Paul Jensen,[c] Eswary Thirthagiri,[d] Hirokazu Hamada[e] and Makoto Chikira[e]

A series of ternary metal(II) complexes {M(phen)(edda); **1a** (Cu), **1b** (Co), **1c** (Zn), **1d** (Ni); H_2edda = N,N'-ethylenediaminediacetic acid} of N,N'-ethylene-bridged diglycine and 1,10-phenanthroline were synthesized and characterized by elemental analysis, FTIR, UV-visible spectroscopy and magnetic susceptibility measurement. The interaction of these complexes with DNA was investigated using CD and EPR spectroscopy. MTT assay results of **1a**–**1c**, screened on MCF-7 cancer cell lines, show that synergy between the metal and ligands results in significant enhancement of their antiproliferative properties. Preliminary results from apoptosis and cell cycle analyses with flow cytometry are reported. **1c** seems to be able to induce cell cycle arrest at G_0/G_1. The crystal structure of **1a** is also included.

1. Introduction

Since the discovery of cisplatin for cancer treatment, numerous transition metal complexes have been synthesized and screened for their anticancer properties. One strategy in such efforts is to synergise the beneficial effect of the ligand and the activity of the metal to produce a complex with enhanced activity.[1] In the present post genomic era, another strategy focusses on the interaction of metal drugs with proteins that regulate apoptosis.[2] Here, selection of organic compounds of known therapeutic action and linking them to the metal has been successfully applied, resulting in platinum and ruthenium anti-metastatic complexes. A recent theoretical study, using clustering analysis and self-organising maps, of more than 1000 metal containing compounds with potential anticancer properties concluded that their cytotoxicity is determined by the identity of the metal and the organic ligand, and the target-specificity can be accomplished by the right metal–ligand combination.[3]

We have been systematically experimenting with such combinations. The present investigation involves the synthesis of a series of neutral ternary transition metal complexes (Co, Ni, Cu, Zn) with a moderately cytotoxic intercalating bidentate ligand, 1,10-phenanthroline, and a non-toxic tetradentate amino acid, N,N-ethylene-bridged diglycine (more commonly called N,N'-ethylenediaminediacetic acid, H_2edda), to evaluate the effect of

varying the type of metal ion. The selection of edda as a second ligand may enhance the affinity of the ternary complexes towards DNA through the formation of hydrogen bonding between the edda and the DNA. Unlike square planar platinum(II) complexes, the six-coordinate M(phen)(edda) complexes are likely to bind to polyanionic DNA *via* non-covalent outer-sphere coordination. Furthermore, neutral metal complexes should be more lipophilic than the corresponding ionic metal complexes and their greater uptake by cells can lead to increased cytotoxicity.

Thus far, most anticancer metal complexes containing 1,10-phenanthroline are cationic.[4-9] These include tris(1,10-phenanthroline)lanthanum(III) trithiocyanate,[4] platinum(II) complexes with 1,10-phenanthroline and acyclovir or penciclovir,[5] platinum(II) or palladium(II) complexes of 1,10-phenanthroline and a series of amino acids,[6] tris(1,10-phenanthroline)chromium(III),[7] and copper(II) complexes.[8,9] Coyle, *et al.* recently reported possible differences in cell death mechanism in mammalian cells incubated with neutral ternary metal complexes (Cu(II), Mn(II) and Ag(I)) of 1,10-phenanthroline and malonic acid.[10] [Cu(phen)$_2$(mal)]·2H_2O induced apoptosis while metal-free phen, and the Mn(II) and Ag(I) ternary complexes did not induced apoptosis but merely caused non-specific DNA degradation. The present paper details the synthesis and characterization of our set of neutral ternary metal complexes, together with their DNA-binding study and anticancer properties towards breast cancer line, MCF-7.

2. Results and discussion

2.1 Synthesis and characterization

The ternary complexes were prepared either by first reacting freshly prepared metal hydroxide with N,N'-ethylenediaminediacetic acid (H_2edda) and then finally by adding a methanolic or ethanolic aqueous solution of 1,10-phenanthroline (phen) or by an *in situ* method where the sequence of added reactants is H_2edda, NaOH, metal(II) salt and alcoholic aqueous phen. The ternary metal(II) complexes of the edda and phen precipitated out on the

[a]Faculty of Engineering and Science, Universiti Tunku Abdul Rahman, 53300, Kuala Lumpur, Malaysia. E-mail: ngch@mail.utar.edu.my; Fax: +60 3 4107 9803; Tel: +60 3 4107 9802
[b]Molecular Pathology Unit, Institute for Medical Research, 50588, Kuala Lumpur, Malaysia
[c]School of Chemistry, University of Sydney, NSW, 2006, Australia
[d]Cancer Research Initiatives Foundation, 47500, Kuala Lumpur, Malaysia
[e]Department of Applied Chemistry, Chuo University, Kasuga 1-13-27, Bunkyo-ku, Tokyo, 112-8551, Japan

Complexes	λ_{1a}/nm (ε/M^{-1} cm^{-1})^a	λ_{1b}/nm (ε/M^{-1} cm^{-1})^a	λ_2/nm (ε/M^{-1} cm^{-1})	λ_3/nm (ε/M^{-1} cm^{-1})
1a (Cu)	225 (21 191)	269 (18 489)	682 (94)	926 (48)
1b (Co)	226 (28 878)	269 (25 124)		942 (6)
1c (Zn)	227 (32 015)	267 (24 730)		
1d (Ni)	227 (32 047)	270 (29 694)	564 (11)	915 (10)

^{a} λ_1 values: π–π* transition bands of phen.

same day or upon slow evaporation of the solution mixtures. FTIR spectra of these complexes show the presence of asymmetrically and symmetrically coordinated carboxylate stretching frequencies at ~1600 and ~1400 cm^{-1} respectively,[11] and of coordinated phen ligand peaks at ~(1517–1522), 852 and ~727 cm^{-1}.[12] Elemental analysis of the isolated complexes, **1**, reveals a general formula, [M(phen)(edda)]·xH$_2$O.

The copper(II) complex, **1a**, has a magnetic moment of 1.91 μ_B while the cobalt(II), **1b**, and nickel(II), **1d**, complexes have μ_{eff} values of 4.89 and 3.06 μ_B respectively. The observed magnetic moments are in the range observed for other octahedral copper(II),[13,14] cobalt(II)[13–18] and nickel(II)[13–18] complexes. These values are higher than their respective spin-only magnetic moments, μ_s, of 1.73, 4.24 and 2.83 μ_B due to significant orbital angular momentum contributions. The diamagnetic zinc(II) complex, **1c**, may be octahedral as evidenced by the very close similarity of its FTIR spectrum with those of **1b** and **1d**. Based on this magnetic property, these four complexes can be classified as being paramagnetic or diamagnetic octahedral complexes.

The ternary complexes seem to be formed from the substitution of the *cis*-coordinated water molecules of the initially-formed [M(edda)(H$_2$O)$_2$] by phen. This is evidenced by comparison of the visible spectra of the aqueous solutions of **1** (Table 1) prepared above and the aqueous solution mixtures (data not included) obtained by adding phen to previously synthesized *cis*-α-[M(edda)(H$_2$O)$_2$] (M = Cu, Ni, Co) complexes.[19] Their visible spectra are identical.

2.2 Crystal structure of 1a

A suitable crystal of **1a** was obtained by allowing the reaction mixture, which was heated in a water bath at 55 °C, to cool overnight. The crystal structure of **1a** (Fig. 1) confirms the octahedral geometry around the copper atom. The coordinated carboxylate oxygen atoms (O(1) and O(3)) of the tetradentate edda ligand are *trans* to each other, with a O(1)–Cu(1)–O(3) angle of 174.02(4)° and an average axial Cu–O bond length of 2.35 Å. The bite angle of the ethylenediamine chelate ring is 86.03(5)° in contrast to those of the glycinate rings which are 75.25(5)° and 76.95(5)°. The corresponding glycinate rings of the octahedral di-aqua[N,N'-ethylenedi(N-hydroxymethylglycinato)]copper(II), derived from the N-hydroxymethylation of Cu(edda), have a bigger bite angle (79.5(1)°).[20] These, together with other angles about the copper atom, show severe distortion of the octahedral geometry.

Interestingly, the tetragonal elongation of the axial bonds (Cu–O) in **1a** lifts up the N(3) atom and pulls down the N(4) atom of the ethylenediamine chelate ring, resulting in an envelope conformation of this chelate ring, such that the plane of the N(4)–N(3)-containing portion is severely tilted from that of the N(1)–
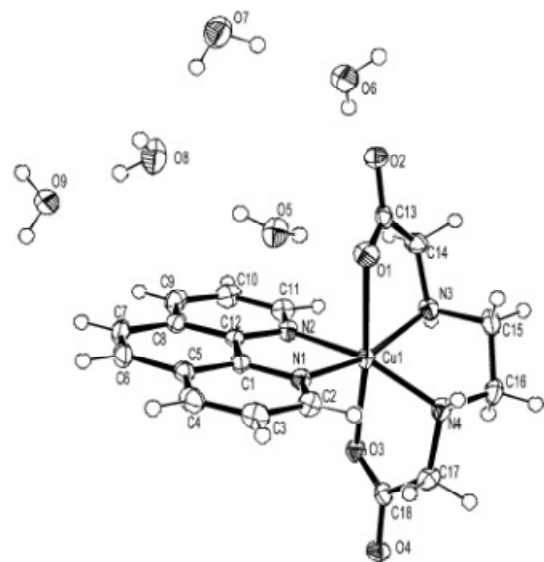

Fig. 1 Molecular structure of (N,N'-ethylenediaminediacetato)(1,10-phenanthroline)copper(II) pentahydrate, **1a**. Selected bond lengths (Å): Cu(1)–O(1) 2.3957(12), Cu(1)–N(4) 2.0263(13), Cu(1)–N(2) 2.0328(13), Cu(1)–N(1) 2.0369(13), Cu(1)–N(3) 2.0429(13), Cu(1)–O(3) 2.3140(11).

N(2)-containing fragment (of the phen ligand), and this results in significant deviation from ideal planarity of the equatorial ligated atoms. The other metal complexes (**1b**, **1c** and **1d**), with symmetric filling of the e$_g$ orbitals (d$_{z^2}$, d$_{x^2-y^2}$) are free from the above Jahn–Teller distortion and their ethylenediamine chelate rings should be conformationally different and their N(1)–N(2)–N(3)–N(4) equatorial atoms should be more planar, as is the case for the equatorial N$_2$O$_2$ atoms of [Co(edda)(H$_2$O)$_2$].[19] Thus, a change in the type of metal(II) ion modulates subtle changes in the conformation of the octahedral geometry of the complexes.

As each edda moiety has H-donor (N(3), N(4)) and H-acceptor (O(2), O(4)) atoms for H-bonding, the above two types of chelate ring conformation may modulate the possible H-bonding interaction of the edda moieties with adjacent base pairs of DNA if the chelated 1,10-phenanthroline moiety intercalates between the DNA base pairs. The resultant conformational change moves the hydrogen bonding sites of the edda moiety away or towards the DNA. Besides the above influence on H-bonding interactions with DNA due to the presence or absence of tetragonal distortion, these octahedral complexes can be classified into two types based on the nature of the distortion of the octahedral geometry.

2.3 DNA binding study

One of the modes of action of anticancer metal-based compounds is the targeting of the DNA of cancer cells. Thus, some basic interaction studies of metal complex–DNA are of relevance. The CD spectra (Fig. 2(a)) of the series of complexes **1a**–**1d** with 40 μM B-form calf thymus DNA (CT DNA) in 20 mM Hepes buffer at pH 7, containing 30 mM NaCl, still shows a positive band at ~276 nm due to base stacking and a negative band at ~245 nm due to DNA helicity. At a DNA : complex mole ratio of 1 : 1, the complexes **1a** (Cu), **1b** (Co) and **1c** (Zn) caused significant enhancement of the DNA band at 276 nm while **1d** (Ni) produced a minor increase in molar ellipticity. No significant shift in the position of the band due to DNA helicity is observed for all complexes, suggesting retention of the B-form conformation. The above enhancement of molar ellipticity at ~276 nm suggests partial intercalation of **1a**, **1b** and **1c**, and this is also observed for similar ternary complexes, [Cu(phen)(L-threo)(H$_2$O)](ClO$_4$) and lathanum(III) complexes containing the phen ligand or its derivative.[21,22]
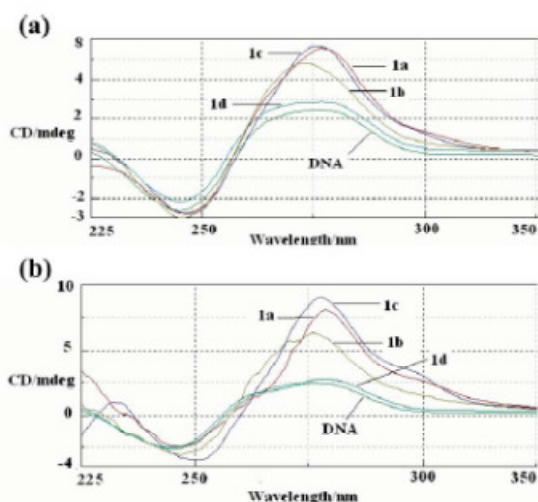

(a)

(b)

Fig. 2 Circular dichroism spectra of CT DNA without and with M(phen)(edda) at 1 : 1 ratio (a) and at 1 : 4 mole ratio (b).

When the DNA : complex ratio was increased to 1 : 4 (Fig. 2(b)), the difference in enhancement of the band at 276 nm is more pronounced, indicating a difference in the extent of intercalation by the various metal complexes. The order of increasing intercalation is **1d** < **1b** < **1a** < **1c**. The zinc complex, **1c**, caused the most significant red shift and enhancement of the band due to DNA helicity at 245 nm. A new positive band at 232 nm also appeared for **1c**. Surprisingly, the increased concentration of **1a** caused a slight decrease in intensity of the DNA helicity band at 245 nm instead of further enhancement as observed for **1b** and **1c**. The nickel complex, **1d**, seems not to significantly effect either DNA band (245 nm and ~275 nm). Thus, the above CD analysis revealed that changing the type of metal ion in **1** affects its binding interaction with DNA.

To elucidate further understanding of the above DNA binding differences, we performed an X-band EPR spectral study on the
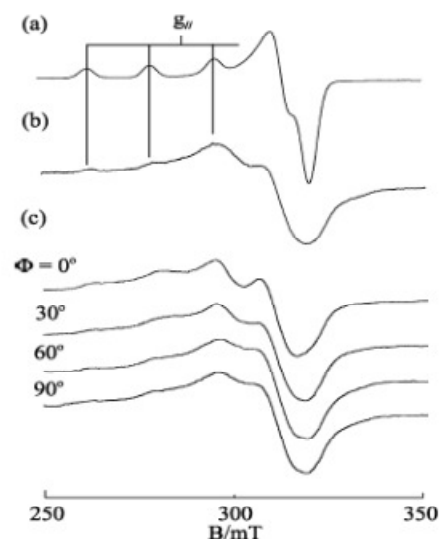

Fig. 3 EPR spectra of **1a** (a) in frozen solution at −150 °C, (b) in DNA-pellet at −150 °C, and (c) in A-form DNA fiber at room temperature. Φ is the angle beween the fiber axis and the static magnetic field.

interaction of the copper complex **1a** with highly oriented DNA fibre. The EPR spectrum of **1a** in frozen aqueous solution at pH 7 (Fig. 3(a)) showed a typical pattern characteristic of a tetragonal Cu(II) complex with $g_{\parallel} = 2.241$ and $A_{\parallel} = 17.0$ mT. The peaks observed in the EPR spectrum of the DNA pellet at −150 °C (Fig. 3(b)) correspond to the $g_{\parallel}$ and $A_{\parallel}$ signals observed for the frozen solution. However, the EPR spectra of **1a** in DNA pellet and in A-form DNA fiber at room temperature (Fig. 3(c)) were broadened considerably, indicating that the copper coordination sphere was deformed inhomogenously on the DNA. The observed small Φ dependence of the EPR spectra of the A-form DNA fiber indicates that the complex is oriented randomly on the fiber.

In contrast to the inhomogenous broadening of the spectra of **1a** in DNA pellet or in A-form DNA fiber, the EPR line shape changed dramatically after the conformational change of the DNA fiber from A- to B-form in a humid atmosphere at ambient temperature (Fig. 4(a)). The conspicuous Φ dependence of the EPR spectra of **1a** in B-form DNA fiber indicates that **1a** was reoriented stereo-specifically with respect to the double helical DNA axis. The intense four line peaks observed at $\Phi = 0°$ indicate that one of the g tensor axes ($g_{\parallel} = 2.20$ and $A_{\parallel} = 12.0$ mT) was oriented along the DNA fiber axis. The considerable decrease in the A value from that observed in frozen solution ($A_{\parallel} = 17.0$ mT) suggests that the tetragonal coordination structure of **1a** changed considerably in the B-form DNA fiber. It should be noted that additional signals (the arrows in Fig. 4(a)) were observed at the low-field end of the spectrum of $\Phi = 0°$ and at the high-field end of the spectrum at $\Phi = 90°$. These signals correspond to another species bound with a different coordination structure.

Freezing of the B-form fiber at −150 °C caused another dramatic change in the EPR line shapes (Fig. 4(b)). The intense four line signals observed at $\Phi = 0°$ at room temperature were replaced with broad signals over the range 290–330 mT and with several weak peaks in the range 250–285 mT. It has been observed
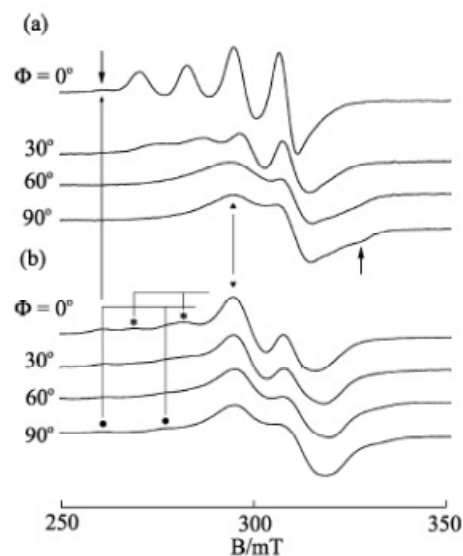
(a)

Φ = 0°
30°
60°
90°

(b)

Φ = 0°
30°
60°
90°

250   300   350
B/mT

Fig. 4 EPR spectra of **1a** in B-form DNA fiber. (a) At room temperature, (b) −150 °C.

that the freezing of B-form DNA fibers sometimes results in the randomization of the orientation of the complexes due to the formation of icebergs in the DNA fibers.[23,24] The intense peak that emerged at 295 mT (marked as ▼ in Fig. 4) indicates that the complex was distorted toward rhombic symmetry. Though the line shapes observed at low temperature did not change with Φ so conspicuously as those at room temperature, the intensity of the peaks marked with asterisks decreased with increasing Φ, indicating that the species has still some preferred orientation on the DNA fiber. On the other hand, the intensity of the peaks marked with a filled circle (●) does not change with Φ, indicating that the species is randomly oriented on the fiber. The $g_{\|}$ and $A_{\|}$ values estimated for latter species are very similar to the $g_{\|}$ and $A_{\|}$ values estimated for the species in frozen solution and DNA pellet. Interestingly, the magnetic field of the peak observed at the lowest end of the spectra at Φ = 0° in Fig. 3(a) almost coincides with those of the peaks at the lowest end of the spectra of frozen solution and DNA-pellet. Therefore, these signals can be assigned as those of the species bound to the DNA keeping the tetragonal structure observed in the crystal or in frozen solution.

It has been shown that ternary complexes of [Cu(phen)]²⁺ with various amino acids bind to DNA with several different binding modes.[25] One is intercalative and the other is groove bound. In some cases, the amino acid was replaced by coordinating groups in DNA. However, it has never been observed that the amino acid ternary complexes were deformed so much toward rhombic form upon binding to DNA. It is evident that the edda moiety in **1a** was preserved at the copper coordination site on the DNA, because no signals from the dissociated [Cu(phen)]²⁺ ($g_{\|}$ = 2.29, $A_{\|}$ = 0.017 cm⁻¹) were detected in the EPR spectra. These results indicate that **1a** binds to DNA, partially intercalating the phenanthroline plane parallel to the DNA base-pair plane with the coordination structure of the phen–edda moiety twisted to form rhombic species. This partial intercalation is correlated by the earlier CD data.

It is obvious that the two axially coordinating carboxyl oxygen atoms of the edda moiety observed in the crystal structure prevented deeper intercalation of the phenanthroline moiety and that the interaction of the carboxyl groups with DNA caused in return the rearrangement of the coordination sphere of the complex on the DNA. It is also possible that solvated water molecules around the carboxyl groups in **1a** exerted stress on the copper coordination sphere when the DNA fibers were frozen to form micro icebergs in the fibers, resulting in the randomization of the orientation of the copper coordination planes.

Though a part of **1a** binds to DNA retaining the initial tetragonal structure on the DNA as judged by the $g_{\|}$ signals in the EPR spectra of DNA-pellet, one can reasonably presume that the rhombic distortion of **1a** on the DNA is the key to understanding the function of this complex.

2.4 Antiproliferative and cell cycle analysis

The antiproliferative activity of M(phen)(edda) complexes on breast cancer cell line MCF-7 was assessed using an MTT assay. The IC₅₀ values of the Cu complex **1a**, Co complex **1b** and Zn complex **1c** were obtained by plotting the cell viability against concentration of the complexes (Fig. 5, Table 2). Due to an initial solubility problem, MTT assay was not done for **1d**. From the plots, the average IC₅₀ values (from two pooled results) were 3.8 μM for **1a**, 11.4 μM for **1b** and 7.0 μM for **1c**.

The trend in the antiproliferative ability of the complexes is **1a** > **1c** > **1b**. MTT assay carried out by incubating the cells with 1,10-phenanthroline gave an IC₅₀ value of 74 μM (Table 2; ESI as Data 1‡). The enhanced IC₅₀ values for the metal complexes suggest that there is synergy between the cytotoxic phen ligand with these metal cations. In other words, chelation of the phen ligand to these metal cations enhanced its cytotoxicity. Such cytotoxic enhancement resulting from chelation of phen to metal cation in binary or ternary complexes is seldom investigated, as far as we know. One such reported synergy involves the octahedral [La(phen)]³⁺ complex.[4] Ranford *et al.* also found that incorparating phen into the copper(II) complexes of 3,5-disubstituted salicylates enhanced their *in vitro* antitumor properties.[26] A similar synergic metal–ligand combination is also reported for a set of dicopper(II) complexes where the IC₅₀ values of the complexes for MCF-7 are in the range 24–54 μM while both the copper(II) chloride and the various non-polypyridyl proligands have IC₅₀ > 100 μM.[27] In contrast, the recent discovery of organic copper complexes as a new class of proteosome-inhibitors and apoptosis inducer for human cancer cells reported the occurrence of the reverse effect for the chosen metal–ligand combination.[28] Here, the 8-hydroxyquinoline slightly inhibits the proteosomal chymotrypsin-like activity of the

Table 2 IC₅₀ values for **1a–1c** on MCF-7

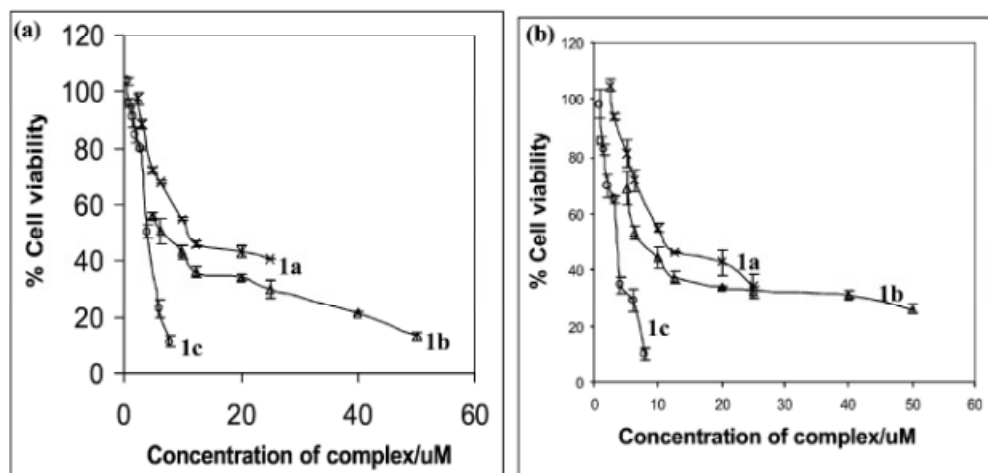| Complexes	1	2	Average
1a (Cu)	3.5	4.0	3.8
1b (Co)	11.4	11.3	11.4
1c (Zn)	7.7	6.3	7.0
phen[a]	74.3		
Cu(edda)[a]			395.5

[a] ESI Data 1 and Data 2.

221

Fig. 5 Viability of MCF-7 cells in the presence of M(phen)(edda) complexes (Cu,**1a**; Co, **1b**; Zn, **1c**). Each complex induced a dose-dependent decrease in cell viability. Plots 5(a) and 5(b) are from two independent sets of experiment.

CuBr$_2$ by forming the bis(8-hydroxyquinoline)copper(II) complex. Devereux *et al.* found that incorporating phen into a binary complex Cu(BZA)$_2$ (benzoate, BZA), to form the water-insoluble ternary complex [Cu(BZA)$_2$(phen)(H$_2$O)] greatly enhances its IC$_{50}$ values from >200 and 130 μM to 9.5 and 21.3 μM for the Hep-G$_2$ and A-498 cancer cell lines respectively.[29] However, IC$_{50}$ value of this ternary complex is not significantly higher than that of the metal-free phen (IC$_{50}$ values for Hep-G$_2$ and A-498 are 4.1 and 5.8 μM respectively) tested for the same cell lines (96 h incubation time). However, our results show that the IC$_{50}$ values of the tested ternary M(phen)(edda) complexes (**1a**, **1b**, and **1c**) are significantly enhanced compared to that of metal-free phen for the MCF-7 cell line (72 h incubation time). The choice of the second ligand may be crucial as we found that Cu(edda), phen and **1a** have IC$_{50}$ values of 395.5, 74.3 and 3.8 μM. In fact, on-going investigations substantiate the significance of choosing an amino acid or its derivative as the second ligand and this will be reported subsequently. In contrast, almost all the nine square planar ternary platinum(II) complexes of phen and various amino acids, [Pt(phen)(aa)]NO$_3$ tested (except [Pt(phen)(pro)]NO$_3$), are found to be not cytotoxic towards a human leukemia cell line.[6] Complex geometry may be a significant contributing factor in ensuring a synergic effect in the rational design of anticancer ternary metal complexes.

Investigation into the nature of the cell death mechanism by incubating MCF-7 cells with the respective complexes by using fluorescence activated cell sorting (FACS) analysis for both apoptosis and cell cycle arrest is in progress. Preliminary results with concentration of complexes lower than their respective IC$_{50}$ values (except for **1c**) are presented herein. FACS of induction of apoptosis was undertaken for MCF-7 cells treated with cisplatin as positive control, and the complexes **1a**, **1b** and **1c** (Fig. 6). Untreated cells showed a majority of viable healthy cells with 86% population after 72 h incubation. Cells treated with 10 μg ml^{-1} of cisplatin for 72 h as positive control exhibited an increased number of cells at late apoptotic stage (76%) compared to an
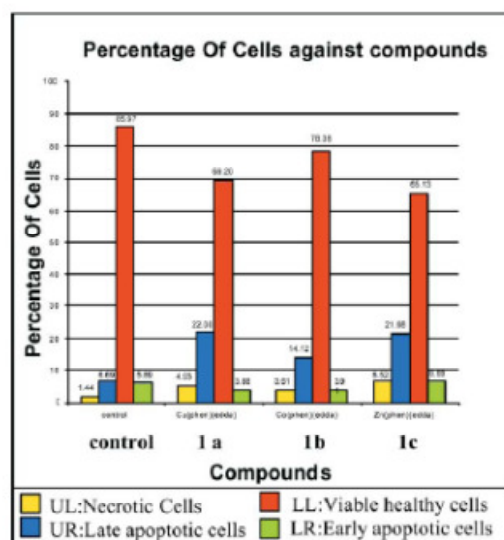

Fig. 6 Percentage of necrotic cells (UL), late apoptosis cells (UR), viable cells (LL) and early apoptotic cells (LR) for untreated MCF-7 cells and cells treated with **1a**, **1b** and **1c**.

untreated control (7%). MCF-7 cells treated with 2.8 μM **1a** (Cu), with 5.3 μM **1b** (Co) and with 9.2 μM **1c** (Zn) for 72 h showed 22%, 14% and 22% of the cell population at late apoptotic stage respectively. The percentage of necrotic cells in the above MCF-7 cells treated with **1a**, **1b** and **1c** were 5%, 4% and 7% respectively compared with 1% for untreated cells. Thus, cell death induced by the metal complexes **1a**, **1b** and **1c** is mainly *via* apoptosis. The total % cell death (apoptosis and necrosis) induced for **1a**, **1b** and **1c** is 31%, 22% and 35% respectively.

The cell cycle progression data of MCF-7 cells treated with **1a**, **1b** and **1c** were obtained using a FACS analysis of DNA
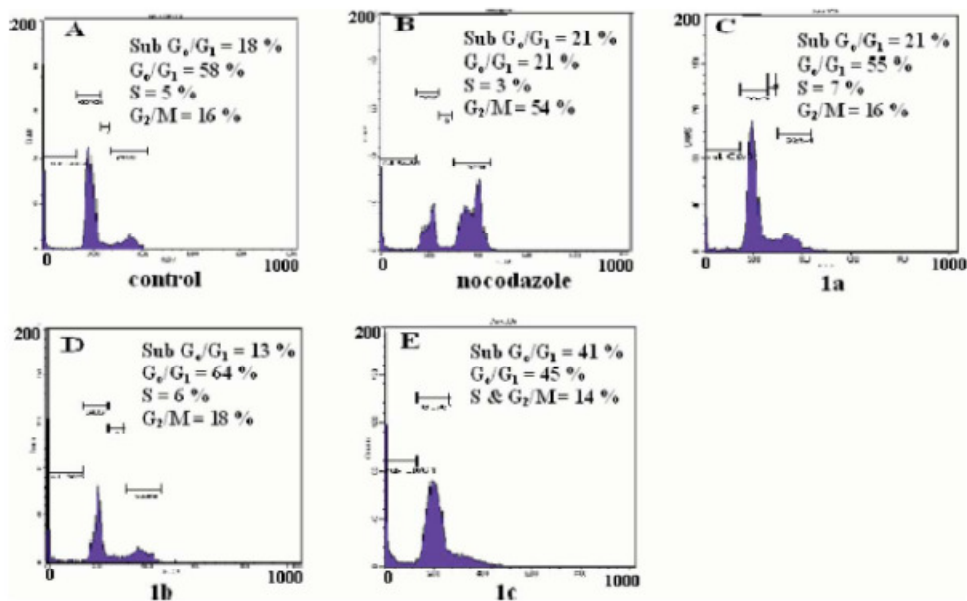
Fig. 7 FACS analysis of cell cycle arrest of untreated MCF-7 cells and those treated with nocodazole (positive control), **1a**, **1b** and **1c**. Percentage of cells in sub G_0/G_1, G_0/G_1, S and G_2/M were determined after staining with propidium iodide (PI).

content (Fig 7). Cells in the G_0/G_1 phase have unreplicated 2N DNA while those in the G2 and M phases have duplicated 4N DNA. Those in the S phase are in the process of replicating their DNA while those in the sub-G_0/G_1 phase have hypodiploid DNA (less than 2N). Our results showed that untreated MCF-7 cells exhibited asynchronous cell cycle profile following 72 h in culture. When the cells were treated with **1a**, **1b** and **1c** at concentrations lower their respective IC_{50} values, the cell cycle profiles of the complexes obtained were quite similar, except that for **1c** (Zn). For **1c**, the cell population at sub-G_0/G_1 (hypodiploid) increased from 18% to 41% after 72 h treatment while the G_0/G_1 population remained high at 45% compared to untreated cells which had a corresponding population of 58% at G_0/G_1. Increases in cell population at sub-G_0/G_1 phase had been taken as evidence of cells entering apoptosis.[4,30,31] There were no distinct S and G_2/M phases; their combined S and G_2/M phases significantly dropped from 20% to 14%, indicating blockage of cell progression into S and G_2/M phases, and thus implying a certain proportion of cells were arrested at G_0/G_1. Accumulation of cells at G_0/G_1 has been associated with activation of cell cycle checkpoint due to DNA damage.[4] In addition, **1b** may also cause cell cycle arrest at G_0/G_1 as there is increase in G_0/G_1 population from 58% to 64% when the cells were treated with **1b** for 72 h. Thus, both **1b** and **1c** induced apoptosis as a major cell death pathway and cell cycle arrest at G_0/G_1 as a minor pathway. This mode of action is in contrast to that of cisplatin which induces cell cycle arrest at G_2/M phase.[32] However, it seems that the complex **1a** induced cell death mainly *via* apoptosis. In this respect, the mode of action of **1a** is similar to the anticancer *octahedral* [Cu(phen)₂(mal)] (H_2mal = malonic acid) complex.[10] On the other hand, the ability of **1c** (Zn complex) to induce cell cycle arrest at G_0/G_1 can be compared to the octahedral [La(phen)₃]³⁺ complex which also

induced expression of p53 and p21 besides inducing a selective decrease in cyclin B_1.[4] The octahedral La(III) complex exhibits very promising results on >60 tumor cell models with low μM values, and low toxicity test on rats. Further work is being carried out to investigate further the molecular mechanism of cell death of the M(phen)(edda) complexes, and confirm the above preliminary observations.

3. Conclusions

The synthesized complexes are found to have octahedral geometries, and they can be classified according to magnetic property or tetragonal distortion. Binding of these complexes to DNA is *via* partial intercalation of the phenanthroline moiety into the base pairs, as evidenced by CD and EPR data. The edda moiety prevents deeper intercalation of the phen of **1a** and this intercalation into DNA in turn results in rhombic distortion; this may similarly occur for the other complexes. The CD data suggest that the extent of intercalation of the octahedral M(phen)(edda) complexes varies with the type of metal(II) ion and this seems to be related to the absence or presence of Jahn–Teller distortion. The enhanced cytotoxicity of the complexes towards MCF-7 cancer cells, as evidenced by their IC_{50} values and in comparison with the IC_{50} value of unchelated 1,10-phenanthroline, suggests synergic combination of the two types of ligand and metal ion used. Compared to the IC_{50} value (1.42 μM) of cisplatin for MCF-7,[33] those of **1a–1c** indicate significant synergic effect. It seems that the choice of the second ligand is important in designing effective anticancer ternary metal complexes. Besides such synergic effect, the type of metal ion can affect the mode of action of these anticancer metal complexes as exemplified by the ability of the zinc complex, **1c**, to induce cell cycle arrest.

223

4. Experimental

4.1 Synthesis of complexes

The metal(II) complexes of 1,10-phenanthroline and N,N'-ethylenediaminediacetic acid were prepared either (i) by reacting freshly prepared metal(II) hydroxide with N,N'-ethylenediaminediacetic acid, followed by addition of methanolic or ethanolic aqueous solutions of 1,10-phenanthroline, or (ii) by an *in situ* method where the sequence of added reactants was H₂edda, NaOH, metal(II) salt and alcoholic aqueous phen. The following is given as an example.

Freshly prepared $Cu(OH)_2$ was obtained by reacting cold aqueous $CuSO_4 \cdot 5H_2O$ (0.54 g, 0.002 mol) with cold aqueous NaOH (0.17 g, 0.004 mol). The solid hydroxide was added to a suspension of N,N'-ethylenediaminediacetic acid in about 30 ml of water. The resultant blue solution was filtered and a methanolic solution of 1,10-phenanthroline (0.43 g, 0.002 mol) was then added. The reaction mixture was heated in a water-bath at 55 °C before cooling overnight. Blue crystals suitable for X-ray structure analysis were obtained on the following day. Yield, 0.47 (46%).

Anal. calc. for **1a**, $CuC_{18}H_{18}N_4O_4 \cdot 5H_2O$: C, 42.55; H, 5.56; N, 11.03%. Found: C, 42.12; H, 5.20; N, 11.22%. FTIR (v/cm^{-1}): 3391 vs (broad, b), 2921 vs, 1590 vs, 1523 m, 1460 m, 1430 vs, 1397 vs, 1352 m, 1328 vs, 1264 s, 1226 s, 1147 w, 1110 m, 1090 m, 1056 w, 1033 m, 987 m, 912 w, 852 s, 816 m, 725 s, 626 s, 581 s.

Anal. calc. for **1b**, $CoC_{18}H_{18}N_4O_4 \cdot 3H_2O$: C, 46.26; H, 5.18; N, 11.99%. Found: C, 45.79; H, 4.67; N, 11.78%. FTIR (v/cm^{-1}): 3401 vs (b), 3275 vs, 2946 s, 1648 vs, 1595 vs, 1517 m, 1455 m, 1424 s, 1366 vs, 1314 s, 1289 m, 1281 m, 1225 m, 1136 m, 1114 w, 1061 m, 1014 s, 951 s, 899 m, 870 m, 852 s, 828 m, 784 s, 728 s, 641 s, 618 s, 571 s, 537 m, 506 m, 422 m.

Anal. calc. for **1c**, $ZnC_{18}H_{18}N_4O_4 \cdot 3.5H_2O$: C, 44.78; H, 5.22; N, 11.60%. Found: C, 44.84; H, 4.61; N, 11.60%. FTIR (v/cm^{-1}): 3370 vs (b), 3277 vs, 2964 w, 1654 s, 1594 vs, 1520 m, 1425 s, 1373 s, 1313 s, 1256 w, 1227 w, 1139 m, 1092 m, 1063 w, 1014 m, 949 m, 902 w, 868 m, 825 m, 785 m, 728 s, 621 m, 582 m, 421 m.

Anal. calc. for **1d**, $NiC_{18}H_{18}N_4O_4 \cdot 3H_2O$: C, 46.28; H, 5.18; N, 11.99%. Found: C, 46.04; H, 4.80; N, 11.85%. FTIR (v/cm^{-1}): 3401 vs (b), 3275 vs, 2946 s, 1648 vs, 1595 m, 1517 m, 1457 m, 1424 s, 1366 vs, 1314 s, 1290 m, 1281 m, 1225 m, 1136 m, 1115 w, 1061 m, 1014 s, 951 s, 899 m, 870 m, 828 m, 784 s, 640 m, 618 m, 571 m, 537 m, 506 m, 422 m.

Crystal data for **1a**. $CuC_{18}H_{28}N_4O_9$, $M = 507.98$, triclinic, $P\bar{1}$, $a = 9.897(1)$, $b = 11.233(2)$, $c = 11.851(2)$ Å, $\alpha = 65.609(2)$, $\beta = 70.409(2)$, $\gamma = 73.771(2)°$, $V = 1115.1(3)$ Å^3, $Z = 2$, $D_c = 1.513$ g cm^{-3}, μ (Mo-Kα) = 1.036 mm^{-1}, $T = 150(2)$ K, blue prism, Bruker CCD-1000 area detector diffractometer, 11229 reflections collected, 5197 independent measured reflections ($R_{int} = 0.0365$), F^2 refinement, $R_1 = 0.0267$ ($I > 2\sigma(I)$), $wR_2 = 0.0759$ (all data), 4638 independent observed absorption-corrected reflections [$I > 2\sigma(I)$, $\theta_{max} = 28.2892°$], 325 parameters.

CCDC reference number 636037.

4.2 Characterization of complexes

The infrared spectra of the complexes were recorded on a Perkin-Elmer FT-IR spectrometer in the frequency range 4000–400 cm^{-1} as KBr discs. The C, H and N microanalysis was carried out with a Perkin Elmer 2400 CHN analyser. UV-visible spectroscopic measurement of the aqueous solutions of the complexes was carried out on a Perkin Elmer Lambda 40 spectrophotometer.

Circular dichroism spectra of the complexes, in 20 mM Hepes buffer pH 7 containing 30 mM NaCl, were measured using a JASCO J-820 CD spectrophotometer. Each sample solution (3000 μL, 3 ml) was obtained by adding the required volume of stock solution of calf thymus DNA (Calbiochem, Merck) and metal complex dissolved in the above Hepes buffer, and finally topping up the solution with an additional volume of the same buffer. Two sets of complex–DNA solutions were used: the ratio of the complex : DNA = 40 μM : 40 μM (1 : 1) in each solution in one set of solutions while the mole ratio for the second set is 160 μM : 40 μM (4 : 1).

4.3 Preparation of DNA-pellets and fibers

Salmon testes DNA was dissolved in 20 mM NaCl to produce a solution of approximately 1 mM DNA base pair concentration. Subsequently, the complex solution was added dropwise to the DNA, and stirred for approximately 12 h at 4 °C. The resulting solutions were adjusted to a pH of 7.0 with sodium hydroxide and hydrochloric acid throughout the experiments. The DNA-pellet was obtained by ultracentrifugation of the mixed solution. The DNA fibers were prepared from the pellet as previously reported.[23,24,34]

4.4 EPR spectra

X-Band (9.2 GHz) EPR spectra at ambient temperature and −150 °C were measured on a JEOL RE-2X spectrometer with 100 kHz field modulation of 0.5 mT. The magnetic field was calibrated with an NMR field meter EFM-2000 (ECHO Electronics LTD). The microwave frequency was measured on an Anritsu MF2412A frequency counter. The EPR spectra were measured at different angles of Φ between the fiber axis and the static magnetic field.

4.5 Antiproliferative screening

All tissue culture reagents were obtained from Sigma and Life Technologies Inc., Gaitherburg, MD. The oestrogen receptor positive human breast adenocarcinoma cell line MCF-7 was cultivated for a minimum of two passages after thawing prior to experimentation. The cells were grown in RPMI 1640 supplemented with 10% FBS, 0.025 M Hepes, 0.024 M sodium bicarbonate, 50 units ml^{-1} penicillin G/streptomycin sulfate at 37 °C in 5% CO_2.

MTT assay was used to test the cytotoxicity of metal complexes. The growing MCF-7 tumour cells were seeded into a 96-well plate at a density of $2.3–3.0 \times 10^5$ cells per well and incubated in a medium containing the complexes at concentration ranging from 0.5–50 μM for 72 h. A 0.25% trypsin EDTA solution was used to detach the cells from the surface. Every experiment was conducted in triplicate wells. Into each well 20 μl of MTT (5 mg ml^{-1}) was added. The plates were then incubated at 37 °C for 4 h to allow MTT to form formazan crystals. The crystals were then solubilized using DMSO for a few minutes. The absorbance of each well was measured in a microplate reader Dynatech MRX at 570 nm with a reference wavelength of 630 nm. The percentage of cell viability was calculated with the formula: Average A_{570} value for live cell

224

(test)/average A_{570} value for live cell (control) $\times$ 100. The IC$_{50}$ values were obtained from the graphs drawn.

4.6 Apoptosis and cell cycle studies with flow cytometry

Apoptosis and cell cycle analysis were determined using a Becton Dickinson flow cytometer FACS Calibur™. For both analyses, MCF-7 cells were plated at a density of 3×10^5 cells ml^{-1} in 60 mm petri dishes and allowed to recover for 24 h. To analyze cell cycle phase distribution, the cells were treated with **1a** (2.8 µM), **1b** (5.3 µM) and **1c** (9.2 µM) for 72 h and washed with PBS. Cells were harvested through trypsinization and resuspended in RPMI 1640 medium. Floating cells were included in the analysis. After centrifugation for 10 min at 1500 rpm, the pellets were fixed in ice-cold 70% ethanol, stored at 4 °C. The fixative was removed by centrifugation. Fixed cells were resuspended in 1 ml of PBS, treated with 15 µL of RNase A (15 µg ml^{-1}) and stained with 10 µL of propidium iodide (Sigma Chemical Co.) for 15 min at room temperature. The cell cycle profiles were determined on FACS by using Cell Quest software. A total of 10 000 events were collected and the cells were properly gated for analysis. The histogram of DNA content (x-axis, PI-fluorescence) *versus* counts (y-axis) was displayed.

After treatment of cells with **1a**, **1b** and **1c** at the respective concentrations (same as above), the cells were washed with PBS, trysinized and resuspended in RPMI 1640 medium. Flow cells were included in the apoptosis analysis. After centrifugation for 10 min at 1500 rpm, the pellets were gently resuspended in 100 µL of binding buffer (Hepes, NaCl, CaCl$_2$ in 6.5 : 22.3 : 1 ratio), 5 µL of Annexin V-FITC (Fharmigen, USA), 5 µL propidium iodide (200 µg ml^{-1} in PBS; Sigma Chemical Co.) in a round bottom polystyrene tube (Becton Dickinson) for 15 min at room temperature. 200 µL of binding buffer was added before analysis by flow cytometry. The cells were similarly analyzed on FACS by using Cell Quest software. A total of 10 000 events were acquired and the cells were properly gated for analysis. The cell populations were displayed as a dot plot divided into four quadrants with Annexin V-FITC fluorescence (x-axis) *versus* propidium iodide fluorescence (y-axis).

Acknowledgements

References

1 P. Christofis, M. Katsarou, A. Papakyriakou, Y. Sanakis, N. Katsaros and G. Psomas, *J. Inorg. Biochem.*, 2005, **99**, 2197.
2 P. J. Dyson and G. Sava, *Dalton Trans.*, 2006, 1929.
3 R. Huang, A. Wallqvist and D. G. Covell, *Biochem. Pharmacol.*, 2005, **69**, 1009.
4 P. Heffeter, M. A. Jakupec, W. Körner, S. Wild, N. G. Von Keyserlingk, L. Elbling, H. Zorbas, A. Koryneuska, S. Knasmüller, H. Sutterlüty, M. Micksche, B. K. Keppler and W. Berger, *Biochem. Pharmacol.*, 2006, **71**, 426.
5 N. Margiotta, A. Bergamo, G. Sava, G. Padovano, E. de Clercq and G. Natile, *J. Inorg. Biochem.*, 2004, **98**, 1385.
6 V. X. Jin and J. D. Ranford, *Inorg. Chim. Acta*, 2000, **304**, 38.
7 K. Balamurugan, R. Rajaram, T. Ramasami and S. Narayanan, *Free Radical Biol. Med.*, 2002, **33**, 1622.
8 H. Jhou, C. Zheng, G. Zou, D. Tao and J. Gong, *Int. J. Biochem. Cell Biol.*, 2002, **34**, 678.
9 S. Zhang, Y. Zhu, C. Tu, H. Wei, Z. Yang, L. Lin, J. Ding, J. Zhang and Z. Guo, *J. Inorg. Biochem.*, 2004, **98**, 2099.
10 B. Coyle, P. Kinsella, M. McCann, M. Devereux, R. O'Connor, M. Clynes and K. Kavanagh, *Toxicol. in Vitro*, 2004, **18**, 63.
11 M. McCann, M. Geraghty, M. Devereux, D. O'Shea, J. Mason and L. O'Sullivan, *Met.-Based Drugs*, 2000, **7**, 185 and reference quoted therein.
12 M. Bernal, J. A. García-Vázquez, J. Romero, C. Gómez, M. L. Durán, A. Sousa, A. Sousa-Pedrares, D. J. Rose, K. P. Maresca and J. Zubieta, *Inorg. Chim. Acta*, 1999, **295**, 39.
13 C. M. Sharaby, *Spectrochim. Acta, Part A*, 2005, **62**, 326.
14 M. S. Masoud, S. A. Abou El-enein, M. E. Ayad and A. S. Goher, *Spectrochim. Acta, Part A*, 2004, **60**, 77.
15 S. Chandra and U. Kumar, *Spectrochim. Acta, Part A*, 2005, **61**, 219.
16 M. El-Behery and H. El-Twigry, *Spectrochim. Acta, Part A*, 2007, **66**, 28.
17 S. Chandra and L. K. Gupta, *Spectrochim. Acta, Part A*, 2004, **60**, 1563.
18 H. Hadadzadeh, M. M. Olmstead, A. R. Rezvani, N. Safari and H. Saravani, *Inorg. Chim. Acta*, 2006, **359**, 2154.
19 C. H. Ng, H. K. Alan Ong, C. W. Kong, K. W. Tan, R. N. Z. R. A. Rahman, B. M. Yamin and S. W. Ng, *Polyhedron*, 2006, **25**, 3118.
20 C. H. Ng, S. B. Teo, S. G. Teoh, H. K. Fun and J.-P. Declercq, *Inorg. Chim. Acta*, 2002, **340**, 81.
21 S. Zhang, Y. Zhu, C. Tu, H. Wei, Z. Yang, L. Lin, J. Ding, J. Zhang and Z. Guo, *J. Inorg. Biochem.*, 2004, **98**, 2099.
22 Z.-M. Wang, H.-K. Lin, S.-R. Zhu, T.-F. Liu and Y.-T. Chen, *J. Inorg. Biochem.*, 2002, **89**, 97.
23 W. Harada, T. Nojima, A. Shibayama, H. Ueda, H. Shindo and M. Chikira, *J. Inorg. Biochem.*, 1996, **64**, 273.
24 M. Chikira, M. Inoue, R. Nagane, W. Harada and H. Shindo, *J. Inorg. Biochem.*, 1997, **66**, 131.
25 M. Chikira, Y. Tomizawa, D. Fukita, T. Sugisaki, N. Sugawara, T. Yamazaki, A. Sasano, H. Shindo, M. Palaniandavar and W. E. Antholine, *J. Inorg. Biochem.*, 2002, **89**, 163.
26 J. D. Ranford, P. J. Sadler and D. A. Tocher, *J. Chem. Soc., Dalton Trans.*, 1993, 33931.
27 Z. Tráníček, M. Maloň, Z. Šindelář, K. Doležal, J. Rolčík, V. Kryštof, M. Strnad and J. Marek, *J. Inorg. Biochem.*, 2001, **84**, 23.
28 K. G. Daniela, P. Gupta, R. H. Harbach, W. C. Guida and Q. P. Dou, *Biochem. Pharmacol.*, 2004, **67**, 1139.
29 M. Devereux, D. O. Shea, A. Kellett, M. McCann, M. Walsh, D. Egan, C. Deegan, K. Kedziora, G. Rosair and H. Müller-Bunz, *J. Inorg. Biochem.*, 2007, **101**, 881.
30 C. C. Sprenger, M. E. Vail, J. Simurdak and S. R. Plymate, *Oncogene*, 2000, **21**, 140.
31 T.-C. Wang, L.-L. Chen, P-J. Lu, C.-H. Wong, C.-H. Liao, K.-C. Tsiao, K.-M. Chang, Y.-L. Chen and C.-C. Tzeng, *Bioorg. Med. Chem.*, 2005, **13**, 6045.
32 A.-R. Ghezzi, M. Aceto, C. Cassino, E. Gabano and D. Osella, *J. J. Inorg. Biochem.*, 2004, **98**, 73.
33 E. Pantoja, A. Gallipoli, S. van Zutphen, S. Komeda, D. Reddy, D. Jaganyi, M. Lutz, D. M. Tooke, A. L. Spek, C. Navarro-Ranninger and J. Reedijk, *J. Inorg. Biochem.*, 2006, **100**, 1955.
34 M. Chikira, S. Suda, T. Nakabayashi, Y. Fujiwara, T. Ejiri, M. Yoshikawa, N. Kobayashi and H. Shindo, *J. Chem. Soc., Dalton Trans.*, 1995, 1325.

225